Studies on the regulation of tissue plasminogen activator activity by physiological templates

A thesis presented by

Stella Claire Williams

for the degree of Doctor of Philosophy

from Imperial College London

Biotherapeutics Division

National Institute for Biological Standards and Control

Blanche Lane, South Mimms, EN6 3QG

Department of Cell and Molecular Biology

Imperial College London, Exhibition Road, South Kensington,

London, SW7 2AZ

Abstract

Myocardial infarction (MI) and ischemic stroke (IS) are caused by blood clots blocking arteries and cutting off the blood supply to tissues in the heart or brain. Clots may be cleared using plasminogen activators ("clot busters") that convert plasminogen into plasmin, which in turn digests fibrin. The major plasminogen activator in the circulation is tissue plasminogen activator (tPA) and a recombinant form Alteplase was developed for use as a thrombolytic drug. However, newer engineered thrombolytics based on tPA have often been disappointing in clinical trials for MI, and there has been little progress in treatment for IS. Some of this lack of success may be due to gaps in our understanding of the details of the action of these drugs during clot dissolution as no rational models exists to understand the quantitative relationship between fibrin binding and plasminogen activation and hence fibrin lysis. Development of such models was the goal of this project. Fibrin binding is central in the regulation of tPA activity and binding is principally via 2 tPA domains, finger (F) and kringle 2 (K2), which were the focus of attention in the design of domain variants of tPA, including fusions with jelly fish fluorescent proteins. Protease activity was investigated initially with amidolytic substrates and then with plasminogen as substrate in the presence of templates: heparin, fibrinogen and fibrin, which co-localise tPA and substrate, plasminogen, to enhance plasmin generation. Kinetics of association and dissociation and equilibrium binding studies were investigated using surface plasmon resonance technology and ELISA-style plate binding assays. The results of these experiments showed that both the strength and pattern of binding of domain variants depends on the template. Models have been developed combining intrinsic enzyme kinetic and binding data to predict plasminogen activation rates in the presence of different templates. These studies are useful for optimising the design of thrombolytic drugs to treat MI and IS.

Acknowledgements

I wish to thank my supervisors Dr. Colin Longstaff and Dr. Craig Thelwell at The National Institute for Biological Standards and Control and Prof. Neil Fairweather and Dr Kate Brown at Imperial College for the huge amount of support, encouragement and advice they have given me throughout this project.

I would also like to thank Dr Marta Silver and Colin Whitton for all their useful advice.

I also thank the British Heart Foundation for the financial support extended for these studies.

Table of contents

Abstract		2
Acknowledgements		3
Table of Contents		4
List of Figures		11
List of Tables		17
Abbreviations		19
Statement of originality		22

CHAPTER 1: INTRODUCTION

1.1	Fibrinolysis	23
1.2	Myocardial infarction and the history of thrombolytics	26
1.3	Domains of plasminogen and tPA involved in binding to fibrin and fibrinogen	27
1.4	Fibrin and Fibrinogen	29
1.4.1	The structure of fibrin and fibrinogen	29
1.4.2	Conversion of fibrinogen to fibrin by thrombin	31
1.4.3	Digestion of fibrin by plasmin	33
1.4.4	tPA and plasminogen binding sites in fibrin and fibrinogen	33
1.5	tPA and plasminogen binding to heparin	35
1.6	tPA glycosylation	38
1.7	Surface plasmon resonance – Biacore	40

1.7.1 The CM range of sensor chips 42

1.7.2 The SA sensor chip 43

1.8 Project aims 44

CHAPTER 2: MOLECULAR BIOLOGY, RECOMBINANT PROTEIN EXPRESSION AND PURIFICATION

2.1 Introduction 49

2.1.1 Recombinant tPA 49

2.1.2 Production of tPA in insect cells 50

2.2 Materials 56

2.2.1 Insect cell lines 56

2.2.2 *Escherichia coli* strains 56

2.2.3 Plasmids 57

2.2.4 Chemicals, reagents and laboratory consumables 58

2.2.5 Buffers 59

2.3 Methods 59

2.3.1 Maintenance of *E. coli* cultures 59

2.3.2 General methods for DNA manipulation 60

2.3.2.1 Transformation of competent α-select *E. coli* cells 60

2.3.2.2 Plasmid isolation from *E. coli* 60

2.3.2.3 Restriction endonuclease digestion of plasmid DNA and agarose gel electrophoresis 60

2.3.2.4 Site-directed mutagenesis 61

2.3.2.5 DNA sequencing 62

2.3.3 Generating plasmid constructs for expression of itPA variants 62

2.3.3.1 Generation of pFastBac-irPA 64

2.3.3.2 Generation of pFastBac-itPA-K1P 64

2.3.3.3 Generation of pFastBac - itPA: P 64

2.3.3.4 Generation of pFastBac-itPA: F del 65

2.3.3.5 Generation of pFastBac- itPA: F del-GFP 65

2.3.3.6 Maintenance of Sf9 cultures 66

2.3.3.7 Generating recombinant bacmid DNA using DH10Bac *E. coli* cells 66

2.3.3.8 Transfection of Sf9 cells to generate recombinant baculovirus 67

2.3.3.9 Baculovirus titre determination 67

2.3.3.10 Baculovirus amplification 68

2.3.4 Protein expression in Sf9 cells 69

2.3.4.1 Purification of recombinant tPA variants expressed in Sf9 cells 69

2.3.4.2 Purification of itPA-GFP 70

2.3.4.3 Ion exchange chromatography 70

2.3.5 Converting itPA into tcitPA using plasmin-Sepharose 71

2.3.6 Determination of protein concentration and purity 72

2.3.6.1 Dialysis 72

2.3.6.2 Protein concentration determination using Bradford assay 72

2.3.6.3 SDS-PAGE 72

2.3.6.4 Western Blotting 73

2.3.7 Fluorescence measurements of itPA-GFP and itPA: F del-GFP 73

2.4 Results 75

2.4.1 Expression and purification of tPA variants 75

2.4.2 tPA-GFP and tPA: F del-GFP 80

2.4.2.1 Fluorescence measurements of itPA-GFP fusions 80

CHAPTER 3: KINETICS

3.1 Introduction 91

3.2 Materials and Methods 94

3.2.1 Materials 94

3.2.2 Methods 95

3.2.2.1 tPA amidolytic activity in solution 95

3.2.2.2 Plasminogen activation with soluble templates 96

3.2.2.3 Plasminogen activation in fibrin clots 98

3.2.3 Data collection and analysis 102

3.2.3.1 Data processing 103

3.2.3.2 Fitting data to the Michaelis-Menten equation 105

3.2.3.3 Combistats 106

3.3 Results 108

3.3.1 Amidolytic activity of tPA variants in solution 108

3.3.2 Plasminogen activation with soluble templates 112

3.3.2.1 Plasminogen activation with fibrinogen as a template 112

3.3.2.2 Plasminogen activation with heparin as a template 121

3.3.3 Fibrin stimulation of tPA activity 126

3.3.3.1 Measuring initial plasminogen activation rates in fibrin and the rate of fibrin lysis 126

3.3.3.2 Fibrin as a template and the effects of plasminogen concentration on the domain variants 127

3.3.3.3 Fibrin as a template and the effects of different types of fibrin on the domain variants 132

CHAPTER 4: BINDING

4.1 Introduction 141

4.2 Materials and Methods 144

4.2.1 Materials 144

4.2.2 Methods 145

4.2.2.1 Fibrinogen plates 145

4.2.2.2 Fibrin plates 147

4.2.2.3 Data Analysis 148

4.2.3 Surface Plasmon Resonance – using the Biacore system 149

4.2.3.1 Lysine immobilization 150

4.2.3.2 Fibrinogen immobilization 150

4.2.3.3 Fibrin immobilization 152

4.2.3.4 Heparin immobilization 153

4.2.3.5 Biacore data analysis 154

4.2.4 Solubility studies 157

4.3 Results 158

4.3.1 Binding to immobilized fibrinogen and thrombin-treated fibrinogen (fibrin) using ELISA style assays 158

4.3.1.1 Determination of fifty percent inhibitory concentration (IC_{50}) of 6-aminohexanic acid against itPA and variants binding to fibrinogen 158

4.3.1.2 Plasminogen activator range binding to immobilized fibrinogen 162

4.3.2 Binding of itPA and variants to immobilized templates measured by Surface Plasmon Resonance –Biacore 170

4.3.2.1 Binding of itPA and variants to immobilized L-lysine on a CM5 Sensor chip 170

4.3.2.2 Interaction of itPA, variants, and plasminogen with fibrinogen immobilized indirectly via anti-fibrinogen antibodies 175

4.3.2.3 Interaction of scitPA (R275E), tcitPA, and itPA with fibrinogen immobilized directly using covalent immobilization (amine coupling) 182

4.3.2.4 Interaction of itPA and domain variants with fibrinogen 195

4.3.2.5 Interaction of itPA, variants, and plasminogen with heparin-biotin immobilized on SA chips 203

4.3.2.6 Investigating conditions for improved tPA solubility 208

CHAPTER 5: MODELLING

5.1 Introduction 212

5.2 Methods 215

5.3 Results 220

5.3.1 Modelling plasminogen activation by scitPA (R275E) and tcitPA with fibrinogen as a template 220

5.3.2 Modelling plasminogen activation by itPA and variants with fibrinogen as a template 223

5.3.3 Modelling plasminogen activation by itPA with heparin as a template in two buffers with different NaCl concentrations 227

CHAPTER 6 DISCUSSION 231

6.1 Future work 252

Reference List 254

List of figures

Figure 1.1: Scheme of fibrinolysis 24

Figure 1.2: Structure of the fibrinogen molecule 30

Figure 1.3: Formation of fibrin from fibrinogen 32

Figure 1.4: Schematic diagram of normal tPA (Alteplase) 45

Figure 1.5: Schematic diagram of normal rPA (Reteplase) 45

Figure 2.1: Expression vector pFastBac1. 54

Figure 2.2: SDS-PAGE of recombinant tPA variants 78

Figure 2.3: SDS-PAGE of scitPA (R275E), itPA and itPA treated with plasmin-Sepharose (tcitPA) 79

Figure 2.4: Fluorescence in relative fluorescence units (RFU) of a 30 μg/ml sample of itPA: F del-GFP 82

Figure 2.5: GFP standard curve 83

Figure 2.6: GFP standard curve 83

Figure 2.7: Coomassie stained SDS-PAGE of GFP fusion variants 84

Figure 2.8: Ruby SYPRO stained SDS –PAGE 84

Figure 2.9: Western blots probed with (1) Anti-GFP antibody, (2) Anti-tPA antibody and (3) an overlay of blots (1) and (2) 86

Figure 2.10: SYPRO Ruby stained SDS-PAGE of itPA: F del-GFP before

and after dialysis 87

Figure 2.11: Silver stained SDS-PAGE of itPA: F del-GFP purifications 89

Figure 2.12: Silver stained SDS-PAGE of itPA: F del-GFP purification with 2 M NaCl wash 89

Figure 2.13: Fluorescence measurements of fractions from itPA: F del purification 90

Figure 3.1 Format of clear clot lysis reaction, representing a single well of a microtitre plate 99

Figure 3.2: Michaelis-Menten curves and 95% confidence intervals for variants in chromogenic substrate S2288 assay 109

Figure 3.3: Michaelis-Menten curves for itPA and scitPA (R275E itPA) before and after plasmin-Sepharose treatment with chromogenic substrate S2288 assay 111

Figure 3.4: Plasminogen activation by itPA and variants in the presence of fibrinogen 115

Figure 3.5: Plasminogen activation rates at the optimum fibrinogen concentration for itPA, irPA and itPA:K1K1 in the presence of 3 plasminogen concentrations 117

Figure 3.6: Plasminogen activation by itPA and variants at 4 activator concentrations in the presence of fibrinogen 118

Figure 3.7: Plasminogen activation by scitPA (R275E itPA) and tcitPA in the presence of fibrinogen 119

Figure 3.8: Plasminogen activation by itPA and variants in the presence

of heparin 123

Figure 3.9: Plasminogen activation by itPA and variants with 3 plasminogen concentrations in the presence of heparin 125

Figure: 3.10: Initial plasminogen activation rates 129

Figure: 3.11: Fibrin lysis rates (measured as time to 50% lysis) 130

Figure: 3.12: Fibrin lysis rates (measured as time to 20% lysis) 131

Figure 3.13: Plasmin generation in normal and CPB-treated fibrin by itPA and irPA 133

Figure 3.14: Example of plots showing the activity of irPA in different fibrins 134

Figure 3.15: Michaelis-Menten curves for clear clot lysis assay 135

Figure 3.16: Rate of plasminogen activation and fibrin lysis for itPA: K1K1 and irPA relative to itPA in 3 fibrin conditions 140

Figure 4.1: Data (circles) and fits (red lines) of the IC50 of 6-aminohexanoic acid on itPA and variants binding to immobilized fibrinogen 160

Figure 4.2: Relative activities of variants compared to full length itPA bound to immobilized fibrinogen 163

Figure 4.3: itPA-GFP (A) and itPA: F del-GFP (B) in plate with immobilized fibrinogen before incubation 166

Figure 4.4: itPA-GFP after incubation with immobilized fibrinogen (after plate had been washed) 167

Figure 4.5: itPA-GFP (A) and itPA: F del-GFP (B) after incubation with

immobilized fibrinogen (after plate had been washed) 168

Figure 4.6: Initial plasminogen activation rates of itPA-GFP and itPA: F del-GFP bound to immobilized fibrinogen 169

Figure 4.7: Immobilization of L-lysine on to a CM5 sensor chip using amine coupling using the Biacore 2000 immobilization wizard 172

Figure 4.8: Overlay of binding curves of 110 nM of itPA and variants binding to immobilized L-lysine 173

Figure 4.9: Interaction of scitPA (R275E), tcitPA and itPA with L-lysine 174

Figure 4.10: Interaction of fibrinogen, tPA and plasminogen with anti-fibrinogen antibody ab6666 177

Figure 4.11: Interaction of fibrinogen (fgn) with anti-fibrinogen β chain (C-20) antibody 179

Figure 4.12: Interaction of tPA (Actilyse) with Sigma (green line) and Calbiochem (pink line) fibrinogens captured on antifibrinogen β chain (C-20) antibody 180

Figure 4.13: Interaction of tPA (Actilyse) with antifibrinogen β chain (C-20) antibody 181

Figure 4.14: Interaction of scitPA (R275E), tcitPA and itPA with fibrinogen 183

Figure 4.15: Global analysis of scitPA (R275E) and tcitPA binding to fibrinogen using a two-step binding model 187

Figure 4.16: Binding constants for scitPA (R275E) interacting with immobilized fibrinogen using a two-step binding model 188

Figure 4.17: Global analysis of scitPA (R275E) and tcitPA binding to fibrinogen using a heterogeneous ligand binding model 189

Figure 4.18: Treatment of immobilized fibrinogen with bovine thrombin 190

Figure 4.19: Global analysis of scitPA (R275E) and tcitPA binding to fibrin* using a two-step binding model 191

Figure 4.20: Global analysis of scitPA (R275E) and tcitPA binding to fibrin* using a heterogeneous binding model 192

Figure 4.21: Interaction of itPA and variants with fibrinogen 196

Figure 4.22: Global analysis of itPA and variants binding to fibrinogen using a heterogeneous binding model 199

Figure 4.23: Single site saturation curve of lys-plasminogen binding to fibrinogen 202

Figure 4.24: Interaction of itPA and variants with heparin 205

Figure 4.25: Interaction of itPA and variants with heparin 206

Figure 4.26: Interaction of glu-plasminogen with heparin 207

Figure 4.27: Absorbance as a measure of tPA precipitation over 5 concentrations in a range of buffers 210

Figure 4.28: TES, Tris, HEPES and HBS-E buffers containing a range of different surfactants to monitor solubility of tPA at 4, 0.8 and 0.4μM 211

Figure 5.1: Kinetic model used to describe plasminogen activation by tPA stimulated by binding to soluble templates 214

Figure 5.2: Plot of raw data from the simulation in Gepasi 217

Figure 5.3: Simulation and kinetic data of plasminogen activation by scitPA (R275E) and tcitPA 222

Figure 5.4: Simulation and kinetic data of plasminogen activation by itPA, itPA: F del and itPA: K1K1stimulated by fibrinogen 225

Figure 5.5: Simulation and kinetic data of plasminogen activation by 4 concentrations of itPA 226

Figure 5.6: Simulation of itPA and kinetic data of itPA, itPA: F del and itPA: K1K1stimulated by heparin to activate plasminogen in buffer D and buffer B 230

List of tables

Table 2.1: Description of the plasmids that were used to generate the proteins 57

Table 2.2: Sequences of primers used in this research 63

Table 2.3: Domain structure and physical properties of commercial and insect expressed tPA variants 77

Table 3.1 KM, Vmax, kcat and kcat/KM values for variant proteins in a S2288 assay 109

Table 3.2: Apparent KM, Vmax, kcat and kcat/KM values for variant proteins in the clear clot lysis overlay assay 137

Table 4.1: The rate equations for binding models used in this study 156

Table 4.2: IC50 values (μM) for 6-aminohexanoic acid on binding of itPA and variants to immobilized fibrinogen 161

Table 4.3: IC50 values (μM) for 6-aminohexanoic acid on binding of itPA and variants to immobilized fibrinogen and fibrin* (thrombin treated immobilized fibrinogen – fibrin-like surface) 161

Table 4.4: Binding constants for scitPA (R275E) and tcitPA binding to fibrinogen and fibrin* generated by fitting to the two-step binding model 193

Table 4.5: Binding constants for scitPA (R275E) and tcitPA binding to fibrinogen and fibrin* generated by fitting to the heterogeneous binding model 194

Table 4.6: Binding constants for itPA, itPA: F del, itPA: K1K1 and irPA binding to fibrinogen generated by fitting to the heterogeneous binding model 200

Table 5.1: The names, reactions and reaction types inputted into the model in Gepasi 218

Table 5.2: The metabolites included in the model and the initial concentrations assigned to the metabolites 219

Table 5.3: The kinetic rate constants for each of the reactions used to model plasminogen activation by scitPA (R275E) and tcitPA with fibrinogen as a template 221

Table 5.4: The kinetic rate constants for each of the reactions used to model plasminogen activation by itPA, itPA: F del and itPA: K1K1 with fibrinogen as a template 224

Table 5.5: The kinetic rate constants for each of the reactions used to model plasminogen activation by itPA in buffer B and buffer D, with heparin as a template 229

Table 6.1: Some of the newly developed thrombolytics with their improvements and shortfalls. 233

Table 6.2: Some of the tPA and variants expressed for studies into the properties of tPA and their source or expression system. 236

Abbreviations

AcMNPV	*Autographia californica* multiple nuclear polyhedrosis virus
AFG	tPA + Plasminogen + template
BEVS	Baculovirus Expression vector system
CHO	Chinese Hamster ovary cells
CI	Confidence intervals
CM3	Carboxymethylated dextran chip 3
CM5	Carboxymethylated dextran chip 5
CNBr	Cyanogen bromide
CPB	Carboxypeptidase B
CPU	Carboxypeptidase U
G domain	Growth factor domain
EDQM	European Directorate for the Quality of Medicines & HealthCare
EGFP	Enhanced green fluorescent protein
endo-H	endo-β-N-acetyl-D-glucosaminidase H
ETI	Erythrina trypsin inhibitor
F domain	Finger domain
FDP	Fibrin degradation products
FRET	Fluorescence Resonance Energy Transfer
GF	Growth Factor like domain
GFP	Green Fluorescent protein
HAS	Human Serum Albumin
HBS-EP	HEPES buffered saline with EDTA and P20
IC_{50}	half maximal (50%) inhibitory concentration

IEX	Ion exchange chromatography
IFC	Integrated Flow cartridge
IFU	integrated microfluidic cartridge
irPA	Insect Reteplase tissue plasminogen activator
itPA K1K1	Insect tissue plasminogen activator kringle 1 kringle 1
itPA-P	Insect tissue plasminogen activator protease domain only
IU	International Units
K1	Kringle 1 domain
K1P	Kringle 1 protease
K2	Kringle 2 domain
K2P	Kringle 2 protease
K3	Kringle 3 domain
K4	Kringle 4 domain
K5	Kringle 5 domain
K_A	Association constant ($1/K_d$)
K_A	Constants for the binding of activator
k_{cat}	Catalytic constant
K_d	Dissociation constant
kDa	Kilodalton
K_G	Constants for the binding of plasminogen
K_M	Michaelis constant
LB	Luria-Bertani broth
M	Molar concentration
MCAC	Metal chelate affinity chromatography
MOI	Multiplicity of infection
n-tPA	Lanoteplase

OD	Optical Density
P	Protease domain
PA	Plasminogen Activator
PAI-1	Plasminogen activator inhibitor-1
PCR	Polymerase chain reaction
Pgn-ECFP	Plasminogen enhanced cyan fluorescent protein
pNA	*p*-nitroaniline
RFU	Relative fluorescents units
R_{max}	theoretical maximum response
rPA	Reteplase
RT-PCR	Real Time-Polymerase Chain Reaction
RU	Resonance Units
scitPA (R275E)	Single chain insect tissue plasminogen activator – non cleavable variant
SDS-PAGE	Sodium dodecyl sulfate polyacrylamide gel electrophoresis
sf9	Spodoptera frugiperda 9 cells
SPR	Surface Plasmon Resonance
TAFI	Thrombin-activatable fibrinolysis inhibitor
tcitPA	Two chain insect tissue plasminogen activator
TNK-tPA	Tenecteplase
tPA	Tissue Plasminogen Activator
uPA	Urokinase plasminogen activator
V	Velocity
V_{max}	Maximum velocity

Statement of originality

Word count: 58,191

The work presented in this thesis is my own unless stated using appropriate references.

CHAPTER 1: INTRODUCTION

1.1. Fibrinolysis

Fibrinolysis is the process whereby a fibrin clot, the product of blood coagulation, is broken down by the serine protease plasmin. A fibrin clot is made up of a collection of cells, proteins, phospholipids and other components, held together by the insoluble structural protein fibrin. During fibrinolysis, fibrin is cleaved by plasmin which is the active form of the zymogen plasminogen (Collen, 1999).

Plasminogen, a circulating plasma protein which binds to fibrin is incorporated into the clot as it is formed (Lucas et al, 1983). Plasminogen contains secondary structure motifs called kringles which bind specifically to lysine and arginine residues in fibrin (Robbins et al, 1967). The plasminogen molecule consists of a 77 amino acid pre-activation peptide, five kringle domains and a protease domain. Full length plasminogen is 791 amino acids and is called glu-plasminogen because the N-terminal amino acid is glutamate. The pre-activation peptide is cleaved by plasmin giving rise to a slightly shorter plasminogen molecule called Lys-plasminogen, so named because it has a lysine as the N terminal residue (Lucas et al, 1983).

Plasminogen activators, such as tissue plasminogen activator (tPA) also bind to fibrin and convert plasminogen to active plasmin. Plasmin initially creates nicks in the fibrin generating C-terminal lysines which provide additional plasminogen (Christensen, 1985; Fleury and Angles-Cano, 1991) and tPA (de Vries et al, 1990) binding sites.

As shown in figure 1.1, fibrinolysis can be seen as a two-step process, (I) the activation of plasminogen to plasmin by a plasminogen activator and (II) is the degradation of the structural protein, fibrin, to fibrin degradation products (FDP).

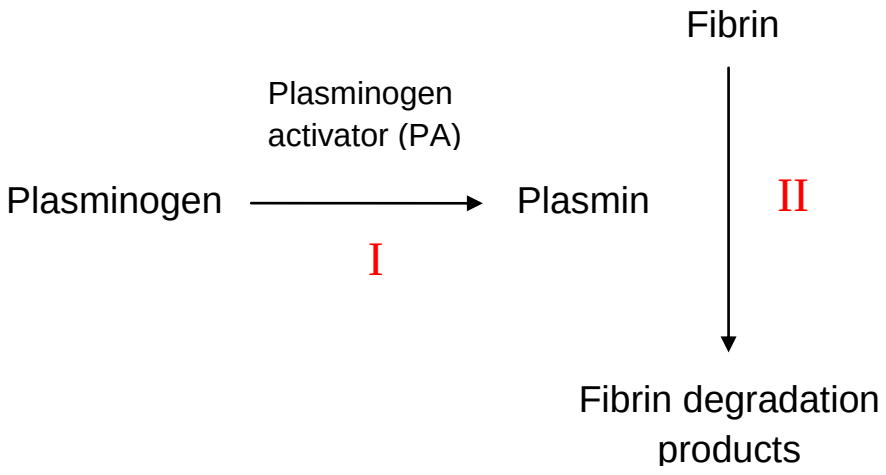


Figure 1.1: Scheme of fibrinolysis.

Plasminogen activator converts plasminogen into plasmin, which then breaks down fibrin into fibrin degradation products. Taken from (Longstaff and Thelwell, 2005; Thelwell and Longstaff, 2007)

However, fibrin is not only a substrate but is also a template and regulator of fibrinolysis. tPA and plasminogen binding to fibrin is critical for the regulation of plasminogen activation. tPA has a low affinity (K_M) for plasminogen in solution, but when they are both bound to fibrin, they are brought together which facilitates plasmin generation. This also means that plasminogen activation is confined to the fibrin clot surface hence, it is clot specific and plasminogen is not activated throughout the body (systemic activation) (de Vries et al, 1990; Lijnen and Collen, 1995).

tPA is a serine protease that is expressed as an active single chain (sctPA) protein but can be converted to a two chain (tctPA) form (held together by disulphide bonds) through cleavage by plasmin between amino acids Arg 275 and Ile 276 (Wallen et al, 1982). In solution tctPA is more active than sctPA (Boose et al, 1989), but in the presence of fibrin(ogen) the differences in activity disappear (Thelwell and Longstaff, 2007).

There are a number of inhibitors of fibrinolysis that regulate activity at different levels of the system. α_2-Antiplasmin (α_2-AP) is an inhibitor of plasmin that is found circulating in the blood at about 1 µM, which is similar to the concentration of plasminogen found in the circulation. Plasminogen activator inhibitor-1 (PAI-1) inhibits the plasminogen activators tPA and urokinase plasminogen activator (uPA) and is found circulating in the blood at a concentration in the same range as tPA (0.1 nM). Another regulator of fibrinolysis is thrombin-activatable fibrinolysis inhibitor (TAFI, also known as carboxypeptidase U, CPU) which down regulates plasminogen activation by cleaving C-terminal lysines in fibrin thus reducing the number of binding sites for plasminogen and tPA. Carboxypeptidase B (CPB) from pancreas may be used as an alternative to TAFI for in vitro studies because it has the same mechanism of action but CPB is more stable than TAFI.

1.2. Myocardial infarction and the history of thrombolytics

Cardiovascular disease is responsible for 17 million deaths per year worldwide and is also the cause of significant morbidity (WHO, 2007). Myocardial infarction (MI) and ischemic stroke (IS) are the two main causes of death and disability in the world. MI and IS are caused by disruption of atheromatous plaques in arteries, which are made up of lipid droplets, matrix constituents, foam cells and necrotic cell debris and form over a number of years. Rupture leads to exposure of collagen to the blood stream, which initiates the coagulation cascade, leading to platelet activation, production of thrombin and formation of occluding arterial thrombus which can cut off the blood supply and lead to tissue death (Davies and Thomas, 1985; Falk, 1991).

Some progress has been made in treating acute MI with thrombolytics ("clot busters"), which are plasminogen activators. However, despite many years of study and huge investment from the pharmaceutical industry, clinical trials of new drugs have often been disappointing (Verstraete, 2000). Furthermore, there has been little progress in treatment for IS. The first generation of thrombolytics (e.g. streptokinase and urokinase) were systemic activators of plasminogen giving rise to large scale plasmin production in the circulation and concomitant loss of circulating plasminogen, fibrinogen, and inhibitors. Second generation thrombolytics, such as recombinant tPA, had fibrin binding domains and were designed with the seemingly rational aim of targeting the activator to a fibrin clot, with the hope that bleeding complications would be reduced. However, all available thrombolytic agents still suffered significant failings, including the need for a large therapeutic dose, short plasma half-life, limited fibrin-specificity and bleeding complications (Collen and Lijnen, 1991). Following on from tPA, in efforts to improve on these shortcomings, the so-called third generation of thrombolytics were engineered which were anticipated to have improved properties (Collen and Lijnen, 1995). These newly cloned and investigated plasminogen activators include

mutants with domain deletions, such as Reteplase and Pamiteplase as well as plasminogen activators from other sources such as Desmoteplase cloned from vampire bat.

1.3. Domains of plasminogen and tPA involved in binding to fibrin and fibrinogen

tPA binding to fibrin is an essential step in the process of plasminogen activation and fibrinolysis and a number of studies have been carried out to elucidate the domains of the tPA molecule that are responsible for binding to fibrin.

The amino acid sequence of tPA was determined in 1983 by Pennica et al.(Pennica et al, 1983) tPA consists of 5 domains, Finger (F), Growth Factor (G), Kringle 1 (K1), Kringle 2 (K2) and Protease (P) (Pennica et al, 1983; Stryer, 1978; van Zonneveld et al, 1986b; van Zonneveld et al, 1986a), where the five domains were found to be homologous with other proteins. One region, the F domain was found to share a high degree of homology with the fingers of fibronectin that are responsible for fibrin binding. Banyai et al hypothesized that the finger domain was the domain that was responsible for fibrin binding and showed that partial plasmin digestion of tPA removing a 10 kDa section of the N-terminus corresponding to the F and G domain led to the loss of fibrin affinity by the remaining 55 kDa section of the enzyme (Banyai et al, 1983). However in 1985 another group designed a domain deletion mutant which had no finger domain but still showed affinity for fibrin (Kagitani et al, 1985) suggesting that the finger domain was not essential for fibrin binding. To further elucidate the domains involved, several groups designed domain deletion/shuffled variants of tPA. Van Zonneveld et al found that the K2 domain and, to a lesser extent, the finger region mediates binding to fibrin whereas the K1 and GF domains do not (van Zonneveld et al, 1986b; van Zonneveld et al, 1986a).

Plasminogen K1 and K4 domains are thought to bind to fibrin through lysine binding sites (Trexler and Patthy, 1983; Vali and Patthy, 1984). These lysine binding sites bind to lysines

that carry a free carboxylate group and these COOH terminal lysines, as well as internal lysines, are the likely ligands on fibrin (Christensen, 1985). Plasminogen K4 domain has 3 residues that are involved in lysine binding, Asp57, Arg74 and Trp72 (Hochschwender and Laursen, 1981; Trexler et al, 1982) and a similar arrangement is seen in the plasminogen K1 domain. tPA K2 domain has identical residues at similar positions, Asp57, Arg70 and Trp73 (van Zonneveld et al, 1986a)

Verheijen et al found that at low concentrations of fibrin and in the absence of plasminogen, the finger domain was responsible for binding, whereas when there were high concentrations of fibrin or in the presence of plasminogen the K2 domain was also involved in binding, which might be explained by the generation of C-terminal lysines under these conditions (Verheijen et al, 1986). The different states of fibrin could be the reason for the differing results seen in the studies by Banyai (Banyai et al, 1983) and the studies by Kagitani (Kagitani et al, 1985) and van Zonneveld (van Zonneveld et al, 1986a). Thus the reason why the 55 kDa protein in the study by Banyai et al did not have fibrin affinity is because the fibrin could have been intact with no C-terminal lysines.

1.4. Fibrin and Fibrinogen

1.4.1. The structure of fibrin and fibrinogen

Fibrinogen is a soluble dimer consisting of two identical subunits formed by three non-identical polypeptide chains Aα, Bβ and γ (McKee et al, 1966) (see figure 1.2). The polypeptide chains are linked together to form a number of independently folded domains, the central E domain, two terminal D regions and the αC domains. The E and D domains are compact and ordered structures of the fibrinogen molecule as determined by electron microscopy, calorimetric studies and SDS-PAGE (Medved et al, 1997; Privalov and Medved', 1982). The E region contains the short NH_2-terminal fibrinopeptides A and B, which are removed by thrombin to convert fibrinogen into fibrin. The middle portion of each coiled coil connector that connects the D regions to the E region contains structures that are easily cleaved by plasmin (Brown et al, 2000; Yang et al, 2001).

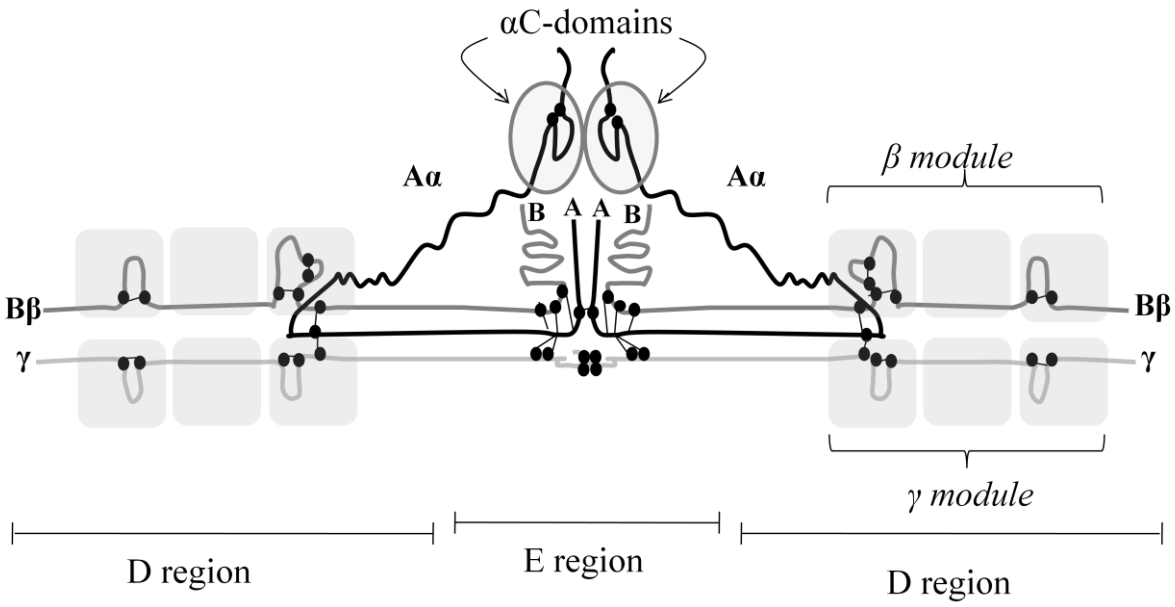


Figure 1.2: Structure of the fibrinogen molecule.

Fibrinogen molecule consisting of the central E domain, two terminal D regions and the αC domains formed by three non identical polypeptide chains Aα, Bβ and γ. The E region is formed by the NH_2-terminal portions of all six chains which are held together by disulphide bonds forming a "disulphide ring". Each terminal D region is formed by the COOH-terminal portions of the Bβ and γ chains (which make up the β and γ modules) and a portion of the Aα chain. The αC domains are each made up of the COOH portion of the Aα chains (Weisel et al, 1985; Weisel and Medved, 2001). The D region is connected to the central E region by a helical coiled coil connector made up of all three chains. Reproduced from (Medved and Nieuwenhuizen, 2003)

1.4.2. Conversion of fibrinogen to fibrin by thrombin

Thrombin converts fibrinogen to fibrin through limited proteolytic cleavage of Aα Arg17Gly and Bβ Arg15Gly, releasing two molecules, fibrinopeptides A and B, respectively. This releases the so called Knobs "A" and "B" on the E region of the fibrinogen molecule which fit into complementary holes "a" and "b" in the γ and β modules respectively of the D region of other fibrinogen molecules (Folk et al, 1959; Litvinov et al, 2007; Lorand, 1952; Yang et al, 2000).

Fibrinopeptide A is removed first, which leads to polymerization of fibrin monomers to form two stranded protofibrils in which A – a interactions cause arrangement of the molecules in a staggered overlap. Fibrinopeptide B is then removed which promotes lateral association through B-b interactions (Litvinov et al, 2007; Yang et al, 2000)

During fibrin assembly the two αC domains dissociate from each other and the central E domain, and re-associate with αC domains of other fibrin molecules (see figure 1.3) (Gorkun et al, 1994; Litvinov et al, 2007; Medved' et al, 1985; Weisel and Medved, 2001).

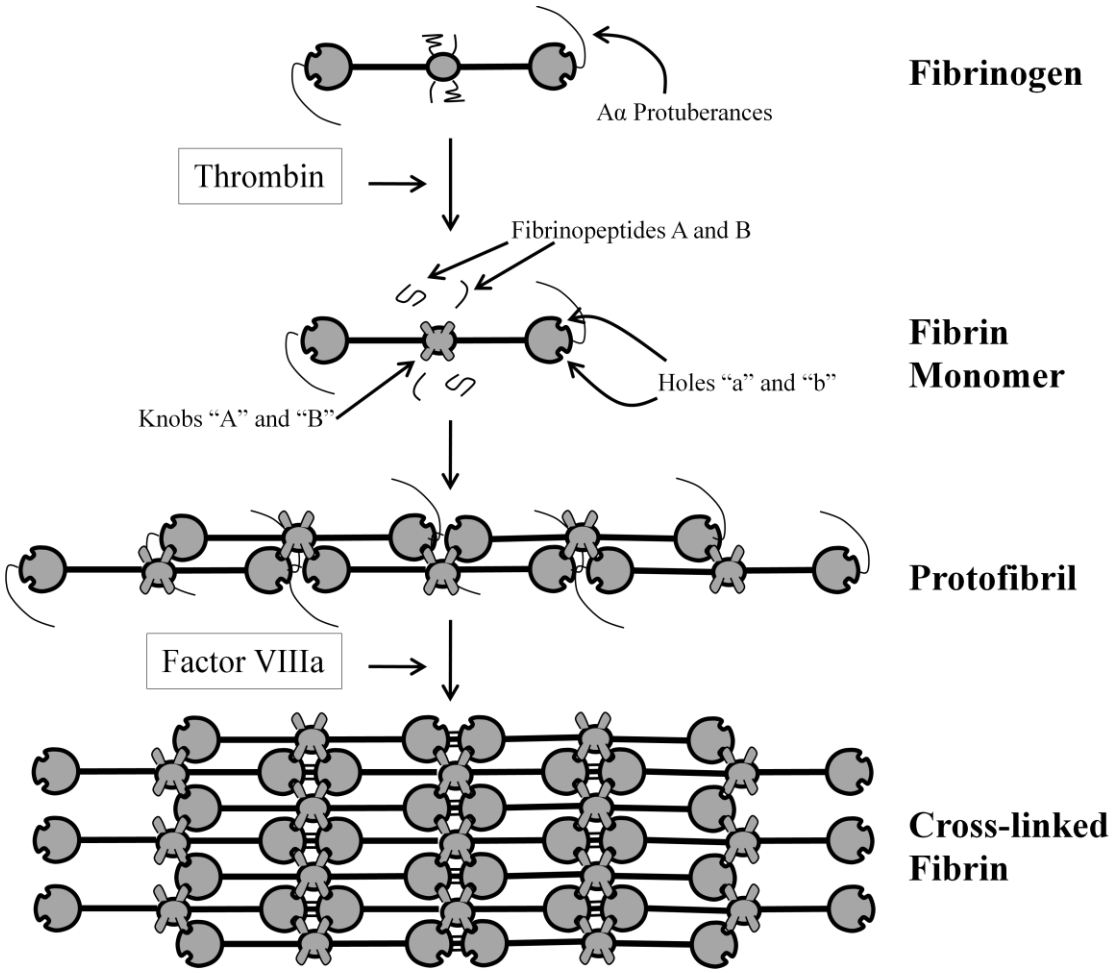


Figure 1.3: Formation of fibrin from fibrinogen.

Thrombin cleaves fibrinopeptides A and B leaving knobs "A" and "B" on the central E region that fit into holes "a" and "b" respectively on the distal D regions of other fibrinogen monomers to form the protofibril. Further cross linking of the protofibrils by Factor VIIIa forms fibrin. Adapted from (Fuss et al, 2001)

1.4.3. Digestion of fibrin by plasmin

Plasmin degradation of fibrin is thought to start by cleavage of the αC domains followed by multiple cleavages between the D and E regions, generating a number of degradation products (Francis et al, 1980; Pizzo et al, 1972). Initially plasmin degradation generates COOH-terminal lysine residues increasing plasminogen and tPA binding (Weinstein and Doolittle, 1972). Larger FDP products have been shown to bind tPA and plasminogen, but further degradation abolishes further binding to fibrin (Tsurupa and Medved, 2001b; Yakovlev et al, 2000). This may serve as a negative feedback mechanism and/or to prevent systemic plasminogen activation stimulated by these degradation products acting as templates for plasminogen and tPA binding while they are in the circulation.

A number of studies have shown that fibrin but not fibrinogen stimulates plasminogen activation by tPA (Nieuwenhuizen, 2001), therefore it was hypothesized that the tPA and plasminogen binding sites are buried in fibrinogen but exposed by conformational changes when fibrinogen is converted to fibrin (Medved et al, 2001; Nieuwenhuizen et al, 1983a). However fibrinogen has been shown to be a weak stimulator of tPA catalysed plasminogen activation by a number of groups (Bringmann et al, 1995; Lucas et al, 1983; Thelwell and Longstaff, 2007).

1.4.4. tPA and plasminogen binding sites in fibrin and fibrinogen

To determine the binding sites on fibrinogen for tPA and plasminogen a number of studies on the ability of plasmin or cyanogen bromide digested fibrinogen fragments to stimulate plasminogen activation by tPA have been performed. The smallest rate enhancing fragments were D_{EGTA} produced from plasmin digestion (Verheijen et al, 1982) and from CNBr digestion producing two fragments called CNBr-cleavage fragment 2 (Gardlund et al, 1977;

Nieuwenhuizen et al, 1983b) and CNBr-cleavage fragment 5 (Yonekawa et al, 1992). D_{EGTA} comprises Aα-111-197 and CNBr-cleavage fragment 2 Aα148-207 and so it was concluded that the common stretch of Aα148-197 contained the rate enhancing section (Nieuwenhuizen et al, 1983a; Nieuwenhuizen et al, 1983b). Further studies narrowed down the rate enhancing section to Aα148-160 with lysine Aα-157 being particularly important (Voskuilen et al, 1987). Antibodies raised to a synthetic peptide of this region bound to fibrin but not fibrinogen, indicating that this region is exposed on conversion to fibrin (Schielen et al, 1989). Binding to this site was found to be lysine dependent indicating binding to this region occurs through the kringle domains, (Bosma et al, 1988) although other studies have found that the binding of tPA to this site is lysine independent (Grailhe et al, 1994).

Another binding region was found near the C-terminus of the γ chain in CNBr-cleavage fragment 5, and it is made up of two γ chain remnants γ311-336 and γ337-379 connected by a single disulphide bond between the cysteines γ-326 and γ-339. The rate enhancing effect of this region is abolished if the remnants are broken down further. tPA but not plasminogen (Yonekawa et al, 1992) binds to this site and is through lysine-independent binding (F domain) (Grailhe et al, 1994). Using a monoclonal antibody it was found that this region is exposed in fibrin but not fibrinogen (Schielen et al, 1991). A region in the αC domain, Aα392-610, has also been found to bind both tPA and plasminogen to individual sites in a lysine- independent manner (Tsurupa and Medved, 2001b). Also sections that bind tPA and plasminogen have been found in the E domain that bind lys-plasminogen (Bosma et al, 1988; Varadi and Patthy, 1983), although the exact position of this site has yet to be fully characterized.

It is believed that conformational changes occur when fibrinogen is converted to fibrin that allows these sites to become exposed. The binding sites in the D domain (Aα148-160 and γ312-324) are thought to become available when the fibrinopeptides are removed and the

knob “A” and hole “a” interaction occurs (Yakovlev et al, 2000). The binding sites in the αC domain (Aα392-610) are thought to become exposed when the interactions of the COOH terminal Aα chains change from intramolecular to intermolecular (Tsurupa and Medved, 2001a).

1.5. tPA and plasminogen binding to heparin

Heparin and heparin sulphate are two sulphated polysaccharides that together are known as heparinoids, they have been found to bind many proteins and are involved in many biological processes (Mulloy and Linhardt, 2001; Saito and Munakata, 2007; Zhang, 2010). Heparin (also known as unfractionated heparin) is a highly sulphated glycosaminoglycan that is used clinically as an anticoagulant, it is made up of a mixture of varying sized repeating disaccharide units containing either D-glucuronic acid or L-iduronic acid and D-glucosamine, which is either N-sulphated or N-acetylated, the disaccharides may be further O-sulfated (Gandhi and Mancera, 2008; Jacobsson et al, 1979). Heparan is an intracellular product found mainly on mast cell granules or on the mucosa. Heparan sulphate has a similar structure to heparin but it is not as sulfated as heparin, it is found on the surface of many cell types and in the extracellular matrix. The fact that heparan sulphate is found much more widely spread throughout the body and is more accessible (i.e on the surface of cells) indicates that heparan-sulphate is the main physiological binding ligand of the heparin-binding proteins (Nader et al, 1999). However because heparan sulphate is produced by so many different types of tissues in the body preparations have found to have varying activities and so for most studies and for commercial use heparin is used as a model (Mulloy and Forster, 2000). Although more and more clinical applications are in varying stages of development (Mousa, 2010) the main use for heparin is still as an anticoagulant. Heparin acts as an anti-coagulant by binding to antithrombin causing a conformational change

allowing the antithrombin to bind more rapidly to thrombin to form a complex that prevents the action of thrombin and therefore inhibits blood coagulation (Bjork and Nordenman, 1976; Rosenberg and Lam, 1979). The anti-coagulant properties are utilized by using heparin in the treatment of venous thromboembolism (Dolovich et al, 2000), pulmonary embolism (Quinlan et al, 2004), unstable angina (Gurfinkel et al, 1995; Theroux et al, 1988), in the treatment of MI alongside thrombolytics (Boland et al, 2003; Genentech Inc, 2005; Mickelson et al, 1988; NICE, 2010) and is also used to prevent coagulation in a number of other circumstances (Hirsh et al, 2001). Heparin is administered alongside thrombolytics to prevent reocclusion of the coronary artery during and after clot dissolution (Cercek et al, 1986) and although heparin has been found to help prevent reocclusion it has also been found to have the undesired effect of increasing bleeding events (Chesebro et al, 1987; Rao et al, 1988; Williams et al, 1986). The increased incidence of bleeding events is likely to be caused by the reduction the ability to form haemostatic plugs due to the inhibition of thrombin however another contributing mechanism was suggested by Andrade-Gordon and Strickland (Andrade-Gordon and Strickland, 1986). They showed that heparin interacted with tPA and plasminogen and stimulated plasminogen activation by tPA at therapeutic concentrations and suggested that if heparin activated plasminogen in vitro then this may result in the degradation of circulating clotting factors leading to bleeding events (Andrade-Gordon and Strickland, 1986). The interaction of heparin with tPA and plasminogen and whether this interaction is likely to be significant in vitro has been the focus of many studies. Using tPA-Sepharose columns it was found that heparin could be separated into high affinity and low affinity fraction, where only the high affinity fraction stimulated tPA activity, the high affinity fraction was also found to be of higher molecular weight (Andrade-Gordon and Strickland, 1990), however others (Edelberg et al, 1991) found that tPA could bind fragments as small as disaccharides but these smaller heparin fragments were not large enough to bind

both tPA and plasminogen and that it was the larger oligosaccharides that bound both tPA and plasminogen. It has also been shown that heparin is more efficient than heparan sulphate at stimulating plasminogen activation by tPA (Edelberg and Pizzo, 1990; Young et al, 1992). The most in depth study into the domains of tPA that interact with heparin was performed by Stein et al, 1989 who used domain variants of tPA to show that the domains of tPA that bind to heparin are the F domain and to a lesser extent the K2 domain, not the K1 or protease domains (Stein et al, 1989) most other studies have supported these findings; Edelberg and Pizzo found that their results indicated that binding to heparin was by the F domain (Edelberg and Pizzo, 1990), others have shown the K2 domain is also involved by using ε – aminocaproic acid (Liang et al, 2000; Pâques et al, 1986) and Reteplase (K2 and protease domains only) was shown to bind to heparin but to a lesser extent to full length tPA (Rijken and Jie, 1996). The actual sequences in these domains that confer binding to heparin have yet to be determined but the experiments with ε – aminocaproic acid (Liang et al, 2000; Pâques et al, 1986) indicate that binding is via lysine and the lack of additive stimulation of tPA activity observed in the presence of both heparin and fibrinogen indicate that binding to heparin is likely to be via the same domains as fibrinogen (Liang et al, 2000). The only available investigation into the domains of plasminogen that interact with heparin was done by Soeda et al who found that the K5 and the protease domains interacted with heparin (Soeda et al, 1987; Soeda et al, 1989), contrary to findings of others they also found that tPA interacted with heparin through the protease domain (Soeda et al, 1987). Other findings of note were that stimulation of glu-plasminogen was found to be more enhanced by a heparin analogue than lys-plasminogen (Takada et al, 1994) and sctPA was found to be stimulated to a higher extent than tctPA by a heparin analogue (Takada et al, 1994) and by heparin (Rijken et al, 1993). The most important finding in these studies in relation to whether the interaction between tPA, plasminogen and heparin is significant in *vivo* was that the interaction was

shown to be salt sensitive and heparin does not appear to stimulate plasminogen activation by tPA at physiological ionic strength (Rijken et al, 1993; Rijken and Jie, 1996; Young et al, 1992). tPA was found to be less salt sensitive than plasminogen (Rijken et al, 1993) and Reteplase was more sensitive to changes in ionic strength that tPA, indicating that the interaction of the K2 domain was more salt sensitive than the F domain (Rijken and Jie, 1996). The heparin stimulated plasminogen activation by tPA was shown to be altered by ionic strength, the presence of divalent cations and chloride ions (Young et al, 1992). The effect of heparin on efficiency of tPA in *vivo* has been investigated and it has shown that the presence of heparin did not affect thrombolytic activity of tPA but does show that heparin leads to more complete reperfusion (Agnelli et al, 1990; Topol et al, 1989; Weitz et al, 1991).

1.6. tPA glycosylation

Native sc-tPA is a glycoprotein with four potential glycosylation sites of which only two are always glycosylated, the third site is glycosylated on around 50% of proteins and the fourth site Asn 218 is never glycosylated (Pohl et al, 1987). Therefore tPA may be isolated as two types based on its glycosylation patterns. Type I has three sites glycosylated Asn-117, -184 and -448 and type II which is only glycosylated at sites Asn- 117 and -448, type I tPA is ~ 2-3 kDa heavier than type II. The reason for the partial glycosylation at position 184 is unknown.

The presence of carbohydrate as well as the different types of carbohydrate present is implicated in many properties of tPA. These include secretion (Dorner et al, 1987), solubility, enzymatic activity (Wittwer et al, 1989) and affinity for fibrin (Parekh et al, 1989). It has been shown that glycosylation increases the tPA specificity for fibrin compared to fibrinogen (Hansen et al, 1988). Clearance from the body is thought to be modulated by

oligosaccharide at position 117 (Hotchkiss et al, 1988). Different cell types produce different oligosaccharide structures, which show different fibrin activated catalytic activity (Wittwer et al, 1989).

Proteins expressed for this project have been produced in an insect cell expression system and therefore may be glycosylated differently from other commercially available proteins that are being used in this project that have been expressed in mammalian expression systems or *Escherichia. coli*. Sf9 (insect) cells and CHO (mammalian) cells both undergo the initial stage of N-glycosylation, which in mammalian cells is the co-translational addition of a high mannose oligosaccharide to the polypeptide chain (Jarvis and Summers, 1989), whereas proteins produced in bacteria have no glycosylation. It is thought that insect cells are incapable of processing the immature oligosaccharide into such a complex form as mammalian cells because glycoproteins derived from sf9 cells remain sensitive to endo-β-N-acetyl-D-glucosaminidase H (endo-H), an endo glycosidase capable of removing only high mannose oligosaccharides (Jarvis and Summers, 1989). Thus insect-cell expressed proteins only carry high-mannose-type and truncated trimannosyl N-glycans (sometimes with a fructose residue attached), which are not found on proteins expressed by mammalian cells and are not intermediate (Wagner et al, 1996). Jarvis and Summers (Jarvis and Summers, 1989) have found that some tPA expressed by sf9 cells remains partially resistant to endo-H and so some N-linked oligosaccharide processing may occur on our proteins (Jarvis and Summers, 1989).

1.7. Surface plasmon resonance – Biacore

The use of surface plasmon resonance in the detection of biomolecular interactions was developed in 1991 by Jönsson et al in 1991 using the BIAcore (Jönsson et al, 1991; Jonsson et al, 1993). It is a biosensor-based technology that can monitor molecular interactions in real time without having to label the components of the interaction. These interactions occur on the surface of a sensor chip which is made up of a thin layer of gold on a glass support. On the gold layer a flexible hydrophobic polymer is added that is used to covalently attach one component of the interaction (called the ligand). The ligand can either be immobilised directly onto the sensor surface or via a capture molecule. The other component of the interaction (the analyte) is passed over the sensor surface where it can interact with the immobilized ligand. The interaction of the ligand and the analyte is followed in real time by monitoring the mass concentration of biomolecules at the sensor surface. This mass concentration at the surface of the sensor chip is detected using SPR technology, which is an optical phenomenon arising in thin metal films under conditions of total internal refraction (Jönsson et al, 1991; Jonsson et al, 1993). The Biacore instrument has a liquid handling system with continuous flow technology which means that samples and buffer can be rapidly exchanged at the sensor chip surface. This liquid handling system has precision pumps and an integrated microfluidic cartridge (IFU) which contains sample loops, pneumatic valves and flow channels to provide accurate delivery of samples to the sensor chip surface. The IFU creates flow cells to provide minimal sample dispersion and efficient mass transport of biomolecules to the sensor chip surface. The IFC allows for single of multichannel analysis in up to four flow cells, additional flow cells can be used on line reference cells so that a blank can be subtracted from the data. The flow cells are created by pressing the flow channels against the surface of the sensor chip, therefore sensor chip surface forms one wall

of the flow cell and this is where the reaction occurs, the gold film is illuminated from the other side through the glass and the interaction of the light energy with the gold film is what generates the SPR (Biacore AB, 1998). Surface plasmons are surface electromagnetic waves that propagate in a direction parallel to the gold/dielectric interface. Since the wave is on the boundary of the gold and the buffer, the oscillations are very sensitive to any change on this boundary such as binding of analyte to ligand. The thin gold conductive film is at an interface between media of different refractive index (the glass and the buffer) and under conditions of total internal reflection (achieved by pressing the glass side of the chip against a semi-cylindrical glass prism) the light incident on the reflecting interface leaks an electric field intensity called an evanescent wave field across the interface into the medium of lower refractive index, without actually losing net energy. At a certain combination of angle of incidence and energy, the incident light excites plasmons in the gold film. This results in absorption of energy via the evanescent wave field and SPR is seen as a drop in the intensity of the reflected light. In the Biacore these plasmons are excited using a high efficiency near infrared light emitting diode. The beam of light is focused onto the sensor chip in a wedge shaped beam giving a fixed range of incident angles. The SPR response is monitored by a fixed array of light-sensitive diodes covering the whole wedge of reflected light (Biacore AB, 2003). The SPR angle detected depends on the refractive index (measure of the bending of a ray of light) of the medium and so changes in the concentration of the solutes changes the refractive index. Consequently, changes in the surface concentration of molecules (other factors being equal) can be monitored in real time. The signal detected from the resonance angle by the optical system is expressed in response units and the changes in response units are plotted against time and the resulting graph is called a sensorgram, it shows the different stages of the binding of a ligand to an analyte, as the ligand flows over the sensor chip surface, the interaction with the analyte is detected as a change in refractive index and

recorded on the sensorgram as an increase in RU. After the injection of analyte is stopped buffer flows over the surface of the sensor chip and the analyte dissociates from the ligand and the signal decreases, the sensor surface can be regenerated bringing the sensorgram baseline back to zero and another cycle can be performed. The sensor chip may be coated with the ligand of interest by directly immobilizing or using a capture molecule such as antibodies or streptavidin covalently attached to a matrix on the gold layer of the sensor chip using a number of different chemistries (Biacore AB, 1998).

1.7.1. The CM range of sensor chips

The CM series of sensor chips have a matrix of linear carboxymethylated dextran covalently attached to the gold layer on the surface of the sensor chip. The CM5 chip is the most commonly used general purpose chip in this range and can be used to covalently immobilize a wide range of proteins, carbohydrates and nucleic acids. The dextran on this chip is around 100 nm thick under physiological conditions. Other chips in the CM range are CM4, which has a lower degree of carboxymethylation than the CM5, resulting in reduced immobilization and the CM3 chip which has the same amount of carboxymethylation as the CM5 but the dextran is shorter. Dextran is a linear polymer of glucose units which exhibits low non-specific binding of biomolecules on the CM5 sensor chip the dextran is carboxymethylated to a level of ~ 1 carboxyl group per glucose residue. This puts a net negative charge on the dextran when it is at physiological pH (pH 7.0), this means that positively charged biomolecules (biomolecules have a positive charge when they are at a pH lower than their isoelectric point (pI)) are attracted electrostatically to the dextran, this allows the biomolecules to be concentrated at the surface of the chip so that efficient immobilization can occur. Biomolecules are attached to the dextran using a number of chemical methods that

utilize functional groups on the ligand such as amine groups, thiol groups or aldehyde groups (Biacore AB, 1998; Biacore AB, 2003). The dextran behaves like a homogeneous layer that creates a hydrophilic environment around the immobilized molecules, it is flexible and so movement of ligand can occur and allows the ligand to accessed easily reducing steric hindrance that would be caused by immobilizing the molecule to a flat surface (Biacore AB, 1998; Johnsson et al, 1991).

1.7.2.The SA sensor chip

The SA sensor chip has streptavidin covalently attached to the dextran matrix. Streptavidin is a bacterial protein homologous to avidin a protein normally purified from chicken egg. Both streptavidin and avidin bind to biotin a B vitamin found in a large number of human cells. The interaction between streptavidin and biotin has the strongest, non covalent biological interaction known, with a dissociation constant (K_d) of ~ 4 x 10^{-14} M (Green, 1990). The bond forms rapidly and is extremely stable in a wide range of conditions (Holmberg et al, 2005; Tong and Smith, 1992). These properties mean that biotin can be introduced into biomolecules of interest (the ligand), this biotinylated ligand is then passed over the streptavidin coated surface of the chip and the biotin binds to the streptavidin resulting in the stable immobilization of the ligand. This method of immobilisation is used for ligands that are difficult to immobilize covalently (Biacore AB, 2003).

1.8. Project aims

To investigate the regulation of fibrinolysis by tissue plasminogen activator and elucidate the roles and relative importance of the structural domains, domain variants of tPA have been designed and expressed in an insect cell system. They have been tested alongside wild type tPA and domain variants that have already been released onto the market as thrombolytic drugs, such as Alteplase and Reteplase. Normal tPA (see figure 1.4) (pharmacopoeial name Alteplase, commercial name Activase in U.S, Actilyse in Europe; see figure 1.4) is produced by recombinant DNA technology and expressed in Chinese hamster ovary (CHO) cells by Genentech (San Francisco, USA). Reteplase (rPA) is a therapeutic product that has been developed by Boehringer Mannheim, produced in *E. coli* and is not glycosylated. It was designed to have a longer half-life (Kohnert et al, 1992) and it also been suggested that it has a lower affinity for fibrin to allow it to penetrate in to the clots and solubilise from the inside (Fischer and Kohnert, 1997). It is comprised of 357 of the 527 amino acids of the original protein: the P and K2 domains (figure 1.5).

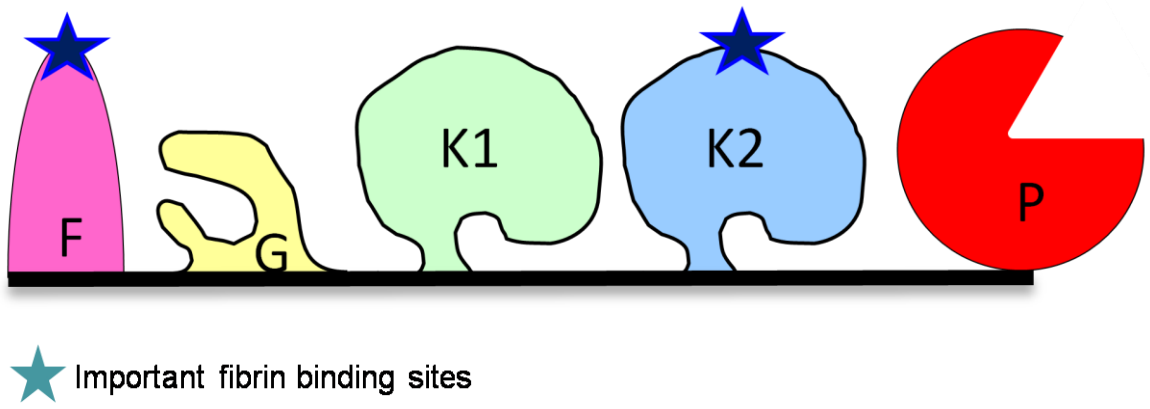


Figure1.4: Schematic diagram of normal tPA (Alteplase)

Containing the finger (F), growth factor (GF), kringle 1(K1), kringle 2 (K2) and protease (P) domains. Adapted from (Longstaff and Thelwell, 2005)

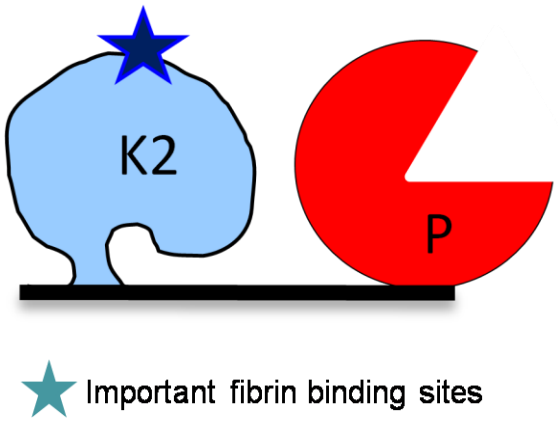


Figure 1.5: Schematic diagram of rPA (Reteplase)

Containing the, kringle 2 (K2) and protease (P) domains. Adapted from (Longstaff and Thelwell, 2005)

As discussed above, initial fibrin binding of tPA is thought to occur through the F domain. Plasmin is then generated from bound plasminogen, implying that some plasminogen binding at least does not require C-terminal lysines. Plasmin then cleaves fibrin exposing C-terminal lysines and increased binding can then occur through the K2 domain of tPA and K domains of plasminogen (Horrevoets et al, 1994; van Zonneveld et al, 1986a). Reteplase has no finger domain and was therefore expected have reduced initial binding, but as C-terminal lysines are generated will begin to bind, accelerating plasminogen activation.

In addition, recombinant forms of these therapeutics were expressed using insect host cells. The therapeutic proteins have been compared against the insect expressed versions to determine if the differences in glycosylation can affect the functional properties of tPA. The insect cell-expressed full length tPA and rPA have also been used as direct comparisons against other variants expressed for this project to assess how the different domains can affect the binding and activity of tPA. Other variants that were expressed for this project were: itPA: K1K1, a domain shuffled variant of tPA, which has a second K1 domain in place of the K2 domain (consisting of domains F-G-K1-K1-P) and was designed to try to keep the structure and folding of full length tPA without the K2 binding domain, so just looking at binding via the finger domain. itPA: K2 del is a domain deletion variant of tPA that has had the K2 domain removed (consisting of domains F-G-K1-P) and was designed to compare with itPA: K1K1 to determine if the resulting change in structure and folding from the deletion of a domain had an effect on the activity. irPA is an insect expressed version of therapeutic product Reteplase and is a truncated variant of tPA consisting of the K2 and protease domains only (K2-P). It was used to investigate binding via the K2 domain. itPA: F del is a domain deletion variant of tPA that has had the finger domain removed (consisting of domains G-K1-K2-P) and was also designed to investigate binding via the K2 domain and as a comparison against irPA to determine if the dramatic change in structure of irPA had an

effect on the functional properties. itPA: K1P is a truncated variant of tPA consisting of the K1 and protease domains (K1-P) of tPA and was designed to investigate any binding properties of the K1 domain and itPA-P consists of only the protease domain of tPA and was designed as a control and was not expected to have any binding properties. The variants itPA and itPA: F del were also expressed as Green fluorescent protein (GFP) fusion proteins with EGFP (enhanced GFP) fused to the C-terminus of the protein. scitPA is insect expressed tPA with a mutation in the cleavage site Arg275Glu preventing conversion into two-chain tPA and tcitPA is itPA that has been treated with plasmin-sepharose until the full length tPA had been completely converted into two-chain tPA.

The tPA and variants described above were used to investigate template binding using a number of different techniques to generate kinetic and binding data. The amidolytic activity of the different insect expressed tPA variants were compared in solution against chromogenic substrate S2288. This gave an idea of the intrinsic activity of the protease domains. No difference in the amidolytic activity of the variants meant that any changes in activity of the variants could be attributed to template binding. The kinetic activity of the insect expressed tPA variants was then investigated in the presence of different fibrin and fibrinogen templates: fibrin(ogen) with no C-terminal lysines and fibrin(ogen) with additional C-terminal lysines. As well as in the presence of heparin in buffers of different ionic strengths. Binding of tPA was then investigated using two methods: ELISA style plate binding assays to investigate binding to immobilized fibrinogen and fibrin measured using activity and fluorescence and SPR technology (Biacore) to look at the binding properties of the insect expressed tPA variants against immobilized lysine, fibrinogen, fibrin and heparin.

The results were then used to investigate the regulation of fibrinolysis by plasminogen activators and elucidate the roles and relative importance of the K2 and F structural domains. The kinetic and binding data collected was used to develop a computer model for optimized

properties of binding activity of plasminogen activator (PA) in a fibrin clot, as no rational model exists to understand the quantitative relationship between fibrin binding and plasminogen activation and hence fibrin lysis.

CHAPTER 2 -MOLECULAR BIOLOGY, RECOMBINANT PROTEIN EXPRESSION AND PURIFICATION

2.1. Introduction

2.1.1. Recombinant tPA

Therapeutic tPA (Actilyse) is produced recombinant in a mammalian CHO cell expression system. Mammalian expression systems produce proteins that are properly folded and assembled, and are capable of performing post-translational modifications such as glycosylation, phosphorylation and disulphide bridges. Expressed proteins are typically soluble and when secreted can be purified from the culture medium. Proper folding of full length tPA is thought to be important for tPA activity and for tPA binding to templates such as fibrin. Glycosylation of tPA has also been shown to influence secretion (Dorner et al, 1987), enzymatic activity (Wittwer et al, 1989), fibrin binding (Parekh et al, 1989) (Hansen et al, 1988) and solubility (Olden et al, 1985). Recombinant proteins from mammalian expression systems are typically more similar to the native human protein than those from other host systems such as bacteria, plants, and yeast. There are however potential drawbacks to mammalian cell expression systems; these include protein yields, which are often much lower than with prokaryotic expression systems, and nutrient requirements which are more complex and cell cultures are more difficult to grow on a large scale (Schmidt, 2004).

Complex recombinant proteins produced in prokaryotic cell expression systems, such as *E. coli*, are often insoluble and may accumulate in the cytoplasm as inclusion bodies. Proteins in inclusion bodies are mis-folded and therefore need to be solubilised and refolded, however it remains uncertain whether all the protein molecules refold correctly. Furthermore the *E.coli* expressed proteins are not glycosylated, and lack many post-translational

modifications. Advantages of expressing recombinant proteins in *E.coli* are the high yields, ease of maintenance and well characterised genetics (Baneyx, 1999).

The properties of different expression systems have been exploited to generate new tPA variants to modify and improve the function of tPA. Full length tPA was expressed in *E.coli*, (strain BM.06.021) in a non-glycosylated form with a view to prolonging half-life and reducing clearance rate for therapeutic use, (Martin et al, 1992) since one mechanism of tPA clearance by the liver appears to be dependent on the high mannose-type oligosaccharide on the kringle 1 domain binding to a mannose receptor on liver endothelial cells (Rijken et al, 1990). Therapeutic tPA variant Reteplase is also expressed in *E.coli* because glycosylation is not desired, and there is evidence that the clearance rate from the body is reduced (Kohnert et al, 1992; Martin et al, 1991).

Tenecteplase (TNK-tPA) a tPA variant with mutations: T103N, N117Q and KHRR(296-299)AAAA, is expressed in CHO cells like Actilyse. For TNK-tPA glycosylation is desirable as the extra glycosylation site on the K1 domain (as a result of mutation T103N) is proposed to decrease the clearance rate from the body (Keyt et al, 1994). Other variants of tPA expressed in CHO cells include Lanoteplase (n-tPA) a deletion variant lacking the F and G domains as well as a point mutation asparagine 117 to glutamine 117 (Smalling, 1997) and Pameteplase (YM866) a tPA variant lacking the K1 domain and containing a point mutation R275E (Kawasaki et al, 1993).

2.1.2. Production of tPA in insect cells

Protein expression in insect cells is a popular method for production of recombinant protein as it generally produces high yields of active protein. It is a more simple system compared to mammalian expression systems because insect cells do not require CO_2, and are grown in suspension so can be scaled up to larger culture volumes more readily. Insect cells perform

many of the post translational modifications of higher eukaryotes, offering an advantage over *E.coli* or other bacterial cell expression systems (Altmann et al, 1999; Jarvis et al, 1993) and insect cells can secrete completely folded, soluble protein into the supernatant (Altmann et al, 1999); however glycosylation is not as complex as that seen on mammalian expressed proteins (Jarvis and Summers, 1989; Jarvis and Finn, 1995) .

Several groups have expressed recombinant tPA (Farrell et al, 1999; Furlong et al, 1988; Jarvis et al, 1990; Jarvis and Summers, 1989; Steiner et al, 1988; Thelwell and Longstaff, 2007) and variants of tPA (Petri et al, 1995) in insect cells. The activity of tPA expressed by insect cells was compared to that produced by different expression systems, and was shown to have relative specific activity comparable to Bowes melanoma derived tPA (Furlong et al, 1988) and higher specific activity compared to tPA expressed in mouse C127 cells (Steiner et al, 1988) although activity in the presence of fibrinogen was observed to be 2-3 fold lower than Bowes melanoma tPA (Furlong et al, 1988). Insect tPA was found to have a lower molecular weight in comparison to mammalian tPA (Furlong et al, 1988; Steiner et al, 1988) which is thought to be due to differences in glycosylation by insect and mammalian expression systems (Furlong et al, 1988; Jarvis and Summers, 1989; Steiner et al, 1988). In all of these studies tPA was secreted in to cell culture media using the native tPA signal peptide, a further study revealed that replacing the native tPA signal peptide with insect-derived signal peptides did not increase secretion of tPA (Jarvis et al, 1993). Insect expression of tPA was performed either using baculovirus expression vector system (BEVS) (Furlong et al, 1988; Jarvis et al, 1990; Jarvis and Summers, 1989; Steiner et al, 1988; Thelwell and Longstaff, 2007) or by stable transformation (Farrell et al, 1999; Jarvis et al, 1990). BEVS uses a recombinant baculovirus in which the polyhedron open reading frame has been replaced by tPA coding sequence. Insect cell cultures can then be infected with the recombinant baculovirus to express tPA from the polyhedron promoter. For stable

transformation a recombinant plasmid encoding tPA is incorporated into the cellular genome under a constitutively active promoter so the cells continually express tPA (Harrison and Jarvis, 2007). It has been suggested that the infection of the cells with the baculovirus has an adverse effect on the host cells secretory pathway as more tPA was found to be secreted with continuous expression than through baculovirus expression, even though the total protein expressed (intracellular and extracellular) was higher using BEVS (Jarvis et al, 1990). Although stable cell lines produce higher protein yields, and do this continuously, the main advantage of using BEVS is that only a single culture is maintained which can be divided and infected with different recombinant baculovirus as required. This is particularly useful if many different proteins are to be expressed but not on an everyday basis. Baculovirus stocks can be stored at 4 ºC for several months or at -80 ºC for long periods of time without causing significant loss in tranducing titre (Tsai et al, 2007).

Recombinant baculovirus have traditionally been generated in insect cells by homologous recombination, but methods have been developed that have improved efficiency (Ma et al, 2006). One such method is the Bac- to-Bac baculovirus expression system (Invitrogen, California, USA) which was used to generate recombinant baculovirus for tPA expression by Thelwell and Longstaff, 2007 (Thelwell and Longstaff, 2007). The Bac-to-Bac (Invitrogen, California, USA) expression system allows for the generation of recombinant bacmid DNA in *E. coli*, rather than through multiple rounds of plaque purification in insect cells to isolate recombinant virus from non-recombinant virus. This process takes less than 2 weeks compared to 4-6 weeks with homologous recombination (Invitrogen Life Sciences, 2004). The general principles of the Bac-to-Bac expression system are described as follows. The donor plasmid pFastBac 1 (see figure 2.1.) is used to generate an expression construct where expression is controlled by the *Autographia californica* multiple nuclear polyhedrosis virus (AcMNPV) polyhedrin promoter, a baculovirus-specific promoter for high level expression

in insect cells. The expression cassette containing the gene of interest is flanked by left and right arms of the Tn7 transposon, and also contains the gentamicin resistance gene and an SV40 polyadenylation signal to form a mini Tn7. The pFastBac 1 plasmid is transformed into DH10Bac *E.coli*. DH10Bac cells contain a baculovirus shuttle vector (bacmid) with a mini-*att*Tn7 target site and a helper plasmid, pMON7124, which enocodes the transposase and confers the resistance to tetracycline. The gene of interest is incorporated into the viral genome by transposition between the mini-Tn7 element on the pFastBac vector and the mini-*att*Tn7 target site on the bacmid. The Tn7 transposition functions are provided by the helper plasmid. This results in the gene of interest becoming an integral part of the baculovirus DNA. The high molecular weight bacmid DNA can then be transfected into Sf9 insect cells to generate a recombinant baculovirus. High titre baculovirus stocks can then be amplified and used to infect insect cells to express the recombinant protein.

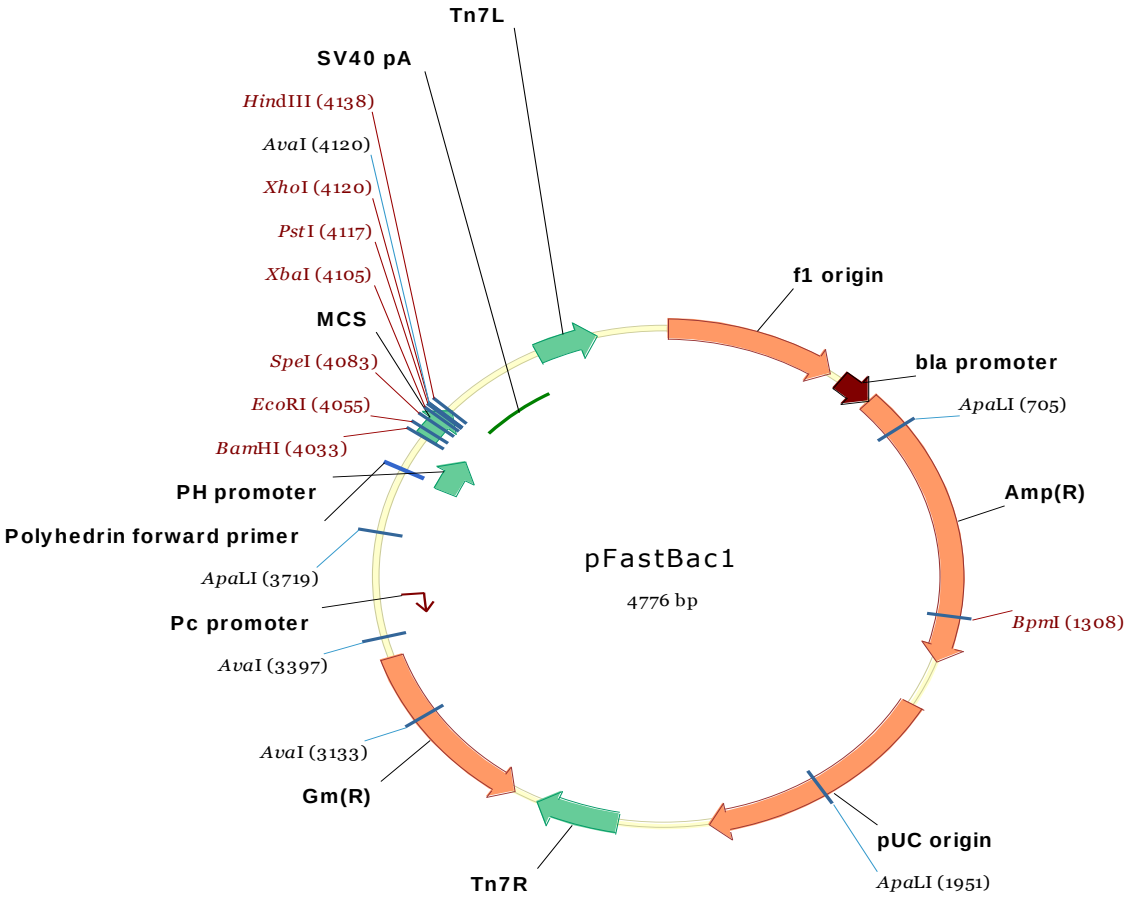


Figure 2.1. Expression vector pFastBac1. Vector map created in Vector NTI showing the f1 origin of replication, the bla prokaryotic promoter, the ampicillin (Amp) resistance gene, the pUC origin of replication, the right arm of the Tn7 transposon (Tn7R), the gentamicin (Gm) resistance gene, the eukaryotic Pc promoter, the polyhedron (PH) promoter, the multiple cloning site (MCS), the SV40 polyadenylation signal (pA)), the left arm of the Tn7 transposon and a number of restriction enzyme recognition sites.

A number of different methods have been used to purify tPA that has been expressed in insect cells and secreted into the culture media, including immunoprecipitation with anti-tPA antibodies (Jarvis and Summers, 1989), metal chelate affinity chromatography (MCAC) followed by immunoaffinity chromatography with a anti tPA mouse monoclonal antibody (Furlong et al, 1988) or by passing the cell supernatant through heparin-agarose column and then passing the eluted protein through a lysine-sepharose column which binds tPA via the K2 domain (Thelwell and Longstaff, 2007). Another alternative method for purification of tPA is using a Erythrina trypsin inhibitor-sepharose (ETI) column. ETI is a 20 kDa protein isolated from the seeds of the legume Erythrina latissima, that inhibits the amidolytic activity of trypsin and tPA. ETI has been shown to specifically recognise tPA and can distinguish between other serine proteases including urokinase (Heussen et al, 1984). The reaction between ETI and tPA is reversible so tPA can be eluted easily from the column still in its active form. ETI binds to the serine protease domain of tPA and so this method of purification can be used for structure/ function studies with tPA variants that have had domain modifications/ deletions. Binding via the serine protease domain gives an advantage over purification using lysine which requires a K2 domain to be present in the protein or using antibodies which may be specific for different parts of the protein. Affinity purification with ETI is also a simple one step method that does not require any preliminary steps (Heussen et al, 1984) unlike heparin/ lysine chromatography or MCAC/ immunoaffinity chromatography and is relatively fast compared to immunoprecipitation which requires an overnight incubation step (Jarvis and Summers, 1989) which could result in loss of activity.

2.2. Materials

2.2.1. Insect cell lines

Sf9 cells, originated from the IPLBSF-21 cell line, derived from the pupal ovarian tissue of the fall army worm *Spodoptera frugiperda* (Invitrogen, California, USA).

2.2.2. Escherichia coli strains

E. coli α-Select Competent Cells (*deo*R *end*A1 *rec*A1 *rel*A1 *gyr*A96 *hsd*R17($r_k^- m_k^+$) *sup*E44 *thi*-1 Δ(*lac*ZYA-*arg*FV169) Φ80δ*lac*ZΔM15 F-) (Bioline, Taunton, MA).

E. coli DH10Bac (F- *mcr*A Δ(*mrr-hsd*RMS-*mcr*BC) φ80*lacZ*ΔM15 Δ*lac*X74 *rec*A1 *end*A1 *ara*D139 Δ (*ara*, *leu*)7697 *gal*U *gal*K λ- *rps*L *nup*G /pMON14272 / pMON7124) (Invitrogen, California, USA,).

2.2.3. Plasmids

All plasmids used during this research are listed in Table 2.1:

Plasmid	**Source**	**Description**
pFastBac-1	Invitrogen	Transfer vector for generating recombinant baculovirus for recombinant protein expression in insect cells
pFastBac-itPA	(Thelwell and Longstaff, 2007)	A derivative of pFastBac-1 for expression of itPA
pFastBac-scitPA	(Thelwell and Longstaff, 2007)	A derivative of pFastBac-itPA for expression of scitPA (R275E)
pFastBac-itPA: K2 del	(Longstaff et al, 2011)	A derivative of pFastBac-itPA for expression of itPA: K2 del
pFastBac-itPA: K1K1	(Longstaff et al, 2011)	A derivative of pFastBac-itPA: K2 del for expression of itPA-K1K1
pFastBac-irPA	Section 2.3.3.1.	A derivative of pFastBac-itPA for expression of irPA
pFastBac-itPA-K1P	Section 2.3.3.2.	A derivative of pFastBac-itPA: K2 del for expression of itPA-K1P
pFastBac-itPA-P	Section 2.3.3.3.	A derivative of pFastBac-itPA: K2 del for expression of itPA-P
pFastBac-itPA: F-del	Section 2.3.3.4.	A derivative of pFastBac-itPA del for expression of itPA-F del
pFastBac-itPA-GFP	(Longstaff et al, 2011)	A derivative of pFastBac-itPA for expression of itPA-GFP
pFastBac-itPA: F-del-GFP	Section 2.3.3.5	A derivative of pFastBac-itPA-GFP for expression of itPA- F del -GFP

Table 2.1.: Description of the plasmids that were used to generate the proteins (see table 2.3.) used in this research

2.2.4. Chemicals, reagents and laboratory consumables

Sf-900 II serum free medium, Penicillin-streptomycin, Trypan Blue, Grace's Media, Fetal Bovine Serum, DMSO, SOC medium, blue juice loading buffer, 1 kb DNA standard, 100 bp DNA standard, CellFectin reagent, 4-12% NuPAGE Bis-Tris polyacrilamide gels, NuPAGE MES SDS Running Buffer NuPage sample reducing agent 10x, NuPage LDS sample buffer, SeeBlue Plus2 pre-stained molecular weight standard, SimplyBlue SafeStain Coomassie reagent, SYPRO ruby stain, Silver xpress kit, magic mark XP western protein standard, PVDF membrane, NuPAGE transfer buffer, western breeze chemiluminescent western blot immunodetection kit (Rabbit), anti-green fluorescent protein rabbit IgG fraction (A11122) were from Invitrogen, California, USA

Gentamicin was from Gibco, Paisley, UK

Erlenmeyer flasks were from Corning, NY

X-gal and IPTG were from Bioline, Taunton, MA

All restriction endonucleases and appropriate reaction buffers, *Pfu* DNA polymerase and Phusion PCR master mix were from New England Biolabs, Hitchin, UK

Ethidium bromide was from Promega, Wisconsin, USA

6-well, tissue-culture treated, polystyrene, flat bottom plates were from BD, Franklin Lakes, NJ

Erythrina trypsin inhibitor was purchased from Landing Biotech Inc, Newton, MA

0.2 µM filters were from Millipore

0.5-3 ml dialysis cassettes were from Pierce, Rockford, IL

All columns were supplied by GE Healthcare, Buckinghamshire, UK

96 well clear, flat bottom black plates were supplied by CoStar, Corning Life Sciences, Amsterdam, The Netherlands.

All other chemicals and reagents were supplied by Sigma-Aldrich, Pool, UK

2.2.5. Buffers

All standard buffers for DNA manipulations, purifications and other manipulations not provided by the manufacturer were prepared according to Sambrook et al (1989). Exceptions and additions are as follows:

(i) Column equilibration buffer contained 50 mM Tris/HCl pH 7.4

(ii) Protein elution buffer contained 0.1 M Sodium Acetate pH 4.0

(iii) Column wash buffer I contained 0.5 M Arginine + 1.0 M NaCl

(iv) Column wash buffer II contained 50 mM Tris/HCl pH 7.4 and 1.0 M NaCl.

(v) Coupling buffer: 0.1 M $NaHCO_3$ pH 8.0 + 0.5 M NaCl

2.3. Methods

2.3.1. Maintenance of E. *coli* cultures

E. coli cells were grown in Luria-Bertani (LB) medium (Sambrook et al., 1989) at 37 ºC with constant shaking, or on solid LB containing 1.5% (w/v) agar. Culture media was supplemented with antibiotics as required for plasmid selection (50 µg/ml kanamycin, 7 µg/ml gentamicin, 50 µg/ml ampicillin and 10 µg/ml tetracycline). For long term storage cultures were frozen at -80 ºC in 1 ml aliquots containing 15% (v/v) glycerol.

2.3.2. General methods for DNA manipulation

2.3.2.1. Transformation of competent α-select *E. coli* cells

The *α-select E. coli* strain was used for routine cloning experiments and competent *α-select* cells were transformed according to manufacturer's instructions. Briefly 2 µl of DNA was added to 50 µl of chemically competent α-select *E. coli* and incubated on ice for 30 min. The mixture was heat shocked at 42 ºC for 45 s, and returned to the ice for 2 min before adding 950 µl SOC medium. The mixture was incubated at 37 °C for 60 min with shaking and plated in 200 µl aliquots on to LB agar plates containing the appropriate antibiotics.

2.3.2.2. Plasmid isolation from *E. coli*

Plasmid DNA was purified from 10 ml overnight *E. coli* cultures using the Wizard plus SV Miniprep DNA Purification System (Promega, Wisconsin, USA) according to the manufacturer's instructions.

2.3.2.3. Restriction endonuclease digestion of plasmid DNA and agarose gel electrophoresis

Restriction digest reactions contained 300 ng of DNA, 1 µl of enzyme, 1x reaction buffer (as recommended by the manufacturer) and 100 µg ml^{-1} bovine serum albumin (if required) in a final volume of 20 µl. Reactions were incubated for 2 h at 37 ºC, unless otherwise directed by the manufacturer.

Digested plasmid DNA was visualised using agarose gel electrophoresis, performed as described by Sambrook et al 1989. Agarose gels (0.8 – 2%) were run according to the size of the DNA fragments to be identified/isolated. Gels were cast with 0.5x TBE buffer including 0.5 μg ml^{-1} ethidium bromide. DNA samples were loaded with Blue juice loading buffer and all samples were run with a 1 kb DNA standard and a 100 bp standard and visualised under UV light. DNA fragments were isolated from the gel using the QIAquick gel extraction kit (Qiagen, Crawley, UK) when required. DNA concentrations were determined either using an Ultrospec 2100 pro spectrophotometer (GE Healthcare, Buckinghamshire, UK) or a nanodrop (Thermo Scientific).

2.3.2.4. Site-directed mutagenesis

Site-directed mutagenesis was performed using the PCR based method 'QuikChange' (Stratagene Ltd, Cambridge, UK) according to the manufacturer's protocol. For each round of mutagenesis two complementary primers were designed which included the desired nucleotide substitutions, or the sequences flanking a region for deletion. Primers were extended using *Pfu* DNA polymerase or Phusion PCR master mix, according to the manufacturer's instructions. The appropriate protocol for insertion/deletions or nucleotide substitutions was followed to replicate the entire plasmid DNA template. Methylated template DNA was digested with the enzyme *DpnI* and the remaining PCR product, that has the desired mutation, was used to transform α-select competent *E. coli* as described in section 2.3.2.1.

2.3.2.5. DNA sequencing

Purified plasmid DNA was sequenced by Mr Adrian Jenkins (Department of Retrovirology, NIBSC), using ABI technology on 3130 XL Prism Genetic Analyser (P.E. Applied Biosystems, CT, USA). Sequencing primers (IX – XVI, table 2.3.3.) were designed using Vector NTI advance 10 (Invitrogen, California, USA), based on the sequence of pFastBac-itPA.

2.3.3. Generating plasmid constructs for expression of itPA variants

All plasmids are described in table 2.1., and primer sequences are given in table 2.2. The sequence of all completed constructs was verified by DNA sequencing.

Primer	Primer sequence
I	5'-CAGAAGAGGAGCCAGATCTTACCAAGGAAACAGTGACTGCTACTTTGG-3'
II	5'-TCCCAAAGTAGCAGTCACTGTTTCCTTGGTAAGATCTGGCTCCTCTTCTG-3'
III	5'-AGGAGCCAGATCTTACCAAATAGATACCAGGGCCAC-3'
IV	5'-GTGGCCCTGGTATCTATTTGGTAAGATCTGGCTCC-3'
V	5'-AGGAGCCAGATCTTACCAATCTGAGGGAAACAGTG-3'
VI	5'-CACTGTTTCCCTCAGATTGGTAAGATCTGGCTCC-3'
VII	5'-GGAGCCAGATCTTACCAACCTGTCAAAAGTTGCAGC-3'
VIII	5'-GCTGCAACTTTTGACAGGTTGGTAAGATCTGGCTCC-3'
IX	5'-TGGAGCACAGCGGAGAGTGG-3'
X	5'-CGGAATCCTGATGGGGAT-3'
XI	5'-GACACTTACGACAATGACATTGC-3'
XII	5'-CACACAGTGCGGACCACG-3'
XIII	5'-AGGAGGGCACATCACAGT-3'
XIV	5'-GCTGCTGTTCCAGTTGGT-3'
XV	5'-TATTCCGGATTATTCATACCGTC-3'
XVI	5'-GTATGGCTGATTATGATCCTC-3'

Table 2.2. Sequences of primers used in this research.

2.3.3.1. Generation of pFastBac-irPA

pFastbac-irPA was generated by site-directed mutagenesis, following the deletion protocol with pFastBac-itPA as template, and primers I and II. The resulting construct, pFastBac-irPA, lacked the 5' 516 bp region that encodes the F-G-K1 region of tPA (amino acids V5 - E175). A test digestion with restriction endonucleases *BamHI* and *XhoI* was used to screen for the deletion, identified by the release of a 1182 bp fragment rather than the 1698 bp fragment of the control template.

2.3.3.2. Generation of pFastBac-itPA-K1P

pFastBac-itPA-K1P was generated by site directed mutagenesis, following the deletion protocol with pFastBac-itPA: K2 del as template and primers III and IV. The resulting construct lacked the 5' 246 bp that encodes the F-G region (amino acids V5-E86) and the 5'246 bp that encode the K2 region (amino acids C215-C296) of tPA. A test digestion using restriction endonucleases *BamHI* and *XhoI* was used to screen for the deletion identified by the release of a 1206 bp fragment, rather than the 1452 bp of the control template.

2.3.3.3. Generation of pFastBac - itPA: P

PFastBac-itPA: P was generated by site directed mutagenesis, following the deletion protocol with pFastBac-itPA: K2 del as template and primers V and VI. The resulting construct lacks the 5' 774 bp that encodes the F-E-K1-K2 region of tPA (amino acids V5-S262). A test digestion using restriction endonucleases *BamHI* and *XhoI* was used to screen for the deletion identified by the release of a 942 bp fragment rather than the 1452 bp of the control template.

2.3.3.4. Generation of pFastBac-itPA: F del

PFastBac-itPA: F del was generated by site directed mutagenesis, using the deletion protocol with pFastBac-itPA as template and primers VII and VIII. The resulting construct lacks the 5' 129 bp that encodes the F region of tPA (amino acids V5-V47). A test digestion using restriction endonucleases *BamHI* and *XhoI* was used to screen for the deletion identified by the release of a 1569 bp fragment rather than the 1698bp of the control template.

2.3.3.5. Generation of pFastBac- itPA: F del-GFP

PFastBac-itPA: F del-GFP was generated by site directed mutagenesis, using the deletion protocol with pFastBac-itPA-GFP as template and primers VII and VIII. The resulting construct lacks the 5' 129 bp that encodes the F region of tPA-GFP (amino acids V5-V47). A test digestion using restriction endonucleases BamHI and XbaI was used to screen for the deletion identified by the release of 1569 bp and 750 bp fragments rather than the 1698 bp and 750 bp fragments of the control template.

2.3.3.6. Maintenance of Sf9 cultures

Sf9 cells were grown in Sf-900 II serum free medium with 100 µg/ml penicillin-streptomycin, in a 250 ml disposable Erlenmeyer flask at 28 ºC with constant shaking at 130 rpm. Cultures were passaged when they reached 2 $x10^6$ cells/ ml to a density of 5 $x10^5$ cells/ ml. To determine the cell density, 0.4 ml of cell culture was diluted with 0.5 ml medium + 0.1 ml of 0.4% (w/v) trypan blue and loaded on to a haemocytometer and the number of cells in one of the $1mm^2$ squares counted. The number of cells were multiplied by 10^4 to estimate the number of cells in the diluted sample, and then multiplied by the dilution factor of 2.5 to find the number of cells/ ml in the original culture. The number of viable cells must exceed 95% by trypan blue exclusion for cultures to be considered healthy. For long term storage, cultures were stored over liquid nitrogen in 1 ml aliquots at 1 x 10^7 cells in 60% Grace's Media, 30% FBS, and 10% DMSO.

2.3.3.7. Generating recombinant bacmid DNA using DH10Bac E. coli cells

100 ng of purified pFactBac construct was added to 100 µl of competent *E. coli* DH10Bac cells and stored on ice for 30 min. The mixture was heat shocked for 45 s at 42 ºC and returned to the ice for 2 min before adding 900 µl of SOC medium at room temperature. The mixture was incubated at 37 ºC for 4 h with shaking and 100 µl aliquots were spread on to LB agar plates containing gentamicin, kanamycin and tetracycline, with 50 µg/ ml Xgal and 40 µg/ ml IPTG. Plates were incubated at 37 ºC for 48 h and colonies containing recombinant bacmid were identified by blue/white selection. A well isolated white colony was picked and re-streaked to verify phenotype. Bacmid DNA was purified from 100 ml

DH10Bac *E. coli* cultures using the QIAfilter plasmid Midi kit (QIAGEN, Crawley, UK) according to the manufacturer's instructions for low-copy plasmids.

2.3.3.8. Transfection of Sf9 cells to generate recombinant baculovirus

Sf9 insect cells were transfected by cationic liposome-mediated transfection, with 1 µg of purified bacmid DNA and 6 µl CellFectin reagent in 6-well tissue culture plates at a density of 9 x 10^5 cells/well, according to the manufacturer's protocol. Virus particles were harvested in the cell culture medium after 72 h incubation at 28 ºC. Cells were removed by centrifugation at 4000 *g* for 10 min and the culture medium was vacuum filtered through a 0.2-µm membrane and stored at 4 ºC, out of light. This preparation is a P1 baculovirus stock.

2.3.3.9. Baculovirus titre determination

The virus titre is determined through the calculation of the number of plaque forming units (pfu)/ ml. A pfu is a measure of the number of virus particles capable of forming plaques in a sample unit, therefore the number of infectious virus particles in a sample. A viral plaque is an area of lysis in a fixed monolayer of host cells contained within a semi-solid medium. A plaque is formed when a virus particle infects a cell, causing it to lyse and infect adjacent which in turn causes them to lyse. The standard method for calculating the pfu is the plaque assay where the monolayer of host cells is infected with varying dilutions of virus. The plaques form within 3-14 days and counted manually. The number of plaques, combined with the dilution factor, is used to calculate the number of plaque forming units; it is assumed that each plaque is formed from 1 infective virus particle.

In this project the virus titre was determined by real time-polymerase chain reaction (RT-PCR) using a LightCycler 2.0 following the method of Lo and Chao, 2004 (Lo and Chao, 2004) In this method viral nucleic acid was extracted from a 200 µl aliquot of baculovirus supernatant using the High Pure viral nucleic acid kit (Roche, Mannheim, Germany) according to the manufacturer's protocol. Using RT-PCR, the viral genomic DNA was amplified with primers designed from ie-1, a baculovirus gene away from the Tn region, this means that the same method can be used regardless of the protein that is being expressed. A fluorogenic dye is used to detect the any ds-DNA PCR products. In this method the LightCycler Faststart DNA Master^{plus} SYBR Green 1 kit (Roche, Mannheim, Germany) was used according to the manufacturer's instructions. SYBR Green dye binds to the double stranded-DNA, when the dye is unbound it emits a relatively low signal but when it is bound it fluoresces brightly. As the amplicon increases the signal from the dye increases, therefore the dye is used to detect the accumulation of PCR product as a function of the number of rounds of amplification. The intensity of the fluorescence signal for each sample can then be compared to that of a sample of virus with known concentration, that has been validated against the plaque forming assay,

2.3.3.10. Baculovirus amplification

P1 viral stocks (from section 2.3.3.8.) were amplified to P2 viral stocks in a 6-well, tissue-culture treated, polystyrene, flat bottom plates. 2 ml of Sf9 cells at 10^6 cells/ ml were added to each well. The cells were incubated at room temperature for 1 h to allow attachment. The appropriate volume of P1 viral stock was added to each well to a multiplicity of infection (MOI) of 0.1 pfu/ cell, calculated according to the equation below.

$$Inoculum\ required\ (ml) = \frac{MOI\ (pfu/cell) x\ number\ of\ cells}{titre\ of\ viral\ stock (pfu/ml)}$$

The plates were incubated for 72 h at 28 ºC. The P2 virus was recovered and titre determined as described in 2.3.3.9

P3 virus stocks were amplified in the same way and volumes were scaled up using suspension cultures in shaker flasks.

2.3.4. Protein expression in Sf9 cells

tPA variants were expressed using P3 and higher generation virus to re-infect 100 ml of sf9 cells at 2 x 10^6 cells/ ml with an MOI of 5 pfu/ cell and incubated at 27 ºC for 72 h in a 250 ml disposable Corning Erlenmeyer flask with continuous shaking. Cells were for centrifuged for 10 min at 4000 *g* and the supernatant culture medium was collected.

2.3.4.1. Purification of recombinant tPA variants expressed in Sf9 cells

The protein purification procedures were carried out using an AKTA Purifier (GE Healthcare, Buckinghamshire, UK). The cell culture medium and all buffers used in purification were vacuum filtered through a 0.2 µM filter and degassed under vacuum until no bubbles were visible. The proteins were purified using affinity chromatography on an Erythrina trypsin inhibitor (ETI) column (Heussen et al, 1984). ETI was coupled to 0.3 g (~1 ml gel when swollen) of cyanogen bromide activated Sepharose 4B in buffer (v) for 2 h at room temperature with constant mixing. Any remaining active groups were then blocked using 1 M ethanolamine pH 8 and the gel was packed into a Tricorn 10/20 column. The ETI

column was equilibrated with buffer (i) until a stable base line was observed. Cell culture medium was loaded on to the ETI column at 1 ml/ min, the column was then equilibrated with buffer (i) until a stable base line was observed. The bound protein was eluted using buffer (ii) and collected in 0.5 ml fractions. Peak fractions observed from the chromatogram were pooled and dialyzed (described in section 2.3.6.1) against 10mM sodium acetate buffer pH 4.0. After determination of protein concentration (described in section 2.3.6.2), the samples were snap frozen in 20 µl or 1 ml aliquots in liquid nitrogen and stored at -40 ºC.

The column was then washed with alternating buffer (iii) and buffer (ii) for 3 min each. 20 % Ethanol was then passed through the column until a steady baseline was observed and the column sealed and stored at 4 °C.

2.3.4.2. Purification of itPA-GFP

itPA-GFP and itPA: F del-GFP were purified as in section 2.3.4.1 with an additional washing step with a gradient of buffer (iv) and buffer (ii) over 15 min, after the proteins were loaded. The column was then equilibrated with buffer (i) and the proteins were then eluted from the column as described in section 2.3.4.1.

2.3.4.3. Ion exchange chromatography

The sample was eluted from the ETI column using buffer (ii) and then loaded it straight onto a resource S cation exchange column that had been equilibrated with buffer (ii). The PI of tPA is around 7 so therefore should bind to the negatively charged medium. Elution from the

resource S column was performed with a gradient up to 2 M NaCl in buffer (ii) over 20 min and 1 ml fractions were collected.

2.3.5. Converting itPA into tcitPA using plasmin-Sepharose

Plasmin-sepharose was made by coupling 1.5 mg glu-plasminogen (chromogenix, Milan, Italy) to 0.3 g (~1 ml gel when swollen) of cyanogen bromide activated Sepharose 4B in 2 ml of buffer (v) for 2 h at room temperature with constant mixing. Any remaining active groups were then blocked using 1 M ethanolamine pH 8.0. The plasminogen-sepharose was then treated with 36 µg streptokinase for 30 min at room temperature with constant mixing, washed and stored as a 50% (v/v) slurry.

The activity of the plasmin-Sepharose was determined using chromogenic substrate S2251. Plasmin-Sepharose was tested over a range of dilutions from neat to 1/64 against a standard curve of the 3rd plasmin international standard (97/536) from 1.060 IU serially diluted 2-fold down to 0.265 IU. The assay was performed with 0.45 mM S2251 in 40 mM Tris/ HCL + 75 mM NaCl pH 7.4 at 37 ºC (final concentrations).

Two-chain tPA was generated by incubating 2 ml of 313 nM itPA in 200 mM Tris/ HCL, 0.75 M NaCl, 0.05% Tween 20, pH 7.6 at 37 ºC with 50 µl of 7.3 nM plasmin-Sepharose for 30 min (optimum time of incubation was determined by a time course experiment visualised by SDS-PAGE, results not shown) with constant agitation at ambient temperature. ScitPA (R275E) was determined non-cleavable using the same procedure.

2.3.6. Determination of protein concentration and purity

2.3.6.1. Dialysis

Proteins were dialyzed using 0.5-3 ml dialysis cassettes (Pierce, Rockford, IL) against 1 L of the desired storage or assay buffer, with 3 buffer changes over 24 h at 4 ºC with continuous stirring.

2.3.6.2. Protein concentration determination using Bradford assay

Protein concentration was determined using the microplate procedure for the Coomassie Plus Protein Assay Kit (Pierce, Rockford, IL) with a standard curve of itPA. The protein concentration of the itPA used to make the standard curve had been determined by amino acid analysis (Alta biosciences, Birmingham University). Samples were diluted into the linear range of the standard curve up to an absorbance of 0.2 to determine the protein concentration.

2.3.6.3. SDS-PAGE

An estimate of protein purity was obtained by visualization of protein samples by electrophoresis in 4-12% NuPAGE Bis-Tris polyacrylamide gels with NuPAGE MES SDS Running Buffer. Protein samples (see individual experiments in the results section for protein concentrations) were heated at 70 ºC for 10 min with 1 part NuPage sample reducing agent (10 x) and 2.5 parts NuPage LDS sample buffer (4 x) and made up to 10 parts with

deionised water. Samples were loaded alongside SeeBlue Plus2 pre-stained molecular weight standard and electrophoresed at 200 V for 45 min.

For visualisation of proteins, gels were stained with SimplyBlue SafeStain Coomassie reagent, SYPRO Ruby stain or Silver stain according to the manufacturer's instructions.

2.3.6.4. Western Blotting

SDS-PAGE was performed as in section 2.3.6.3. using 5 µl magic mark XP western protein standard instead of SeeBlue Plus2 pre-stained molecular weight standard. Blotting was then performed in an XCell II Blot Module (Invitrogen, California, USA) following manufacturer's instructions, with NuPage transfer buffer, transferring the proteins on to a PVDF transfer membrane. Proteins transferred to the PVDF membrane were then probed using rabbit anti-GFP at 1 µg/ ml or rabbit anti-tPA at 3 µg/ ml and then detected with the WesternBreeze chemiluminescent western blot detection kit (anti-rabbit) following the manufacturer's instructions. The chemiluminescent signal was visualised by exposing the PVDF membrane to Amersham hyperfilm ECL for 1 and 5 min.

2.3.7. Fluorescence measurements of itPA-GFP and itPA: F del-GFP

The fluorescence signal from itPA-GFP and itPA F del-GFP was tested in a number of different buffers, including 10 mM Sodium Acetate buffer pH 4.0, 0.1 M HEPES pH 7.6, 50 mM Tris/ HCl pH 7.7 at 25 ºC and 10 mM Sodium phosphate pH 8.0 with 0.005 % Triton-X-100 and 1 mM EDTA. Fluorescence was measured, in cuvettes using 1 ml of sample (see individual experiments for concentrations) and in 96 well, flat bottom, clear bottom, black

sided plates with 100 µl sample/ well, readings were taken from the bottom of the plate. The excitation wavelength used was 475 nm with a cut off set at 495 nm, the emission was measured as a scan from 500 nm – 550 nm in 2 nm increments or as a single measurement at 510 nm. Conditions were optimised using a GFP standard from the GFP quantification kit from BioVision, CA, USA and a standard curve was generated according to the manufacturer's instructions. All measurements were taken on a Molecular Devices Spectramax M5 fluorescent plate reader and results were analysed using plate reader software; Softmax Pro version 5.0, Molecular Devices, Sunnydale, CA, USA.

2.4. Results

2.4.1. Expression and purification of tPA variants

Full length tPA, and mutated derivatives, were expressed in Sf9 insect cells using the Bac-to-Bac baculovirus system. Expressed proteins were secreted into the culture medium using the native tPA signal peptide, and purified by affinity chromatography on an ETI-sepharose column. Estimates of protein concentration were made using the Bradford assay and a typical 100 ml culture yielded approximately 300 μg protein. Cultures expressing GFP fusion proteins generally produced lower yields, typically 100 μg per 100 ml.

All recombinant tPA variants expressed are shown in table 2.3. together with commercial full length tPA (Actilyse) and truncated variant rPA (Reteplase). The theoretical molecular weights of the insect-expressed variants were based on the amino acid sequence, calculated using Vector NTI advance software (Invitrogen, California, USA). The molecular weight of the expressed glycosylated proteins differ from the theoretical values and the predicted glycosylation state is given for each variant in table 2.3., based on the domain structure. The molecular weight of Actilyse, the full length glycoprotein produced in mammalian CHO cells, is 65 kDa (European Pharmacopoeia, 1998); Reteplase, a non-glycosylated variant produced in *E. coli*, has a molecular weight of 39 kDa (Waller et al, 2003)..

Commercial and insect expressed tPA variants were visualised by SDS-PAGE under reducing conditions to provide an estimate of purity, and size relative to molecular weight markers (Figure 2.2.). Each variant was expressed predominantly in the single-chain form and by Coomassie staining appeared to be highly purified. A small amount of the two-chain form of each variant was also present, represented by faint lower molecular weight bands. The position of each band, relative to the molecular weight markers, was consistent with the

theoretical value in table 2.3., with apparent differences accounted for by the glycosylation state. For example, the insect-expressed rPA (lane 5) has an apparently higher molecular weight than the non-glycosylated *E. coli*-derived rPA (lane 6).

Two-chain tPA was generated by plasmin-Sepharose treatment of a sample of itPA, lane 3 in figure 2.3. shows the sample of itPA before treatment in a predominantly single-chain form when visualized by Ruby SYPRO stained SDS-PAGE. Lane 4 shows that the sample of itPA after 30 min of plasmin treatment was completely converted to two-chain tPA. ScitPA (R275E) is a derivative of tPA in which the plasmin cleavage site has been mutated from Arg to Glu and as a result it can be seen in figure 2.3. that only the single chain form was expressed and purified. Figure 2.3. also shows that conversion into two-chain tPA did not occur after a 30 min incubation with plasmin-Sepharose.

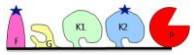
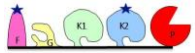
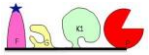
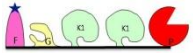
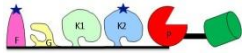
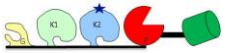
Name	Domains in variant	Fibrin binding F	Fibrin binding K	Glycosylation	Expression system	Theoretical Mw, kDa	Gel Fig./ Lane
tPA (Alteplase)	FGK1K2P 	✓	✓	processes 2-3 immature high-mannose oligosaccharides into more complex forms than insect cells	Mammalian (CHO)	65	2.2A/ 1
itPA *	FGK1K2P 	✓	✓	2 or 3 immature high-mannose oligosaccharides	Insect (sf9)	59	2.2A/ 2
itPA:K2 del	FGK1P 	✓	-	2 immature high-mannose oligosaccharides	Insect (sf9)	50	2.2A/ 4
itPA:K1K1	FGK1K1P 	✓	-	3 immature high-mannose oligosaccharides	Insect (sf9)	59	2.2A/ 3
rPA (Reteplase)	K2P 	-	✓	no glycosylation	*E.coli*	39	2.2A/ 5
irPA	K2P 	-	✓	1 or 2 immature high-mannose oligosaccharides	Insect (sf9)	39	2.2A/ 6
itPA: F del	GK1K2P 	-	✓	2 or 3 immature high-mannose oligosaccharides	Insect (sf9)	54	2.2B/ 7
itPA: K1P	K1P 	-	-	2 immature high-mannose oligosaccharides	Insect (sf9)	41	2.2B/ 8
itPA: P	P 	-	-	1 immature high-mannose oligosaccharides	Insect (sf9)	31	2.2B/ 9
itPA-GFP	FGK1K2P-GFP 	✓	✓	2 or 3 immature high-mannose oligosaccharides	Insect (sf9)	88	2.7/ 1
itPA F del-GFP	GK1K2P-GFP 	-	✓	2 or 3 immature high-mannose oligosaccharides	Insect (sf9)	83	2.7/ 2

Table 2.3.: Domain structure and physical properties of commercial and insect expressed tPA variants. For each variant the expression host and glycosylation state are shown. Immature high-mannose oligosaccharide refers to reduced processing of side chains compared to that seen with mammalian cells. The domain structure is represented by F (finger), G (growth factor), K1 (kringle 1), K2 (kringle 2) and P (protease) with a diagram of the structure. The presence or absence of the fibrin binding domains F and K2 are indicated. The theoretical molecular weight was calculated from the amino acid sequence of each insect expressed protein and is the published molecular weight for the commercial proteins Actilyse (McCluskey et al, 2003) and Reteplase (Waller et al, 2003) * sc-itPA (R275E) (non cleavable itPA) has the same structure and physical properties described in this table as itPA and tc-itPA is itPA that has been cleaved into two-chain tPA by plasmin.. i denotes insect cell expression.

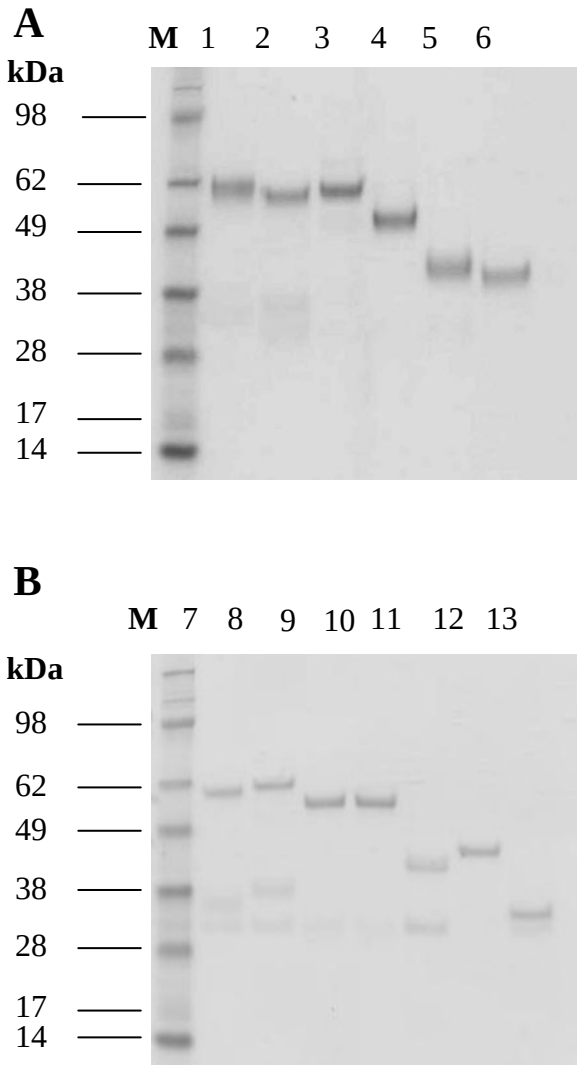


Figure 2.2. SDS-PAGE of recombinant tPA variants. Gels were loaded with 580 ng protein and stained with Coomassie reagent. Molecular weight markers (M) were included in each gel and the numbered lanes (A: 1-6; B: 17-13) contained the following tPA variants: 1: Actilyse; 2: itPA; 3: itPA:K1K1; 4: itPA:K2 del; 5: irPA; 6: Reteplase. 7: itPA, 8: itPA: K1K1, 9: itPA F del, 10: itPA F del 11: irPA. 12: itPA: K1P, 13: itPA: P.

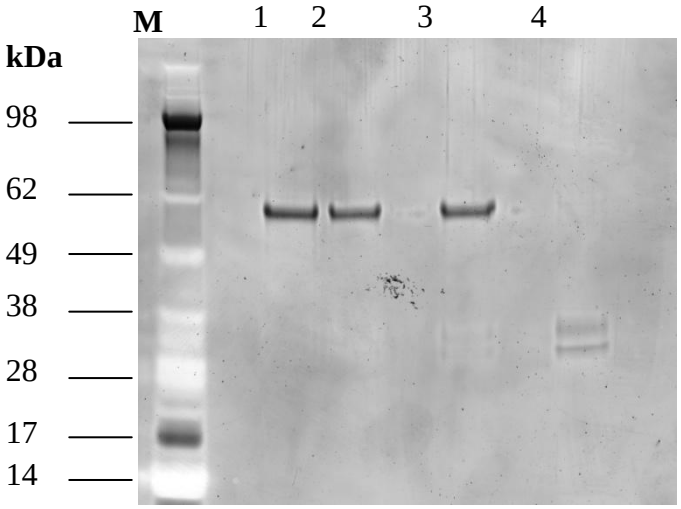


Figure 2.3. SDS-PAGE of scitPA (R275E), itPA and itPA treated with plasmin-Sepharose (tcitPA). Gels were loaded with 390 ng protein and stained with SYPRO Ruby reagent. A molecular weight marker (M) was included in the gel and the numbered lanes (1 -4) contained the following: 1: scitPA (R275E); 2: scitPA (R275E) treated for 30 min with plasmin-Sepharose; 3: itPA; 4: itPA treated for 30 min with plasmin-Sepharose (tctPA)

2.4.2. tPA-GFP and tPA: F del-GFP

2.4.2.1. Fluorescence measurements of itPA-GFP fusions

Initially GFP fusion proteins were purified, dialysed and stored in 10 mM Sodium Acetate buffer pH 4.0 following the same procedure as the other tPA variants. These conditions were optimised to keep tPA stable and reduce precipitation. GFP fusions purified and stored this way were found to give little or no fluorescence, (e.g. figure 2.4.).

A GFP standard kit was used to investigate the optimal conditions for measurement of the GFP fluorescence signal and to compare the level of fluorescence with our GFP fusion variants. A standard curve of the commercial GFP was prepared in 3 different buffers, 10 mM Sodium Acetate pH 4.0, 50 mM Tris/ HCl pH 7.7, and 10 mM Sodium phosphate pH 8.0 with 0.005 % Triton-X-100 and 1 mM EDTA (figure 2.5.). Consistent with the GFP fusion proteins, the GFP standard curve prepared in 10 mM Sodium Acetate buffer gave little or no fluorescence signal. The highest fluorescent signal was found in the 10 mM Sodium Phosphate buffer at pH 8.0. In 50 mM Tris/ HCl pH 7.7 GFP produced a lower fluorescence signal that was unstable when measured over time (figure 2.6.) The reason that the GFP did not show any fluorescence signal in the 10 mM Sodium Acetate pH 4.0 and gave inconsistent readings in the 50 mM Tris/ HCl pH 7.7 is likely to be because GFP pH sensitive (Bizzarri et al, 2009). Therefore the inconsistent readings seen with GFP in the Tris buffer could be because the pH of Tris is temperature dependent and so fluctuations in temperature may have changed the pH and as a result affected the fluorescence of the GFP. When the GFP fusion proteins were tested in the optimised conditions they still showed little or no fluorescence.

GFP fusion proteins were visualised by SDS-PAGE under reducing conditions and by coomassie staining (figure 2.7.) and SYPRO Ruby staining (figure 2.8.), both GFP fusion variants showed a predominant band at a position on the gel that appeared to be consistent

with the theoretical molecular weight relative to the molecular weight marker. There also appeared to be a number of fainter lower molecular weight bands indicating the samples were not highly purified compared with the non-GFP fusion variant itPA-F del (figure 2.8.).

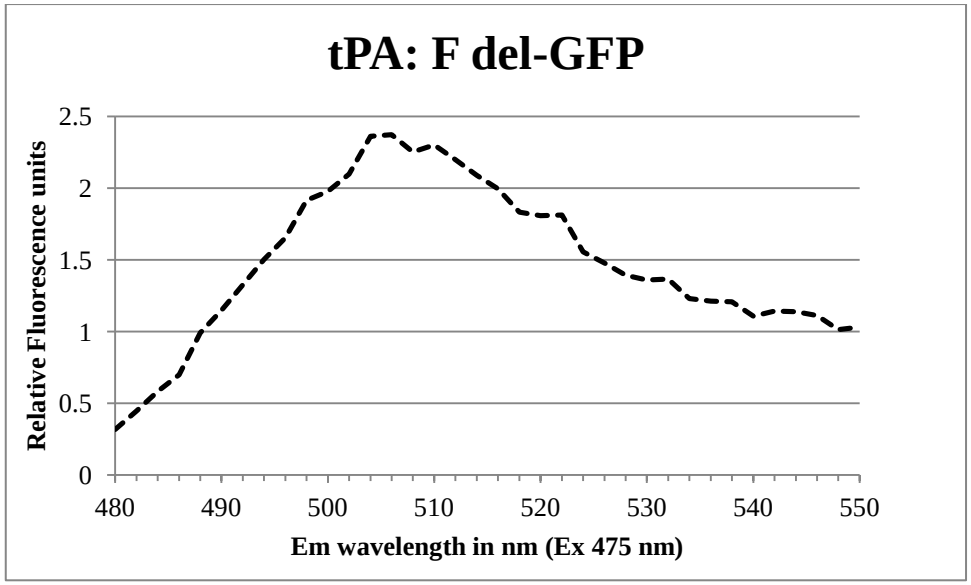


Figure: 2.4. Fluorescence in relative fluorescence units (RFU) of a 30 µg/ml sample of itPA: F del-GFP in 10 mM Sodium Acetate buffer pH 4.0. The sample has been excited at 475 nm and the emission has been read over a range of wavelengths from 480 nm to 550nm. The Maximum fluorescence 2.4 RFU was observed at 506 nm.

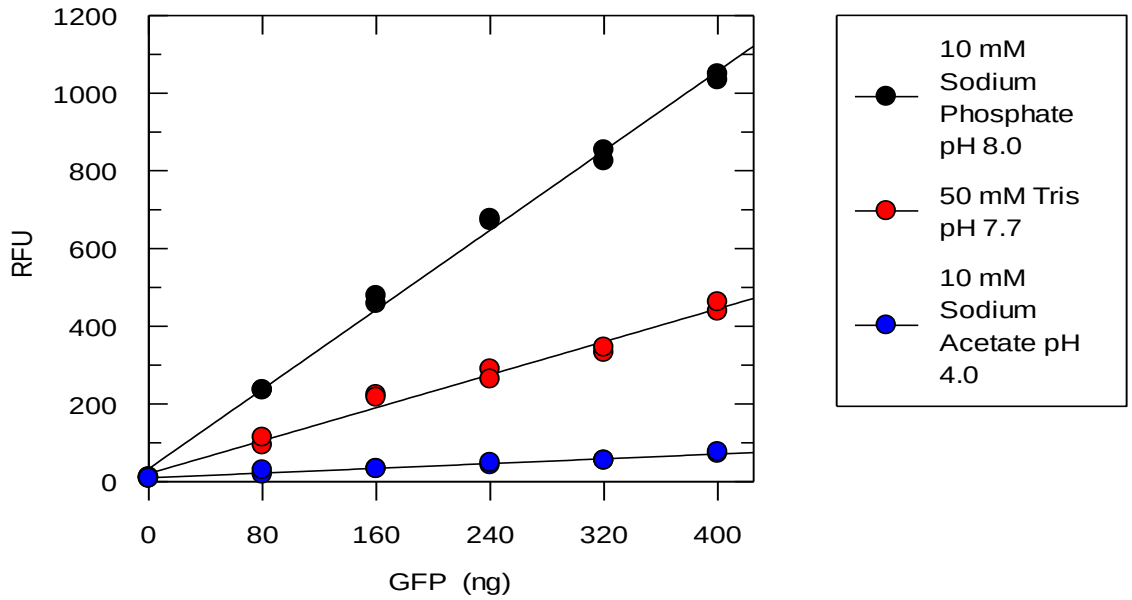


Figure 2.5: GFP standard curve. A GFP standard curve was made up in 3 different buffers: 10 mM Sodium Acetate buffer pH 4.0, showing almost no fluorescence, 10 mM Sodium Phosphate buffer pH 8.0 gave the highest fluorescence signal and 50 mM Tris/HCL pH 7.7 showed about half the fluorescence of the GFP in 10 mM Sodium Phosphate pH 8.0. Samples were excited at 475 nm and the emission was read at 509 nm.

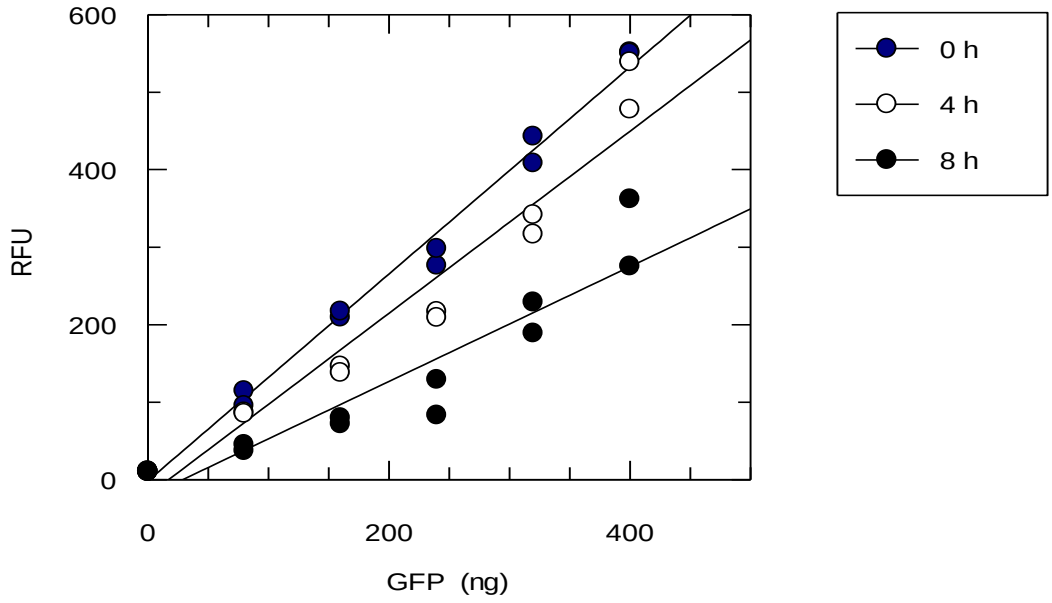


Figure 2.6: GFP standard curve. The GFP standard curve was made up in 50 mM Tris/HCL pH 7.7 and then read at 3 time points; 0 h, 4 h and 8 h. Samples were excited at 475 nm and the emission was read at 509 nm.

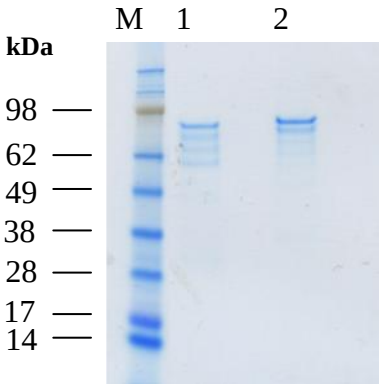


Figure 2.7: Coomassie stained SDS-PAGE of GFP fusion variants. The gel was loaded with 780 ng protein/ lane. A molecular weight marker was included in the gel and lane 1 contained itPA: F del-GFP and lane 2 contained itPA-GFP.

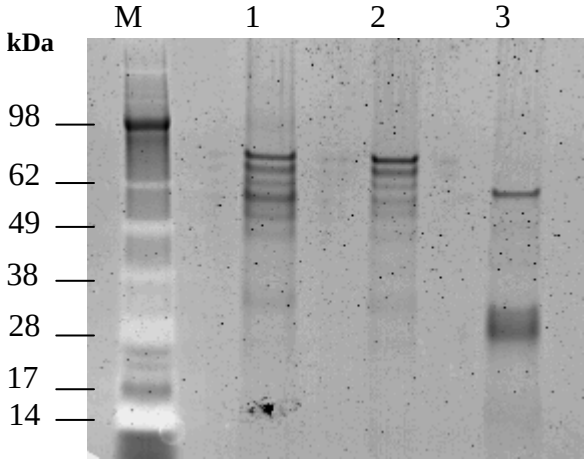


Figure 2.8: Ruby SYPRO stained SDS –PAGE. The gel was loaded with 390 ng protein/ lane and each numbered lane (1-3) contained 1: itPA-GFP. 2: itPA-F del-GFP and 3: itPA: F del. A molecular weight marker was included in the gel.

Western blots of itPA: F del-GFP probed with 1) anti-GFP antibodies and 2) anti-tPA antibodies, revealed that the contaminating bands were detected by one or both of the antibodies (figure 2.9). A control sample of itPA: F del was detected by the anti-tPA antibody as two bands at the expected molecular weight for the single and two chain forms and was not detected by the anti-GFP antibody. The control sample of commercial GFP was detected by the anti-GFP antibody as a band at the expected molecular weight, relative to the molecular weight marker for GFP with another band at a molecular weight at around double that of the expected molecular weight for GFP, which is presumably a GFP dimer. Further experiments visualised by SDS-PAGE stained with SYPRO Ruby revealed that a sample of protein snap frozen instantly after purification remained as a single band, whereas a sample of the same protein that had been dialysed after purification had been cleaved into a number of bands, see figure 2.10. This indicated that there may have been proteases co-purifying with the itPA: F del-GFP that was cleaving the protein.

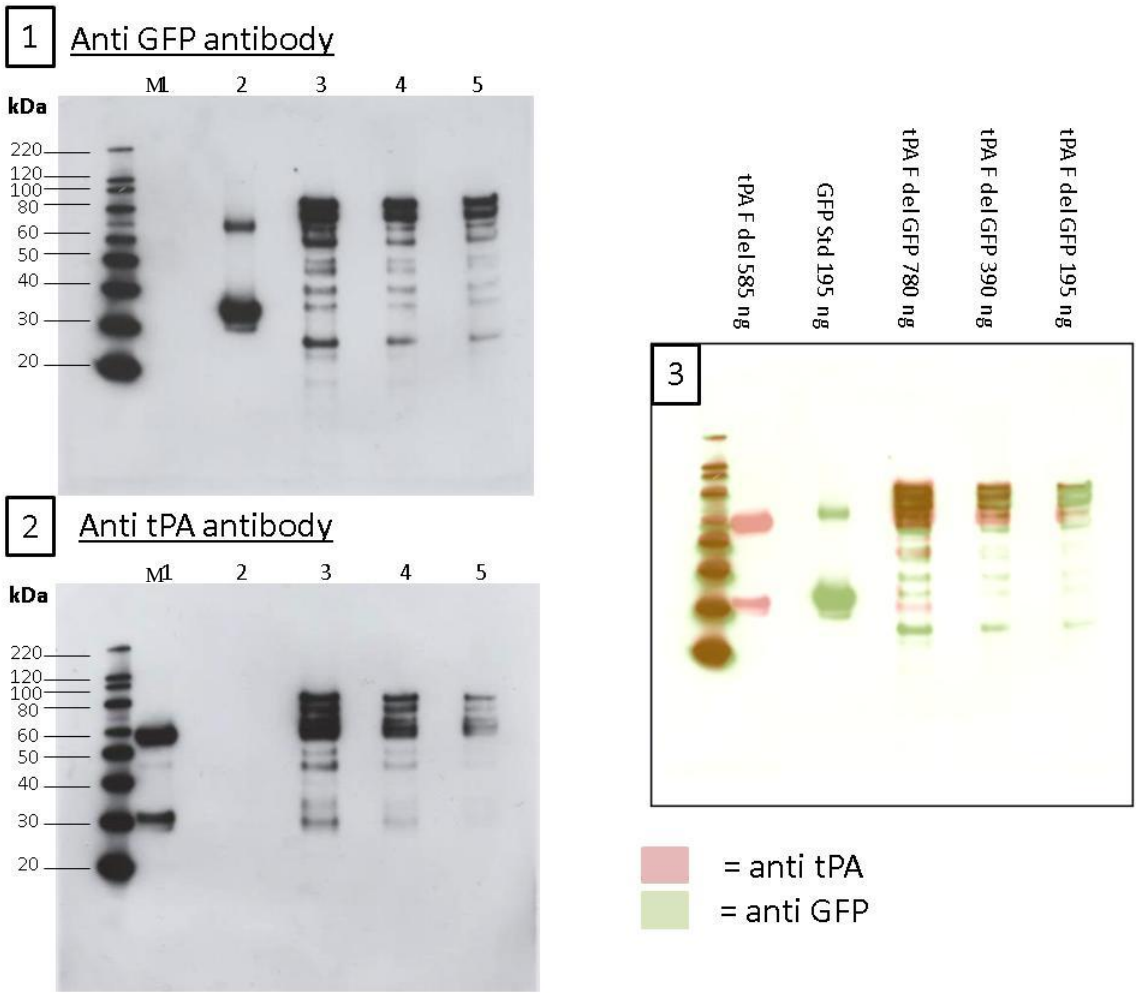


Figure 2.9.: Western blots probed with (1) Anti-GFP antibody, (2) Anti-tPA antibody and (3) an overlay of blots (1) and (2): A molecular weight marker was included in both blots and in both blots and numbered lanes (1-5) contained: 1: itPA: F del at a concentration of 585 ng/ lane, 2: commercial GFP at a concentration of 195 ng/lane and 3-5: itPA: F del-GFP at concentrations of 780, 390, and 195 ng/ lane respectively. Blot number 3 is an overlay of blots 1 and 2 with the anti-tPA in red and the anti-GFP in green.

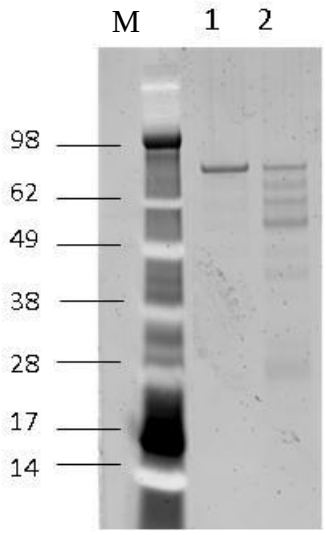


Figure 2.10. SYPRO Ruby stained SDS-PAGE of itPA: F del-GFP before and after dialysis. Each lane was loaded with 390 ng of protein and a molecular weight marker was included on the gel. Numbered lane 1was loaded with itPA: F del-GFP snap frozen in liquid nitrogen immediately as it was eluted from the column. Lane 2 was loaded with itPA: F del-GFP after dialysis in 10 mM Sodium Phosphate buffer pH 8.0.

Further purification of the samples using Ion exchange chromatography (IEX) was attempted to try to separate the GFP fusion proteins from any impurities. The sample eluted over a large number of fractions and much of the sample was shown to have been lost when viewed SDS-PAGE with silver stained, see figure 2.11.

A different approach for further purifying the proteins was to remove any loosely bound proteins i.e. proteins bound to the column non-specifically, by washing with a gradient of NaCl solution before the final elution of the GFP variants. Samples of itPA: F del-GFP, that has been washed with a gradient of NaCl up to 1 M and up to 2 M show fewer unexplained bands when visualised by SDS-PAGE with silver staining (figures 2.11. and 2.12. respectively) than previous purifications, even after dialysis. Fractions collected during the NaCl wash were seen to contain a large number of bands. The GFP variants eluted after a NaCl wash gave good fluorescence signals (see figure 2.13) and the protein that was eluted during the NaCl wash showed very little fluorescence. itPA; F del-GFP from purification with a 1 M NaCl wash showed a maximum fluorescence of ~1350 RFU. itPA; F del-GFP from purification with a 2 M NaCl wash showed a maximum fluorescence of ~1800 RFU, protein from the 1 M NaCl wash showed a maximum fluorescence of ~16 RFU, and a control sample of 10 mM Sodium Phosphate pH 8.0, showed no fluorescence. All samples had been dialysed in to 10 mM Sodium Phosphate pH 8.0.

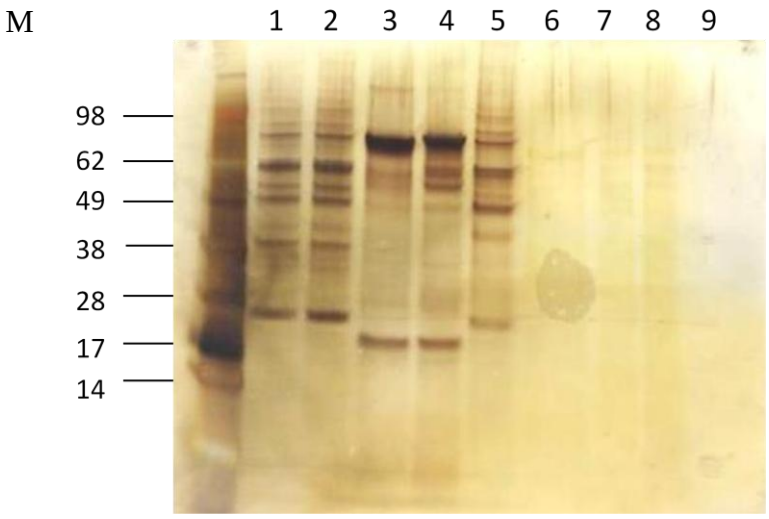


Figure 2.11: Silver stained SDS-PAGE of itPA: F del-GFP purifications. A molecular weight standard was included in the gel and the numbered lanes (1-9) contained the following: 1: 195 ng of protein from the 1 M NaCl wash before dialysis, 2: 195 ng of protein from 1 M NaCl wash, after dialysis into 10 mM Sodium Phosphate buffer pH 8.0, 3: 585 ng of itPA: F del-GFP before dialysis, 4: 585 ng of itPA: F del-GFP after dialysis into 10 mM Sodium Phosphate buffer pH 8.0, 5: 390 ng of tPA: F del-GFP as it was eluted from the ETI column onto the resource S column, 6-9: Pooled and concentrated samples from elution peaks off IEX column.

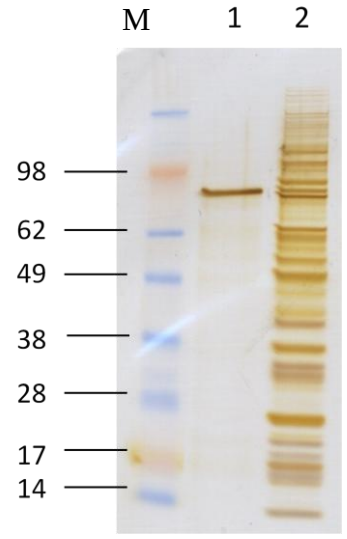


Figure 2.12. Silver stained SDS-PAGE of itPA: F del-GFP purification with 2 M NaCl wash. A molecular weight marker was included and numbered lanes contained: Lane 1: 585 ng itPA: F del-GFP eluted from ETI column after wash with a gradient of NaCl up to 2.0 M. Lane 2: Neat pooled fractions from 2.0 m NaCl gradient wash

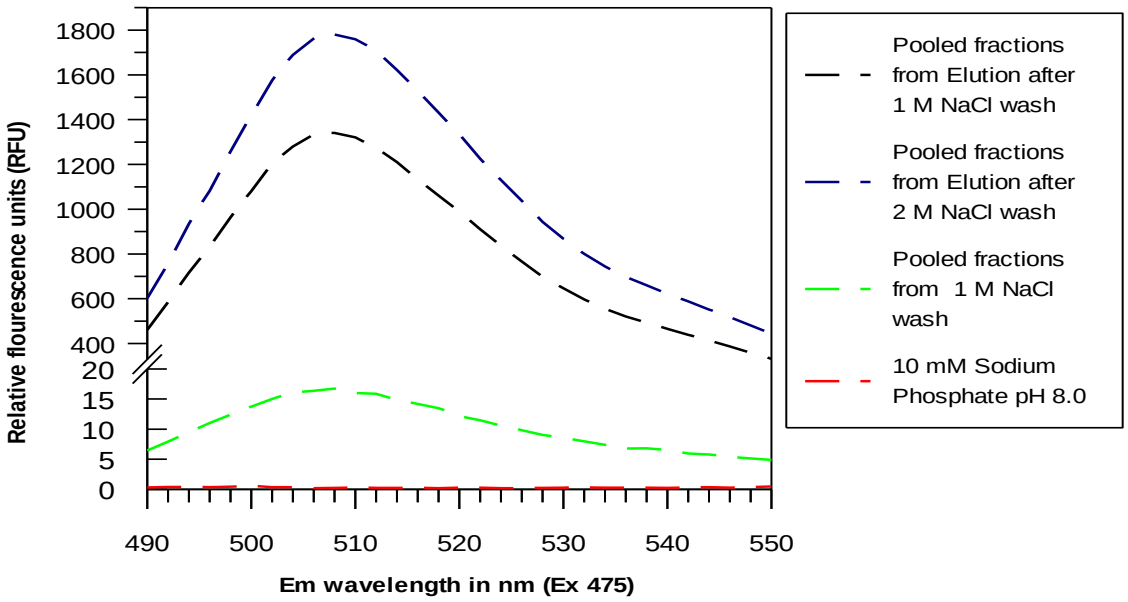


Figure 2.13: Fluorescence measurements of fractions from itPA: F del purification. Fluorescence in relative fluorescence units (RFU) of 1 ml samples of 30 µg/ ml excited at 475 nm and the emission read over a spectrum of wavelengths from 480 nm to 550nm in a cuvette.

CHAPTER 3 - KINETICS

3.1. Introduction

Enzyme kinetics is the study of chemical reactions catalysed by enzymes. Historically enzyme catalysed reactions have been described in terms of measures of the affinity with which the enzyme binds substrate and the rate at which the substrate gets turned over to generate product.(Cornish Bowden, 2004)

The general reaction pathway for an enzyme catalysed reaction is:

$$E + S \underset{k_{-1}}{\overset{k_1}{\rightleftharpoons}} ES \underset{k_{-2}}{\overset{k_2}{\rightleftharpoons}} E + P$$

In this pathway, E refers to the enzyme, S is the substrate, ES is the enzyme-substrate complex and P is the product. The rate constants for the various steps in the reaction are k_1 = the rate of formation of ES, k_{-1} = the breakdown of ES back to E and S, k_2 = the rate that enzyme catalyses the conversion of substrate into product (also referred to as the k_{cat}) and k_{-2} = rate of the reverse reaction where enzyme and product reform to form a complex.

To simplify the interpretation of the data the reverse reaction (k_{-2}) can usually be safely ignored as experimental data is collected at the beginning of the reaction the concentration product is low. This leads to the simplified pathway:

$$E + S \underset{k_{-1}}{\overset{k_1}{\rightleftharpoons}} ES \xrightarrow{k_2} E + P$$

Using this simplified pathway Leonor Michaelis and Maud Menten developed the Michaelis-Menten equation that can be used to interpret enzyme kinetic data.

Enzyme kinetic experiments are performed using a fixed enzyme concentration and varying substrate concentrations. The increase in substrate concentration leads to an increased rate of product formation until the enzyme reaches saturation. At this point increase in substrate concentration does not increase the rate, as all the enzyme molecules are in a complex with a substrate molecule. The initial rates or velocity (V) are plotted against substrate concentration producing hyperbolic plots, that can be interpreted using the Michaelis-Menten equation, which describes the relationship between catalytic rate, the concentration of enzyme and substrate to the individual rates and is as follows:

$$V = \frac{V_{max}[S]}{([S] + K_M)}$$

Where V is velocity, V_{max} is the maximum velocity. [S] is substrate concentration and K_M is the concentration of substrate that leads to half maximum velocity.

The hyperbolic plot can be used to determine kinetic parameters. The V_{max} is the maximal velocity that can be achieved by an enzyme, the rate approaches Vmax asymptotically. At low substrate concentrations the rate of the reaction is dependent on the substrate concentration (first order kinetics) and at high substrate concentrations the rate of the reaction is independent of substrate concentration (approaching zero-order kinetics). The K_M is the Michaelis constant, which corresponds to the substrate concentration producing a rate of ½ V_{max}. The K_M is measured in molar units and is a rough measure of the enzyme substrate affinity (Bisswanger, 2008; Longstaff and Whitton, 2004). Before the advent of personal computers enzyme kinetic parameters were often determined by linear transformations of the

Michaelis-Menten equation, but nowadays non-linear regression to raw data is the preferred method of deriving K_M and V_{max} values from experimental data.

Plasminogen activation by tPA requires both enzyme (tPA) and substrate (plasminogen) to be brought together by binding to a template, due to low affinity for one another in solution (Sinniger et al, 1999). This means that simple Michaelis-Menten kinetics do not apply. Further complications may be present due to the competitive inhibition of the plasmin product by fibrin(ogen). However, the kinetics of plasmin generation should still be measured using initial rates, as usually recommended for enzyme kinetics studies to avoid depletion of substrates (Longstaff and Whitton, 2004).

In this chapter the effect of binding to different templates on the kinetics of plasminogen activation were investigated using tPA variants described in table 2.3. The solid template fibrin is the main target of plasmin (the product of tPA mediated plasminogen activation) in the body and is therefore likely to be a strong template for tPA and plasminogen. Fibrinogen the precursor of fibrin as well as heparin a glucosaminoglycan used as an injectable anticoagulant will be investigated as soluble templates. Measurement of amidolytic activity in solution (no template) will also be studied. In some cases the activity of tPA and variants is studied over a range of plasminogen (substrate) concentrations so apparent K_M and V_{max} parameters can be derived. These parameters are labelled "apparent" because they apply only to the experimental conditions used, including the particular template concentration present in the reaction. In other situations, the tPA and variant enzyme concentration is varied at a fixed template concentration; or enzyme and substrate concentrations are held constant and the template concentration is varied. In all cases slightly different measures of enzyme activity are determined which do not provide a simple statement of enzyme activity. However, these data can be used to help model complex systems involving templates which is dealt with later in Chapter 5.

3.2. Materials and Methods

3.2.1. Materials

Buffer A: 0.5 M Tris pH 8.4 at 37 °C

Buffer B: 40 mM Tris/HCL, 75 mM NaCl and 0.01% (v/v) Tween 20, pH 7.4 at 37 ºC

Buffer C: buffer B + 1 mg/ml HSA

Buffer D: 40 mM Tris/HCL, 37.5 mM NaCl and 0.01% (v/v) Tween 20, pH 7.4 at 37 ºC

Buffer E: buffer D + 1 mg/ml HSA

Buffer (v): Coupling buffer: 0.1 M $NaHCO_3$, 0.5 M NaCl, pH 8.0

Blocking buffer: 1 M ethanolamine pH 8.0

Fibrinogen, Human, Calbiochem, Merck, Darmstadt, Germany

Fibrinogen, Human, Sigma, Pool, UK

Glu-Plasminogen, Chromogenix, Milan, Italy

Lys plasminogen,

Plasmin

Bovine thrombin, Diagnostic Reagents Thame, Oxon

Sodium heparin, Multiparin, Artex, New Zealand

tPA, Actilyse, Boehringer Ingelheim, Ingelheim, Germany

Reteplase, Boehringer Ingelheim, Ingelheim, Germany

tPA variants, see section 2.3.3.

Plasmin chromogenic substrate S-2251 (H-D-Val-Leu-Lys-pNA•2HCL), Chromogenix, Milan, Italy

tPA chromogenic substrate S-2288 (H-D-Ile-Pro-Arg-pNA•2HCL), Chromogenix, Milan, Italy

96 well microtitre plates, PS, Flat bottom (Greiner bio one, Germany).

3.2.2. Methods

The mechanism of tPA stimulation requires binding to a template and the co-localisation of tPA enzyme and plasminogen substrate. The assay methods below describe the measurement of amidolytic activity in solution (no template) and studies with soluble template, fibrinogen and heparin and the solid template fibrin in a 2 phase heterogeneous system.

3.2.2.1. tPA amidolytic activity in solution

Kinetic parameters, K_M and V_{max} (thence k_{cat}, calculated as V_{max}/ protein concentration) were determined using a range of S-2288 concentrations (0.15 – 6 mM) with 4.22 nM tPA (see section 2.3.6.2. for determination of tPA concentration), final concentrations in the microtitre plate well containing a reaction volume of 100 µl. Aliquots of 20 µl of buffer A, 20 µl of 21 nM tPA and 60 µl of a range of S-2288 concentrations from 0.25 to 10 mM were added the wells of 96 well microplates and 60 µl of mineral was added to the top of the reactions to prevent evaporation. Readings were taken every 30 s for up to 1.5 hours. Data processing and analysis is described in section 3.2.3.2.

3.2.2.2. Plasminogen activation with soluble templates

Where an enzyme and substrate bind to a common template a characteristic bell shape profile of activity versus log of template concentration is seen. This profile progresses to a peak at optimum template concentration and then the activity declines with increasing template concentration. The position of the optimum template concentration and the apparent K_M and k_{cat} of the enzyme are all interdependent. Hence there is no saturating template concentration so apparent K_M and k_{cat} values are valid under given conditions at a particular template concentration. Similarly the optimum template concentration depends on the concentrations of tPA and plasminogen in the system. Full characterisation of the system requires all components be varied. Soluble templates, fibrinogen and heparin, were investigated as follows.

a) Fibrinogen

The rate of plasmin production over a range of fibrinogen (Sigma or Calbiochem) concentrations from 13.2 mg/ml (40 µM) to 0.0092 mg/ml (29 nM) of clottable protein was measured in the presence of 0.84 nM tPA, 0.15 mM S-2251 (chromogenix, Milan, Italy) and either 0.32, 0.16, 0.1 or 0.08 µM glu-plasminogen (chromogenix, Milan, Italy) final concentrations.

All buffers and solutions were pre heated in a 37 ºC water bath. Aliquots of 40 µl each of 3-fold serial dilutions of fibrinogen 33 mg/ml to 0.023 mg/ml, were added to the wells of a 96-well microtitre plate, that had been heated to 37 ºC using a heating block. Then 20 µl each of either 1.6, 0.8, 0.5 or 0.4 µM plasminogen, 0.75 mM chromogenic substrate S-2251 and 4.13 nM tPA, were then added to the fibrinogen. All dilutions were made in buffer B, except for

tPA where dilutions were made in buffer C (buffer B + 1 mg/ml HSA). 60 µl of mineral oil was added to top of the reaction in each well to prevent evaporation. The rates of plasminogen activation were calculated as described in section 3.2.3.1 a. These rates were then plotted against the log concentrations of fibrinogen.

b) Heparin

The rate of plasmin production over a range of heparin sodium (Multiparin, Artex, New Zealand) concentrations from 2000 IU/ml to 0.0339 IU/ml was measured in the presence of tPA, S-2251 (chromogenix, Milan, Italy) and glu-plasminogen (chromogenix, Milan, Italy). Aliquots of 40 µl each of 3-fold serial dilutions of heparin from 5000 IU/ml to 0.085 IU/ml were added to the wells of a blocked 96- well microtitre plate, heated to 37 ºC using a heating block. Then 20 µl each of plasminogen, chromogenic substrate S-2251 and tPA, warmed to 37 ºC using a water bath, were then added to the heparin. 60 µl of mineral oil was added to top of the reaction in each well to prevent evaporation.

The concentration of S-2251 was added at 0.15 mM (final concentration) in all experiments. Two types of buffer were tested in this system; the first was buffer B. The second buffer was buffer D, which contains half the concentration of NaCl as buffer B and therefore had a lower ionic strength. All dilutions were made in buffer B or D, except for tPA where dilutions were made in buffers C or E.

A range of tPA concentrations from 13.2 nM to 0.1 nM and tPA variants at a final concentration of 6.6 nM and 0.826 nM were investigated in both buffers, with a final glu-plasminogen concentration of 0.2 µM. tPA at 0.826 nM was also investigated in the presence of 0.4 and 0.1 µM glu-plasminogen in buffer D.

The rates of plasminogen activation were calculated as described in section 3.2.3.1.a. These rates were then plotted against the log concentrations of heparin.

3.2.2.3. Plasminogen activation in fibrin clots

tPA and plasmin chromogenic substrate were added to pre-formed fibrin clots containing plasminogen. As activator enters the clot, the concentration of plasmin generated, was followed by monitoring the rate of hydrolysis of plasmin chromogenic substrate. In these assays the condition of the fibrin can be modified to have more or less C-terminal lysines, by forming the clots with fibrinogen that has been treated with either plasmin or using fibrin clots incorporating carboxypeptidase B, respectively. All buffers and reagents were pre warmed in a 37 ºC water bath.

a) Plasminogen activation in clear clots

Fibrin clots were made in microtitre plates (blocked for at least 4 h with 0.01% Tween 20) under conditions of ionic strength that produce clear clots (Longstaff and Whitton, 2004), by mixing 20 µl of bovine thrombin at 4 IU/ml (Diagnostic Reagents Thame, Oxon), 60 µl of human fibrinogen at 7.5 mg/ml clottable protein (Sigma) and 20 µl each of 2-fold serial dilutions of Glu-plasminogen (Chromogenix, Milan, Italy) from 1.6 µM to 0.025 µM. Dilutions of plasminogen were made in buffer B. The clots were left to form for 30 min at 37ºC. tPA diluted in buffer C and plasmin chromogenic substrate S2251 (Chromogenix, Milan, Italy) were mixed to a final concentration of 400 pM tPA and 0.64 mM S2251 and 40 µl added to the pre-formed clots. Mineral oil (60 µl) pre-warmed to 37ºC was overlaid to prevent evaporation. An overview of this is shown in figure 3.1.

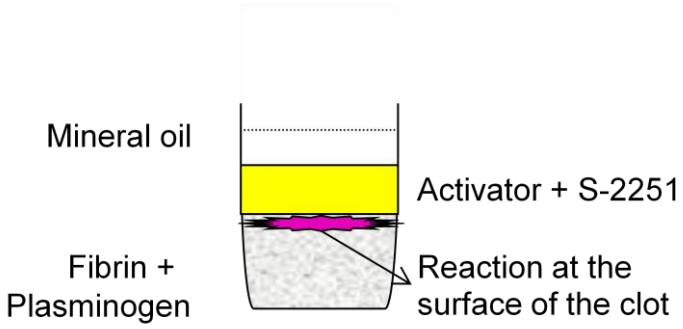


Figure 3.1: Format of clear clot lysis reaction, representing a single well of a microtitre plate. The fibrin and plasminogen forming the clot at the bottom of the well with the activator (tPA) and substrate (S2251) added to the top followed by mineral oil. The reaction occurs at the interface of the clot and plasmin is released cleaving the substrate to produce pNA. Adapted from (Longstaff and Whitton, 2004).

The change in absorbance at 405 nm which corresponds to the pNA cleaved by plasmin is then monitored at 37ºC for 90 min with readings every 30 s. Rates of plasminogen activation were then calculated as in section 3.2.3.1 a. and were converted from units of absorbance/s^2 to rates of plasmin generation Ms^{-1} using the method by Longstaff et al, 1995 (Longstaff et al, 1995). The rates of plasmin generation were then plotted over a range of plasminogen concentrations producing hyperbolic plots as described in section 3.2.3.2. a.

Modified fibrin with additional C-terminal lysines was made by pre-treating fibrinogen with plasmin-Sepharose at 73 pM for 20 min at room temperature with continuous mixing using a roller mixer. The plasmin-Sepharose was removed by filtration prior to use. Plasmin-Sepharose was made by coupling 1.5 mg glu-plasminogen (chromogenix, Milan, Italy) to 0.3 g of cyanogen bromide activated Sepharose 4B. The Sepharose was swollen in 1 mM HCl giving about 1 ml of gel, then washed three times with 30 ml of 1 mM HCl for 5 min each. The final HCl wash was removed and the gel transferred into 2 ml of 0.75 mg/ml glu-

plasminogen (Chromogenix, Milan, Italy) in buffer (v) (see buffers section 3.2.1) and was incubated for 2 h at room temperature with constant mixing. Any remaining active groups were then blocked using blocking buffer (see section 3.2.1) for 2 h at room temperature on the roller mixer. Any remaining excess absorbed proteins were washed away using alternate high /low pH by alternating 3 times each, 5 ml of 0.1 M Tris pH 8.0 and 0.1 M Acetate, 0.5 M NaCl pH 4.0 for 5 min each and the final wash removed. The plasminogen-Sepharose gel was then re-suspended in 1 ml of buffer B and then treated with 12 µl of streptokinase (Streptase, CSL Behring) (giving a final concentration of 1800 IU of streptokinase) for 30 min at room temperature with constant mixing, washed and stored as a 50% (v/v) slurry in 20 % ethanol.

To investigate the importance of C-terminal lysine formation during fibrinolysis, clots were made that incorporated CPB. CPB, 16 units was added to 7.5 mg/ml fibrinogen solution in buffer B, 20 min before clotting.

b) Plasminogen activation and simultaneous fibrinolysis in fibrin clots

To investigate both plasminogen activation and fibrin lysis by tPA, simultaneously, the method for the clear clot plasminogen assays (a) above was modified. Fibrinogen (Calbiochem) was dissolved in buffer B to give a solution of 50 mg/ml clottable protein and this solution was flash frozen in small aliquots in liquid nitrogen and stored at -40 °C until needed. Clots made with this fibrinogen solution were slightly turbid and fibrin lysis could be monitored by following absorbance changes in fibrin as the clot is broken down. Simultaneously, plasminogen activation was monitored by following generation of pNA, as described above in section 3.2.2.3.a. Measuring plasminogen activation and fibrinolysis was performed using two approaches, the first was measuring both plasminogen activation and

fibrin lysis in the same plate by taking readings at 2 wavelengths simultaneously throughout the kinetic run, 405 nm for plasminogen activation and 650 nm for changes in clot turbidity. The second approach was to make up two plates using the same solutions, one plate containing chromogenic substrate, used to monitor plasminogen activation at 405 nm and the second plate was without chromogenic substrate monitor at fibrin lysis at 405 nm by changes in clot turbidity. The method where simultaneous dual wavelength readings were taken was less sensitive as clot turbidity readings are lower at 650 nm than at 405 nm, measurement of clot lysis at 650 nm was selected because there is no interference from the pNA generated by plasmin.

As with method (a) above, clots were formed in a 96-well plate, pre blocked with 0.01% Tween 20, turbid clots were formed by adding 10 µl of a mixture containing 20 mg /ml fibrinogen (in buffer B) and 91 µg /ml of glu plasminogen, the clotting process was started by adding 50 µl of bovine thrombin to give 2 IU /ml final concentration in the clots. Clotting was allowed to proceed for 30 min before addition of tPA. Plasminogen activation and fibrinolysis was initiated with the addition of tPA (in buffer B or in 3 mM S-2251 in buffer B see below). Where a range of tPA concentrations were examined, aliquots of 160 µl each of 2 fold serial dilutions of tPA from 1.56 nM to 0.195 nM were mixed with 40 µl of 3 mM S-2251 and then 40 µl of that mixture were added to the surface of up to 4 clots. To prevent evaporation 60 µl of mineral oil was added to the top of the reactions and the plate was monitored at 405 nm, and 650 nm simultaneously, with readings 45 s for 5 h at 37 ºC. To remove the interfering absorbance caused by the turbidity of the clot at 405nm, absorbance readings at 650nm were multiplied by 3 and subtracted from the absorbance at 405nm (using Excel, because the absorbance of the clot at 405nm is 3 times higher than at 650nm). Where separate plates were used to monitor fibrinolysis and plasminogen activation, both plates were monitored at 405 nm, in one plate tPA was made up as above, in the second parallel

plate tPA was diluted and mixed with buffer B rather than 3 mM S-2251 and clot turbidity was followed. Data collection and processing is described in section 3.2.3.1 and 3.2.3.3. Results were presented as initial rates of plasminogen activation, using absorbance changes due to S-2251 hydrolysis up to 0.1, where there is also < 10 % depletion of plasminogen, where data were collected in the presence of S-2251 chromogenic substrate. Alternatively, fibrinolysis rates were assessed as time to 50 % lysis (or some other lysis point could be selected, see section 3.3.3.2)

3.2.3. Data collection and analysis

Enzyme activities were measured using a microtitre plate reader (Molecular Devices, Sunnydale, CA, USA).

Where tPA activity on a direct chromogenic substrate, S-2288 (X-Y-Z-pNa, Chromogenix, Milan, Italy) was studied, rates of substrate hydrolysis were monitored as release of p-nitroaniline (pNA) by following changes in absorbance at 405 nm over time. The rate of change in absorbance was calculated by the plate reader software (Softmax Pro version 5.0, Molecular Devices, Sunnydale, CA, USA) over the portion of the curve representing the maximum initial rates, where substrate depletion was < 10 %. Absorbance readings were converted to rates of pNA produced in moles per litre per second (Ms^{-1}), using an apparent molar extinction coefficient for pNA of 2940 absorbance/M which is predetermined under conditions of the assay in this microtitre plate format

To determine the rate of plasminogen activation catalysed by tPA, the generation of plasmin was monitored using the plasmin chromogenic substrate, S-2251 (X-Y-X-pNa, Chromogenix, Milan, Italy). Initial rates with excess plasminogen substrate are expected to result in a linear increase in plasmin concentration, which corresponds to an exponential increase in hydrolysis

of the plasmin substrate, S-2251 as followed by generation of pNA. Generation of pNA was measured by following absorbance at 405 nm for 1.5 h at 37 ºC. Initial rates of plasmin production were calculated from the slope of plots of absorbance versus time squared, up to a change in absorbance of 0.1. In this transformed plot of absorbance versus time squared the slope is proportional to the rate of plasminogen activation and in an ideal situation is linear and where less than 10% of substrates plasminogen and S-2251 have been consumed.

3.2.3.1. Data processing

The large amounts of data generated in kinetic assays to study plasminogen activation were processed in one of 2 ways, as follows.

a) GraFit

Raw data from Softmax Pro were exported into an Excel spreadsheet as a table of 96 columns of absorbance readings over time corresponding to the individual wells of a microtitre plate. The values not including the data labels were then copied into the data table in a GraFit template. A function was then applied to each column which subtracts the value in row 1 (the absorbance reading at time zero) from the rest of the values in that column. If the resulting absorbance change is less than 0.1 nm then the absorbance value is then written in to a new column. This generates a new table giving the absorbance readings up to a change of 0.1 nm. These are then plotted against time squared (as it is an autocatalytic reaction it shows a $time^2$ dependence) and linear regression is performed to calculate the rate of pNA production. These rates are then used in further analysis of the data.

b) Matlab

Raw data from Softmax Pro were exported into and Excel spreadsheet as a table of 96 columns of absorbance readings over time corresponding to the individual wells of a microtitre plate. A Matlab routine (written by Dr Colin Longstaff, personal communication) was then applied to sort the data and write a new Excel workbook consisting of 96 sheets corresponding to raw data from each well, including graphs of absorbance versus time squared and corresponding rate of plasmin generation.

A second Matlab routine was also used to analyse exported data from Softmax Pro to deal with changes in clot turbidity when fibrinolysis was being studied rather than plasminogen activation. In this case, Excel tables of absorbance versus time representing a kinetic run from a 96 well microtitre plate were sorted into a new Excel workbook consisting of 96 sheets corresponding to each well including raw data of absorbance versus time and a time to 50 % lysis (other endpoints of % lysis could also be readily selected) was calculated.

3.2.3.2. Fitting data to the Michaelis-Menten equation

Data collected to determine enzyme parameters, Km and kcat was analysed in one of two ways, as follows.

a) GraFit

Kinetic parameters, K_M and V_{max} were determined for both direct amidolytic substrate assays (tPA with S-2288) and where plasminogen was substrate and plasmin generation rates were monitored using S-2251. To determine apparent K_M and V_{max} values, the appropriate rate was plotted against substrate concentration, S-2288 or plasminogen, using Grafit software (Leatherbarrow, 2003) and data were fitted to the Michaelis-Menten equation below by non-linear regression.

Michaelis-Menten equation:

$$V = \frac{V_{max}[S]}{([S] + K_M)}$$

Where V is velocity expressed as molar concentration (M) of pNA or plasmin produced per second. V_{max} is the maximum velocity. [S] is substrate concentration expressed in M and K_M is the concentration of substrate that leads to half maximum velocity, also expressed in units of concentration, M. k_{cat} values were calculated from V_{max} / enzyme concentration. At this time there is no simple way of performing active site titration on tPA so protein concentration of the pure enzyme was used as an approximation for the concentration of active enzyme concentration, see section 2.3.6.2.

b) Excel

To compare enzyme amidolytic activities of tPA variants it was useful to plot Michaelis-Menten curves with 95% confidence intervals. In this way it was possible to test for significant differences between variants by checking for overlapping confidence intervals. Data from plots of substrate concentration ([S2288]) versus rate of pNA release were fitted to determine Vmax and Km using a modified version of an Excel routine developed for non-linear regression analysis using "Solver" as described by Brown (Brown, 2001), the fitting routine generated values for the fitted parameters, Vmax and Km along with the residual standard error and the number of degrees of freedom (DF, in this case the number of data points minus 2, which is the number of fitted parameters). The value for the 95 % confidence interval was then calculated as a 2 tailed t-distribution of 0.025 % and 0.975 % which is multiplied by the square root of the squared residual standard error divided by the DF. Values for the t-distribution are supplied automatically by functions in Excel.

t-dist(0.975, DF) x sqrt[resid std error^2/ DF]

3.2.3.3. Combistats

To measure concentrations of tPA in a solution versus a known standard, Combistats (European Directorate for the Quality of Medicines & HealthCare (EDQM) software was used. Combistats is a program for the statistical analysis of data from biological dilution assays or potency assays. Calculations were performed according to chapter 5.3 of the European Pharmacopeia to determine the concentration of a test substance relative to the concentration of a known standard. To measure the concentration of tPA in a test solution,

sample responses (e.g. enzyme activity, which is proportional to concentration) are entered in to the program along with each dose, to produce a dose response curve for activity against dose of tPA. A parallel-line model was then applied to give a potency ratio of standard and test sample, as well as 95 % confidence intervals of the unknown sample in relation to the standard. The Combistats program performs statistical tests to determine if the dose-responses were linear, have a significant slope and if standard and sample response curves were parallel. If the probability of non-linearity and non-parallelism was found to be significant to a probability of < 0.05, then the potency of the sample was not determined and the assay was deemed invalid. For an assay to be valid there also had to be significant regression and linearity (i.e., non-linearity and non-regression had to be non-significant at the 5 % level).

3.3. Results

3.3.1. Amidolytic activity of tPA variants in solution

The activity of full length tPA and variants expressed in chapter 2 were tested alongside commercial products Actilyse (full length tPA expressed in CHO cells) and Reteplase (rPA, kringle 2 and protease domain expressed in *E.coli*) using chromogenic substrate S2288 to show any differences between the proteolytic activity of the variants irrespective of the fibrin binding abilities. Figure 3.2. displays an example of the variants in a S2288 chromogenic substrate assay showing that the variants appear to have similar activities to each other and the Actilyse and rPA appear to have similar activities to the insect expressed versions itPA and irPA. The K_M, V_{max}, k_{cat} and k_{cat}/K_M values were calculated and are shown in table 3.1. k_{cat} values are calculated from V_{max} / enzyme concentration. At this time there is no simple way of performing active site titration on tPA so protein concentration of the pure enzyme is used as an approximation for the concentration of active enzyme (see section 2.3.6.2. for determination of protein concentration). To determine whether the variants are actually different, the 95% confidence intervals of the fits were calculated in Microsoft Excel (Brown, 2001) (Figure 3.2) Figure 3.2. shows the activation rate versus substrate concentration for all the variants studied from a representative assay and the 95% confidence intervals for the itPA:K2 del variant, as they were the widest. Overall, the data suggest that the amidolytic activity of each variant was not significantly different from any other variant at the 5% level.

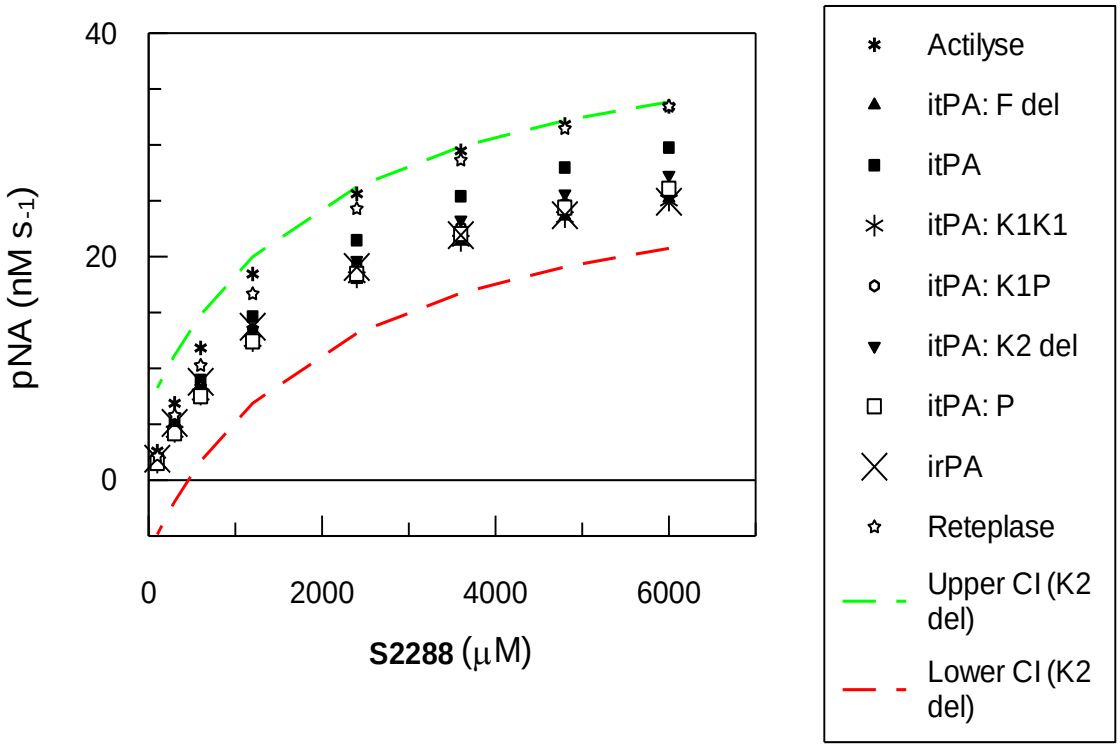


Figure 3.2.: Michaelis-Menten curves and 95% confidence intervals for variants in chromogenic substrate S2288 assay

The Michaelis-Menten plot for the itPA: K2 del variant in a S2288 assay, and the experimental data from the other variants. All the data points are within the 95% confidence intervals (dashed lines) based on the fit from the itPA: K2 del.

Table 3.1.: K_M, V_{max}, k_{cat} and k_{cat}/K_M values for variant proteins in a S2288 assay.

	K_M (μM)	V_{max} (nM s^{-1})	k_{cat} (s^{-1})	k_{cat}/K_M (μM^{-1} s^{-1})
Actilyse	1533	42	9.9	0.0065
itPA: F del	2221	35	8.3	0.0037
itPA	2090	40	9.5	0.0045
itPA: K1K1	2027	33	7.8	0.0038
itPA: K1P	1845	34	8.1	0.0044
itPA:K2 del	2090	37	8.8	0.0042
itPA: P	2280	36	8.5	0.0037
irPA	1533	31	7.3	0.0048
Reteplase	2020	45	10.7	0.0053

Amidolytic activity of insect expressed itPA converted to tcitPA with plasmin-Sepharose was compared to itPA, and scitPA, (non cleavable itPA variant – R275E itPA) before and after treatment with plasmin-Sepharose. Figure 3.3. shows that scitPA (R275E) has very similar rates to scitPA (R275E) after plasmin-sepharose treatment, tying in with results from the SDS-PAGE in chapter 2.4.1. showing that plasmin treatment of scitPA (R275E) has no effect due to the mutation in the cleavage site. itPA shows very similar rates to the scitPA (R275E) as would be expected as itPA was shown to be in the predominantly single chain form when visualised by SDS-PAGE seen in figure 2.3. tcitPA has significantly higher rates than itPA and scitPA (R275E) indicating that the protease domain is more efficient when tPA is in the two-chain form.

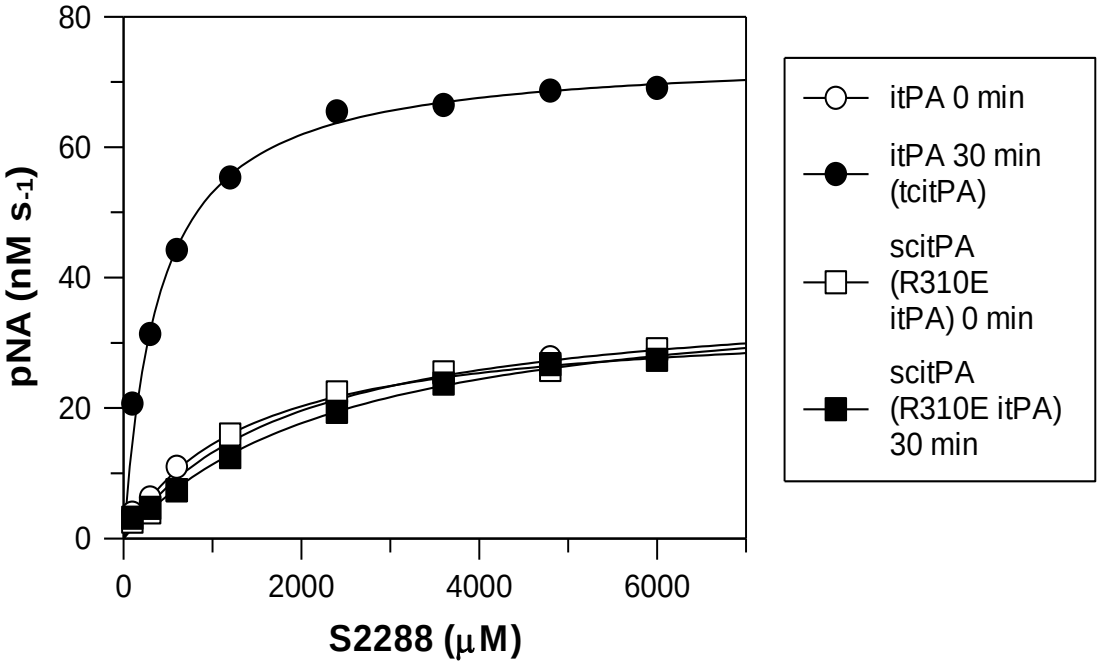


Figure 3.3. Michaelis-Menten curves for itPA and scitPA (R275E) before and after plasmin-Sepharose treatment with chromogenic substrate S2288 assay

Michaelis-Menten plots for itPA and scitPA (R275E) before and after treatment with plasmin-Sepharose in a S2288 assay. The times given in the legend box indicate the incubation period with plasmin-Sepharose. The plots for scitPA (R275E), before and after plasmin-Sepharose treatment as well as the plots for itPA before plasmin-Sepharose treatment are all very similar, where as the rates for the itPA after plasmin-Sepharose treatment (tcitPA) are much faster.

3.3.2. Plasminogen activation with soluble templates

Soluble templates follow a template model such that tPA and plasminogen are bound and brought into close proximity, giving higher local concentrations, and thus increasing the rate of plasminogen activation. Increasing template concentrations lead to a maximum activation rate after which increased template leads to the binding of tPA and plasminogen to different template molecules causing a reduction in plasminogen activation resulting in a bell shaped curve of plasmin generation rate versus log template concentration. The position of the optimum template concentration depends on the concentration of the other reactants and their strength of binding to the template.

3.3.2.1. Plasminogen activation with fibrinogen as a template

The effect of fibrinogen as a template in the activation of plasminogen was investigated as fibrinogen is known to be a weak stimulator of natural, full length tPA (Bringmann et al, 1995). Fibrinogen is easier to study than fibrin as it is a soluble template for the binding of tPA and plasminogen and forms a homogeneous system rather than the heterogeneous fibrin system described in chapter 3.3.3. The stimulation of tPA mediated-plasminogen activation by fibrinogen follows a template model described above.

The connection between enzyme activity and the binding properties of the tPA variants shown in table 2.3 in the molecular biology section, were investigated by looking at initial plasminogen activation rates in the presence of three different types of fibrinogen (1) carboxypeptidase-B-treated fibrin, where C-terminal lysines are rapidly removed when formed by plasmin; (2) plasmin-treated fibrinogen with additional C-terminal lysines formed by pre-treating fibrinogen with plasmin; (3) normal fibrinogen that has had no treatment, that

contains no C-terminal lysines but which will develop C-terminal lysines as plasmin is generated in the assay. The K2 domain relies on lysines to bind to fibrin, whereas the F domain does not. The aim is to improve our understanding of roles of the tPA K2 and F domains in fibrinogen binding and the importance of different modes of binding in plasminogen activation. We also hope to understand the relative contribution of C-terminal lysines on acceleration of plasminogen activation through increased tPA binding and increased plasminogen binding.

In these assays the optimum fibrinogen concentration and height of the peak are looked at to get idea of stimulation and binding strength. Figure 3.4. shows that binding of tPA to fibrinogen is required for stimulation of plasminogen activation to occur (as the itPA: P and itPA: K1P variants which contain no known binding sites, show no stimulation of plasminogen activation) and that both the F and K2 domain are involved in binding. The itPA: F del variant shows a higher rate of plasminogen activation than the itPA: K1K1 and irPA variants, which themselves show similar rates of plasminogen activation. However, it has been consistently seen that a lower concentration of fibrinogen is required for optimal stimulation of irPA and itPA: K1K1 than for itPA: F del indicating tighter binding by irPA and itPA:K1K1. The optimal stimulation of itPA: K1K1 is at a fibrinogen concentration between itPA: F del and irPA. These results show that the K2 domain is more important in initial plasminogen activation than the F domain, despite the fact that the F domain appears to bind with higher affinity to fibrinogen than the K2 (when in the itPA: F del variant). The more dramatic change in the structure of irPA (only consisting of the K2 and P domains, see table 2.3.) may allow the K2 domain to bind with higher affinity but this appears to result in a loss of plasminogen activation capacity. The itPA variant shows the highest plasminogen activation rates and has a broad activation profile which suggests that both F and K2 domain bind fibrinogen where available. The activity of itPA is greater than the sum of the parts

(itPA: F del and itPA: K1K1), shown as a dashed line in figure 3.4.A, suggesting some synergy between the K2 and F domains in tPA.

The treatment of fibrinogen with CPB to remove C-terminal lysines as they are generated decreased the strength of binding of all the variants, figure 3.4.B shows that the activation profile of itPA has become less broad and that optimum stimulation occurs at a higher fibrinogen concentration. Optimum stimulation of all the variants occurs at a higher fibrinogen concentration with CPB-treated fibrinogen compared to normal fibrinogen but the optimal stimulation of itPA: K1K1 and irPA still takes place at a lower concentration of CPB-treated fibrinogen than itPA: F del. The removal of the C-terminal lysines appears to have reduced the affinity of the variants for fibrinogen, so that more fibrinogen is required to bind the same amount of activator and plasminogen. The itPA: K1K1 variant contains no K2 domain therefore no reduction in binding by this variant was expected but was observed suggesting other domains besides K2 can interact with C-terminal lysine residues. Figure 3.4.B also shows that the rates of plasminogen activation by itPA: K1K1 have increased relative to the other variants and are similar to the rates shown by itPA: F del, whereas in un-treated fibrinogen the rates were lower than those shown by itPA: F del.

Figure 3.4.C shows that the treatment of fibrinogen by plasmin broadened the activation peak of itPA and itPA: F del across the lower concentrations of fibrinogen compared to un-treated fibrinogen. The increase in K2 binding sites could allow for more binding to occur even at lower fibrinogen concentrations. The affinity of the itPA: K1K1 variant was lower for plasmin-treated fibrinogen than un-treated fibrinogen, this agrees with the results of the CPB-treated fibrinogen indicating that binding of plasminogen blocks or interferes with binding by the F domain.

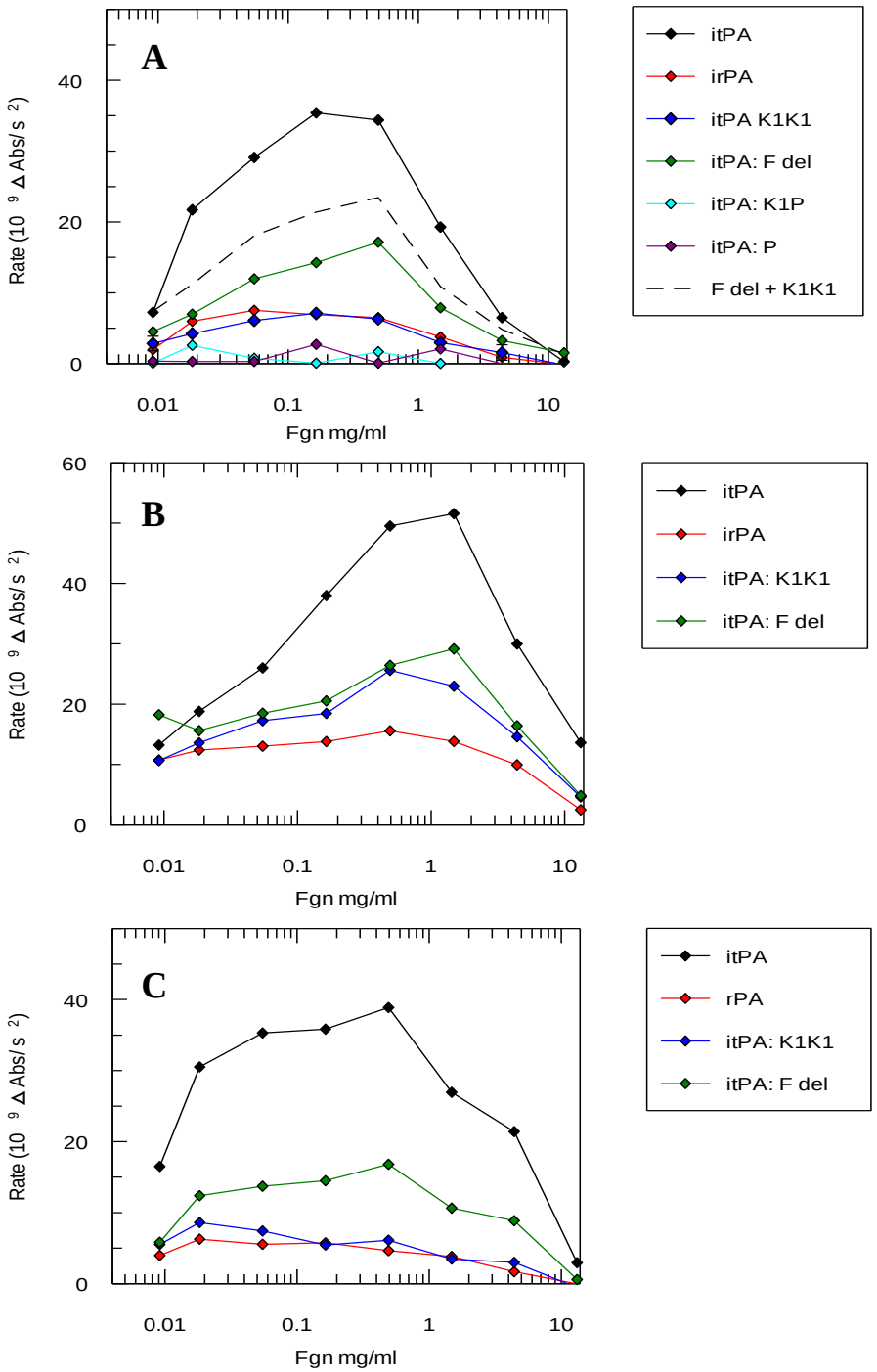


Figure 3.4: Plasminogen activation by itPA and variants in the presence of fibrinogen. Plasminogen activation rates of itPA and variants were measured over a range of concentrations of A) normal untreated fibrinogen, B) CPB-treated fibrin and C) plasmin--treated fibrinogen. Activation rates are represented as a change of absorbance over time squared, measured by the release of *p*NA from S2251 as plasmin is generated. Mean rates of 2 replicates are plotted against log fibrinogen concentration.

Fibrinogen stimulated plasminogen activation by tPA and variants was tested over a range of plasminogen concentrations and the results can be seen in figure 3.5. Increasing the plasminogen concentration increased the rates of plasminogen activation of all three variants as expected. Detailed Michaelis-Menten curves were not performed with all tPA variants, but these results show that there were no major differences in K_M values for these variants. It was also noted that at the highest plasminogen concentration tested: (1.6 μM) more fibrinogen was required for optimal plasminogen activation than at 0.4 and 0.8 μM (data not shown).

The effect of varying activator concentration was also investigated and figure 3.6 shows that the plasminogen activation rates of the three variants tested; itPA, itPA: K1K1 and itPA: F del decreased with decreasing activator concentration, as expected. The concentration of fibrinogen for optimal plasminogen activation to occur remained the same at all activator concentrations with itPA and itPA: F del but changes in peak activation rate were non-linear with itPA: K1K1 and appeared to be accompanied by a shift in optimum fibrinogen concentration. These results suggest binding of the finger domain in itPA:K1K1 may be heterogeneous, involving multiple interactions.

Fibrinogen stimulated plasminogen activation by scitPA (R275E) and tcitPA variants were investigated over a range of untreated fibrinogen concentrations. Figure 3.7. shows that both sc and tcitPA are stimulated by fibrinogen but scitPA (R275E) is stimulated to give greater plasminogen activation rates and shows peak activity at a lower fibrinogen concentration than tcitPA. This is at odds with the results of the amidolytic activity with S2288 in which the tcitPA shows much greater activity to the scitPA (R275E) (see section 3.3.1). These results suggest scitPA (R275E) binds fibrinogen with higher affinity than tcitPA and this leads to greater stimulation of plasminogen activation.

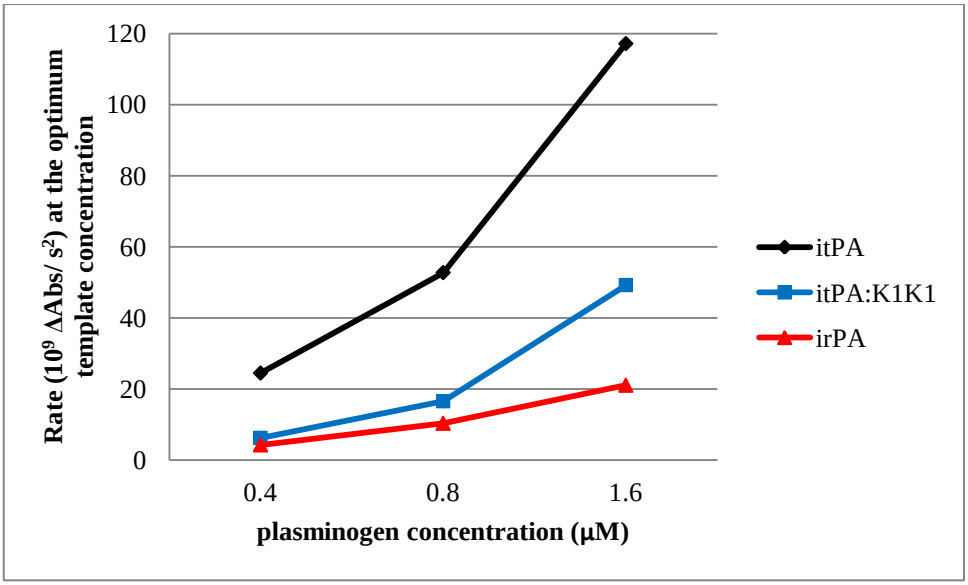


Figure 3.5 Plasminogen activation rates at the optimum fibrinogen concentration for itPA, irPA and itPA:K1K1 in the presence of 3 plasminogen concentrations. Plasminogen activation rates of itPA, irPA and itPA:K1K1 variants were measured over a range of untreated fibrinogen concentrations and the activation rates at the optimum fibrinogen concentration are displayed for 3 different plasminogen concentrations. The optimum fibrinogen concentration was 0.165 mg/ml for all the variants at 0.4 and 0.8 µM plasminogen and 0.493 mg/ml at 1.6 µM plasminogen.

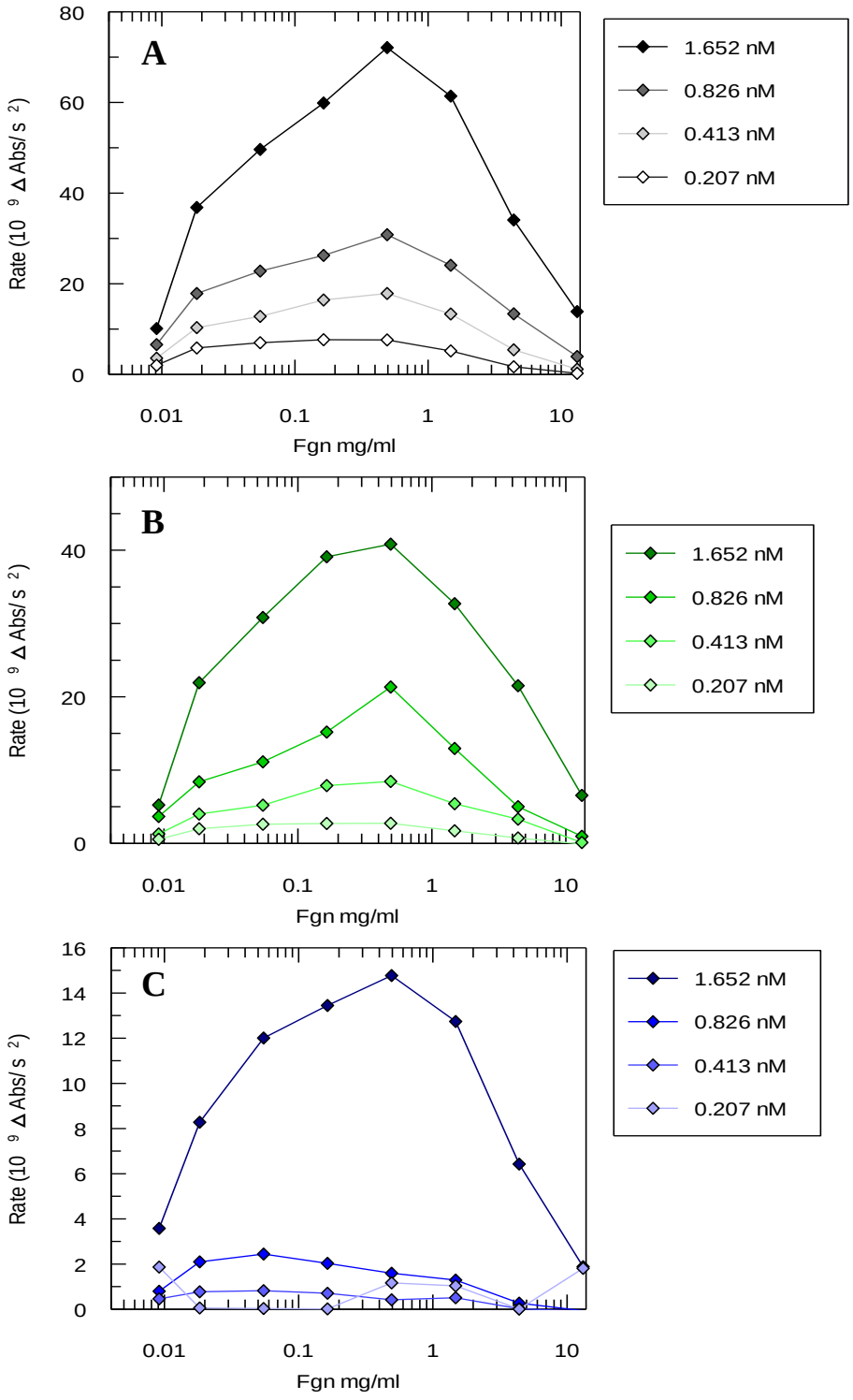


Figure 3.6.: Plasminogen activation by itPA and variants at 4 activator concentrations in the presence of fibrinogen. Plasminogen activation rates at 4 concentrations of A) itPA B) itPA: F del and C) itPA:K1K1 were measured over a range of fibrinogen concentrations. Activation rates are represented as a change of absorbance over time corresponding to the release of *p*NA from S2251 by plasmin. Rates are plotted against log fibrinogen concentration.

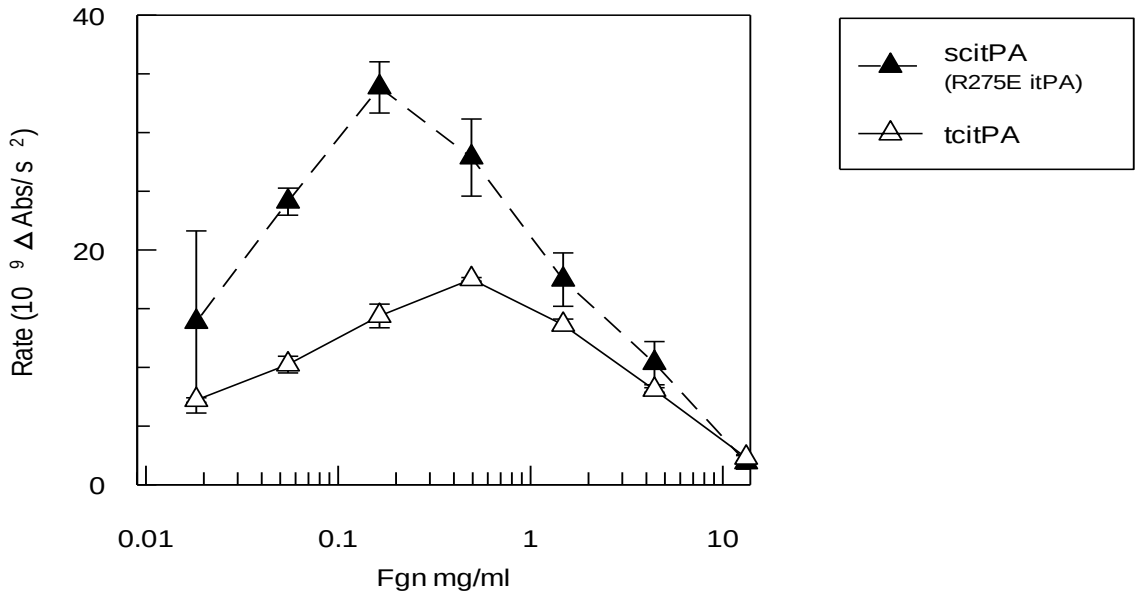


Figure 3.7: Plasminogen activation by scitPA (R275E) and tcitPA in the presence of fibrinogen. Plasminogen activation rates of 4.22 nM scitPA (R275E) and tcitPA were measured over a range of fibrinogen concentrations. Activation rates are represented as a change of absorbance over time corresponding to the release of *p*NA from S2251 by plasmin. Rates are plotted against log fibrinogen concentration.

In summary binding to fibrinogen is required for plasminogen activation to occur and is greatest when both K2 and F domains are available to bind. Binding by the K2 domain is best for plasminogen activation and the F domain appears to bind more tightly to fibrinogen when the structure of the protein is more similar to full length itPA. The itPA: F del shows higher plasminogen activation than the irPA even though both contain the K2 binding sites, indicating the more dramatic change in the structure of irPA has affected the binding and activity or that there are other sites in tPA that contribute to binding to fibrinogen. The rates of plasminogen activation do not appear to correlate with the affinity of the variants for fibrinogen. sctPA appears to bind with higher affinity to fibrinogen than tctPA, which causes greater stimulation of plasminogen activation. Thus the activity of sctPA catches up with tctPA, which is more active in solution. The differences between sc- and tctPA in binding and activity complicates our understanding in kinetic studies as sctPA will be converted to tctPA during the course of the reaction. Furthermore, it should be remembered that lysines are also involved in plasminogen binding to fibrinogen and generation of C-terminal lysines will affect tPA and plasminogen binding. Nevertheless, the kinetic data generated in these studies will be useful in the modeling chapter to get a better understanding of the regulation of tPA activity.

3.3.2.2. Plasminogen activation with heparin as a template

The effect of heparin as a template for plasminogen activation by tPA was investigated as heparin is a potent anti-coagulant that is often administered alongside tPA in the treatment of myocardial infarction to prevent reocclusion of a coronary artery. Other studies have found that heparin can stimulate plasminogen activation by tPA and it has been suggested that this could potentially cause systemic activation of plasminogen by tPA rather than at the site of the clot (Andrade-Gordon and Strickland, 1986; Liang et al, 2000). Heparin like fibrinogen is also a soluble template and appears to follow a template profile. Due to the fact that heparin also follows template profile as an activator of tPA, it provides an interesting alternative system to fibrinogen stimulation. Significantly, heparin differs from fibrinogen in not being a substrate for plasmin, which simplifies the analysis and future modelling of the kinetics.

The effect of heparin as a template for plasminogen activation by tPA and variants was investigated over a range of heparin concentrations in buffer B and in buffer D, which contains only half the NaCl of buffer B and therefore has a lower ionic strength. Ionic strength has been shown to be important in tPA binding to heparin (Rijken et al, 1993) and that ionic strength lower than physiological ionic strength results in higher affinity of tPA for heparin. In binding experiments using surface plasmon resonance (see section 4.3.2.5), binding to heparin by itPA was found to be too weak in buffer B to calculate kinetic or equilibrium binding constants, hence buffer D was introduced for kinetic studies. Kinetic data presented in figure 3.8 and 3.9 show a typical template profile of heparin stimulation with a broad peak over a concentration range of 10^{5} IU heparin. As seen with fibrinogen in section 3.3.2.1, both the F domain and the K2 domain are involved in binding to heparin for plasminogen activation to occur but in heparin the itPA: K1K1 variant showed higher

plasminogen activation rates than the itPA: F del and irPA variants (see figure 3.8), indicating that the F domain binding is more important than K2 domain binding for plasminogen activation to occur. The itPA: F del had higher plasminogen activation rates than the irPA even though both contain the K2 binding site. This was also seen with fibrinogen as a template (figure 3.4) and suggests there are more binding sites for heparin over the length of the tPA molecule or more drastic structural rearrangements in the truncated irPA affect binding and/or kinetics. Full length tPA showed the highest plasminogen activation rates and the sum of the parts (itPA: F del and itPA: K1K1) seem more additive in heparin than in fibrinogen. When heparin stimulated plasminogen activation was investigated in buffer D, see figure 3.8(B), the rates of plasminogen activation increased approximately 10-fold and the heparin concentration that gave optimal stimulation was lower for all the variants, compared to the results in buffer B (figure 3.8.(A)). This suggests that at lower ionic strength, binding of tPA to heparin is tighter when binding via both the F and K2 domain, but of course the binding of heparin and plasminogen must also be taken into account. Clearly, this tighter binding leads to both a shift in optimum heparin concentration an increase in plasminogen activation.

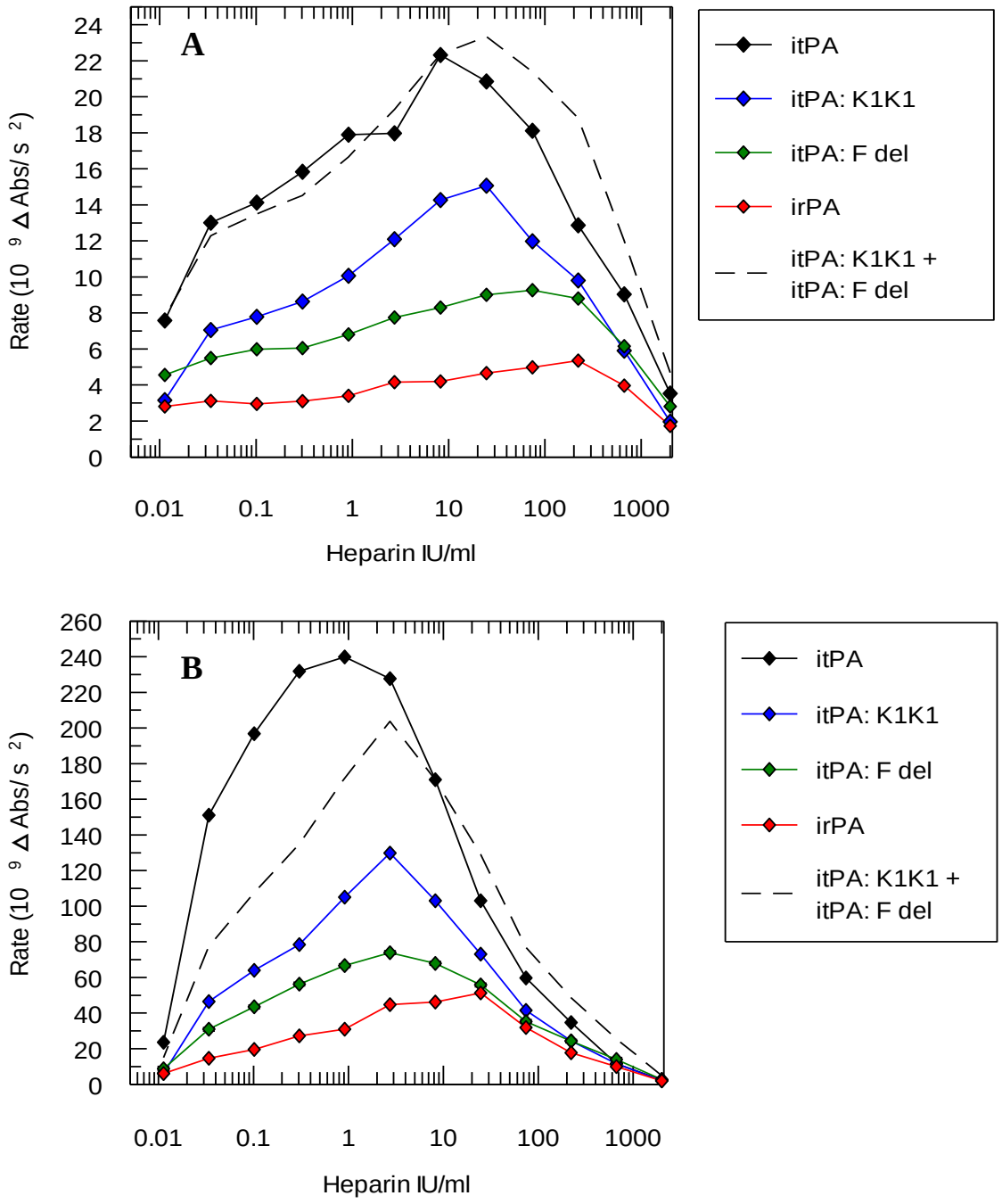


Figure 3.8. Plasminogen activation by itPA and variants in the presence of heparin. Plasminogen activation rates were measured over a range of heparin concentrations. itPA and variants were investigated at A) 0.826 nM activator concentration in buffer B, B) 0.826 nM activator concentration in buffer D. Activation rates are represented as a change of absorbance over time corresponding to the release of *p*NA from S2251 by plasmin. Rates are plotted against log heparin concentration.

To investigate the effect of itPA concentration on the rate of plasminogen activation when stimulated by heparin, 8 concentrations of tPA were each tested over a range of heparin concentrations. The initial rates of plasminogen activation were calculated and plotted against log heparin concentration to produce the expected bell shaped curve. The concentration of heparin that gave the optimum plasminogen activation rates and also the optimum rates were plotted for each tPA concentration, these experiments were performed in both buffer B and D. The result (data not shown) showed a linear relationship between variant concentration and rate of plasminogen activation and an increase in the concentration of heparin required for optimal stimulation.

To investigate the effect of plasminogen concentration on plasminogen activation and strength of binding to heparin, 3 concentrations of plasminogen were each tested over a range of heparin concentrations with 4.33 nm (0.826 nM final concentration) of tPA, itPA: K1K1, itPA: F del and irPA. The initial rates of plasminogen activation were calculated and plotted against log heparin concentration to produce a bell shaped curve. The activation profiles of the 4 variants in 2, 1, and 0.5 μM plasminogen in buffer D are shown in figure 3.9. Higher plasminogen concentration resulted in higher plasminogen activation rates but the optimum heparin concentration also shifted when F binding was dominating as in figure 3.9. B,

In summary both the F and K2 domains are involved in binding to heparin with F binding appearing to be more important than K2 domain. itPA: F del has higher activity than irPA suggesting that other sites on tPA may contribute to binding or that the gross structure of tPA is important. Activation and binding are dependent on ionic strength and the lower the ionic strength the tighter the binding, the template profile means that plasminogen also binds to heparin and the ionic strength is also likely to modulate plasminogen binding.

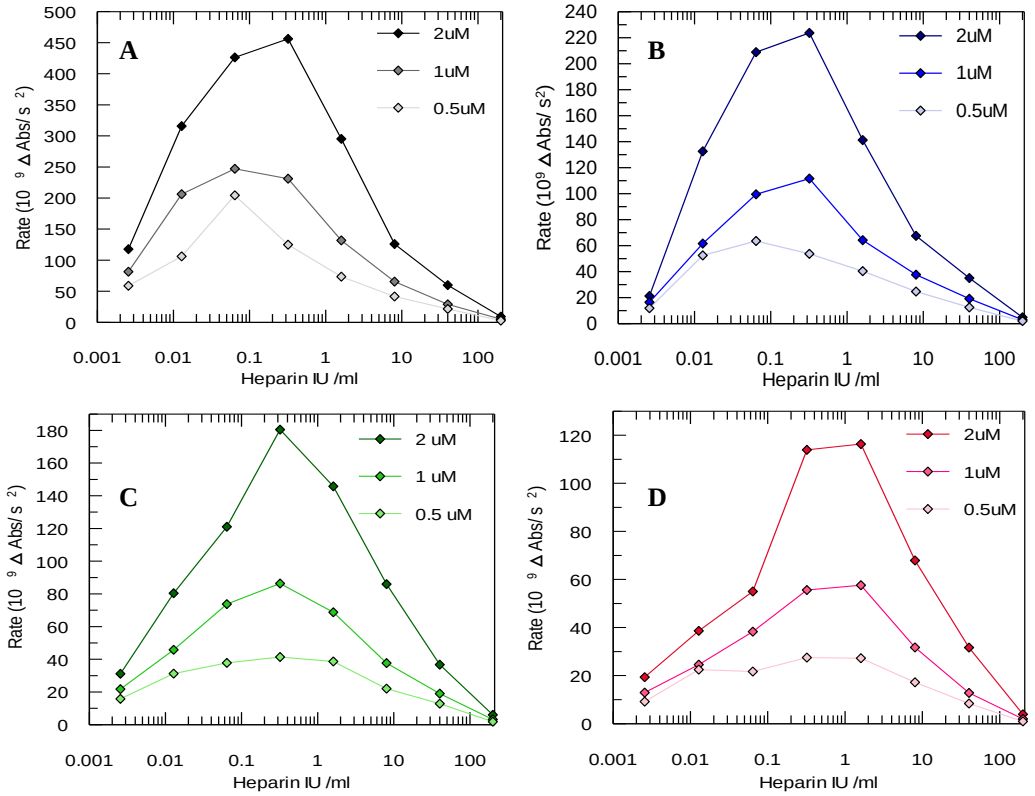


Figure 3.9. Plasminogen activation by itPA and variants with 3 plasminogen concentrations in the presence of heparin. Plasminogen activation rates of A) itPA, B) itPA: K1K1, C) itPA: F del, and D) irPA at a concentration of 0.826 nM were measured over a range of heparin concentrations with 3 plasminogen concentrations as shown, in buffer D. Activation rates are represented as a change of absorbance over time squared measured by the release of *p*NA from S2251 as plasmin is generated. Rates multiplied by 10^9 are plotted against log fibrinogen concentration.

3.3.3. Fibrin stimulation of tPA activity

3.3.3.1. Measuring initial plasminogen activation rates in fibrin and the rate of fibrin lysis.

Three clot overlay methods were used to measure the initial rates of plasminogen activation by tPA in the presence of fibrin described in detail in section 3.2.2.3. The first; is the clear clot lysis assay (Longstaff and Whitton, 2004), where a transparent fibrin clot is made in a buffer of optimized ionic strength and the rate of plasmin production is calculated from the change in absorbance at a wavelength at 405 nm caused by the generation of pNA. Two variations of the method to measure fibrin lysis by changes in clot turbidity were used. In one method, the dual wavelength clot lysis assay, both fibrin lysis and plasmin production were measured simultaneously in the same plate by taking readings at two wavelengths at each time point throughout the kinetic run, 405 nm for plasminogen activation and 650 nm for changes in clot turbidity. The alternative to this was to use 2 simultaneous plates made up using the same solutions but one plate included chromogenic substrate, used to monitor plasminogen activation at 405 nm and the second plate was without chromogenic substrate to monitor fibrin lysis at 405 nm by changes in clot turbidity. This method required two plate readers. The method where simultaneous dual wavelength readings were taken was less sensitive as clot turbidity readings are lower at 650 nm, which was selected because there is no interference from the pNA generated by plasmin, see methods section 3.2.2.3. for more details.

When using fibrin as a template it is not possible to vary the fibrin concentration as it would result in a change in the structure of the clot, therefore more emphasis was placed on varying the concentration of plasminogen or the concentration of activator. Where plasminogen concentration was varied results could be summarised as changes in apparent Km for

activation within the clot. Where activator concentration was varied results were summarised by comparing observed potencies of activators using parallel line analysis and Combistats software (section 3.2.3.3).

3.3.3.2. Fibrin as a template and the effects of plasminogen concentration on the domain variants

The dual wavelength assay performed with two plates using the same solutions, one to monitor plasminogen activation and the second to monitor fibrin lysis both monitored at 405 nm was used to investigate the activity of all the variants and itPA at three different plasminogen concentrations over a range of activator concentrations. The rates of plasminogen activation and fibrin lysis of each variant were compared against the rates of full length itPA and the relative potency calculated using a parallel line model in Combistats (see section 3.2.3.3.). The results shown in figure 3.10 are for initial rates of plasminogen activation monitoring S-2251 hydrolysis and are expressed as % activity relative to full length itPA at the highest plasminogen concentration; 0.5 μM (which is set as 100%). Figure 3.10. shows that relative potencies of activators are itPA> itPA: K1K1> itPA: F del indicating that binding to fibrin by the F domain is more important than binding by the K2 domain in fibrin. As noted with soluble templates in the previous sections, the rates of the irPA are lower than the itPA: F del which again may be due to the more dramatic change in the structure of irPA or indicates that additional binding sites are available throughout the tPA molecule. The itPA: K1P and the itPA: P variants show little or no fibrin stimulation of plasminogen activation. These trends are observed in all 3 plasminogen concentrations tested.

When looking at fibrin lysis (rather than plasminogen activation), time to reach 50% lysis for tPA and the variants, shown in figure 3.11, the itPA: F del variant increases relative to the

itPA: K1K1 variant at the higher plasminogen concentrations (this is not observed at the lower 0.05 μM plasminogen concentration). This discrepancy between plasminogen activation and fibrin lysis is most likely due to the assay method where 50% lysis takes a significant time to occur and during this time C-terminal lysines are generated which bind itPA: F del but not itPA: K1K1. The method used to calculate initial rates of plasminogen activation in fibrin works on initial rates and only uses the early stage of the reaction. This explanation is supported if data in Figure 3.11 are reanalyzed to look at time to 20% lysis, as shown in figure 3.12 where itPA:K1K1 is still more potent than itPA: F del. The catch up of activity of itPA: F del is a late phenomenon.

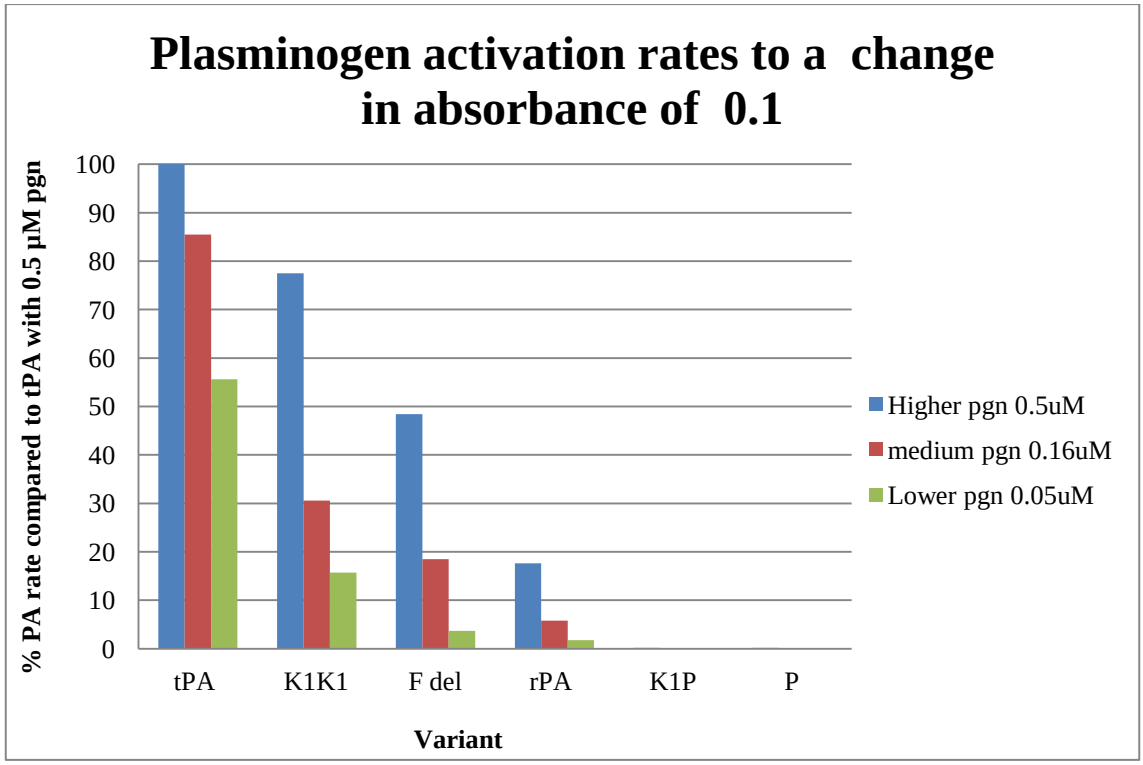


Figure: 3.10: Initial plasminogen activation rates itPA and variants at 3 plasminogen concentrations in un-treated fibrin clots. The results are displayed as % activity relative to itPA in 0.5 µM plasminogen.

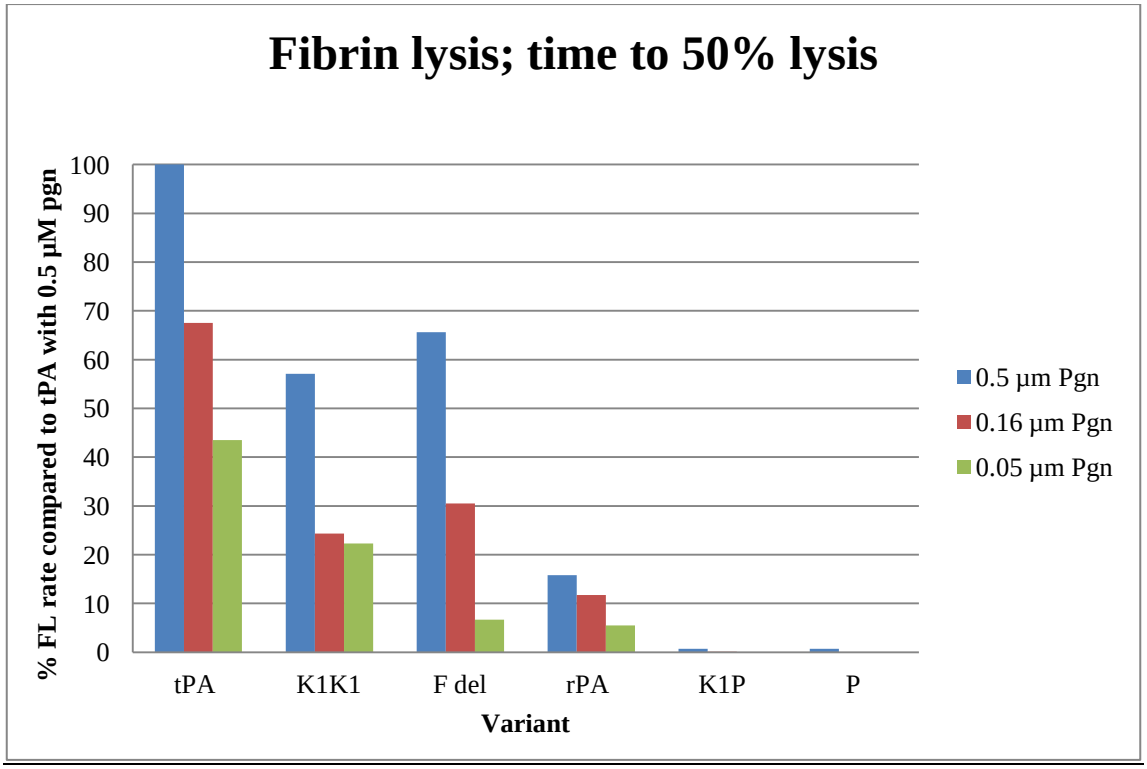


Figure: 3.11.: Fibrin lysis rates (measured as time to 50% lysis) itPA and variants, itPA: K1K1, itPA: F del, irPA, K1-protease and protease domain alone at 3 plasminogen concentrations in untreated fibrin clots. The results are displayed as % activity relative to itPA in 0.5 µM plasminogen.

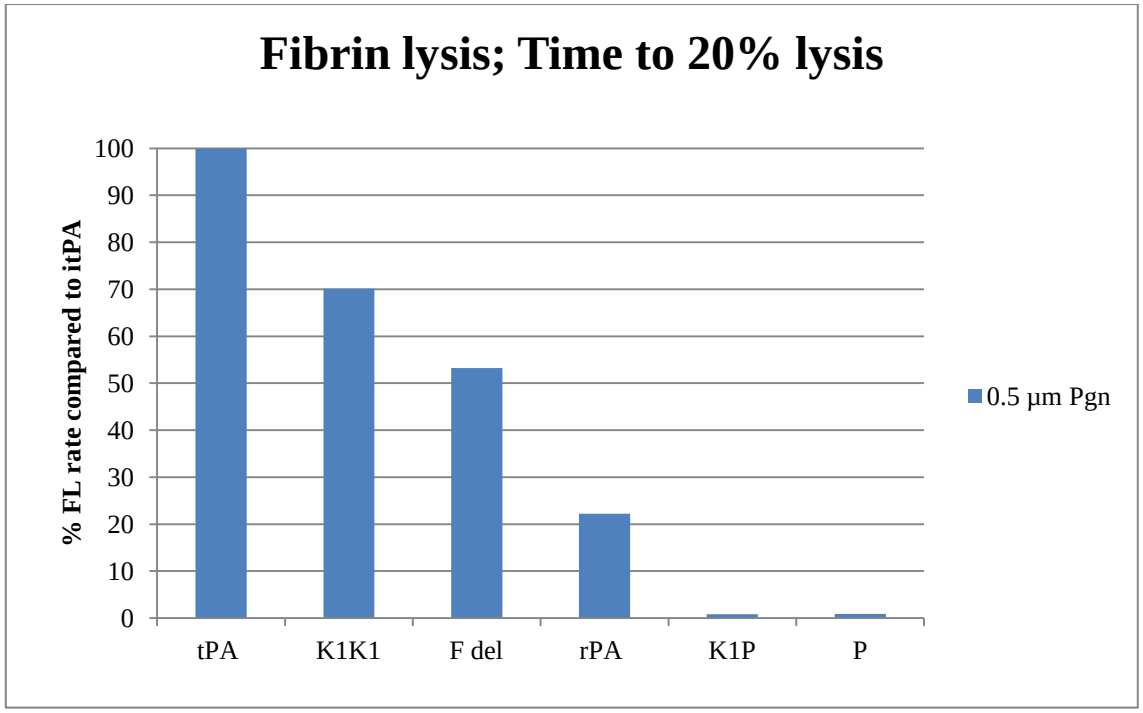


Figure: 3.12.: Fibrin lysis rates (measured as time to 20% lysis) itPA and variants at 0.5 µM plasminogen in un-treated fibrin clots. The results are displayed as % activity relative to itPA.

3.3.3.3. Fibrin as a template and the effects of different types of fibrin on the domain variants.

The activity of tPA variants was investigated in fibrin clots that were made with fibrinogen that was modified as described in chapter 3.3.2.1, to produce different fibrin conditions to try to distinguish between different binding mechanisms. The clear clot lysis overlay assay was used and the concentration of plasminogen was varied. Initial rates of plasminogen activation were calculated as described in section 3.2.3.1.a. and then plotted against plasminogen concentration producing hyperbolic plots from which kinetic parameters can be calculated using the Michaelis-Menten equation (see section 3.2.3.2).

rPA and irPA do not have a finger domain and rely solely on binding to fibrin through the K2 domain. The K2 binding sites on fibrin are lysines. When new generated C-terminal lysines in fibrin are removed by the addition of CPB the rPA will experience reduced binding to fibrin and it is expected that the rate of plasminogen activation will be reduced (Suenson et al, 1984). The effect of the reduced irPA binding to fibrin is that the rate of plasminogen activation is greatly reduced which can be seen in figure 3.13 at a single concentration of plasminogen and in figure 3.14(A) over a range of plasminogen concentrations. In Figure 3.14(A) no hyperbolic plot is produced and apparent K_M and k_{cat} values cannot be calculated but apparent k_{cat}/K_M is estimated assuming a linear plot for the data shown in figure 3.14(A). When fibrin is treated with plasmin, C-terminal lysines are produced therefore providing rPA and plasminogen with nascent kringle binding sites (Christensen, 1985; Fleury and Angles-Cano, 1991; Hoylaerts et al, 1982). Increased plasminogen activation is observed with plasmin-treated fibrin (figure 3.14(B)) compared to normal fibrin (Figure 3.14 (C)). There is a reduction in the apparent K_M value of 1.21 μM in normal fibrin to 0.41 μM in plasmin-treated fibrin.

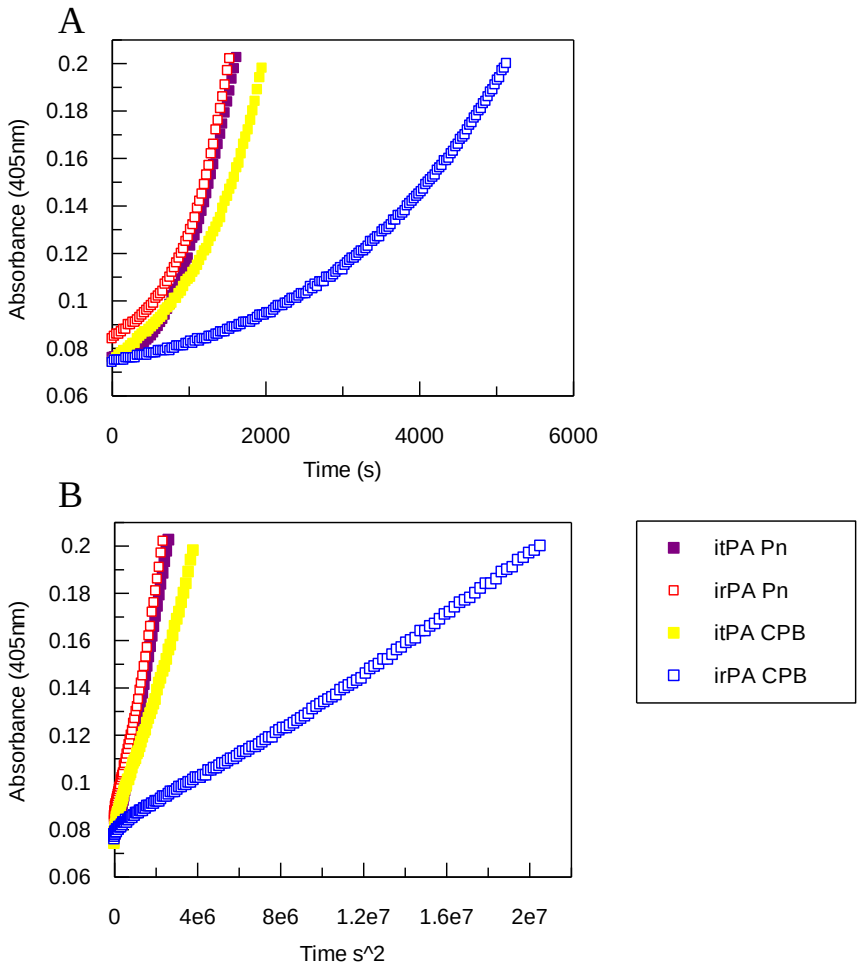


Figure 3.13: Plasmin generation in normal and CPB-treated fibrin by itPA and irPA.

A: Plot of absorbance versus time, showing plasminogen activation by itPA in plasmin (pn) treated fibrin and CPB added to the fibrin. Plasmin treatment shows increased acceleration compared with CPB addition.

B: transformed plot of absorbance versus time squared where the slope is proportional to the rate of plasmin production (plasminogen activation) and in an ideal situation is linear.

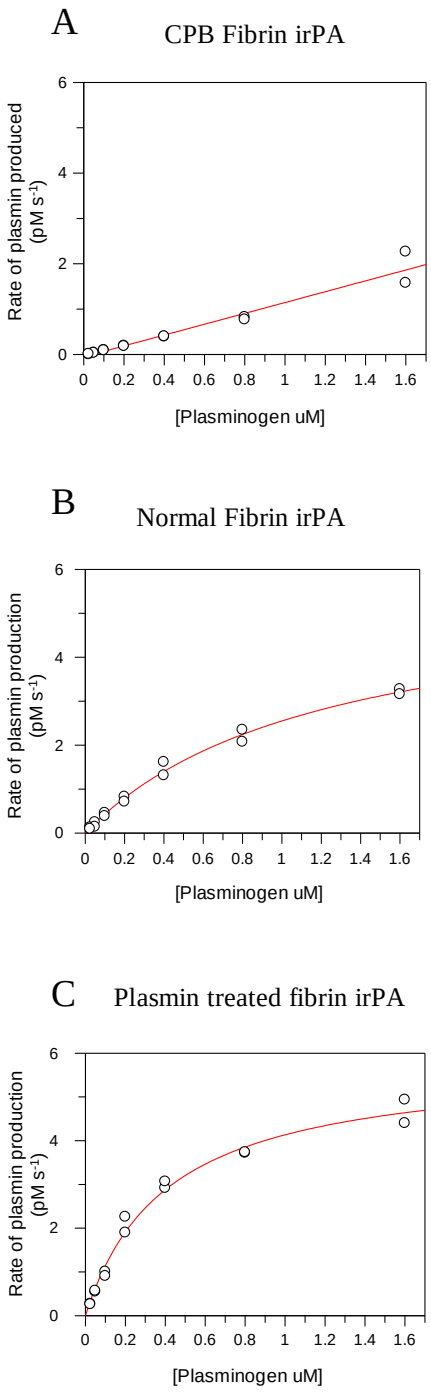


Figure 3.14: Example of plots showing the activity of irPA in different fibrins.

(A) Rate of plasmin produced in fibrin with CPB as a function of plasminogen concentration, not showing hyperbolic plots (B): Rate of plasmin produced in plasmin-treated fibrin as a function of plasminogen concentration (C): Rate of plasmin produced in normal fibrin as a function of plasminogen concentration. Curves in B and C are fitted to the Michaelis-Menten equation and A is fitted to a straight line.

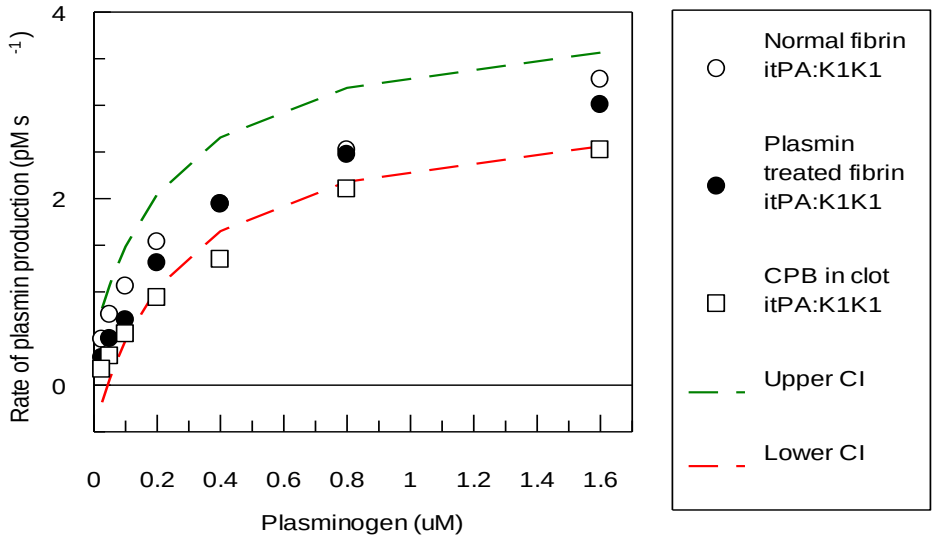


Figure 3.15: Michaelis-Menten curves for clear clot lysis assay.

Michaelis-Menten curves for the experimental data for the itPA: K1K1 in the three types of fibrin and the 95% confidence intervals for the normal fibrin (dashed lines) around the fit.

There appears to be little change in the rate of plasmin production by itPA, itPA:K1K1 and itPA: K2 del variants with the plasmin treated fibrin compared to normal fibrin but a small consistent decrease in the rate of plasmin production is observed when CPB is added to the clot. As an example, figure 3.15 shows the Michaelis-Menten curves for itPA: K1K1 in the three types of fibrin and the 95% confidence intervals for normal fibrin (see section 3.2.3.2.b). itPA: K1K1 in the presence of CPB-treated fibrin is seen to be close to the lower 95% confidence interval but not significantly different from the rates seen with normal fibrin or plasmin-treated fibrin. Using the clear clot lysis assay it has not been possible to definitely demonstrate the significance of CPB-treated fibrin on the rate of plasminogen activation using the variants with the exception of irPA beyond the variability between assays. Analysis of the ratio of the k_{cat}/K_M values from repeated experiments for normal and CPB-treated fibrin shows that the itPA: K1K1 is ~2 times less efficient in the presence of CPB than in normal fibrin. A similar pattern is also observed in the majority of repeats with itPA (2 times) and itPA: K2 del (2 times). It is likely that this reduction in efficiency is due to reduced plasminogen binding. However the effect of CPB reducing plasminogen activation is much less pronounced in these variants than is seen with the irPA which shows a 9-10 times reduction in efficiency expressed as apparent k_{cat}/K_M values (see table 3.2).

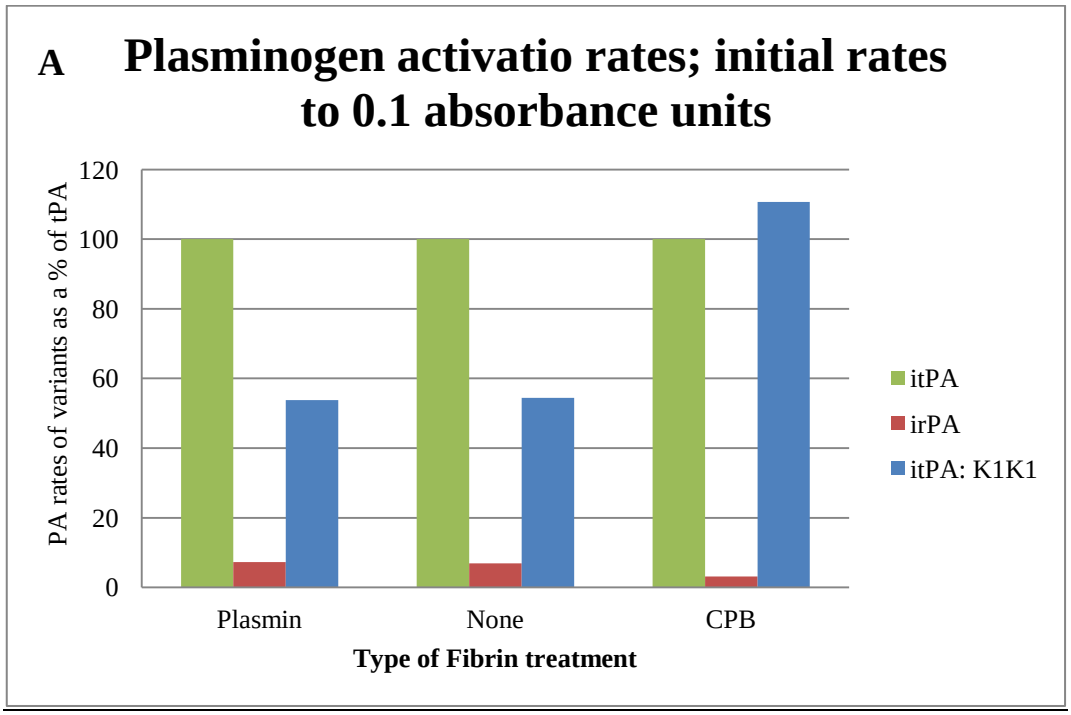
The data show no reproducible difference between the itPA, itPA: K1K1 and the itPA: K2 del in the normal and plasmin-treated fibrin. Notably, these are the three variants with the ability to bind to fibrin with the finger domain.

Assay No	irPA				K1K1: tPA				itPA				tPA: K2 del			
	Km (μM)	*Vmax (pM s-¹)*	*kcat (s-¹)*	*kcat/Km (μM-`¹s-¹)*	*Km (μM)*	*Vmax (pM s-¹)*	*kcat (s-¹)*	*kcat/Km (μM-`¹s-¹)*	*Km (μM)*	*Vmax (pM s-¹)*	*kcat (s-¹)*	*kcat/Km (μM-`¹s-¹)*	*Km (μM)*	*Vmax (pM s-¹)*	*kcat (s-¹)*	*kcat/Km (μM-`¹s-¹)*
CPB treated fibrin																
1	-	-		0.00	0.59	3.39	0.01	0.01	0.61	5.18	0.01	0.02				
2	-	-		0.00	0.52	1.87	0.00	0.01					0.78	2.81	0.01	0.01
3					0.54	1.65	0.00	0.01	0.58	2.23	0.01	0.01	0.58	2.33	0.01	0.01
Normal fibrin																
1	1.16	10.71	0.03	0.02	0.27	2.99	0.01	0.03	0.28	6.23	0.02	0.06				
2	1.22	9.26	0.02	0.02	0.26	1.72	0.00	0.02					0.36	2.45	0.01	0.02
3					0.19	1.46	0.00	0.02	0.18	2.26	0.01	0.03	0.23	1.90	0.00	0.02
4	1.21	5.64	0.01	0.01	0.27	2.93	0.01	0.03					0.23	4.60	0.01	0.05
5	0.80	9.82	0.02	0.03	0.37	9.97	0.02	0.07	0.25	12.51	0.03	0.13				
6	0.38	4.87	0.01	0.03	0.19	1.32	0.00	0.02	0.41	2.37	0.01	0.01				
Plasmin treated fibrin																
4	0.41	5.83	0.01	0.04	0.47	4.11	0.01	0.02	0.50	3.15	0.01	0.02	0.37	5.45	0.01	0.04
5	0.48	11.18	0.03	0.06	0.34	10.54	0.03	0.08								
7									0.21	13.21	0.03	0.16				

Table 3.2: Apparent K_M, V_{max}, k_{cat} and k_{cat}/K_M values for variant proteins in the clear clot lysis overlay assay. The kinetic constants are shown for each variant in plasmin-treated, normal, and CPB treated fibrin. Each assay number represents results from experiments that were performed in the same plate. Due to variability between assays comparisons were made only from data that were performed in the same assay

To further elucidate which domains are involved in the activity of tPA with fibrin as a template the dual wavelength clot lysis assay was used to investigate plasminogen activation and fibrinolysis in the same clots simultaneously. In these experiments the concentration of tPA and variants were varied and the initial plasminogen activation rates and the fibrin lysis rates were calculated. The rates of each variant were compared against the rates of full length itPA and the relative potency calculated using a parallel line model in Combistats (see section 3.2.3.3.). The relative activity expressed as a percentage of full length itPA (set to 100%) in each fibrin condition can be seen in figure 3.16 (A). In this system the itPA: K1K1 variant showed about half of the plasminogen activation activity of full length itPA in both normal and plasmin treated fibrin, indicating that increased C-terminal lysines does not increase binding by the itPA: K1K1 variant. In CPB-treated fibrin the activity of itPA: K1K1 increased to around 110% of the activity of itPA in normal fibrin. In these conditions it seems removal of K2 binding by tPA allows for enhanced plasminogen activation. The plasminogen activation rates of irPA were lower than those of itPA: K1K1, only around 7% of the activity of itPA in both normal and plasmin treated fibrin. This also highlights the importance of F domain binding to fibrin to activate plasminogen. There was no increase in plasminogen activation for irPA when fibrin was treated with plasmin, this was unexpected as an increase in K2 binding sites was expected to increase binding, these results differ from the results seen with in the clear clot lysis assay where plasmin-treatment of fibrin was shown to increase plasminogen activation by irPA. This lack of effect may be technical problems with the plasmin treatment since CPB-treated fibrin decreased plasminogen activation rates of irPA to only 3% of that of itPA. The rates of fibrin lysis (to 50% lysis) showed a very similar pattern to that seen in the rates of plasminogen activation this can be seen in figure 3.16(B), though with somewhat higher relative activities for irPA in the absence of CPB, probably due

to the longer reaction times to 50% lysis compared to initial rates of plasminogen activation, as noted above.



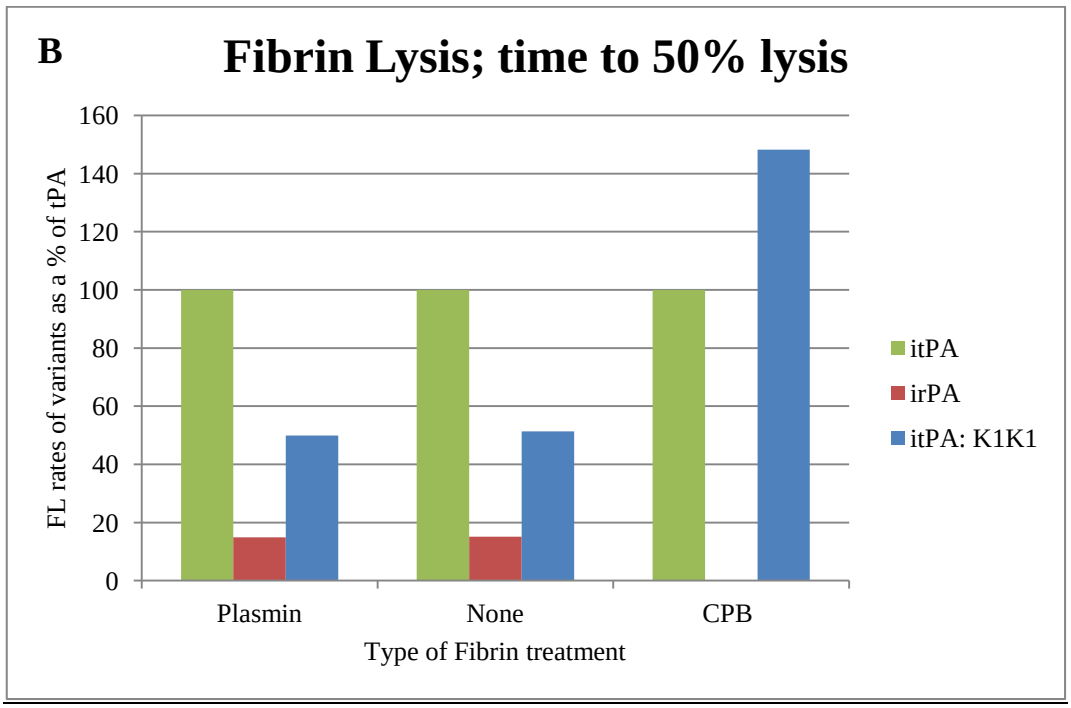


Figure 3.16.: Rate of plasminogen activation and fibrin lysis for itPA: K1K1 and irPA relative to itPA in 3 fibrin conditions. (A) Initial plasminogen activation rates and (B) Time taken to reach 50% lysis by itPA: K1K1 and irPA compared to itPA in fibrin clots made with forms of fibrinogen. The results are expressed as percentage activity relative to itPA.

CHAPTER 4 - BINDING

4.1. Introduction

Many biological processes require recognition and specific binding of molecules. Knowledge of the strength of these interactions is important in determining the function of the molecules involved and the regulation of biological pathways. The strength of an interaction can be measured quantitatively by determining the affinity between two molecules. In the process of plasminogen activation the affinity between tPA, plasminogen and the templates that stimulate this reaction is required since tPA stimulation is known to follow a co-localisation mechanism in which template binding of tPA and plasminogen is responsible for bringing enzyme and substrate together. Fibrin is not a simple molecule to study and a number of methods can be employed to look at strength of binding and affinity qualitatively and quantitatively for binding of tPA and plasminogen. Many methods have been used previously such as affinity chromatography (Christensen, 1985), NMR spectroscopy (Byeon et al, 1995), measuring binding directly to fibrin clots using radioactively labelled (Bok and Mangel, 1985; Larsen et al, 1988; Lucas et al, 1983; Nesheim et al, 1990) or fluorescently labelled (Horrevoets et al, 1996) tPA and plasminogen. Fibrinogen can be immobilized onto microtitre plates or other surfaces and converted to fibrin with treatment with thrombin, the amount of tPA and plasminogen that bind to this fibrin surface can be measured by radioactively labelling tPA (de Vries et al, 1989), using antibodies to tPA and plasminogen that are detected as they are conjugated to fluorescent or chemical indicators (ELISA) (Bosma et al, 1988; Tsurupa and Medved, 2001a; Tsurupa and Medved, 2001b) or by directly measuring the amount of tPA bound by measuring plasminogen activation (Angles-Cano, 1986; Fleury et al, 1993). Even though radioactive labels produce robust reproducible assays it can be problematic primarily due to labelling

chemistry which can disrupt protein binding sites. Similarly, fluorescently labelling of tPA and plasminogen by large reactive aromatic molecules such as FITC can be used but this is method is difficult to control as it is difficult to ensure that optimal conjugation between variants due to differences amino acid sequence and structure (Holmes and Lantz, 2001). Another method to generate fluorescent tPA is by expressing tPA fused to GFP, this ensures that there is one GFP molecule fused to each tPA molecule. The Green Fluorescent Protein (GFP) is a 29 kDa protein that has been isolated from the jellyfish *Aequorea victoria*, which emits green fluorescence when exposed to blue light (Prendergast and Mann, 1978; Tsien, 1998). It was first discovered in 1962 by Shimomura et al (Shimomura et al, 1962) and has since become a very useful and widely used biological marker. GFP can be used as a fluorescent marker in vitro and in vivo as it has been found that the use of GFP as a tag does not affect the normal function of the fusion partner and requires no other cofactor to fluoresce. It has been used in many different applications including looking at protein-protein interactions and following processes in living tissues (Lippincott-Schwartz and Patterson, 2003).

Detection of bound tPA and plasminogen to immobilised templates using antibodies is also potentially useful but problems may arise when investigating variants of target molecules. Measurement of the amount of tPA bound using plasminogen activation activity is simple and does not involve the use of any labels or other binding partner. However the different plasminogen activation activities of the domain variants could complicate the interpretation of binding and requires appropriate methodology or correction of results.

Surface plasmon resonance (Biacore) (described in detail in chapter 1.8) is a technique that is used to measure binding of analyte to an immobilized ligand in real time and does not require labelling of the either binding partner. This technique can be used to generate high-quality data on binding affinity and kinetics. However, there are many considerations that need to be

addressed when using SPR, including non-specific binding, steric hindrance and suitable immobilization techniques. Development of working protocols can take time to optimise ligand levels, and surface regeneration methods (Schuck, 1997). Fibrinogen has previously been immobilized on to the surface of Biacore sensor chips and converted to fibrin with thrombin to monitor the interactions between tPA and fibrinogen with some success (Dunn et al, 2006; Mutch et al, 2010). The interaction of tPA and plasminogen with fibrinogen fragments has also been investigated using SPR by immobilizing tPA and plasminogen on to the surface of the sensor chip (Yakovlev et al, 2000). The immobilization of heparin on to the sensor surface is more complicated due to the chemical properties of heparin. Immobilization of highly sulfated heparin oligosaccharides by amine coupling is difficult as there is only a single reducing end amine group which means that amine chemistry is difficult (Zhang et al, 2002). The presence of negatively charged sulphate groups means that heparin is extremely negatively charged preventing electrostatic preconcentration at the sensor surface and so high enough levels of immobilization cannot be achieved (de Paz et al, 2007). Therefore other immobilization methods are required, one such method is using biotinylated heparin and binding to streptavidin coated sensor chips. Ultimately however, it may be possible to study the binding of tPA and plasminogen to physiological templates to derive values for kinetic and equilibrium constants. These constants can be used, along with parameters derived from enzyme kinetic studies, to construct working models which explain how templates regulate tPA enzyme activity.

4.2. Materials and Methods

4.2.1. Materials

High binding plates were from Sterilin ltd, (Caerphilly, UK). tPA-GFP and F del tPA-GFP were generated as described in section 2.3.2. Na Phosphate, 10 mM sodium phosphate buffer pH 8.0, containing 1 mM EDTA and 0.001% Triton-X-100 was used where stated. All SPR experiments were performed on a Biacore 2000 instrument with dextran coated sensor chips, CM5, CM4, CM3, and carboxymethylated dextran pre-immobilized with streptavidin (sensor chip SA). Other Bicore reagents and buffers were, surfactant p20 and amine coupling kits, containing EDC- 0.4 M 1-ethyl-3-(3-dimethylaminopropyl)-carbodiimide, NHS-0.1 M N-hydroxysuccinimide in water and 1 M ethanolamine-HCl pH 8.5, supplied as kits. Biacore and related materials were from GE Healthcare, Bucks, UK. HBS-EP buffer, 10 mM HEPES (free acid), 150 mM NaCl, 3.4 mM EDTA and 0.005% p20 surfactant was prepared as 10x stock, made up and degassed as needed. Goat polyclonal anti human fibrinogen (ab6666) and Goat polyclonal anti human plasminogen (ab11523) antibodies were purchased from Abcam (Cambridge, UK) and goat polyclonal anti fibrinogen β chain (C-20) antibodies were purchased from Santa Cruz (Santa Cruz, CA, USA). Heparin-Biotin was from Calbiochem (Merck, Darmstadt, Germany) Goat anti rabbit IgG, L-lysine, arginine and poly L-lysine and all other chemicals were purchased from Sigma Aldrich. and all other materials and proteins are listed in section 3.2.1.

4.2.2. Methods

4.2.2.1. Fibrinogen plates

The efficiency of binding of tPA and variants to fibrinogen was investigated using fibrinogen immobilized to the surface of 96 well microtitre plates, using two methods, described in sections a) and b) below. In both cases plates containing immobilised fibrinogen were prepared in the same way. Immobilization of fibrinogen was performed by adding aliquots of 100 µl of fibrinogen at 1 mg/ml (clottable protein) diluted in buffer B (section 3.2.1) but containing no Tween 20, to the wells in a 96 well microtitre plate. The plate was covered and incubated over night at 4 °C. The fibrinogen solution was then emptied from the plate and excess removed by patting on a tissue. The plate was blocked with 200 µl per well, of buffer B diluted 10x containing 0.1% Tween 20 (w/v), for 3 h. The fibrinogen coated plate was then washed three times using 200 µl per well of buffer B and used immediately.

a) tPA range

To investigate the relative binding of tPA variants to immobilised fibrinogen, a range of of tPA concentrations were added to the plate and incubated for 1h. Aliquots of 100 µl of 2-fold serial dilutions of tPA from 100 to 12.5 nM diluted in buffer C (section 3.2.1), were added to the plate and for each concentration at least 4 replicates were performed. The plate was then sealed and incubated for 1 h at 37 °C. Excess unbound tPA was then washed off using 3 x 200 µl of buffer B and the concentration of tPA bound to the fibrinogen was then estimated by following activation of plasminogen. Aliquots of 20 µl of 3 mM chromogenic substrate S-2251 (section 3.2.1) were added to all wells followed by, 80 µl of a mixture of 2 mg/ml fibrinogen (template for tPA and plasminogen) and 10 µg/ml glu-plasminogen (section

3.2.1), in buffer B. Final concentrations in the activation reaction mixtures were 0.6 mM S-2251, 1.6 mg/ml fibrinogen and 8 µg/ml of glu-plasminogen. Finally 60 µl of mineral oil was added to all reaction wells to prevent evaporation. The rate of pNA production was measured by following absorbance at 405 nm for 1.5 h at 37 ºC. The Initial rates of plasminogen activation were calculated as described in section 3.2.3.1.a and then analysed using the program Combistats as described in section 3.2.3.3.

A direct binding assay method was also developed for use with fluorescent fusion proteins, tPA-GFP and F del-GFP (section 2.4.2). Aliquots of 100 µl of 2-fold serial dilutions from 353-0.353 nM diluted in 10 mM NaPhosphate buffer pH 8.0 were incubated in the fibrinogen coated wells. Washing steps were as described above and bound fluorescent protein were then measured as described in section 2.3.7.

b) Aminohexanoic acid range

The second method, a competition binding assay, was performed with a fixed concentration of tPA and a range of dilutions of 6-aminohexanoic acid, analogue of the amino acid lysine. The 6-aminohexanoic acid blocks binding via tPA lysine binding sites and a range of dilutions of 6-aminohexanoic acid was used to determine the IC_{50} (half maximal (50%) inhibitory concentration), at which only 50% of binding of tPA to fibrinogen can occur. Plates were coated with fibrinogen as described in section 4.2.2.1. a). and aliquots of 100 µl of 2-fold serial dilutions, from 20 to 0.00976 mM of 6-aminohexanoic acid, diluted in buffer C, were performed across the plate from column 1 to 11. In column 12, a blank was included, containing no 6-aminohexanoic acid. Aliquots of 50 µl of tPA, diluted to 50 nM in buffer C, were added to each of the coated wells, in duplicate at each aminohexanoic acid

concentration, giving final concentrations of 10 mM to 0.00488 mM of 6-aminohexanoic acid and 25 nM tPA. The plate was then sealed and incubated at 37 °C for 1 h. The plates were then washed 3x with 200 µl/ well buffer B and initial rates of plasminogen activation were then determined as described above in section 3.2.3.1.a. Rates of plasminogen activation were analysed using the program Combistats as described in section 3.2.3.3. and by calculating the IC_{50} using Grafit as described in section 4.2.2.3.

4.2.2.2. Fibrin plates

The efficiency of binding of tPA and variants to fibrin was investigated by converting fibrinogen immobilized to the surface of 96-well microtitre plates into fibrin by incubation with thrombin. After immobilization of fibrinogen to a 96-well microtitre plate as described above the plate was blocked with 0.01% Tween 20 (section 4.2.2.1), and 100 µl aliquots of bovine thrombin at 4 IU/ ml, diluted in buffer B were added to each well. The plate was then incubated for 1 hour at 37 °c and then washed twice with 200 µl buffer B. The remainder of the assay was performed as described in section 4.2.1.1 b).

4.2.2.3. Data Analysis

a) Grafit

The rates of plasminogen activation were calculated as in section 3.2.3.1 and multiplied by 10^9. The rates at each concentration of 6-aminohexanoic acid were then converted into a percentage of the plasminogen activation rates where no aminohexanoic acid had been added to the reaction. These percentage values are then plotted against the log concentration of 6-aminohexanoic acid and then fitted to the IC50 – 4 parameter logistic equation in Grafit:

$$y = \frac{Range}{1 + \left(\frac{x}{\mathrm{IC}_{50}} \right)^{s}} + \mathrm{Background}$$

The four parameters being:

-Background: the minimum point of the curve * 0.95

-Range: the fitted uninhibited value minus the Background (max*1.05 - min*0.95)

-s: the slope factor or the steepness of the slope (gradient)

-IC_{50}: the x value for the curve point that is midway between the max and min parameters (1/exp(intercept))^(1/gradient)

From which the IC50 (the concentration of 6-aminohexanoic acid that inhibits plasminogen activation by 50%) values are calculated.

b) Combistats (Using a Standard)

See section in chapter 3.2.3.3.

4.2.3. Surface Plasmon Resonance – using the Biacore system

Immobilisation procedures and assessment of the amount of ligand to immobilized on to the chip was accomplished by following Biacore software wizards and guidelines from Biacore Sensor Surface Handbook (Biacore AB, 2003). pH immobilization scouting was performed to determine the pH that appeared to give the best conditions for immobilization. Ligands were immobilized to dextran coated sensor chips CM5, CM4 and CM3 by amine coupling using the immobilization wizard (Biacore 2000 Control software 3.2.1). Carboxyl groups on the on the sensor surface were activated with a mixture of EDC and NHS (Biacore, Uppsala, Sweden) to give reactive succinamide esters. Ligand was then passed over the surface and the esters on the dextran react with primary amine (NH_2) groups on the ligand. Ethanolamine was then injected to deactivate any excess reactive groups. Biotinylated heparin was immobilized to sensor chip SA by non-covalent capture (binding to streptavidin). Analytes, tPA or plasminogen, were dialysed (as described in section 2.3.6.1.) or diluted 1/10 in to running buffer HBS-EP (10 mM HEPES, 3.4 mM EDTA, 150 mM NaCl, and 0.005% p20) unless otherwise stated and injected over the immobilised ligand at various flow rates and lengths of time (flow rates and length of injection of individual experiments are reported in Results).

After each injection of analyte the chip surface was regenerated by removing bound analyte but leaving ligand attached to the surface of the chip. The regeneration conditions were determined by regeneration scouting to test the effectiveness of different regeneration solutions (Biacore 2000 Control software 3.2.1, GE Healthcare, Bucks, UK) injected as consecutive short injections of acids, bases, high salt concentrations or a competing ligand (see Results section) with a higher affinity for the analyte than the immobilized ligand. Surface performance tests were also performed to assess whether the regeneration conditions

removed all analyte while retaining ligand binding activity over a number of analyte binding and regeneration cycles.

4.2.3.1. Lysine immobilization

L-lysine was diluted to 0.2 M in 10 mM Sodium acetate buffer pH 4.0 or HBS-EP pH 9.0 and immobilized to a CM5 sensor chip by amine coupling using the Biacore immobilization wizard at a rate of 10 µl/min for 7 min. Actilyse at various concentrations was then injected over the surface of the chip to determine the efficiency of immobilization at both pH values. Increased binding was observed with lysine immobilized at pH 9.0. A number of regeneration solutions were tested including 25 mM HCl (+/- 150 mM NaCl), 50 mM NaOH, 10 mM glycine-HCL pH 3.0, and arginine at various concentrations. The regeneration solution that was found to work most effectively was 0.5 M Arginine + 0.5 M NaCl in HBS-EP buffer. tPA and variant samples were either dialysed or diluted into HBS-EP running buffer, filtered in a spin-x-tube in a table top centrifuge for 1 min at 8000 rpm and immediately injected on to the chip at various concentrations, flow rates and times (see results section 4.3.2.1 for individual experiments)

4.2.3.2. Fibrinogen immobilization

a) Antibodies

Two different antibodies to fibrinogen, one from Abcam and the other from Santa Cruz were immobilized both individually and combined onto flow cells of a CM5 sensor chip with anti-rabbit IgG on a second flow cell on the same chip as a reference to check for non-specific binding. Immobilization was by amine coupling using the Biacore immobilization wizard,

aiming for an immobilized level of 500, 1000 or 5000 RU using the antibodies diluted to a concentration of 30 µg/ml in sodium acetate buffer at pH 5.0 for the Abcam antibody and pH 4.0 for Santa Cruz antibody. After antibody immobilization was completed, 1 mg/ml or a concentration series of 5 concentrations from 1 mg/ml to 200 µg/ml in 200 µg/ml increments of Sigma and Calbiochem fibrinogen (clottable protein) were injected onto the chip for 1 min at a flow rate of 10-20 µl/ml. tPA (Actilyse), glu-plasminogen, and lys-plasminogen diluted into HBS-EP and both at various concentrations (see results section for individual experiments) were immediately injected on to the fibrinogen for variable lengths of time (see individual experiments in results section 4.3.2.2.) in consecutive injections at a flow rate of 10 or 20 µl/min. All experiments were performed by manual injections or using the Biacore kinetic analysis application wizard with HBS-EP as running buffer. A number of regeneration solutions to strip the fibrinogen from the antibodies were investigated including 10 mM glycine, pH 3.0, 2.5, 2.0, and 1.5, 50 mM and 10mM NaOH, 20 mM HCl, HBS-EP + 1M NaCl + 1% p20, and 2 M and 4 M guanidine HCl. The most effective being 1 injection of 10 mM glycine, pH 1.5 for 30 s for the antibody from Abcam and 1 injection of 10mM NaOH for 45 s, followed by 1 injection of 20 mM HCl for 45 s for the antibody from Santa Cruz.

b) Direct immobilization (covalent immobilization)

Fibrinogen was immobilized directly onto the surface of a CM5 sensor chip by amine coupling using the Biacore immobilization wizard. Sigma fibrinogen at 30 µg/ml in 10 mM sodium acetate buffer, pH 4.5 was injected on to the surface of a flow cell on the sensor chip aiming for 5000 RU of immobilized ligand. The immobilization procedure without fibrinogen additions was also performed in a second flow cell on the same sensor chip to act

as a reference cell. Prior to each experiment the fibrinogen coated and reference cells were treated with regeneration solution. The regeneration solution used was 0.5M Arginine + 0.5 M NaCl in running buffer as determined as the most effective regeneration solution from the results of the regeneration scouting test. The running buffer used was either HBS-EP, 0.1 M HEPES buffer (0.1 M HEPES + 3.4 mM EDTA + 0.1 M NaCl + 0.005% p20 pH.7.4) or buffer B (see individual results, section 4.3.2.3). tPA (Actilyse), itPA, itPA variants or plasminogen (glu or lys) were either dialysed or diluted into running buffer and filtered in spin-x-tubes using a table top centrifuge or diluted by the Biacore into the appropriate running buffer at various concentrations immediately prior to use. Samples of analyte were then injected over the surface of the chip for different lengths of time and flow rates depending on samples (see results section 4.3.2.3 and 4.3.2.4), after which dissociation of bound complex was allowed to proceed for up to 1.2 min. Finally remaining bound material was removed by 2 x 30 s injections of 0.5 M arginine + 0.5 M NaCl regeneration solution. After regeneration the chip was left to stabilize for 2 min before the next cycle or analyte injection.

4.2.3.3. Fibrin immobilization

Immobilized fibrinogen was converted to a fibrin like surface by injecting 4 IU/ml of bovine thrombin onto the fibrinogen coated sensor chip surface for 1 h at a flow rate of 2 µl/ min. The surface was then washed with HBS-EP with the NaCl content made up to 1 M for 3 min at a flow rate of 2 µl/min. Binding of analytes itPA, sctPA and tctPA to the fibrin like surface was then tested by injecting each analyte, diluted to 110 nM in 0.1 M HEPES running buffer, into the flow cell for 4 min using a customised application wizard. Kinetic analysis of sctPA and tctPA binding was also investigated over a range of concentrations 110, 90, 70, 50, and

30 nM with injection times of 1 min using the Biacore kinetic analysis application wizard. For both experiments the flow rate was 10 µl/min with a dissociation time of 2 min. The surface was regenerated using the same method described in section 4.2.3.2. For each analyte this procedure was repeated for two cycles.

4.2.3.4 Heparin immobilization

Biotinylated heparin was immobilized to the surface of a SA sensor chip. The surface of the surface of the sensor chip was conditioned by injecting 3 consecutive 1 min injections of 1M NaCl in 50 mM NaOH. The heparin-biotin diluted to 100 µg/ml in HBS-EP buffer was then injected over the surface of the chip at a flow rate of 10 µl/ min, as many times as it is required to reach saturation. The chip was then washed with 5 µl of 10 mM NaOH + 0.2 M NaCl. Using the Biacore control software kinetic analysis application wizard, samples were then tested for binding to heparin by injecting a concentration series of 20, 30, 50, 70, 90, and 110 nM of tPA variants and 12.5, 25, 50, 100, 400, 800 nM of glu- and lys- plasminogen over the surface of the chip. The flow rate was 10 µl/ min and the contact time was 5 min with a dissociation time of 1.2 min and a stabilization time of 2 min, two replicates were performed for each concentration. A number of buffers were tested such as 0.1M HEPES, HBS-EP, buffer B (40 mM Tris + 75 mM NaCl + 0.005% p20, pH 7.4) and buffer D (40 mM Tris + 37.5 mM NaCl + 0.005% p20, pH 7.4). The buffer that showed the best results was 40 mM Tris + 37.5 mM NaCl + 0.005% p20, pH 7.4 and the chip was regenerated using 1 30 s injection of 10 mM NaOH + 0.2 M NaCl and then 1 30 s injection of 0.2 M NaCl with a stabilization time of 4 min after regeneration before the next cycle.

4.2.3.5. Biacore data analysis

Biacore data was analysed using Biacore evaluation software 3.2. Association rate constants (k_{on}) and dissociation rate constants (k_{off}) were calculated from sensorgrams using pre-defined or user defined models by non linear regression. Using the kinetic evaluation wizard, sensorgrams were overlaid and the curves aligned. The base line was set to zero, all unwanted data e.g. disturbances from air segments, were removed and the section of data to be analysed was selected. The appropriate model to fit the data was then selected, a simple 1:1 (Langmuir) binding model was used primarily and the results inspected. A number of diagnostic checks were performed to test validity of the results. Visual examination of the fitting was useful to see if the fitted curves deviated too much from the experimental data. The residual plots were checked to see if the scatter was excessive or showed systematic deviations between the experimental data and fitted curves. The fitted parameters were checked for consistency and to see how reasonable they appeared. Chi squared values were compared between models. If there were problems, refitting using different starting estimates was attempted. Often, the simple Langmuir 1:1 binding model was not adequate to fit the data and more complex models were required. A diagnostic test for more complicated patterns of association and dissociation was performed using the dissociation phases of the sensorgrams in isolation. Simple 1:1 Langmuir binding would be accompanied by single exponential curve dissociation. However, where dissociation is better fitted by double or triple exponential curves, more complicated complex dissociation (and association) such as two step binding or multiple simultaneous reactions are evident. In these cases more complicated models were investigated. The aim of fitting was to identify the simplest model that would fit the data and provide reasonable estimates for the corresponding rate constants (and equilibrium constants). Rate equations for the models discussed in this study can be

seen in table 4.1. If simple 1:1 binding models were ruled out, dissociation phases were fitted to double exponential curves which were then fixed as dissociation rate constants (kd_1 and kd_2) in the model formula in the Biaeval fitting program. Subsequent rounds of fitting were then used on the whole sensorgram curves (global fitting) to derive values for the association rate constants and Rmax values. Sensorgrams were fitted as a complete set over a range of analyte concentrations where possible, otherwise better fits were obtained when sensorgrams were fitted one at time at each analyte concentration. Where complex models were used, the selection of the most appropriate model was based on reasoning of the type of reactions likely to be taking place on the sensor surface with prior knowledge of the system under study. It was not possible to definitively identify the correct model with complete certainty.

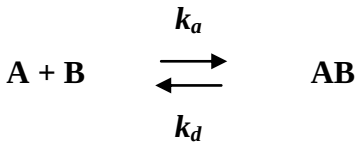
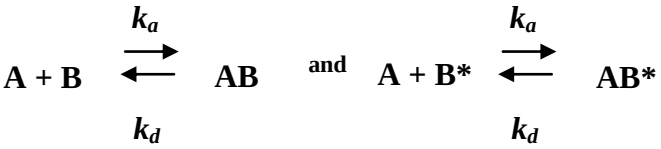
Reaction Scheme	Rate equations
Scheme 1: **Simple 1:1 Langmuir binding** **(One complex)**	
Scheme 2: **Two-step or conformational change binding** **(Two complexes)**	
Scheme 3: **Heterogeneous ligand binding**	

Table 4.1: The rate equations for binding models used in this study.

4.2.4. Solubility studies

tPA is poorly soluble at concentrations over 0.1 mg/ml and a range of conditions and buffers were investigated to maximise solubility for Bicaore studies. The amount of precipitation of tPA in different buffers over time was investigated to determine conditions to maximize tPA solubility.

The amount of precipitation of tPA in different buffers over time was investigated to determine conditions to maximize tPA solubility.

Actilyse (therapeutic full length tPA) was dialysed (as described in section 2.3.6.1.) into 10 mM sodium acetate pH 4.0 containing 0.1 M NaCl, to remove arginine which is added to the Actilyse to keep it soluble. The protein concentration of the dialysed Actilyse was then determined as described in section 2.3.6.2. The Actilyse was diluted to get a range of concentrations from 5 µM to 0 µM in 10 mM sodium acetate pH 4.0. and 11 biological buffers all at a concentration of 0.5 M and with neutral pH. The buffers containing different surfactants were made up in the same way but adding the correct volume of each surfactant to get 0.005% (v/v) p20 or 0.1% (v/v) and 0.01% (v/v) of each of the other surfactants tested. Each sample containing Actilyse at the concentrations described above was then diluted 4 parts Actilyse to 1 part buffer to get buffer concentrations of 0.1 M at pH values as close to pH 7.4 as possible while keeping within the useful buffering range of each buffer. 60 µl mineral oil was added to the top of each solution to prevent evaporation. The absorbance at 405 nm was measured over 16 h at room temperature.

4.3. Results

4.3.1. tPA and variants binding to immobilized fibrinogen and thrombin-treated fibrinogen (fibrin) using ELISA-style assays

Two methods were used to investigate the binding of tPA and variants to fibrinogen immobilized to the surface of 96 well plates. The first method used a fixed plasminogen activator concentration and range of dilutions of 6-aminohexanoic acid to determine the IC_{50} (half maximal (50%) inhibitory concentration), at which only 50% of binding of tPA and variants to fibrinogen can occur. The second method used a range of plasminogen activator concentrations to compare the binding behaviour of each variant to immobilised fibrinogen, using itPA as a standard.

4.3.1.1. Determination of fifty percent inhibitory concentration (IC_{50}) of 6-aminohexanic acid against itPA and variants binding to fibrinogen

In these assays the concentration of tPA was held constant and a range of 6-aminohexanoic acid was added with the tPA before incubation with fibrinogen. The 6-aminohexanoic acid (a lysine analogue) binds to the tPA via lysine binding sites (K2 domain). The concentration of 6-aminohexanoic acid to block binding to fibrinogen by 50% (IC_{50}) was calculated in Grafit. The plasminogen activation rates obtained when no 6-aminohexanoic acid was added to the reaction was designated 100% binding and the plasminogen activation rates at the highest concentrations of 6-aminohexanoic acid where the sigmoidal curve plateaus were taken as 100% inhibition. The concentration of aminohexanoic acid in the reaction at the half way point between 100% binding and 100% inhibition is the IC_{50} value. The curves were not expected to go down to zero plasminogen activation in the variants with a F and K2 domain as 6-aminohexanoic acid only blocks binding via the K2 domain. The higher the

concentration required to inhibit binding by 50% the stronger the binding of the variant to fibrinogen. The IC_{50} values generated for itPA and variants are shown in table 4.2 and representative graphs for each variant can be seen in figure 4.1. The results of these assays were quite variable and therefore it was difficult to determine a precise IC50 value for each variant, especially for those variants which contain both the K2 and F domains. Analysis of the results from itPA, scitPA (R275E), and tctPA revealed no pattern to indicate that there was any difference in the strength of binding to fibrinogen between these variants and it is likely that the IC50 values for these variants is between 150 and 250 μM 6-aminohexanoic acid. Interestingly no reproducible difference was observed with the itPA: F del variant compared to itPA (again an IC50 of between 150 and 250 μM is likely). The irPA variant also binds via the K2 domain only and a lower IC_{50} value of 87 μM was observed but this variant was only tested once and due to the variability of this assay no definitive conclusions can be drawn. However if this result is true it would further corroborate results from the kinetics experiments with fibrinogen (section 3.3.2.1), fibrin (section 3.3.3) and heparin (section 3.3.2.2) that there may be additional sites that are involved in binding. The variants that do not contain the K2 domain and rely on binding via the F domain only; itPA: K1K1 and itPA: K2 del, have much higher IC_{50} values <3000 μM although an IC_{50} value is unlikely to be accurate as looking at the graphs in figure 4.1. very little downward trend of the data is observed and so no sigmoidal curve is generated. The small downward trend seen with these variants is likely to be due to ionic interactions or affects on fibrinogen or some other reason rather than blocking a specific binding site.

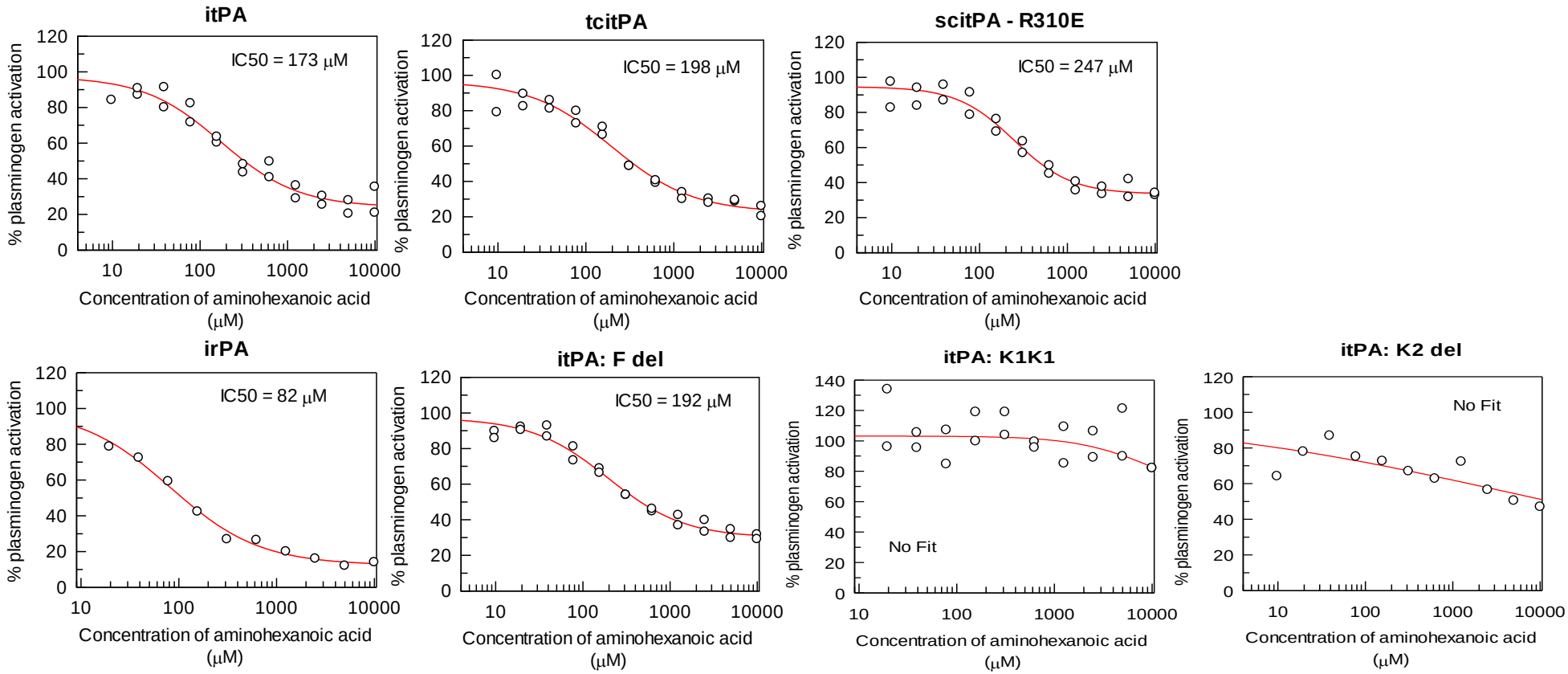


Figure 4.1: Data (circles) and fits (red lines) of the IC50 of 6-aminohexanoic acid on itPA and variants binding to immobilized fibrinogen. Initial plasminogen activation rates of itPA and variants over a range of 6-aminohexanic acid concentrations converted to a percentage with 100% being the initial plasminogen activation rates when no 6-aminohexanoic acid is present. The IC50 is calculated from the fits of the data.

Assay No	itPA	tcitPA	scitPA	itPA: F del	irPA	itPA: K1K1	itPA: K2 del
1	248	155	96	156			
2		160	138			no fit	no fit
3	173		173		82	no fit	
4	111	198	247	192			
5	168	408	209	238			
6	169	150	163	160			
Mean	138	214	171	187	82	-	-
S.E.	18.9	49.1	28.2	19	0	-	-

Table 4.2: IC50 values (µM) for 6-aminohexanoic acid on binding of itPA and variants to immobilized fibrinogen The results are shown for 6 independent assays, with 4 variants tested in each assay with the mean and standard error (S.E.) for each variant.

Immobilized fibrinogen was treated with thrombin to try to generate a fibrin-like surface for binding to see if any difference could be observed between this and fibrinogen. Preliminary experiments indicated that there was a small reduction in the strength of binding to the fibrin-like surface compared to the immobilized fibrinogen in the 3 variants tested and the IC50 values are shown in table 4.3, more repeats are needed to confirm these results.

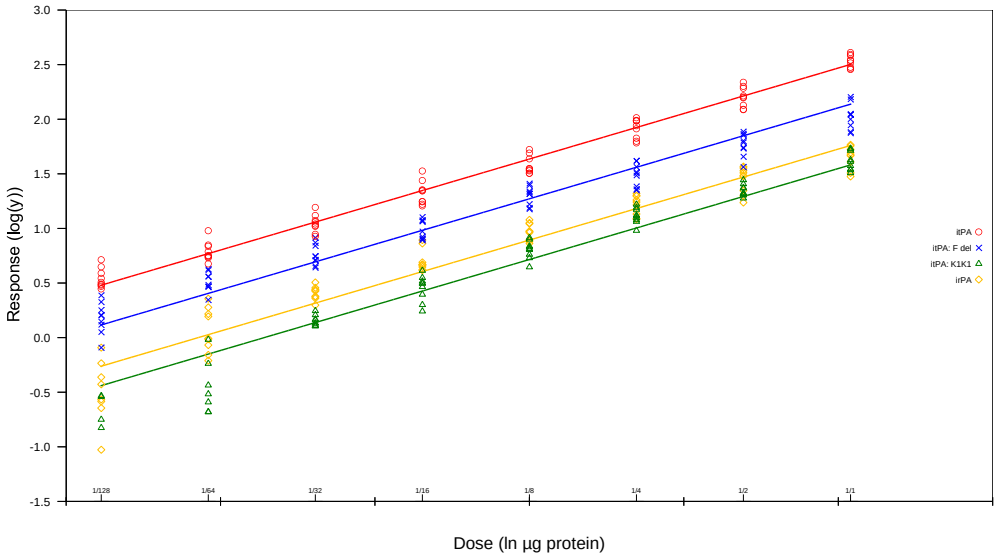
	scitPA	itPA	itPA: K1k1
Fibrin*	140	354	no fit
Fibrinogen	642	499	no fit

Table 4.3: IC50 values (µM) for 6-aminohexanoic acid on binding of itPA and variants to immobilized fibrinogen and fibrin* (thrombin treated immobilized fibrinogen – fibrin-like surface).

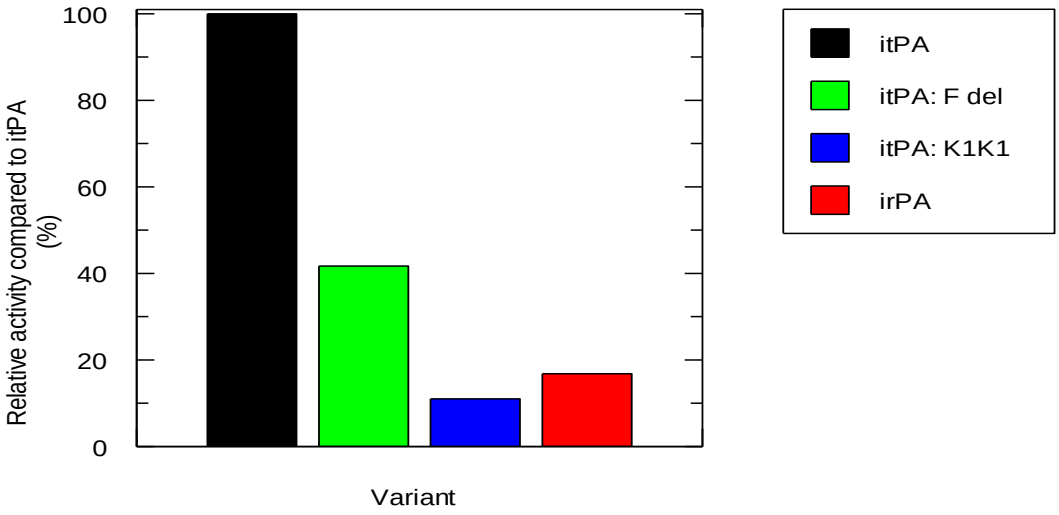
4.3.1.2. Plasminogen activator range binding to immobilized fibrinogen

After incubation of a range of tPA and variants with immobilized fibrinogen, excess plasminogen activator was washed off and the plasminogen activation rates of the remaining bound plasminogen activator were measured and calculated. The rates from a range of concentrations of each variant were compared against the rates of full length itPA and the relative potency calculated using a parallel line model in Combistats (see section 3.2.3.3.) and the resulting graph from generated from combistats is shown in figure 4.3 A and the graph shown in figure 4.2 B is the % activity relative to full length itPA of each of the variants tested. It can be seen that both the F and K2 domain are involved in binding to fibrinogen and that the K2 domain (itPA: F del and irPA) binds better than the F domain (itPA: K1K1), confirming results of plasminogen activation in soluble fibrinogen assays (section 3.3.2.1.). Interestingly, irPA consistently showed higher activity than itPA: K1K1 in this system unlike in soluble fibrinogen, although irPA still shows lower activity than itPA: F del, confirming results that the K2 domain binds more tightly than the F domain and that it is likely that the change in structure of irPA affects it ability to activate plasminogen or that there are additional sites in tPA that work with the K2 domain to increase binding and plasminogen activation.

A



B



Variant	Lower 95% CI	Percentage activity compared to itPA (100%)	Upper 95% CI
itPA: F del	39	41.7	45.7
itPA: K1K1	9.9	11	12.1
irPA	15.3	16.8	18.6

Figure 4.2 Relative activities of variants compared to full length itPA bound to immobilized fibrinogen. A) The plasminogen activation rates of each variant was compared to full length itPA over a range of concentrations and the resulting graph produced in combistats is shown (including all 9 replicates for each variant). B) The relative activity was calculated and expressed as a percentage of itPA which is set at 100%, the values with the 95% confidence intervals (CI) are displayed under the graph, it can be seen that none of the CI overlap and so the activities of the variants are significantly different at the 5% level.

In this system analyzing the data in Combistats, scitPA (R275E) has about 85-100% of the activity of itPA and tcitPA showed around 40-50% activity compared to itPA (data not shown). These results agree with the results from the assays with fibrinogen in solution (section 3.3.2.1) that scitPA (R275E) appears to bind to fibrinogen with higher affinity than tcitPA.

One drawback to this type of assay is that the amount of itPA and variants bound to fibrinogen is measured using activity and differences in plasminogen activation activity by the variants complicate the interpretation of binding. However, the approach used does allow for a simple comparison between these results using immobilized fibrinogen and kinetic data discussed in chapter 3.3.2.1. A different approach was tested in which fluorescence was used to measure bound tPA. itPA and itPA: F del were expressed as GFP fusion proteins. An initial assay was performed and the fluorescence signal of a range of itPA-GFP and itPA: F del-GFP was measured immediately after addition to the plate containing immobilized fibrinogen and is shown in figure 4.3. A) and B) respectively. Another reading was taken after incubation and before the plate was washed, the results were very similar to those shown in figure 4.3. (data not shown). After the plate was washed, the amount of itPA-GFP and itPA: F del-GFP that remained bound to the immobilized fibrinogen was measured. Figure 4.4. shows that initially no fluorescence peak was observed and only interference from the excitation light can be seen, however after subtracting blank data from wells with no itPA-/itPA: F del-GFP added some peaks were visible, see figure 4.5., although it is difficult to say if these peaks are in fact fluorescence from the GFP variants. The plate was then measured for plasminogen activation and the results in figure 4.6. show that there was active itPA-GFP and itPA: F del-GFP bound to the immobilized fibrinogen but the activity or the binding appears to be weaker than observed with non-fluorescent variants (data not shown). Measuring activity appears to be much more sensitive as plasminogen activation can be

detected at concentrations of itPA-GFP as low as 1.38 nM in figure 4.6 whereas the lowest concentration that fluorescence was observed was 44 nM. Furthermore the intrinsic fluorescence of the variants appears to be different with itPA: F del-GFP showing higher fluorescence than the itPA-GFP. It is clear that much more work would be required to make this into a valid and reproducible assay.

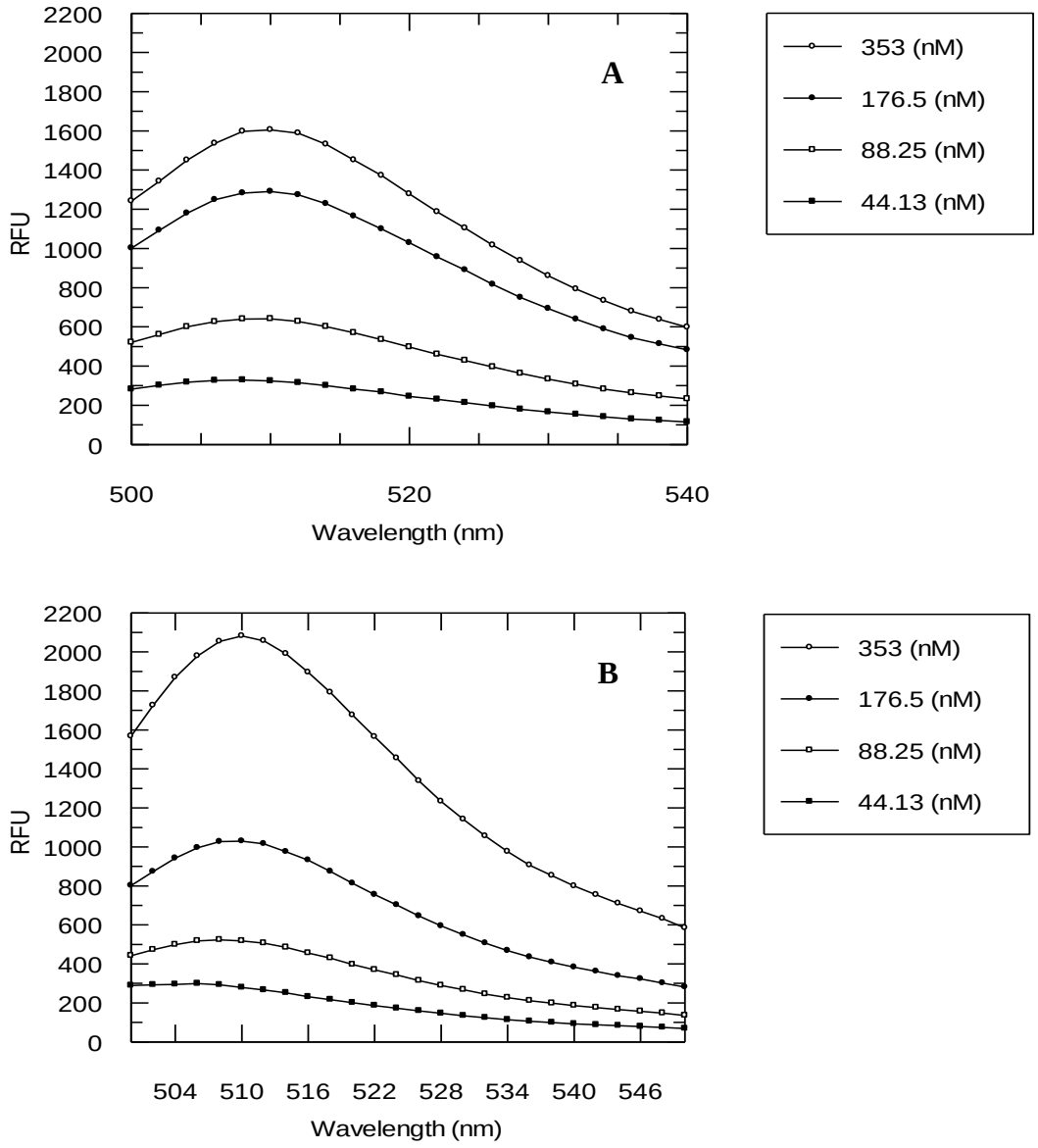


Figure 4.3: itPA-GFP (A) and itPA: F del-GFP (B) in plate with immobilized fibrinogen before incubation. The samples were excited at 475 nm (cut off 495 nm) and the emission wavelength was scanned from 500 nm – 550 nm. Scanning over a range of emission wavelengths rather than taking a single emission reading at 1 wavelength ensures that the result is not interference from the excitation light. Concentrations of 353 nM to 44.13 nM are shown as at concentrations lower than 44 nM the interference from the excitation light is too great.

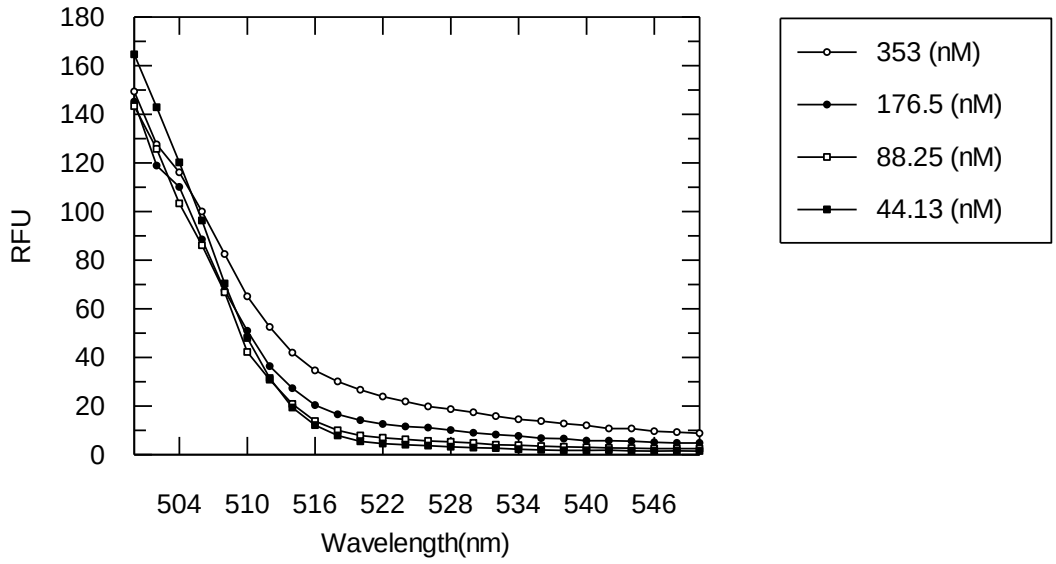


Figure 4.4. itPA-GFP after incubation with immobilized fibrinogen (after plate had been washed). The samples were excited at 475 nm (cut off 495 nm) and the emission wavelength was scanned from 500 nm – 550 nm. Concentrations of 353 nM to 44.13 nM are shown. No blank had been subtracted.

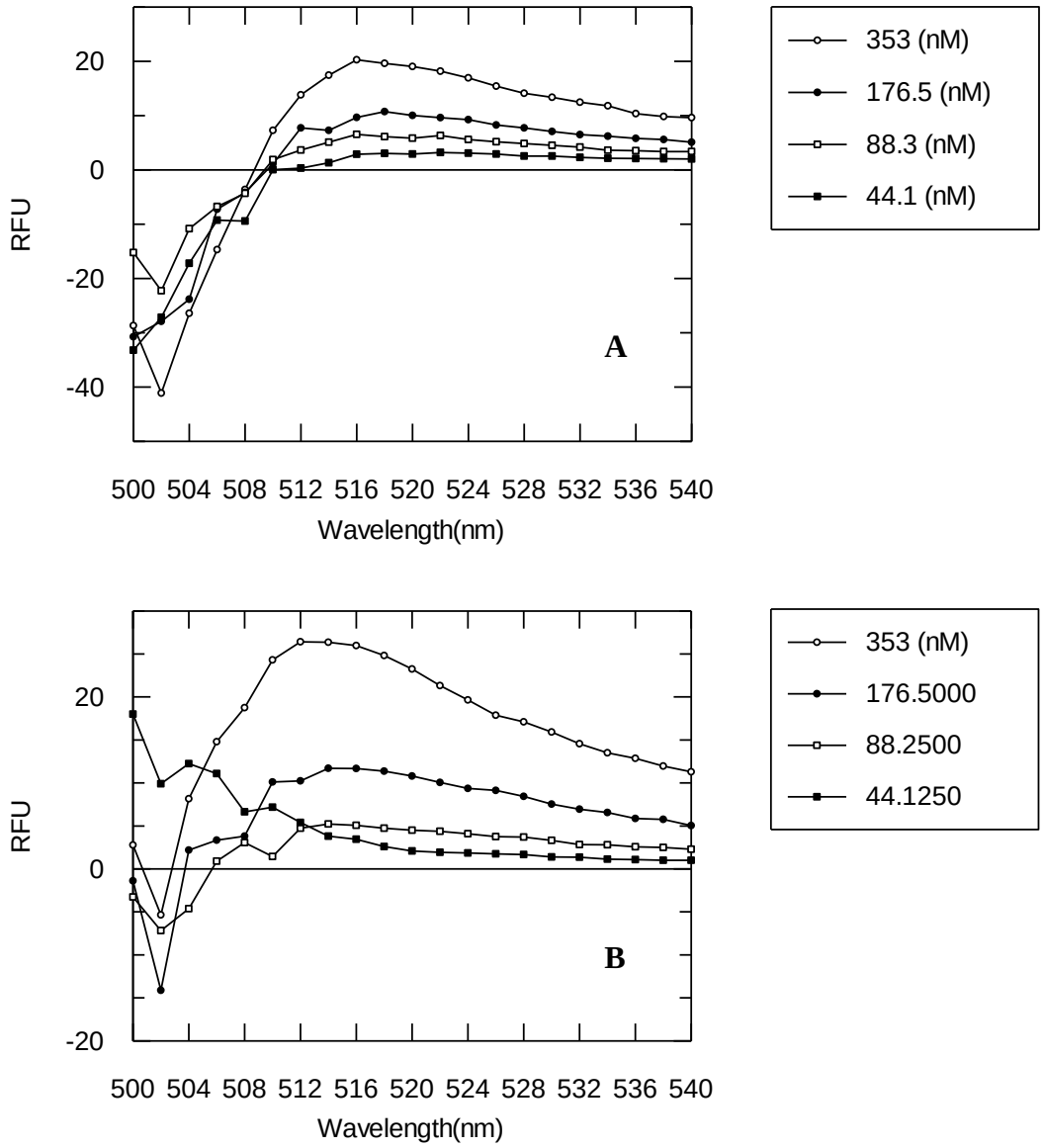


Figure 4.5. itPA-GFP (A) and itPA: F del-GFP (B) after incubation with immobilized fibrinogen (after plate had been washed). The samples were excited at 475 nm (cut off 495 nm) and the emission wavelength was scanned from 500 nm – 550 nm. Concentrations of 353 nM to 44.13 nM are shown. Blank had been subtracted.

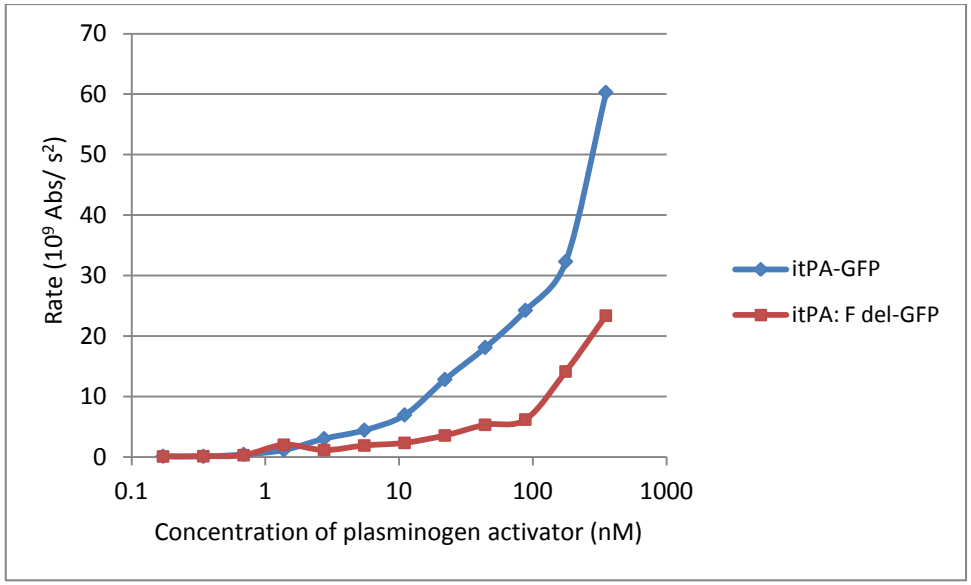


Figure 4.6: Initial plasminogen activation rates of itPA-GFP and itPA: F del-GFP bound to immobilized fibrinogen. Activation rates are represented as a change of absorbance over time squared, measured by the release of *p*NA from S2251 as plasmin is generated. Rates are plotted against log fibrinogen concentration.

4.3.2. Binding of itPA and variants to immobilized templates measured by Surface Plasmon Resonance –Biacore

Measuring binding using surface plasmon resonance is a label free way to generate binding constants without using activity and binding can be observed in real time. itPA and variants were investigated binding to immobilized L-lysine (to mimic C-terminal lysines in proteins), plasminogen, fibrinogen, fibrin (thrombin-treated fibrinogen – fibrin-like surface) and heparin.

4.3.2.1. Binding of itPA and variants to immobilized L-lysine on a CM5 sensor chip

Figure 4.7 demonstrates a typical immobilization of L-lysine onto the surface of a CM5 sensor chip. Typically immobilized levels of 182±80 RU (mean±SD) were obtained. Any loosely bound L-lysine was removed by washing the sensor chip surface by injecting 0.5 M NaCl for 20 s at a flow rate of 20 µl /min.

Binding of 110 nM of itPA and variants to L-lysine was investigated by injecting 40 µl of each sample over the surface of the immobilized L-lysine at a flow rate of 10 µl/ ml in HBS-EP running buffer. Figure 4.8 A shows an overlay of the resulting sensorgrams and looking at the initial results, the itPA: K1K1 appears to show a higher level of binding than itPA: F del and irPA. This result was unexpected as L-lysine is a model surface to attempt to emulate binding to C-terminal lysines on fibrin. Binding to lysine by tPA is via the K2 domain and as itPA: K1K1 has no K2 domain no binding by this variant would have been expected. itPA: F del and irPA show much lower levels of binding than itPA, all three variants would be expected to show similar levels of binding via the K2 domain. Furthermore small levels of

binding are observed with the itPA: K1P variant, which contains no known binding sites. The levels of binding appear to be in order of size of the variants and so the sensorgrams of each variant were adjusted proportionally according to size compared to itPA and can be seen in figure 4.8 B. This did not appear to make any significant difference to the results with the exception of itPA: F del and irPA (the variants with the K2 binding site) which showed more similar levels of binding. These results could be due to non-specific binding, although no non-specific binding was observed in the reference cell and results of the surface performance test showed a steady baseline using 0.5 M Arginine + 0.5 M NaCl as a regeneration solution. If these results are not due to non-specific binding they indicate that the K1 domain contains sites that interact with lysine. Further experiments with a range of concentrations of tPA and variants need to be performed to calculate binding constants as they may reveal differences in affinity that are not apparent when looking at total RU.

Binding of scitPA (R275E), tcitPA and itPA to immobilized lysine in HBS-EP running buffer was also investigated. A small difference in binding was observed, see figure 4.9 for an overlay of the sensorgrams at 110 nM. The results show that binding of itPA > scitPA (R275E) > tcitPA. It would have been expected that scitPA (R275E) would show the strongest binding of the variants with itPA showing similar or less binding as itPA was seen to be predominantly single-chain but containing a small proportion of two-chain. The difference in binding between these variants is small and so it cannot be concluded that there is any significant difference in the strength of binding by these variants.

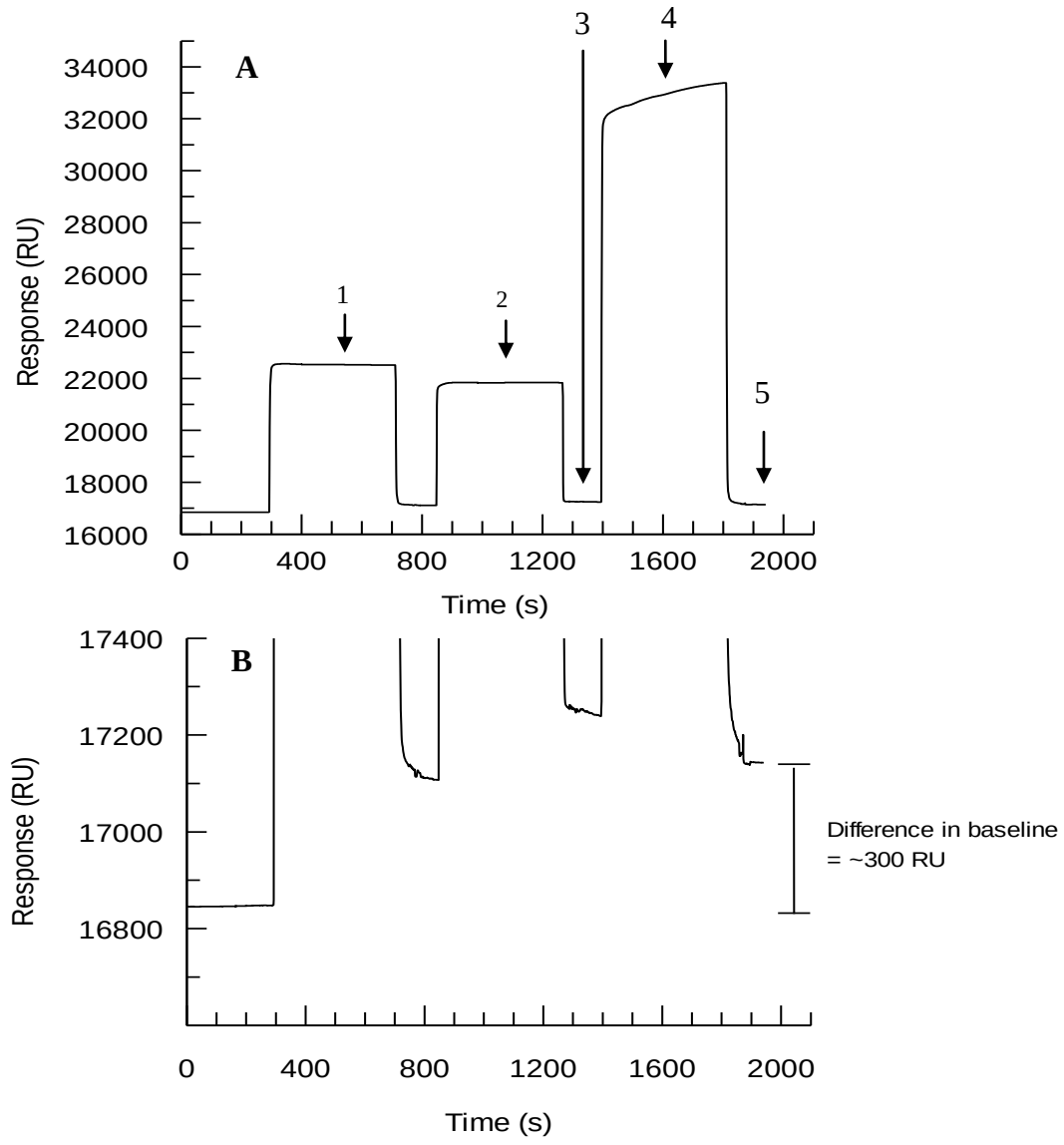


Figure 4.7: Immobilization of L-lysine on to a CM5 sensor chip using amine coupling using the Biacore 2000 immobilization wizard. A) The sensorgram starts with HBS-EP buffer flowing over the surface and this gives the initial baseline of 16848 RU with no ligand bound to the surface. Report point 1 represents the injection of NHS/ EDC to activate the surface, report point 2 is the injection of ligand onto the activated surface and report point 3 shows the amount of ligand that remains bound to the sensor chip surface. Ethanolamine is then injected over the chip to deactivate any remaining active sites that are not bound to the ligand and is shown in report point 4 and the final immobilized ligand is indicated in report point 5 and is the difference between the initial baseline and the final baseline; 296 RU. B) Close up of the bottom section of the sensorgram to show change in baseline after immobilization of L-lysine.

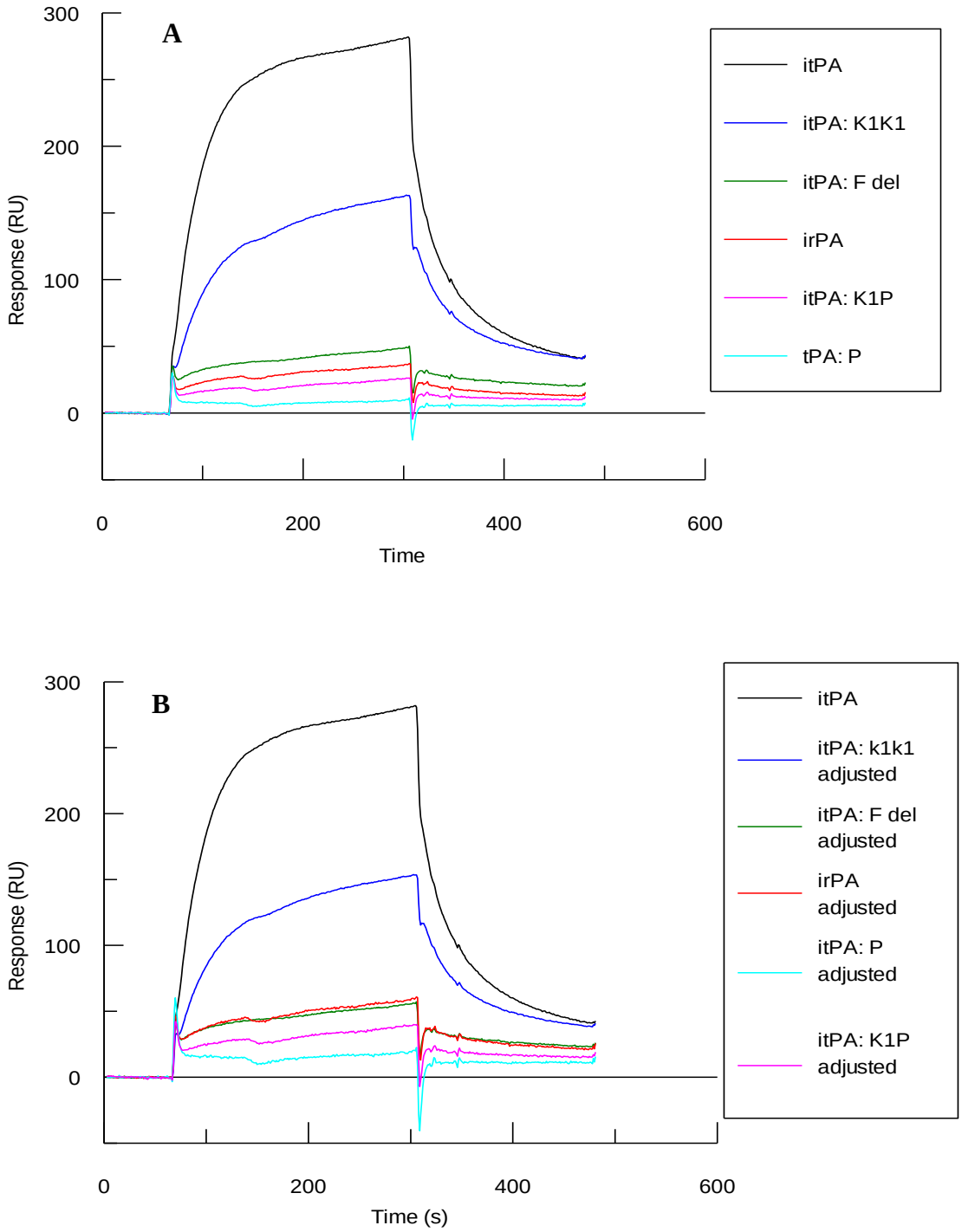


Figure 4.8: Overlay of binding curves of 110 nM of itPA and variants binding to immobilized L-lysine. Sensorgram A shows the original data and sensorgram B shows the data adjusted according to size of all the variants relative to itPA.

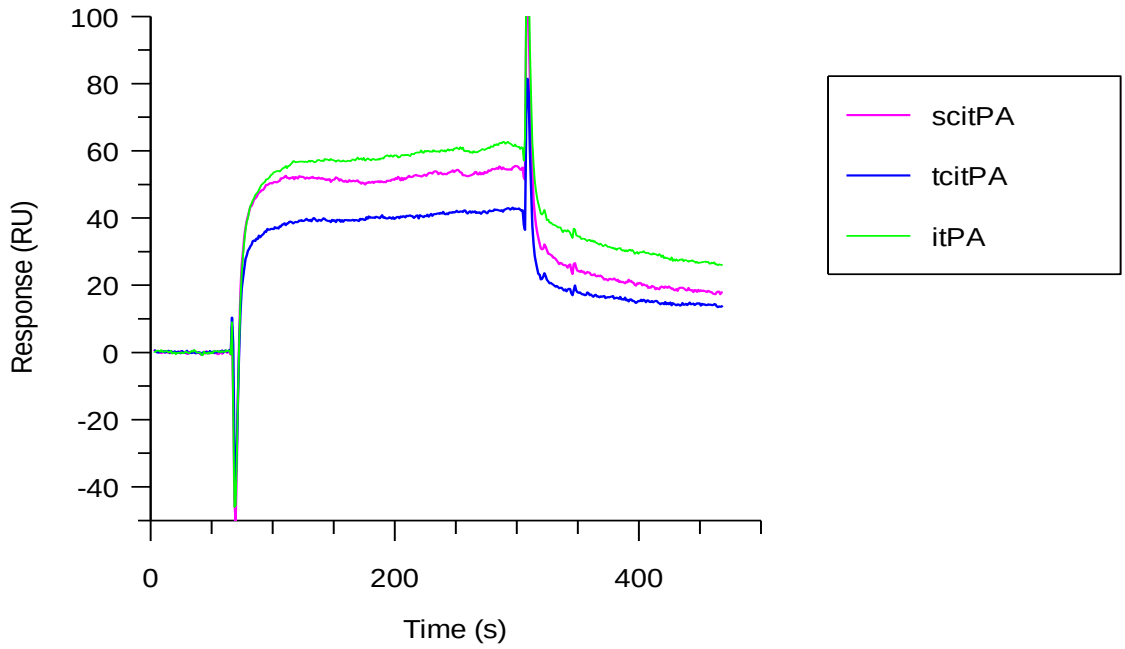


Figure 4.9: Interaction of scitPA (R275E), tcitPA and itPA with L-lysine. Overlays of the sensorgrams (solid lines) of 110 nM of scitPA (R275E), tcitPA and itPA binding to immobilized lysine injected at a flow rate of 10 µl/ min for 4 min.

4.3.2.2. Interaction of itPA, variants, and plasminogen with fibrinogen immobilized indirectly via anti-fibrinogen antibodies.

Anti-fibrinogen antibodies were covalently immobilized to the sensor surface of CM5 chips using amine coupling (as shown in figure 4.7 with L-lysine). Fibrinogen was then injected over the surface of the immobilized antibody, creating a surface of immobilized fibrinogen captured by the immobilized antibody, on which the interaction between fibrinogen and protein could be measured. After the injection of protein, regeneration of the sensor surface involves removing the fibrinogen from the antibody and so for each cycle fibrinogen is recaptured onto the antibody surface. The benefit of using a capture molecule is that fresh fibrinogen is immobilized every cycle and so does not become denatured after numerous cycles. Two anti-fibrinogen antibodies were tested, one was goat polyclonal anti human fibrinogen (ab6666) and the other was goat polyclonal anti fibrinogen β chain (C-20).

Antibody ab6666 was immobilized at a level of 1464.4 RU (aimed for 1000 RU) and 1 mg/ml of sigma fibrinogen diluted into running buffer (HBS-EP) was injected onto the chip for 6 min at a flow rate of 10 µl/ min, resulting in an immobilized fibrinogen level of 51.2±4 RU (Mean ±SD, n= 4). Surfaces were tested by binding of 1.5 µM tPA (Actilyse), that has been dialysed into 10 mM Sodium Acetate to remove any arginine (added by the manufacturer to maintain solubility) and then diluted into HBS-EP running buffer, glu-plasminogen and lys-plasminogen, also diluted into HBS-EP running buffer, by injecting 20 µl at a flow rate of 10 µl /min over the immobilized fibrinogen. The results are shown in figure 4.10 and it can be seen that a small amount of binding was observed with tPA (Actilyse) at around 10 RU and lys-plasminogen at around 25 RU but no binding was observed with glu-plasminogen. Binding of tPA (Actilyse) and lys-plasminogen was then tested on the immobilized antibody surface with no fibrinogen. Similar levels of binding

were observed indicating that regeneration of the chip was not stringent enough and fibrinogen still remained bound to the antibody or that ab6666 binds tPA and plasminogen, see figure 4.10. Another problem that was observed was that ab6666 did not appear to bind fibrinogen with high enough affinity and a high rate of dissociation was observed.

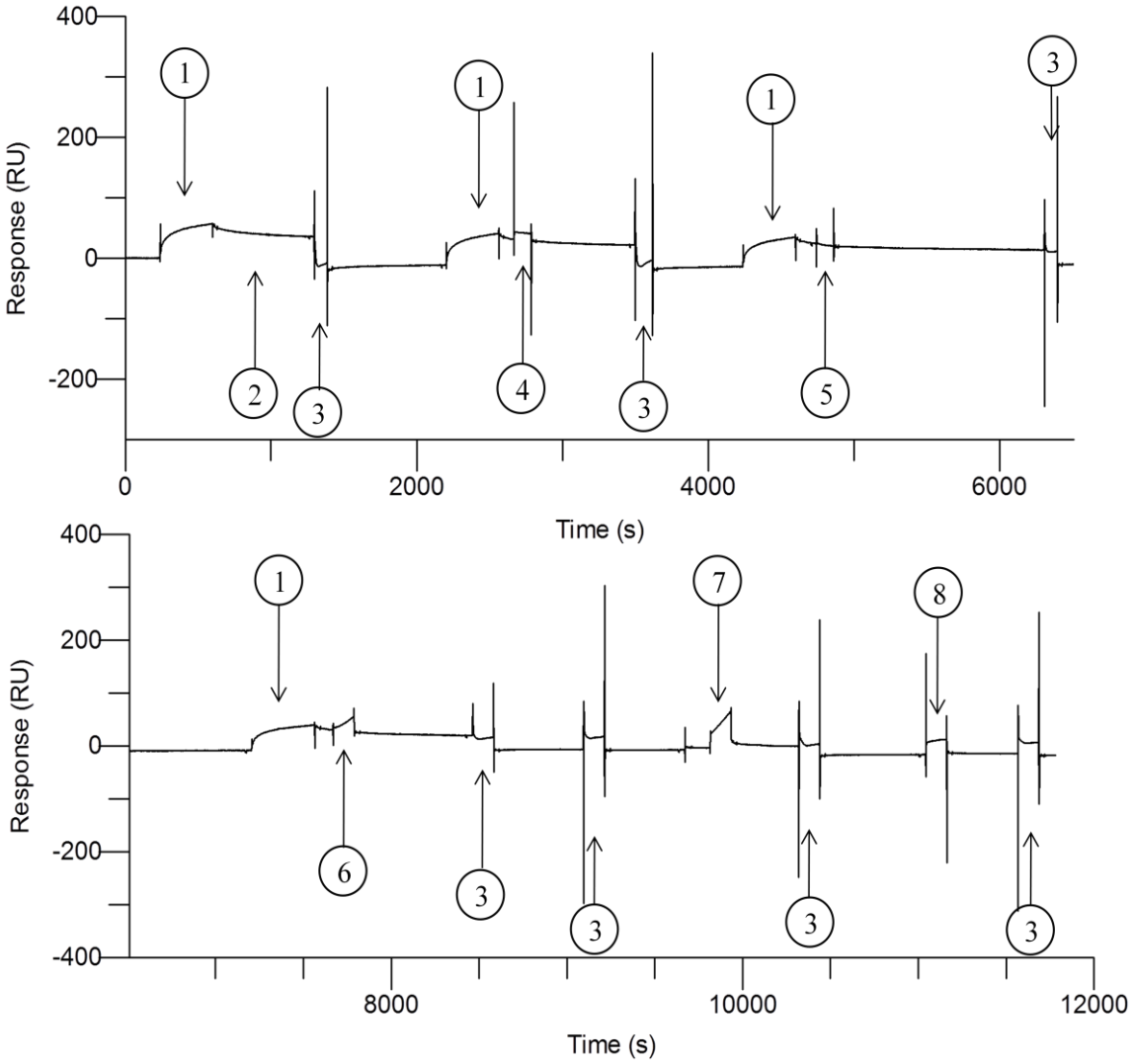


Figure 4.10: Interaction of fibrinogen, tPA and plasminogen with anti-fibrinogen antibody ab6666. Sensorgram of binding to ab6666, the flow rate was set at 10 µl/ min in 0.1 M HEPES buffer and the two panels are one continuous experiment. The spikes in the sensorgram are a result of the subtraction of the control surface to remove the effects of any non-specific binding. The numbers relate to different responses and correspond to (1) injection of 1 mg/ ml fibrinogen for 6 min (2) the dissociation of fibrinogen after the injection was stopped (3) regeneration with 10 mM glycine, pH 1.5 for 30 s (4) injection of 1.5 µM tPA (Actilyse) for 2 min onto captured fibrinogen (5) injection of 1.5 µM glu-plasminogen for 2 min onto captured fibrinogen (6) injection of 1.5 µM lys-plasminogen for 2 min onto captured fibrinogen (7) injection of 1.5 µM lys-plasminogen for 2 min onto antibody surface (no fibrinogen) (8) injection of 1.5 µM tPA (Actilyse) for 2 min onto antibody surface (no fibrinogen)

Higher immobilization levels of anti fibrinogen β chain (C-20) antibody were aimed for (10000 RU) and typically resulted in 8638.9 ± 195 RU (mean ± SD, n=5). Immobilization of fibrinogen was then performed by injecting 2 mg/ ml of sigma fibrinogen onto the antibody surface at 20 µl /min for 5 min; this resulted in an immobilized level of 1176 RU. Bleeding of the fibrinogen from the antibody was observed over a period of several minutes. Binding of both Sigma and Calbiochem fibrinogen was investigated and the results shown in figure 4.11 shows that both fibrinogens are lost from the surface.

Binding of tPA (Actilyse) to both of these fibrinogens was then tested by injecting 1 mg/ml fibrinogen onto the surface of the antibody for 5 min at a flow rate of 20 µl/ min in HBS-EP. 1.5 µM Actilyse was then injected on to the fibrinogen for 2 min at a flow rate of 20 µl/ min. To try to accommodate the response for the dissociating fibrinogen on the binding curves of the tPA, a separate cycle of only fibrinogen (no tPA) was performed and the resulting sensorgrams were subtracted from the sensorgram with the tPA on fibrinogen. The results, seen in figure 4.12, show that this did not completely solve the problem particularly with the tPA on Calbiochem fibrinogen. The results do show that it appears that tPA binds to both fibrinogens by about the same amount. Testing of 1.5 µM tPA (Actilyse) on the antibody chip (no fibrinogen) showed binding, to confirm that tPA was actually binding to the anti-fibrinogen antibody and not to fibrinogen that had not been completely removed during regeneration, antibody was immobilized onto a fresh chip and 1.5 µM tPA (Actilyse) was injected over the surface for 1 min at a flow rate of 20 µl/ min. The results, shown in figure 4.13, were that tPA bound to the antibody to an even greater level ~ 150 RU (figure 4.13) than tPA binding to fibrinogen captured on the antibody ~ 50 RU (figure 4.12). This may mean that the response observed in figure 4.12 is genuinely tPA binding to fibrinogen but it would be hard to entirely trust any results generated using this system.

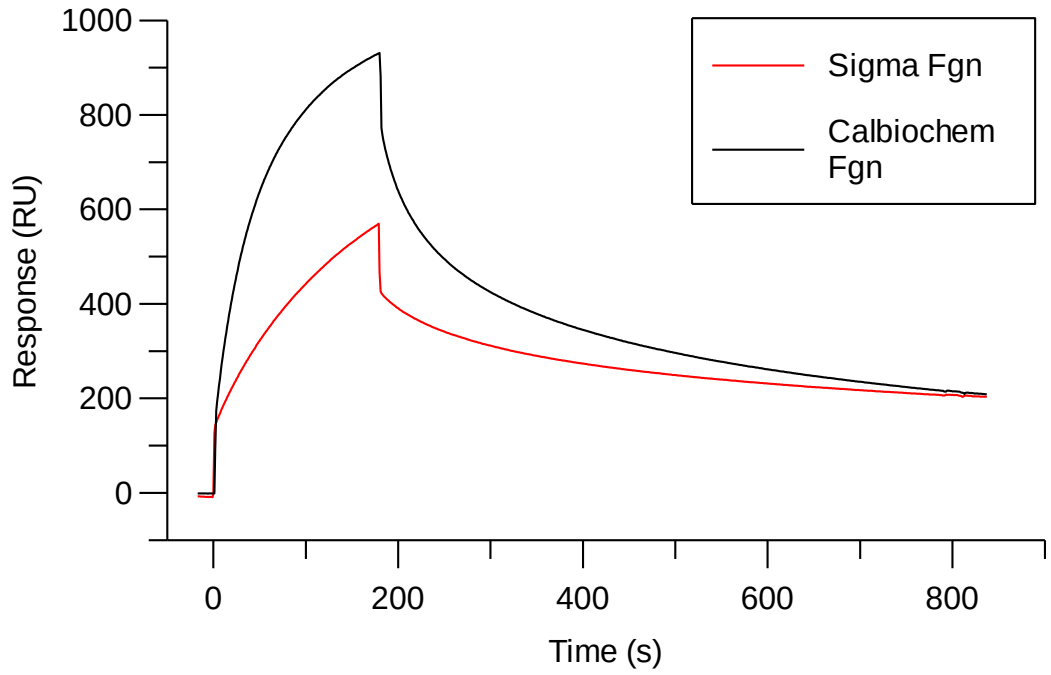


Figure 4.11: Interaction of fibrinogen (fgn) with anti fibrinogen β chain (C-20) antibody. Overlays of the sensorgrams of 2.35 µM Calbiochem and Sigma fibrinogen at a flow rate of 20 µl/ min binding to 8638.9 ± 195 RU (mean ± SD) immobilized anti fibrinogen β chain (C-20) antibody in HBS-EP buffer.

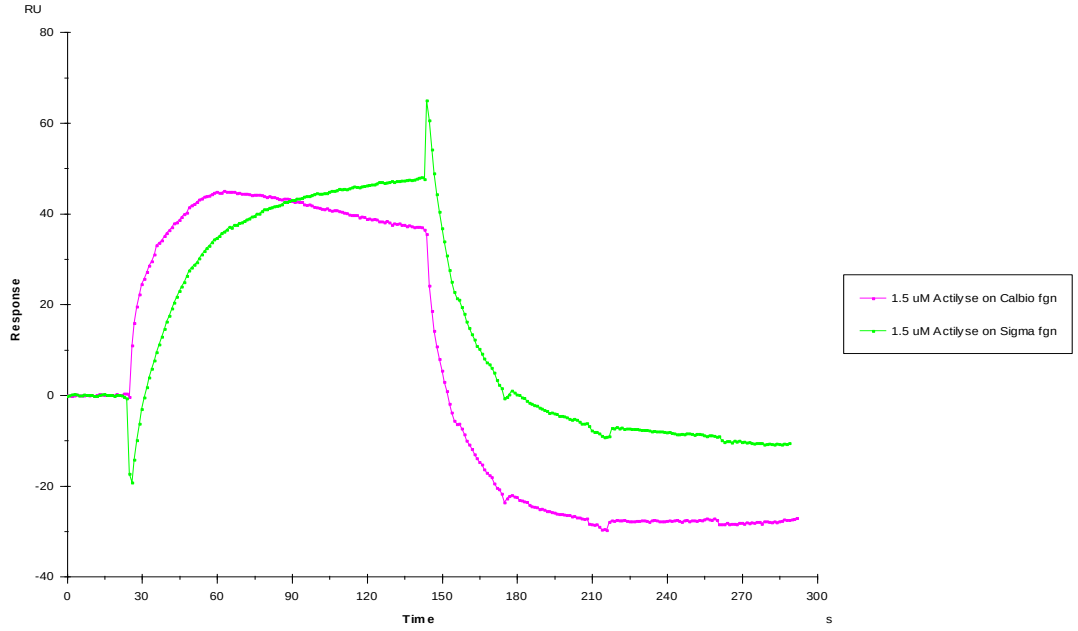


Figure 4.12: Interaction of tPA (Actilyse) with Sigma (green line) and Calbiochem (pink line) fibrinogens captured on anti fibrinogen β chain (C-20) antibody. Overlays of sensorgrams of 1.5 µM tPA (Actilyse) injected at a flow rate of 20 µl/ min for 2 min with HBS-EP running buffer, binding to 1 mg/ml Sigma (green line) or Calbiochem (pink line) fibrinogen that had been injected for 5 min at 20 µl/min on to immobilized antibody minus data of 1 mg/ml Sigma (green line) or Calbiochem fibrinogen (pink line) that had been injected for 5 min at 20 µl/min on to immobilized antibody only (no tPA).

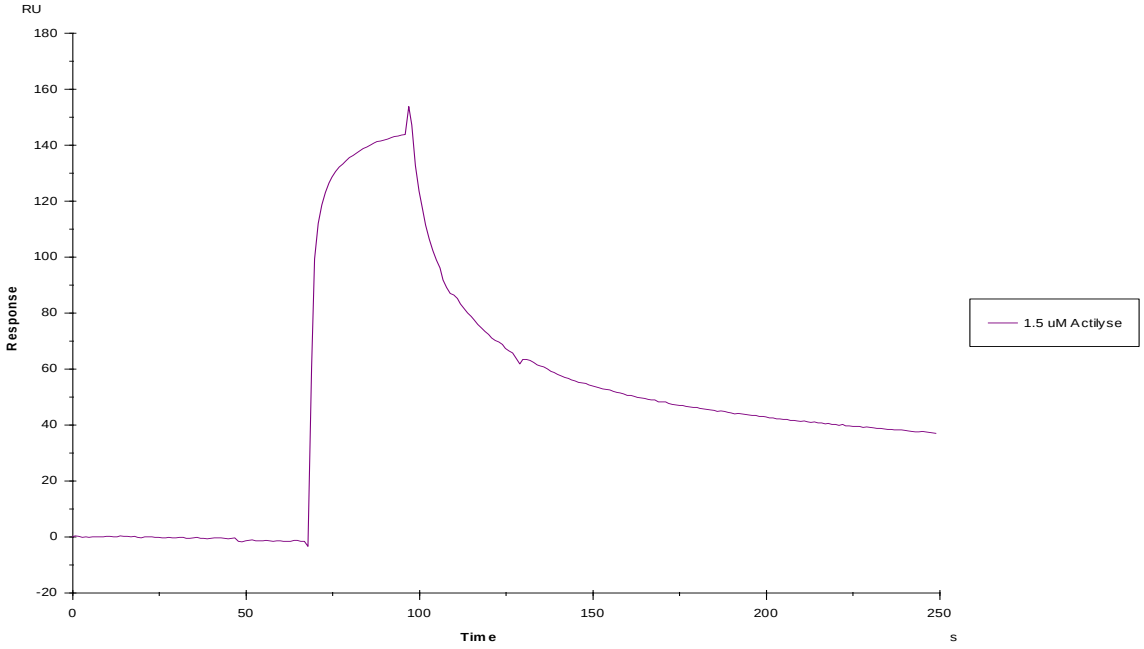


Figure 4.13: Interaction of tPA (Actilyse) with anti fibrinogen β chain (C-20) antibody. Sensorgram of 1.5 μM tPA (Actilyse) injected for 1 min at 20 μl/ min over immobilized anti fibrinogen β chain (C-20) antibody (no fibrinogen) with HBS-EP running buffer.

4.3.2.3. Interaction of scitPA (R275E), tcitPA, and itPA with fibrinogen immobilized directly using covalent immobilization (amine coupling).

The problems faced when using antibodies to capture fibrinogen suggested that direct immobilization of fibrinogen to the sensor chip surface might be a better option. Immobilization was performed by amine coupling of 30 μg/ ml Calbiochem fibrinogen to a CM5 sensor chip aiming for an immobilized level of 2500 RU and typically resulted in an immobilized level of 2428.85 ±68.5 RU (mean ± S.D, n= 7).

The interaction of scitPA (R275E), itPA and tcitPA with the immobilized fibrinogen was observed by injecting each variant diluted to 110 nM in 0.1 M HEPES running buffer on to the fibrinogen for 4 min at 10 μl/ min, the overlay of the resulting sensorgrams are shown in figure 4.14 and show that the levels of binding were scitPA (R275E) > itPA > tcitPA. That itPA showed an intermediate level of binding between the scitPA and tcitPA is logical as itPA was shown to be mostly single-chain with some two-chain, see figure 2.3 and that scitPA (R275E) showed more binding than tcitPA agrees with the results of the plasminogen activation experiments in section 3.3.2.1, figure 3.7, where higher levels of plasminogen activation were seen with scitPA (R275E) at a lower optimum concentration of fibrinogen than tcitPA.

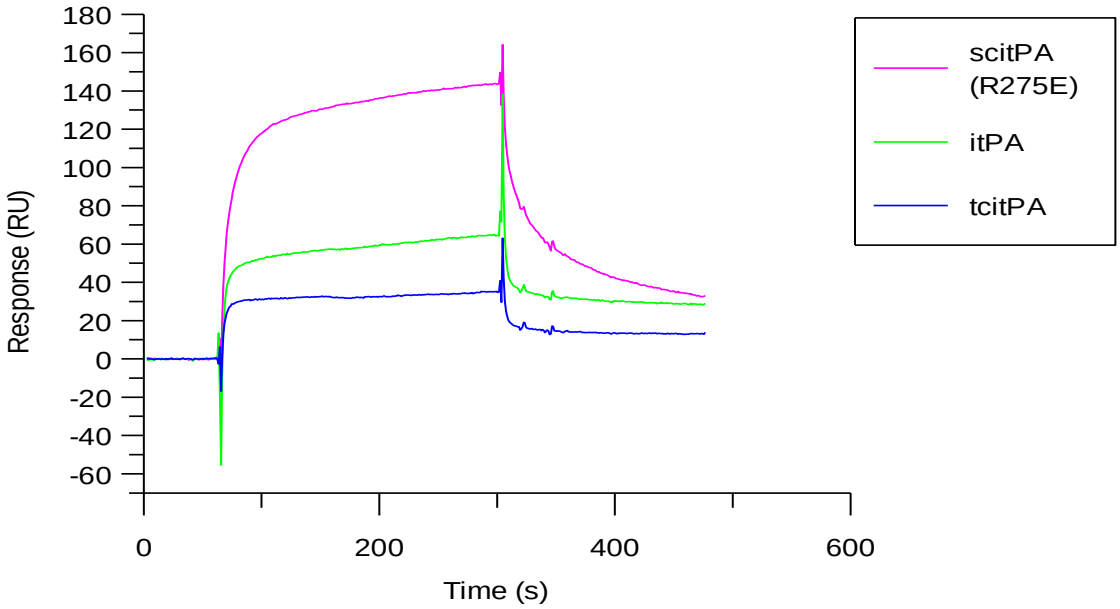


Figure 4.14: Interaction of scitPA (R275E), tcitPA and itPA with fibrinogen. Overlays of the sensorgrams of 110 nM of scitPA (R275E), tcitPA and itPA binding to immobilized fibrinogen injected at a flow rate of 10 µl/ min for 4 min in 0.1 M HEPES running buffer.

The interaction of scitPA (R275E) and tcitPA was investigated in more detail by performing a concentration series experiment by binding 30-110 nM of each variant diluted in to 0.1 M HEPES buffer onto immobilized fibrinogen for 1 min at a flow rate of 10 µl/ min. Binding constants were calculated from the data by fitting to the two-step and heterogeneous ligand binding models as these more complex models were found to show improved fitting over the simple 1:1 Langmuir binding model. Overlays of the sensorgrams of 30-110 nM of scitPA (R275E) and tcitPA binding to fibrinogen are shown in figure 4.15 A and B respectively with the fits from the two step models and 4.16 A and B respectively with the fits from the heterogeneous model, in both the coloured lines represent the experimental data and that black lines represent the fits. The kinetic parameters derived from the two-step or heterogeneous binding models are shown in tables 4.4 and 4.5 respectively. It is difficult to distinguish which model fits the data best and neither model fits the data perfectly; this is likely to be due to the complex nature of tPA binding to fibrinogen and the heterogeneous nature of fibrinogen. tPA has two known binding sites for fibrin/ fibrinogen and there are likely to be multiple sites in fibrin/ fibrinogen that bind tPA. Further complications may arise from alterations to the fibrinogen molecule resulting from the immobilization chemistry and washing procedures that can cause some denaturation or gross changes in the structure of this large complex protein. However looking at the curves and the binding constants derived from the fitting it can be seen that using the two-step binding model (figure 4.15 A and B and table 4.4) that scitPA (R275E) has a higher level of binding and a higher affinity for the immobilized fibrinogen, K_D = 68 nM than the tcitPA, K_D = 113 nM, figure 4.16 shows how the K_D is calculated for the binding constants generated using the two-step binding model, using sctPA (R275E) as an example. The first step in the reaction being the part that is different between the variants, with tcitPA showing a faster k_{d1} (0.45 s^{-1}) than scitPA (R275E) (0.11 s^{-1}). When that data was analysed with the heterogeneous binding model (figure 4.17

and table 4.5) it can be seen that for both scitPA (R275E) and tcitPA there are two reactions with reaction 1 accounting for ~2/3 of the overall response and has faster kd values and lower affinity than the second reaction. Reaction 1 is also the where the difference between the variants can be seen with scitPA showing higher affinity K_{D1} = 46 nM than tcitPA K_{D2}= 135 nM, whereas the second reaction shows similar kinetics for the two variants ~20 nM. Although it is difficult to distinguish between the two models it can be seen that with both the variants the R_{max} total (R_{max1} + R_{max2}) values from the heterogeneous binding model (scitPA (R275E) = 181 RU and tcitPA = 127 RU) are similar to the R_{max} values derived from the two step binding model (scitPA (R275E) = 150 RU and tcitPA = 124 RU). Similarly the K_D values from the two-step binding model (scitPA (R275E); K_D= 68 nM and tcitPA; K_D= 113 nM) are in a similar range to the K_D values for the first reaction and major component in the heterogeneous binding model (scitPA (R275E); K_{D1}= 46 nM and tcitPA; K_{D1}= 135 nM).

The immobilized fibrinogen was then treated with 10 nM bovine thrombin for 1 h at a flow rate of 2 µl/ min in HBS-EP to try to generate a more fibrin-like surface (fibrin*) and see if there was any change in the kinetics. After the injection of thrombin the surface was washed with 1 M NaCl for 30 s to try to remove any loosely bound structures, this resulted in a reduction in baseline (from starting baseline) of ~ 40 RU (figure 4.18). It is possible that this reduction in baseline could be a result of the cleavage of the fibrinopeptides by the thrombin. The resulting surface is unlikely to be very similar to fibrin due to the fact that the fibrinogen is immobilized, it is unlikely that the molecules will be able to cross link in the way that they would in solution but it may reveal sites in the fibrinogen molecule that are exposed in fibrin but not in fibrinogen. A range of 30-110 nM of scitPA (R275E) and tcitPA were injected over the fibrin* for 1 min at 10 µl/min, as with the fibrinogen. The resulting sensorgrams were fitted with the two-step and heterogeneous binding models and can be seen in figures 4.19 and 4.20 respectively, where in each figure graph A is the data from the scitPA and

graph B is the data from tcitPA, the colored lines represent the response data and the black lines are the fits. The kinetic constants from the two-step binding model are shown in table 4.4 and for the heterogeneous binding model in table 4.5. The patterns observed are very similar to those described with the variants binding to fibrinogen using the heterogeneous binding model; the K_D values were lower indicating a higher affinity for the fibrin* than the fibrinogen although the R max values and the responses from the curves are lower. Whereas the results of the two-step model show that fibrin* has lower affinity for fibrin than fibrinogen. It is difficult to determine which model describes the data and the binding best and it would be nice to believe that the variants have higher affinity for fibrin* than fibrinogen but due to the fact that fibrin* is unlikely to be very similar to fibrin it is entirely possible that the treatment has changed the protein and the variants bind to it with lower affinity.

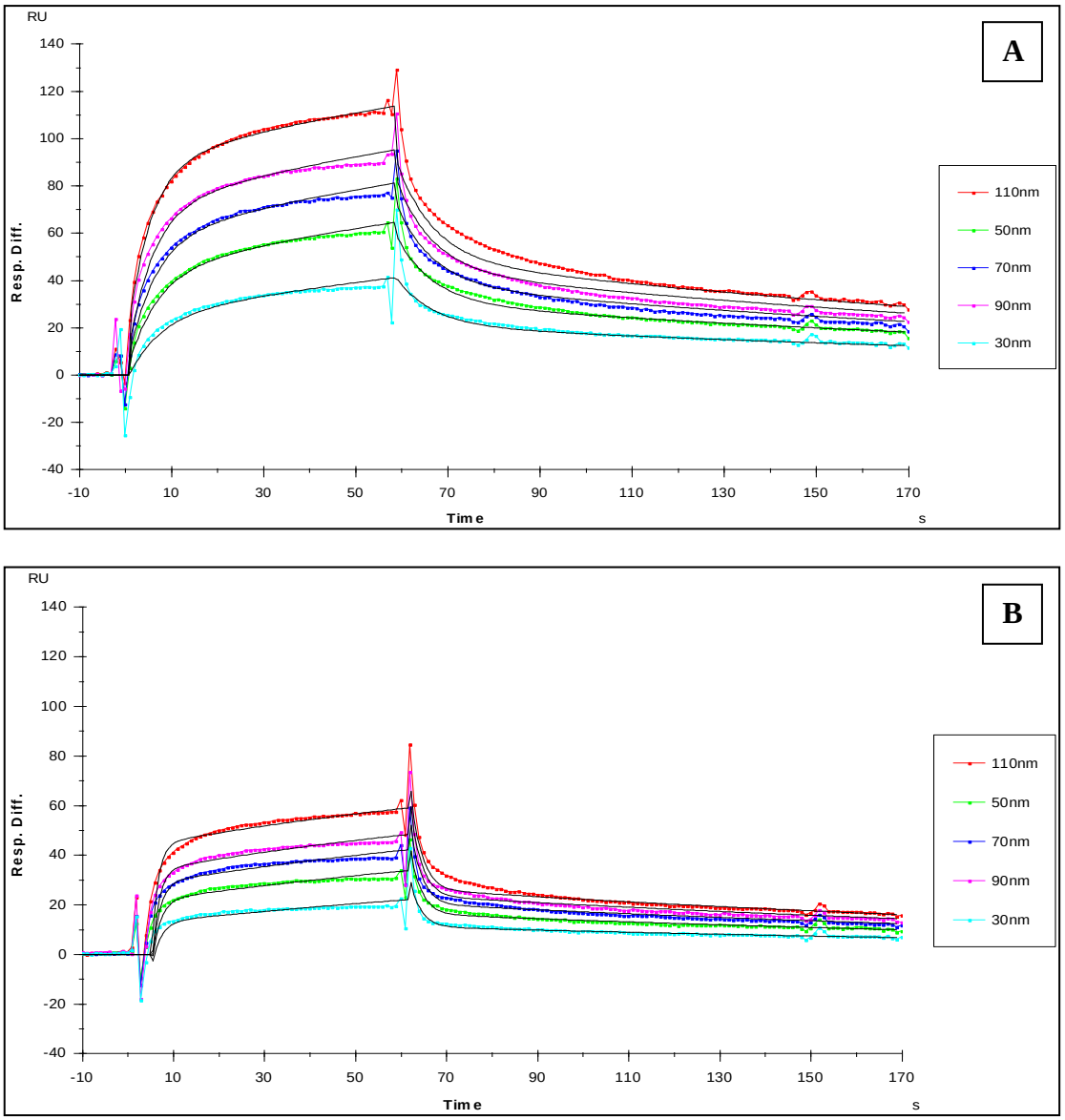


Figure 4.15: Global analysis of scitPA (R275E) and tcitPA binding to fibrinogen using a two-step binding model. Overlays of sensorgrams of 30-110 nM of A) scitPA (R275E) and B) tcitPA binding to immobilized fibrinogen in 0.1M HEPES buffer. The coloured lines represent the response data and the black lines represent the fit to a two-step binding model.

Variant	Rate and affinity constants	R_{max} (RU)
scitPA (R275E)	**A + B** $\underset{0.109\ s^{-1}}{\overset{845000\ M^{-1}\ s^{-1}}{\rightleftharpoons}}$ **AB** $\underset{0.0055\ s^{-1}}{\overset{0.016\ s^{-1}}{\rightleftharpoons}}$ **AB*** $K_{D\ initial} = \frac{k_{d1}}{k_{a1}} = 128.9$ nM $K_{D\ final} = K_{D\ initial} * \frac{k_{d2}}{(k_{a2} - k_{d1})} = 67.5$ nM	150

Figure 4.16: Binding constants for scitPA (R275E) interacting with immobilized fibrinogen using a two-step binding model. 30-110 nM of scitPA (R275E) was injected on to immobilized fibrinogen. Data were analysed using the BIAevaluation 3.2 software using the two step binding model and the binding constants obtained are shown. The R_{max} represents the maximum binding capacity of the surface in RU.

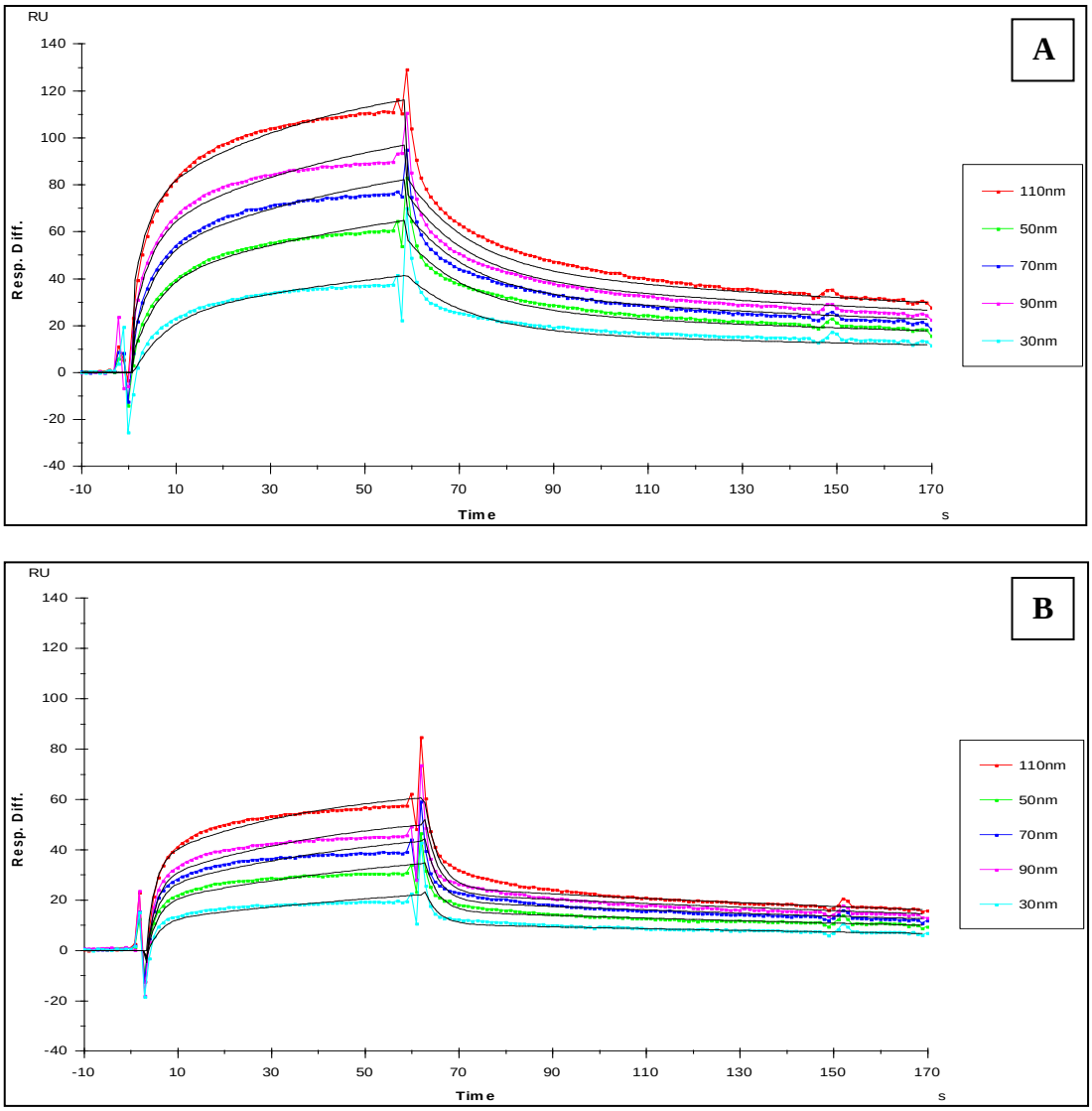


Figure 4.17: Global analysis of scitPA (R275E) and tcitPA binding to fibrinogen using a heterogeneous ligand binding model. Overlays of sensorgrams of 30-110 nM of A) scitPA (R275E) and B) tcitPA binding to immobilized fibrinogen in 0.1M HEPES buffer. The coloured lines represent the response data and the black lines represent the fit to a heterogeneous binding model.

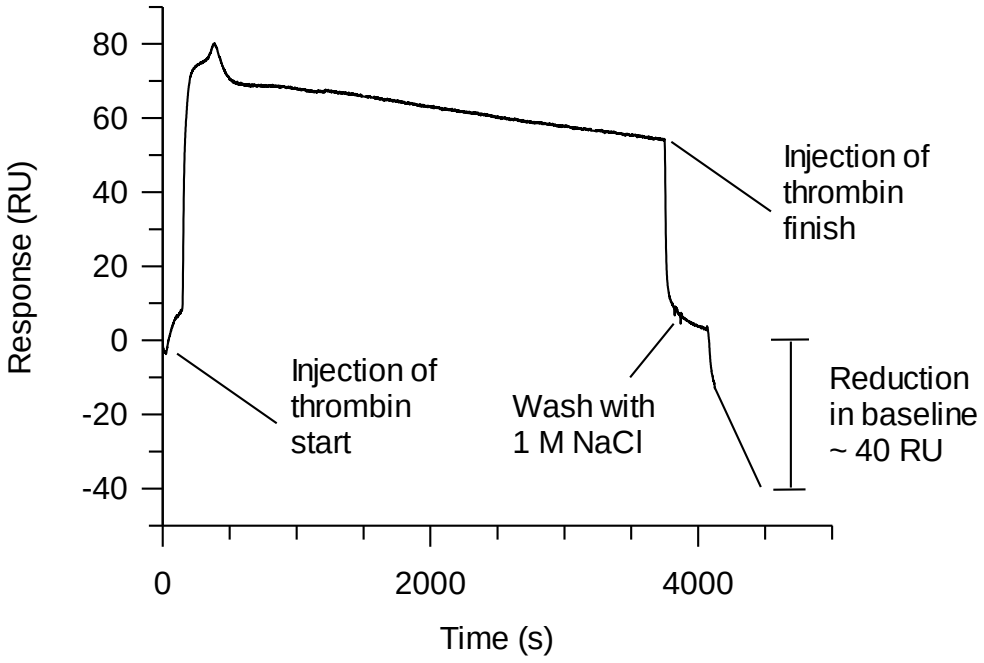


Figure 4.18: Treatment of immobilized fibrinogen with bovine thrombin. Sensorgram showing a 1 h injection at a flow rate of 2 µl/ min of bovine thrombin over ~2500 RU immobilized fibrinogen to generate fibrin* - a fibrin like surface.

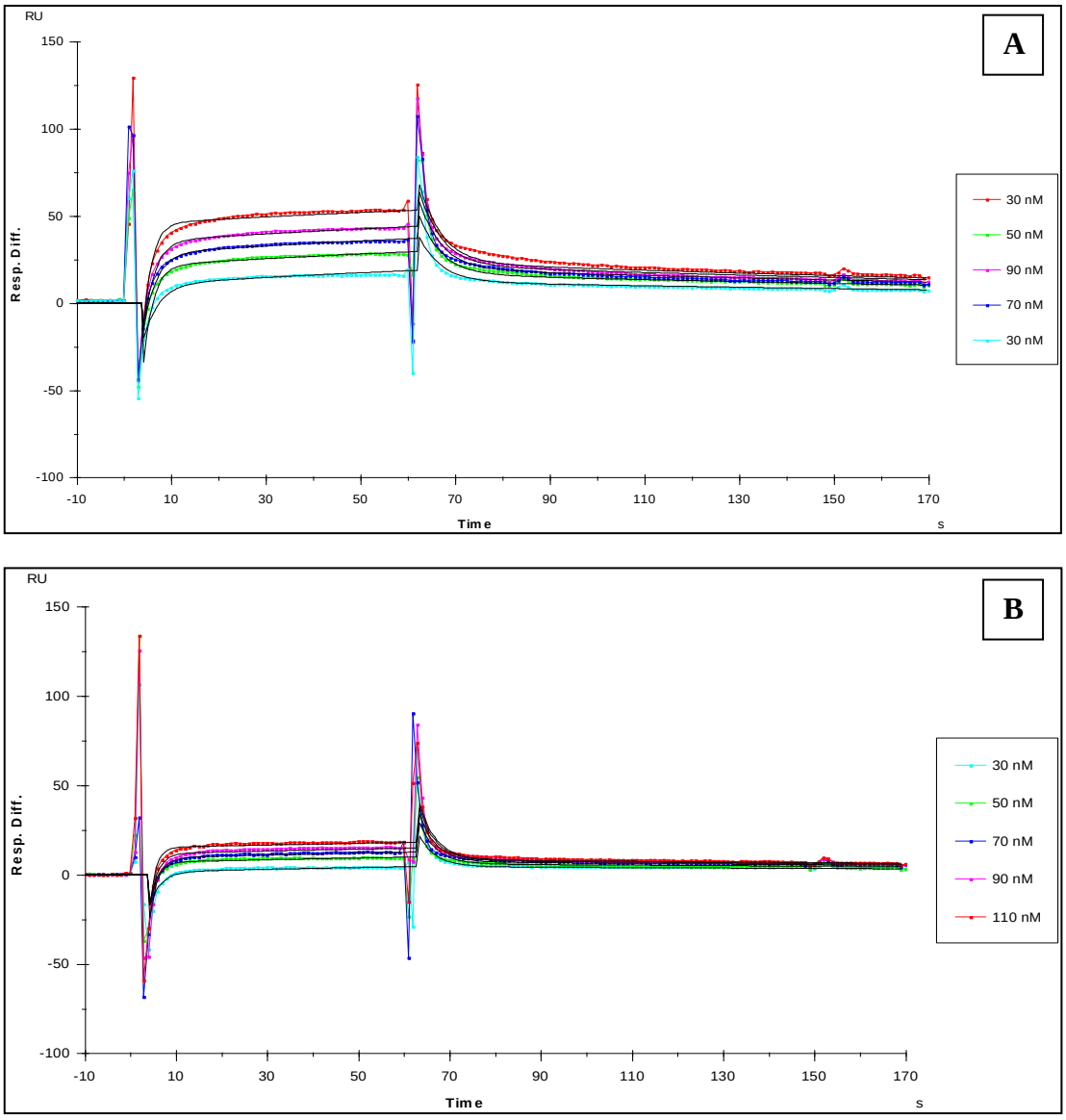


Figure 4.19: Global analysis of scitPA (R275E) and tcitPA binding to fibrin* using a two-step binding model. Overlays of sensorgrams of 30-110 nM of A) scitPA (R275E) and B) tcitPA binding to immobilized fibrin* in 0.1M HEPES buffer. The coloured lines represent the response data and the black lines represent the fit to a two-step binding model. (fibrin* is thrombin treated immobilized fibrinogen)

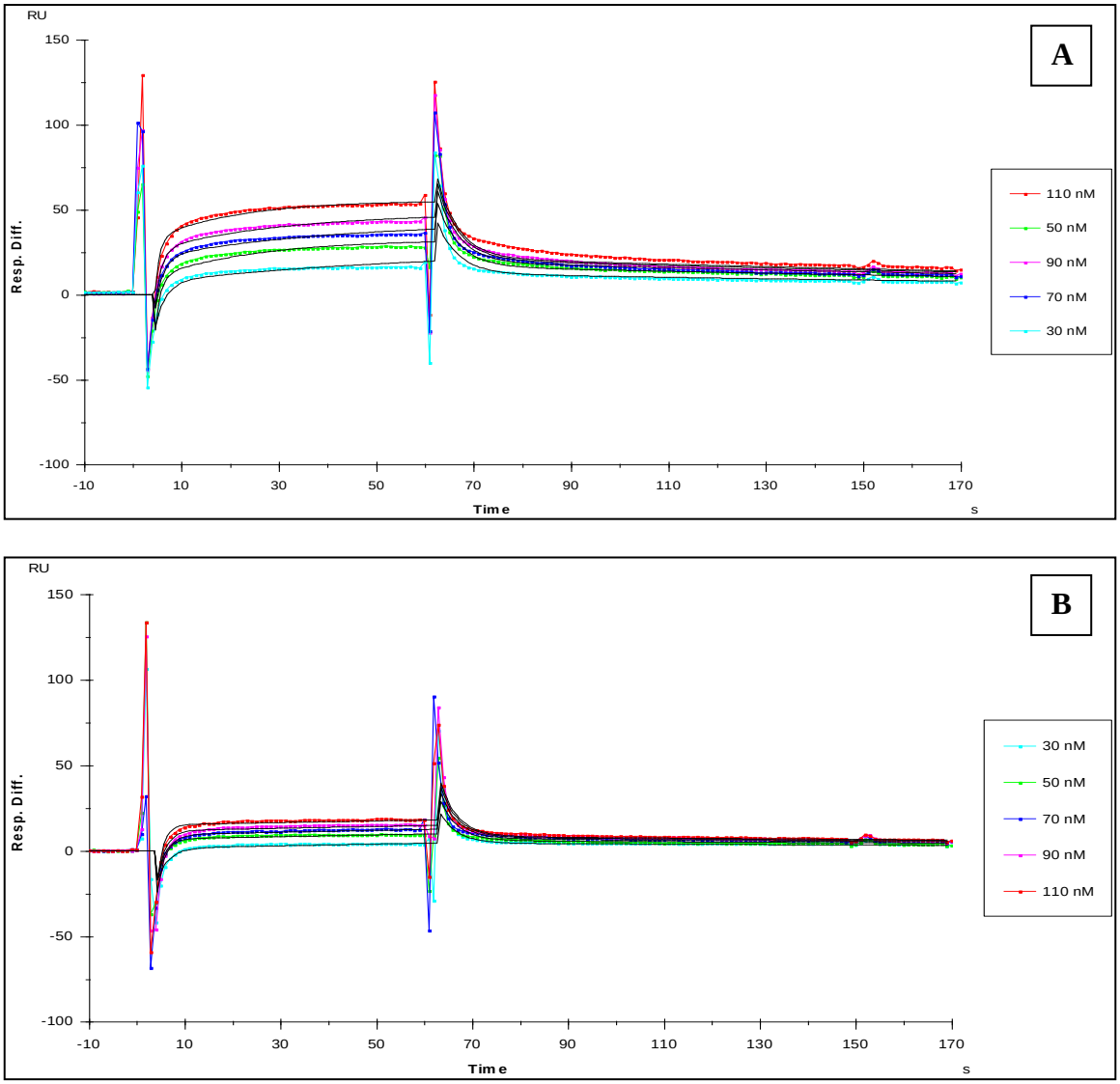


Figure 4.20: Global analysis of scitPA (R275E) and tcitPA binding to fibrin* using a heterogeneous binding model. Overlays of sensorgrams of 30-110 nM of A) scitPA (R275E) and B) tcitPA binding to immobilized fibrin* in 0.1M HEPES buffer. The coloured lines represent the response data and the black lines represent the fit to a heterogeneous binding model. (fibrin* is thrombin treated immobilized fibrinogen)

Surface	Variant	k_{a1} M^{-1} s^{-1}	k_{d1} s^{-1}	k_{a2} s^{-1}	k_{d2} s^{-1}	K_D (nM)	R_{max}
Fibrinogen	scitPA (R275E)	8.5E+05	1.1E-01	1.6E-02	5.5E-03	68	150
	tcitPA	2.9E+06	4.2E-01	1.1E-02	4.8E-03	113	124
Fibrin*	scitPA (R275E)	3.4E+06	2.1E-01	8.0E-03	4.6E-03	92	99
	tcitPA	4.6E+06	2.7E-01	4.0E-03	2.8E-03	128	60

Table 4.4: Binding constants for scitPA (R275E) and tcitPA binding to fibrinogen and fibrin* generated by fitting to the two-step binding model. Response data and fits are shown in figures 4.15 and 4.19 and the data were analysed using the BIAevaluation 3.2 package.

		Reaction 1				***Reaction 2***					
Surface	**Variant**	k_{a1} **M^{-1} s^{-1}**	k_{d1} **s^{-1}**	K_{D1} **(nM)**	R_{max1} **(RU)**	k_{a2} **M^{-1} s^{-1}**	k_{d2} **s^{-1}**	K_{D2} **(nM)**	R_{max2} **(RU)**	R_{max} ***total***	***% reaction #1***
Fibrinogen	scitPA (R275E)	3.5E+06	1.6E-01	46	107	2.2E+05	4.7E-03	22	74	181	59
	tcitPA	2.3E+06	3.1E-01	135	91	2.3E+05	4.1E-03	18	36	127	72
Fibrin*	scitPA (R275E)	7.5E+06	2.3E-01	30	65	4.8E+05	4.1E-03	9	25	90	73
	tcitPA	5.9E+06	4.7E-01	79	86	9.8E+05	3.5E-03	4	8	95	91

Table 4.5: Binding constants for scitPA (R275E) and tcitPA binding to fibrinogen and fibrin* generated by fitting to the heterogeneous binding model. Response data and fits are shown in figures 4.17 and 4.20 and the data were analysed using the BIAevaluation 3.2 package.

4.3.2.4. Interaction of itPA and domain variants with fibrinogen

The interaction of itPA; itPA: K1K1, itPA: F del and irPA with the immobilized fibrinogen was observed by injecting 20-110 nM of each variant diluted in to buffer B used as running buffer onto immobilized fibrinogen for 2.5 min at a flow rate of 10 µl/ min. The running buffer used was changed to buffer B (from 0.1 M HEPES used in analysis of scitPA and tcitPA) to bring it into line with the buffer used for the analysis of these variants with heparin, which required a change in buffer to reduce the ionic strength to increase the levels of binding. Buffer B was also the buffer used in the experiments with plasminogen activation in the presence of fibrinogen. Binding constants were calculated from the data by fitting to the heterogeneous binding model as the data was found not to follow a simple 1:1 Langmuir binding model. Overlays of the sensorgrams of 110 nM of tPA and variants as an example concentration are shown in figure 4.21 and just looking at the binding curves it can be seen that levels of binding were itPA > itPA: F del > itPA: K1K1 > irPA. These results agree with the results seen in the plasminogen activation assays in section 3.3.2.1. that binding is most when K2 and F domain are present and that binding by K2 domain is better than binding by F domain and that the dramatic change in structure of rPA has affected its ability to bind or that there are other site in the tPA molecule that contribute to binding.

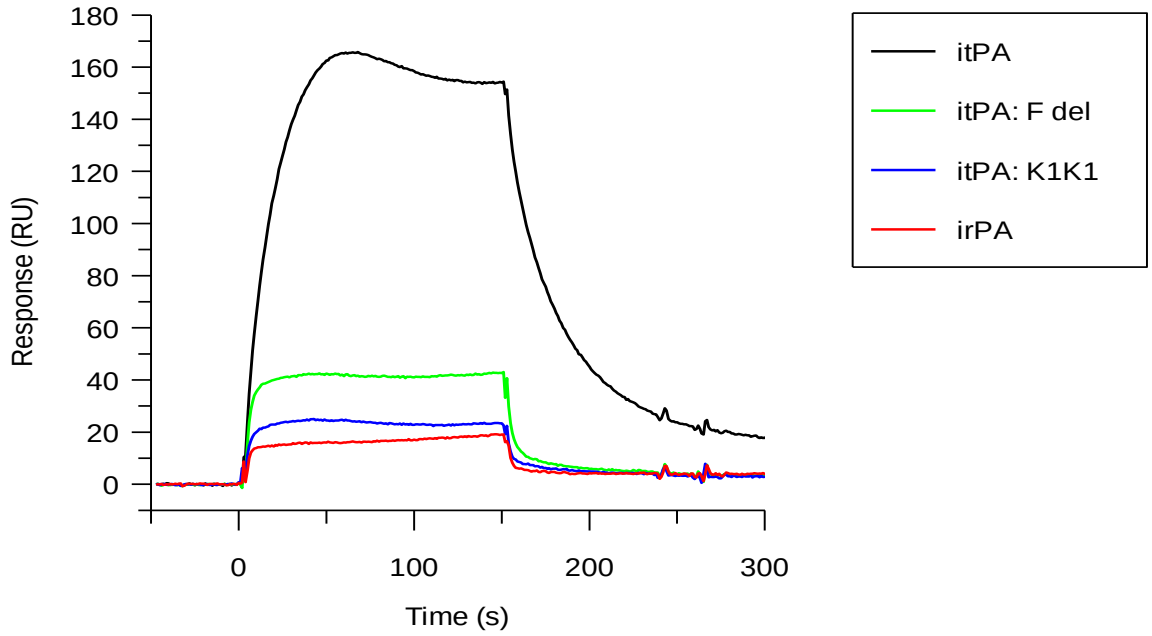


Figure 4.21: Interaction of itPA and variants with fibrinogen. Overlays of sensorgrams of 110 nM of itPA; itPA: K1K1, itPA: F del and irPA binding to immobilized fibrinogen for 2.5 min at a flow rate of 10 µl/ min with buffer B as running buffer.

The fitting of itPA and variants to generate kinetic constants was difficult due to the fact that the variants reached only low RU values and had weak affinity and although itPA had higher RU, looking at the sensorgrams they suggest that binding is complex. Figure 4.22 A-D show the overlays of the response data and the fits from the heterogeneous binding model of itPA, itPA: K1K1, itPA: F del and irPA binding to immobilized fibrinogen for 2.5 min at a flow rate of 10 µl/ min with buffer B as running buffer. Table 4.6 shows the kinetic constants generated from fitting to the heterogeneous binding model and looking at the data it can be seen that k_{d1} is fast for variants and is not well estimated as it is outside Biacore specifications. The R_{max} is difficult to estimate as RU and required range for study is < 50 RU and estimates for R_{max} are over 300 RU. Based on the results of the plasminogen activation experiments in section 3.3.2.1 it is clear that interactions between tPA and fibrinogen are complicated and multiple interactions are anticipated, therefore making it difficult to apply a suitable kinetic model for fitting. Assuming a heterogeneous ligand with separate distinct binding sites the data suggest that there are 2 reactions (at least). The first reaction is weak with fast kinetics generating K_D values of between 2-4 µM for the variants and 0.15 µM for itPA, this reaction accounts for 85% of the overall response. The second reaction is a small proportion and has higher affinity than the first reaction due to the slower k_d values, it is possible that this reaction may be background. itPA is clearly much better at binding to fibrinogen than the variants and the R_{max} appears to be better estimated because the RU observed is getting closer to the R_{max} fitted. These RU values suggest there is several 100 RU binding capacity on these fibrinogen chips.

The differences in the shapes of the binding curves generated when comparing the interactions of itPA, scitPA (R275E) and tcitPA (figure 4.14), and when comparing itPA and the other variants (figure 4.22) is likely to be due to the different running buffers used 0.1 M HEPES and buffer B, respectively. The investigation into tPA solubility shown in section

4.3.2.6 showed that less precipitation of tPA occurred in 0.1 M HEPES buffer than in buffer B but at the concentration of tPA used in the Biacore experiments only a very small change in absorbance due to precipitation was observed (see figure 4.27).

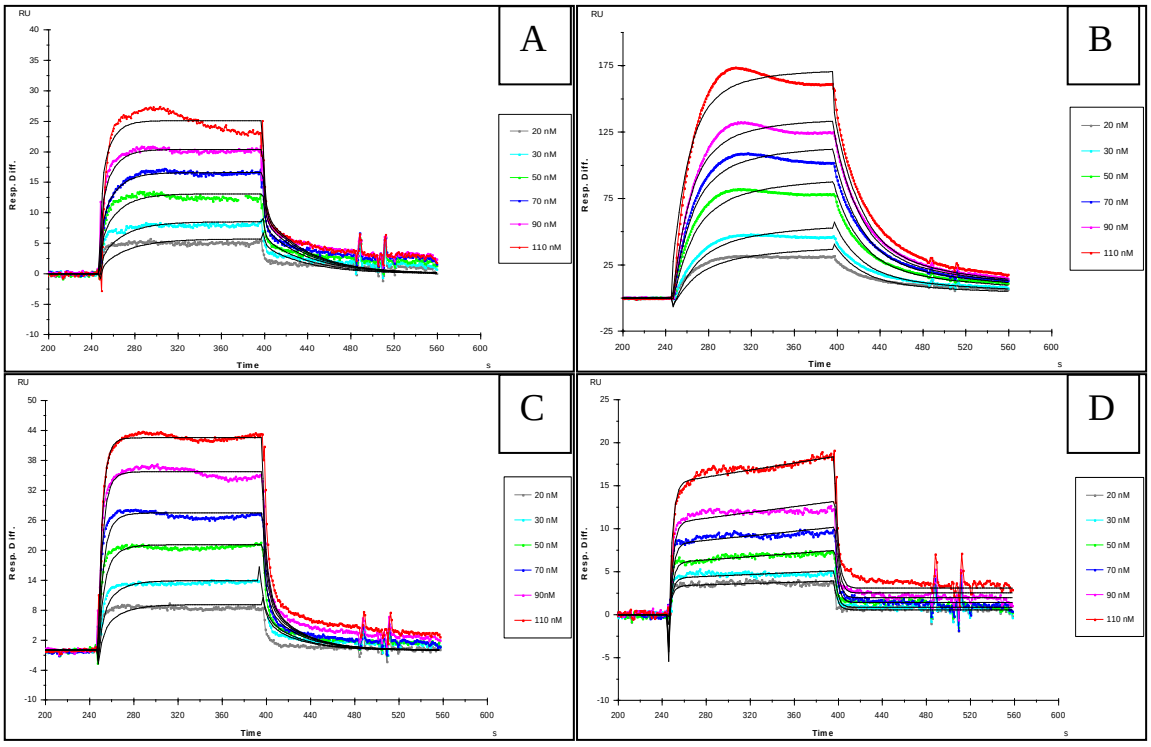


Figure 4.22: Global analysis of itPA and variants binding to fibrinogen using a heterogeneous binding model. Overlays of sensorgrams of 20-110 nM of A) itPA, B) itPA: F del, C) itPA: K1K1 and D) irPA binding to immobilized fibrinogen in buffer B. The coloured lines represent the response data and the black lines represent the fit to a heterogeneous binding model.

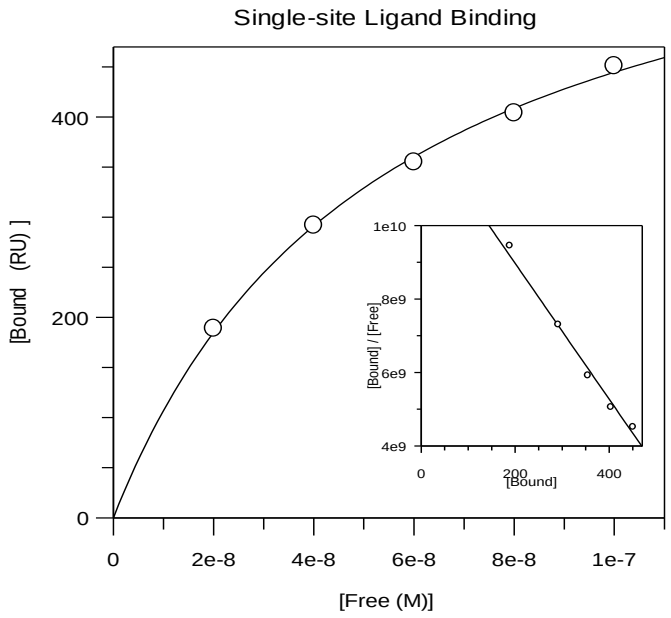
	Reaction 1				*Reaction 2*					
Variant	k_{a1} **M^{-1} s^{-1}**	k_{d1} **s^{-1}**	K_{D1} **(nM)**	R_{max1} **(RU)**	k_{a2} **M^{-1} s^{-1}**	k_{d2} **s^{-1}**	K_{D2} **(nM)**	R_{max2} **(RU)**	R_{max} ***total***	***% reaction 1***
irPA	2.1E+05	3.6E-01	1744	353	4.3E+03	2.0E-03	519	59	412	86
itPA: F del	1.5E+05	2.8E-01	1833	578	1.3E+06	3.4E-02	26	15	593	97
itPA: K1K1	1.1E+05	5.0E-01	4564	457	6.8E+05	2.5E-02	37	14	471	97
itPA	2.6E+05	4.1E-02	158	278	1.5E+05	5.0E-03	34	45	323	86

Table 4.6: Binding constants for itPA, itPA: F del, itPA: K1K1 and irPA binding to fibrinogen generated by fitting to the heterogeneous binding model. Response data and fits are shown in figures 4.20 A-D and the data were analysed using the BIAevaluation 3.2 package.

The interaction of plasminogen with immobilized fibrinogen was also investigated, a range of glu-plasminogen from 0.2 μM-1 μM and a range of lys-plasminogen from 20-100 nM diluted in buffer B running buffer were injected over immobilized fibrinogen for 2.5 min at 10 μl/ min. The data were not well fitted using the 1:1 Langmuir binding model or any more complex binding model and so kinetic constants could not be obtained. To obtain an idea of the affinity of each plasminogen the association phase of the response curves were fitted with the Langmuir association binding model (separate k_a/k_d). The Req (RU) generated from this fit was used to find an estimate of the K_d using single site ligand binding equation in Grafit which fits data to a single site saturation curve, where the amount of ligand bound is plotted as a function of the amount free:

$$[Bound] = \frac{Capacity.[Free]}{K_d + [Free]}$$

The graphs for lys-plasminogen are shown in figures 4.23. Binding of glu-plasminogen to immobilised fibrinogen is too weak to generate a binding curve over this range of ligand and no K_d can be estimated. Lys-plasminogen appears to have a much higher affinity for fibrinogen such that K_d = 54.1 nM.



Parameter	Value	Std. Error
Capacity	6.9e2	2.3e1
Kd value	5.4e-8	4.1e-9

Figure 4.23: Single site saturation curve of lys-plasminogen binding to fibrinogen. Req (RU) of response curves from 20 – 100 nM lys-plasminogen binding to immobilized fibrinogen fitted to equation 4.1

4.3.2.5. Interaction of itPA, variants, and plasminogen with heparin-biotin immobilized on SA chips

Immobilization of heparin was performed by binding biotinylated heparin to streptavidin coated chips (SA). The interaction of itPA; itPA: F del, itPA: K1K1, and irPA with the immobilized heparin was observed by injecting 20-110 nM of each variant diluted in to buffer D used as running buffer onto immobilized heparin for 2.5 min at a flow rate of 10 µl/ min, overlays of these sensorgrams are shown in figure 4.24 (A-D). Looking at the curves of itPA, figure 4.24 A, it can be seen that there are some problems with the binding of the highest concentrations (110 and 90 nM), where the shape of these curves are different from the curves at the lower concentrations and there is some bulk shift effects at the beginning of the injections. When the reference cell was examined it was seen that there was some unspecific binding to the reference cell which was observed with all the variants, non-specific binding to streptavidin by heparin binding proteins has been observed by others (Marks et al, 2001; Yakovlev et al, 2003). There was no real binding observed with itPA: F del and irPA (variants binding with the K2 domain) and there was no correlation between the height of the curve and the concentration of variants was seen. The itPA: K1K1 variant showed about half the amount of binding as the itPA. The problems with non-specific binding plus the fact that binding of tPA to heparin is likely to complicated due to the heterogeneity of heparin and likely multiple possible interactions, it was not possible identify a suitable model and derive any kinetic constants. However looking at the overlay of the variants in figure 4.25 it can be seen that the results of the binding agree with the results of the kinetic experiments in section 3.3.2.2, that the F domain binds more to heparin than the K2 domain. The interaction of glu-plasminogen with heparin was also observed by injecting 12.5-800 nM diluted in to buffer D, used as running buffer onto immobilized heparin for 2.5 min at a flow rate of 10 µl/ min, overlays of these sensorgrams are shown in figure 4.26. A similar problem with non-specific

binding to the reference cells was observed and as with tPA no suitable binding model was identified.

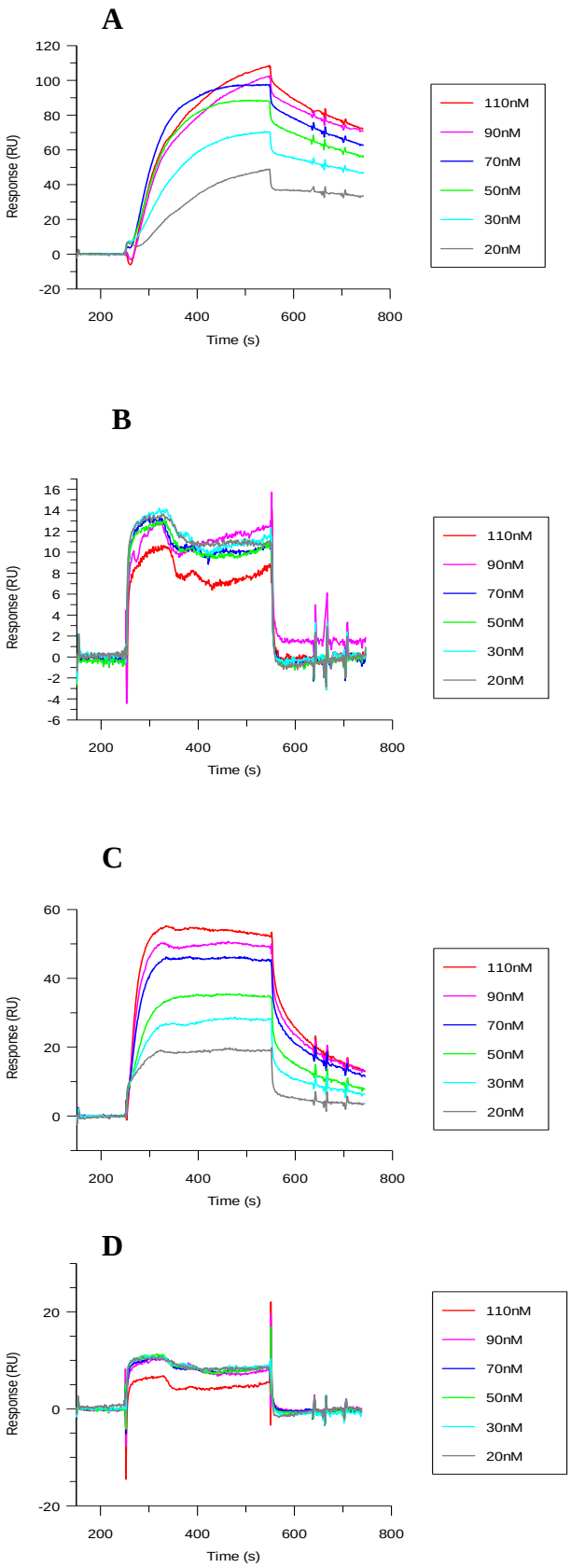


Figure 4.24: Interaction of itPA and variants with heparin. Overlays of sensorgrams of 30-110 nM of A) itPA, B) itPA: F del, C) itPA: K1K1 and D) irPA binding to immobilized heparin for 2.5 min at a flow rate of 10 µl/ min with buffer D as running buffer.

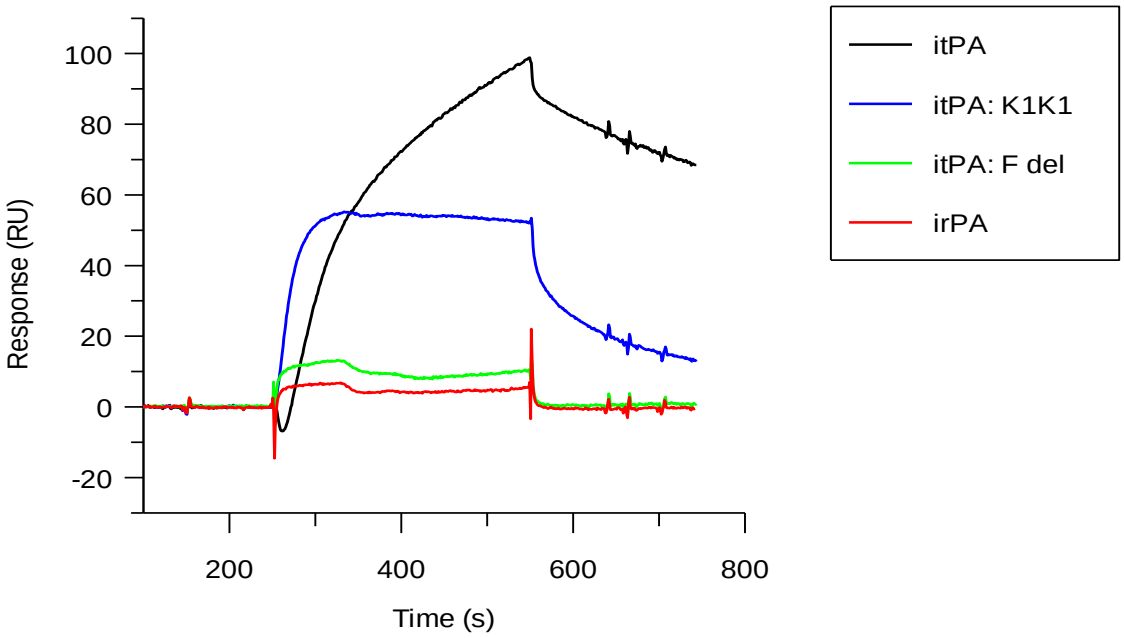


Figure 4.25: Interaction of itPA and variants with heparin. Overlays of sensorgrams of 110 nM of itPA; itPA: K1K1, itPA: F del and irPA binding to immobilized heparin for 2.5 min at a flow rate of 10 µl/ min with buffer D as running buffer.

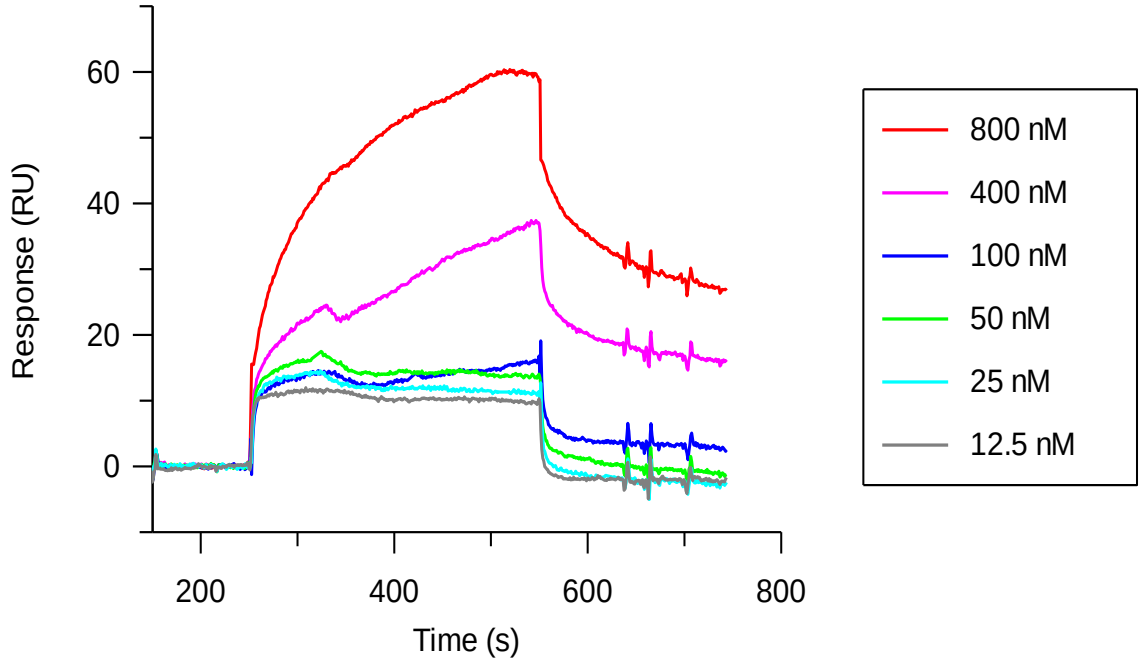


Figure 4.26: Interaction of glu-plasminogen with heparin. Overlays of sensorgrams of 12.5 nM-800 nM of glu-plasminogen binding to immobilized heparin for 2.5 min at a flow rate of 10 µl/ min with buffer D as running buffer.

4.3.2.6. Investigating conditions for improved tPA solubility.

tPA is rather insoluble and the clinical product Actilyse is formulated in a high concentration of arginine which improves the solubility profile. However, this will probably interfere with binding studies and alternative conditions were investigated that might optimise solubility under conditions that would be less likely to affect binding studies and were similar to conditions used for kinetic studies (where very low concentrations of tPA and variants are needed). The amount of precipitation of tPA was investigated with different buffers over time to determine which buffer systems were best suited to maximise tPA solubility. As tPA is more soluble at low pH a range of tPA concentrations in 10 mM sodium acetate pH 4.0 were added to 5 times strength buffer, bringing the solutions up to the desired pH. This was done with of a range of buffers. The absorbance at 405 nm was measured over 16 h, to monitor precipitation, at room temperature and the results after 0 h and 16 h are shown in figure 4.27.

The 10mM sodium acetate buffer pH 4.0 caused the least amount of precipitation, even after 16 h (although maximum precipitation appears to occur in < 3 h, data not shown), but is not suitable for Biacore studies due to unphysiological pH. The Tris buffer containing 0.1M Arginine also reduced precipitation but again cannot be used as the arginine inhibits binding of the tPA to ligands of interest. The other buffers that showed the least precipitation were 0.1 M HEPES, 0.1 M NaCl pH 7.4l and HBS-E (0.01 M HEPES, 0.15 M NaCl) with EDTA. HBS-EP which is HBS-E containing P (p20 surfactant) is the buffer that is recommended for use in SPR by Biacore. 0.1 M HEPES was tested to see if the higher concentration of HEPES reduced precipitation.

The effect of different surfactants was then investigated with one of the buffers that resulted in the most precipitation of tPA, the two buffers that showed the least precipitation, and the Tris buffer pH 7.4 at 37 ºC because this is the buffer that is used for the clot overlay assays.

The results show that there is very little difference between any of the surfactants as can be seen from figure 4.28. The results show that tPA diluted, rather than dialysing into HEPES-based buffers immediately before use is best for prevention of precipitation for use in SPR studies.

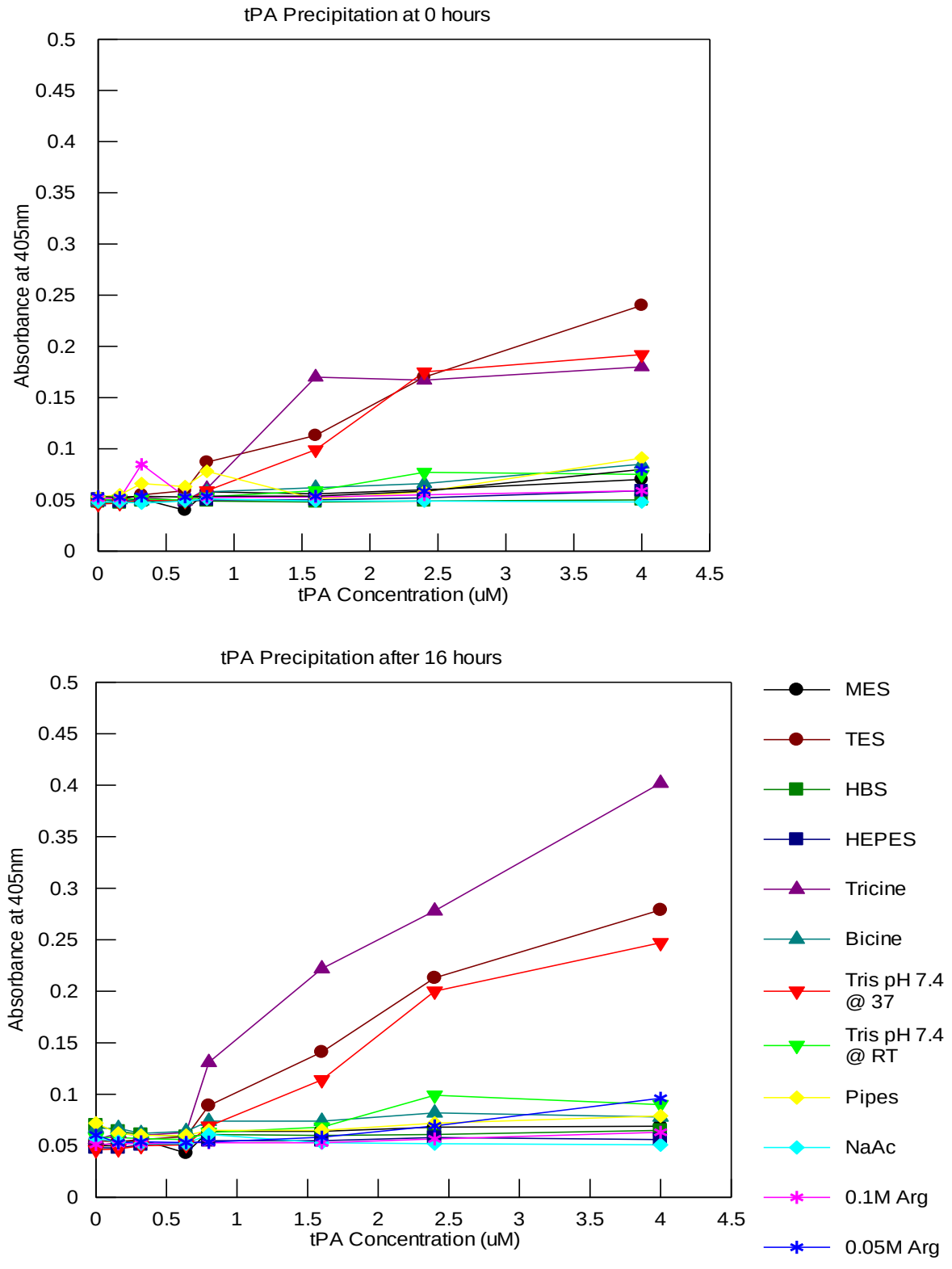


Figure 4.27: Absorbance as a measure of tPA precipitation over 5 concentrations in a range of buffers.

A: Shows the amount of precipitation of tPA in a range of different buffers at 0 h, over a range of starting concentrations of tPA. B: Shows the amount of precipitation of tPA in a range of different buffers at 16 h, over a range of starting concentrations of tPA.

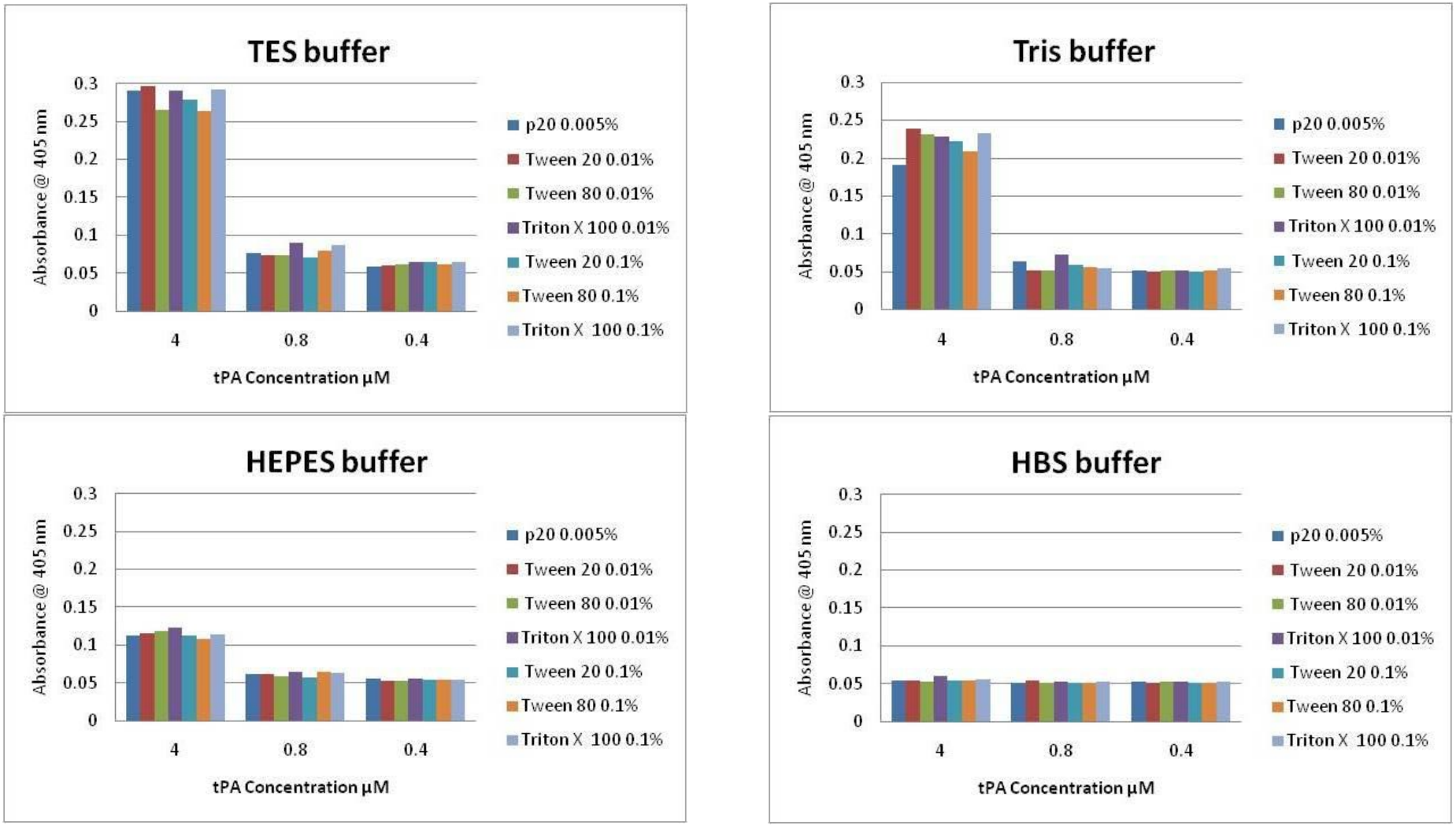


Figure 4.28: TES, Tris, HEPES and HBS-E buffers containing a range of different surfactants to monitor solubility of tPA at 4, 0.8 and

CHAPTER 5: MODELLING

5.1. Introduction

Computer modelling of biological systems is a useful tool in the study of biochemical kinetic systems. Modelling can be used to compare theories with experimental results, to observe the effects of changing any parameter of the pathways and to find estimates of kinetic parameters. The way kinetic simulation software works is to use kinetic functions, with values for their parameters and the concentrations of the metabolites to calculate the metabolite concentrations over time, at specified intervals. The majority of kinetic models are based on the generation of differential equations. Often, the differential equations can be derived from a set of chemical reactions presented using a specified script that can be read and converted into differential equations by the software package (Mendes et al, 2009). The basis of the model used to describe the reaction of plasminogen activation by tPA stimulated by templates is shown in figure 5.1. In this model the template (F) can either bind to tPA (A) or plasminogen (G) in a random order and then bind to the second component to generate the tPA + Plasminogen + template (AFG) complex. Once this complex is formed tPA (A) activates plasminogen (G) into plasmin (E). Because the binding events are proposed to happen in a random order, the energetic of AFG formation via the upper or lower routes in figure 5.1 should be the same Therefore $K_A \times K_G' = K_G \times K_A'$ e.g. (Wells and Fersht, 1986). To adhere to these conditions constants were selected such that template binding remained the same whether or not the other partner in the complex was already bound (i.e $K_A=K_A'$ and $K_G=K_G'$). The model as proposed in the current work supposes that the tPA and plasminogen binding to the template does not necessarily need to form a defined complex as shown but reactants are being concentrated close to the template surface. Thus the effective local concentrations of tPA and plasminogen are higher than those added. This type of formulation

has been applied to the stimulation of tPA activity by cell surfaces (Sinniger et al, 1999) and elsewhere (Griffith, 1982; Nesheim et al, 1984), but not previously for numerical simulations as used here.

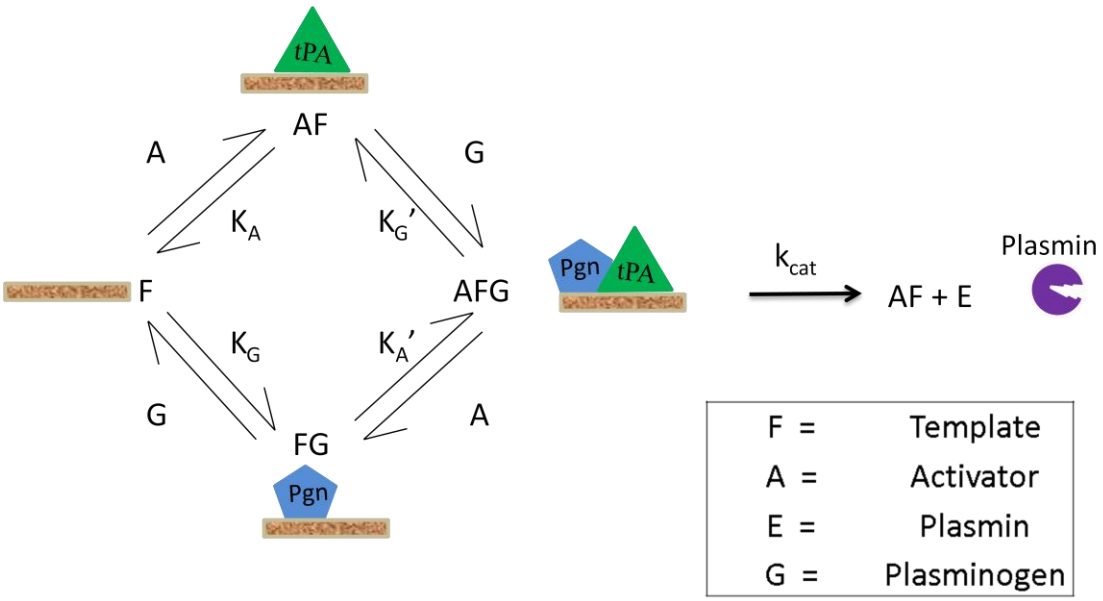


Figure 5.1. Kinetic model used to describe plasminogen activation by tPA stimulated by binding to soluble templates. K_A, K_A', K_G and K_G' are equilibrium constants for the binding of activator (A) or plasminogen (G) to template.

5.2. Methods

Modelling was performed using the computer program Gepasi (Mendes, 1997), a free computer software that is designed to simulate biochemical pathways, using numerical methods. An updated version of Gepasi is available by the same developer called Copasi (Mendes et al, 2009) but the simple and user friendly interface of Gepasi presents some advantages. The first step in creating a model in Gepasi is to list all of the chemical reactions. A list and description of reactions used in the model representing the scheme shown in figure 5.1 are listed table 5.1. In addition there are reactions for the action of plasmin on the chromogenic substrate S-2251 (reactions 1 and 2) and a term for the inhibition of plasmin by template (fibrinogen) (reaction 8) which behaves as a competing substrate. There is also a reaction describing the solution activation of plasminogen by activator (reactions 9 and 10), which can take place slowly. The model does not contain any reaction to include any information for the destruction of fibrinogen as plasmin is generated but as we are only looking at initial rates any effects caused by this should be minimal and would only be likely to effect the lower concentrations of fibrinogen. When heparin is the template there is no term for the inhibition of plasmin by heparin which is not a substrate for plasmin. The kinetics of each of the reactions in the model were defined as mass action and the reactions containing the "->" symbol the reaction is irreversible and reactions containing "=" are reversible reactions. Values were then assigned to the kinetic constants, which were taken from experimental results (see individual simulations in the results section) or from work previously done in the lab under the conditions of the kinetic assay. For the reaction of plasmin on S2251 (S + E = ES) $K_{M.}$ = 300 μM, (ES -> E), k_{cat} = 20 s^{-1} (Thelwell and Longstaff, 2007) and for the binding of plasmin with competing fibrinogen substrate K_M = 1.39 μM (Longstaff and Whitton, 2004) or from taken from the literature, again see

individual simulations in the results section. All reaction parameters need to be entered as rate constants. For equilibrium reactions a forward and reverse reaction need to be supplied, but since these are rarely known precisely it is common to enter an association rate constant ($k_{f,}$ in units of $M^{-1}s^{-1}$) in a reasonable range of 10^5 to 10^6 $M^{-1}s^{-1}$ and then adjust the dissociation rate constant (k_r, units s^{-1}) to give the appropriate equilibrium constant ($K_D=k_r/k_{f,}$ units M). Initial concentrations were assigned to the metabolites and were the concentrations used in kinetic assays in section 3.2.2.2, as shown in table 5.2. These are the starting concentrations but of course will vary throughout the reaction. Simulations were set up to scan a range of fibrinogen (or heparin) template concentrations for 5000s and over 100 points, generating slopes of absorbance versus time for each template concentration, as with real kinetic data. Figure 5.2 shows an example plot of the raw data generated by the model in Gepasi over 12 concentrations of fibrinogen template. These data were then exported as a single text file listing each time course at each fibrinogen concentration into Microsoft Excel. An initial rate of plasminogen activation was then calculated using these data from plots of absorbance (up to 0.1 absorbance units) versus time squared, replicating the methods used during actual kinetic assays. This provides a set of data of plasminogen activation rate (in familiar units of absorbance change per seconds ^{2}) which can be plotted against log of template concentration.

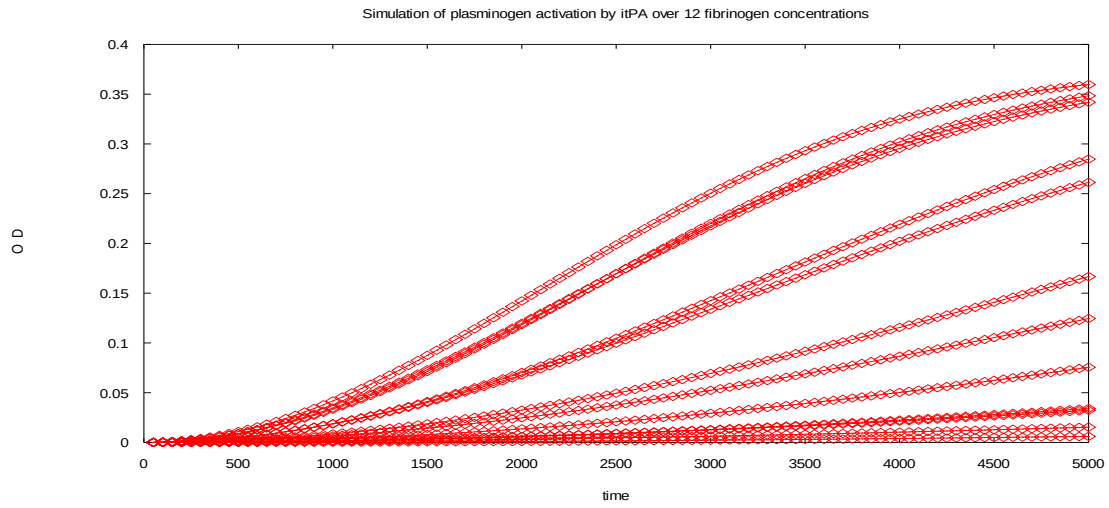


Figure 5.2: Plot of raw data from the simulation in Gepasi. Simulated plots of absorbance over time of plasminogen activation by itPA over 12 fibrinogen concentration (plotted in Gnuplot – free software supplied with Gepasi)

Reaction No.	Reaction	Kinetic type	Explanation of reaction
1	**S + E = ES**	Mass action (reversible)	The substrate S-2251 (S) forms a complex with plasmin (E)
2	**ES -> E + P**	Mass action (irreversible)	Plasmin (E) converts S2251 (S) into pNA (P) releasing the enzyme
3	**F + A = AF**	Mass action (reversible)	tPA (A) binds to template (F) to form a complex (AF)
4	**AF + G = AFG**	Mass action (reversible)	The tPA + template (AF) complex binds to plasminogen to form a complex (AFG)
5	**F + G = FG**	Mass action (reversible)	Plasminogen (G) binds to template (F) to form a complex (AF)
6	**FG + A = AFG**	Mass action (reversible)	The plasminogen + template complex (FG) binds to tPA to form a complex (AFG)
7	**AFG -> AF + E**	Mass action (irreversible)	The template bound tPA converts template bound plasminogen into plasmin (E) leaving the tPA + template complex (AF)
8	**E + F = EF**	Mass action (reversible)	Plasmin (E) binds to template (F) forming EF complex
9	**A + G = AG**	Mass action (reversible)	tPA (A) binds to plasminogen (G) to form a complex (AG)
10	**AG -> A + E**	Mass action (irreversible)	tPA (A) converts plasminogen (G) into plasmin (E) releasing tPA (A)

Table 5.1: The names, reactions and reaction types inputted into the model in Gepasi.

Metabolite	Initial Conc. M
S	1.50E-04
E	3.90E-11
ES	0
P	0
G	1.00E-07
A	8.26E-10
F	0
AF	0
AFG	0
FG	0
EF	0
AG	0

Table 5.2: The metabolites included in the model and the initial concentrations assigned to the metabolites.

5.3. Results

5.3.1. Modelling plasminogen activation by scitPA (R275E) and tcitPA with fibrinogen as a template.

Fibrinogen stimulated plasminogen activation by scitPA (R275E) and tcitPA was simulated using the model shown in figure 5.1. The kinetic constants assigned to the reaction are shown in table 5.3. The kinetic parameters used for reactions 1 and 2 were from (Thelwell and Longstaff, 2007) and (Longstaff and Whitton, 2004) respectively. The parameters for reactions 3 and 6 were initially approximated from the results of the Biacore binding experiments, scitPA K_D = 50 nM and tcitPA K_D = 150 nM. (section 4.3.2.3). However, these values did not give satisfactory results and were manually adjusted to provide a better fit to the data. In simple terms, the optimum fibrinogen concentration for plasminogen activation in a model is adjusted by changing the K_D value for tPA, that is reactions 3 and 6 (the model is relatively insensitive to the plasminogen binding K_D, reactions 4 and 5). Lower affinity binding of tPA shifts the optimum fibrinogen concentration to higher values and vice versa. The peak height for plasminogen activation rate is also affected by the K_D for tPA binding but is also adjusted by varying the k_{cat} for the breakdown of the AFG complex (reaction 7). These updated K_D values were significantly different from estimates obtained from Biacore studies but were in the range of other published values and are shown in table 5.3, (Nesheim et al, 1984) and reviewed in (Longstaff et al, 2008). These generated simulated curves that were similar to the actual kinetic results obtained, see figure 5.3.

Reaction No	Reaction	Kinetic Parameters	
		scitPA	tcitPA
1	S + E = ES	k1 = 1.0e+06 k2 = 3.0e+02	k1 = 1.0e+06 k2 = 3.0e+02
2	ES -> E + P	k = 2.0e+01	k = 2.0e+01
3	F + A = AF	k1 = 1.0e+06 k2 = 2.0e-01	k1 = 1.0e+06 k2 = 1.2e+00
4	AF + G = AFG	k1 = 1.0e+06 k2 = 2.0e+01	k1 = 1.0e+06 k2 = 2.0e+01
5	F + G = FG	k1 = 1.0e+06 k2 = 2.0e+01	k1 = 1.0e+06 k2 = 2.0e+01
6	FG + A = AFG	k1 = 1.0e+06 k2 = 2.0e-01	k1 = 1.0e+06 k2 = 1.2e+00
7	AFG -> AF + E	k = 2.75e+00	k = 2.75e+00
8	E + F = EF	k1 = 1.0e+06 k2 = 1.32e+00	k1 = 1.0e+06 k2 = 1.32e+00
9	A + G = AG	k1 = 1.0e+06 k2 = 6.0e+01	k1 = 1.0e+06 k2 = 6.0e+01
10	AG -> A + E	k = 1.0e-02	k = 1.0e-02

Table 5.3: The kinetic rate constants for each of the reactions used to model plasminogen activation by scitPA (R275E) and tcitPA with fibrinogen as a template. Kinetic parameters are in units of $M^{-1}s^{-1}$ for forward reactions, k1 and k, and in units of s^{-1} for reverse reactions, k2.

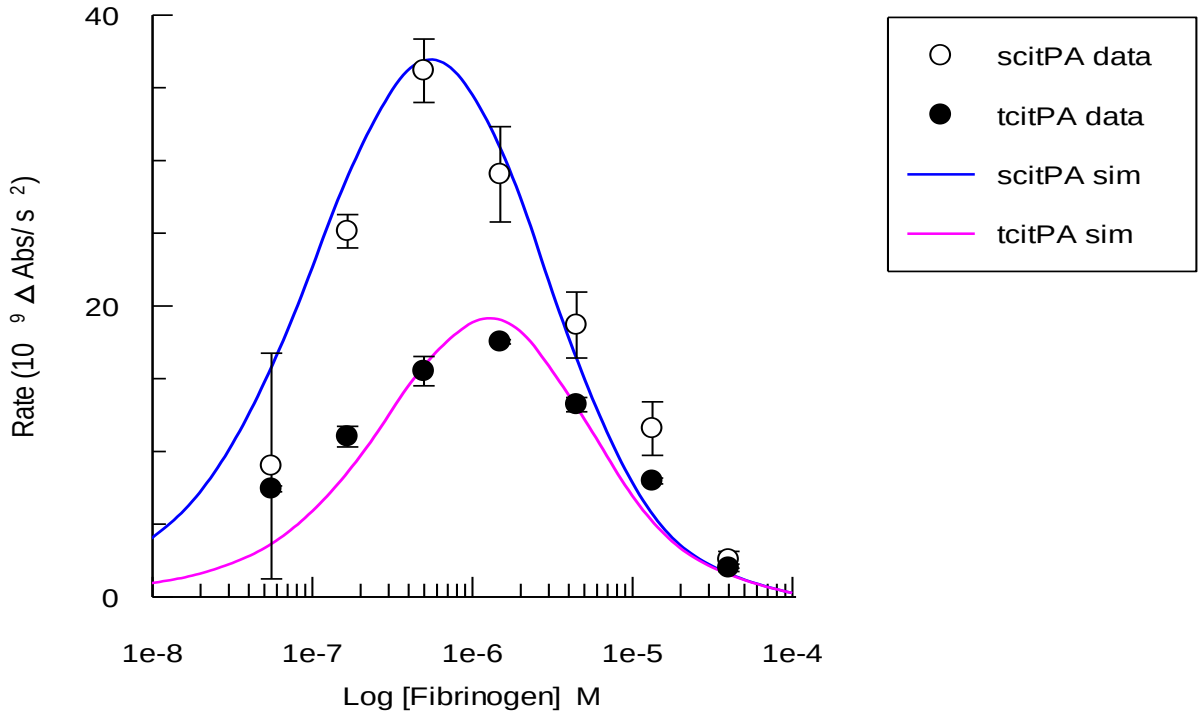


Figure 5.3: Simulation and kinetic data of plasminogen activation by scitPA (R275E) and tcitPA. Simulation (lines) and kinetic data (circles) of plasminogen activation by 0.826 nM of scitPA (R275E) (blue lines and open circles) and tcitPA (pink line and closed circles) stimulated by fibrinogen. The K_D values used to simulate the kinetic data were scitPA (R275E) = 0.2 μM and tcitPA: = 1.2 μM, and the k_{cat} values for both variants were = 2.75 s^{-1}.

5.3.2. Modelling plasminogen activation by itPA and variants with fibrinogen as a template.

Fibrinogen stimulated plasminogen activation by itPA, itPA: F del and itPA: K1K1 was simulated using the model shown in figure 5.1. The kinetic constants assigned to the reactions are shown in table 5.4 and are for the most part the same as entered for modelling with the scitPA and tcitPA, above. As was the case with scitPA and tcitPA data from Biacore analysis of itPA and variants (table 4.6) did not generate particularly good data and so the K_D values were updated in the model for reactions 3 and 6 (affinity of activator to template). Because the data for itPA: F del looked very similar to the data for tcitPA the same affinity was assumed for itPA: F del, with the results shown in figure 5.4. matching the actual kinetic data well. The itPA: K1K1 shows peak activity at around the same concentration of fibrinogen as itPA but the rates are much lower. Because the optimum fibrinogen concentration is the same for itPA and itPA: K1K1 this suggests a similar affinity for fibrinogen (reactions 3 and 6), but a lower kcat value (reaction 7) to account for the low rate of plasminogen activation. Results from simulations using the conditions listed in table 5.4 are shown in figure 5.4.

Simulations over a range of itPA concentrations were also investigated. Fibrinogen stimulated plasminogen activation by itPA at 1.652, 0.826, 0.413, and 0.207 nM was simulated and the simulations and kinetic data are shown in figure 5.5 (A) and (B) respectively. The KD values that were found to best simulate this data were the same as those used in the model when simulating tcitPA. This observation may be explained by the tPA preparation used in these experiments having a high proportion of tctPA initially, or tctPA is formed quickly during the course of the experiment. The resulting simulations show that the variation in tPA concentration is broadly in line with the data.

Reaction No	Reaction	Kinetic Parameters		
		itPA	itPA: F del	itPA: K1K1
1	S + E = ES	k1 = 1.0e+06 k2 = 3.0e+02	k1 = 1.0e+06 k2 = 3.0e+02	k1 = 1.0e+06 k2 = 3.0e+02
2	ES -> E + P	k = 2.0e+01	k = 2.0e+01	k = 2.0e+01
3	F + A = AF	k1 = 1.0e+06 k2 = 2.0e-01	k1 = 1.0e+06 k2 = 1.2e+00	k1 = 1.0e+06 k2 = 2.0e-01
4	AF + G = AFG	k1 = 1.0e+06 k2 = 2.0e+01	k1 = 1.0e+06 k2 = 2.0e+01	k1 = 1.0e+06 k2 = 2.0e+01
5	F + G = FG	k1 = 1.0e+06 k2 = 2.0e+01	k1 = 1.0e+06 k2 = 2.0e+01	k1 = 1.0e+06 k2 = 2.0e+01
6	FG + A = AFG	k1 = 1.0e+06 k2 = 2.0e-01	k1 = 1.0e+06 k2 = 1.2e+00	k1 = 1.0e+06 k2 = 2.0e-01
7	AFG -> AF + E	k = 2.75e+00	k = 2.75e+00	k = 4.50e+01
8	E + F = EF	k1 = 1.0e+06 k2 = 1.32e+00	k1 = 1.0e+06 k2 = 1.32e+00	k1 = 1.0e+06 k2 = 1.32e+00
9	A + G = AG	k1 = 1.0e+06 k2 = 6.0e+01	k1 = 1.0e+06 k2 = 6.0e+01	k1 = 1.0e+06 k2 = 6.0e+01
10	AG -> A + E	k = 1.0e-02	k = 1.0e-02	k = 1.0e-02

Table 5.4: The kinetic rate constants for each of the reactions used to model plasminogen activation by itPA, itPA: F del and itPA: K1K1 with fibrinogen as a template. Kinetic parameters are in units of $M^{-1}s^{-1}$ for forward reactions, k1 and k, and in units of s^{-1} for reverse reactions, k2.

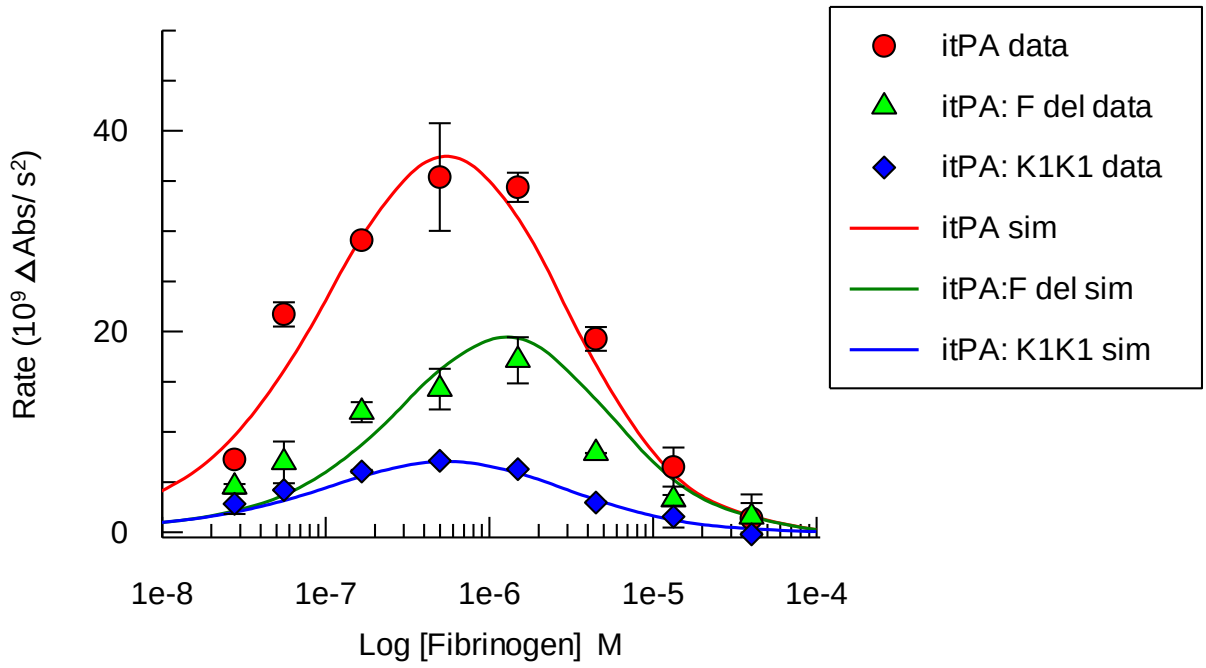


Figure 5.4: Simulation and kinetic data of plasminogen activation by itPA, itPA: F del and itPA: K1K1stimulated by fibrinogen. Simulation (lines) and kinetic data (points) of plasminogen activation by 0.826 nM of itPA (red), itPA: F del (green) and itPA: K1K1 (blue) in the presence of fibrinogen. The K_D values used to simulate the kinetic data were itPA = 0.2 μM, itPA: F del = 1.2 μM, itPA: K1K1 = 0.2 μM and the k_{cat} values itPA = 2.75 s^{-1}, itPA: F del = 2.75 s^{-1}, itPA: K1K1 = 45 s^{-1}.

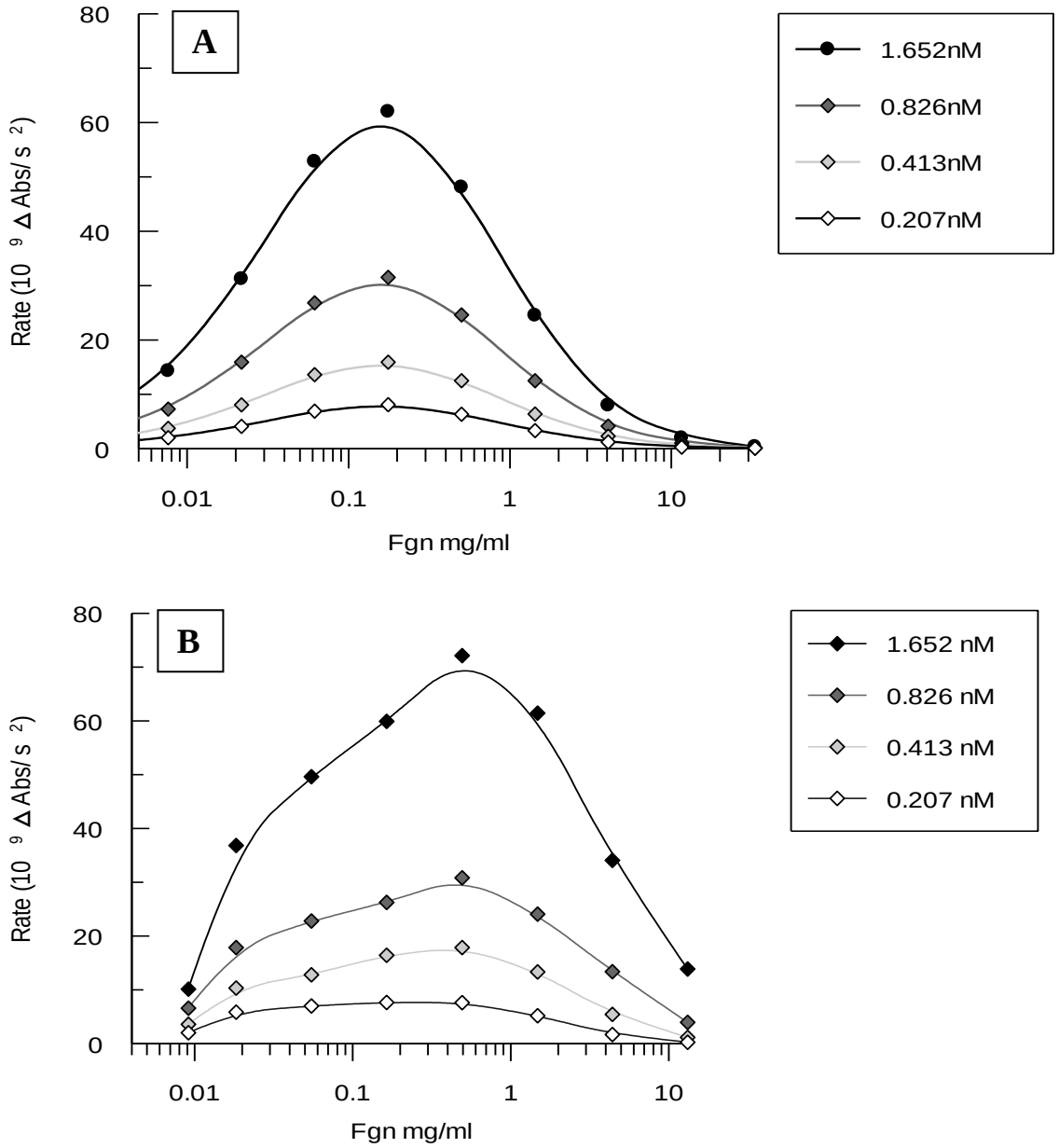


Figure 5.5: Simulation and kinetic data of plasminogen activation by 4 concentrations of itPA. Simulation (A) and kinetic data (B) of plasminogen activation by 1.652, 0.826, 0.413, and 0.207 nM of itPA stimulated by fibrinogen. The K_D = 1.2 μM and the k_{cat} = 2.75 s^{-1}

5.3.3 Modelling plasminogen activation by itPA with heparin as a template in two buffers with different NaCl concentrations.

Heparin stimulated plasminogen activation by itPA was simulated using the model shown in figure 5.1. In kinetic experiments the concentration of NaCl had been shown to affect the rates of plasminogen activation by itPA (section 3.3.2.2, figure 3.8), therefore heparin as a template for plasminogen activation by tPA was simulated for comparison with kinetic data collected using buffer B containing 75 mM NaCl and buffer D containing half the amount of NaCl as buffer B (37.5 mM). The effect of sodium chloride in this system is to weaken binding (Rijken et al, 1993) and hence increase the K_D for the binding of tPA and plasminogen to heparin. Table 5.5 shows the kinetic parameters entered into the model for plasminogen activation by itPA with heparin as a template, in the presence of high and low NaCl. The kinetic parameters for itPA and plasminogen binding to heparin could not be taken from Biacore as binding of itPA to heparin in buffer B was too weak to generate binding curves and the binding curves generated in buffer D showed that the interaction between heparin and tPA was complex and the data could not be fitted to any binding models. A search of the literature uncovered only one set of K_D values for this interaction tPA = 1.9 μM and glu-plasminogen = 120 μM (Andrade-Gordon and Strickland, 1986). However, these values were generated in buffer of different ionic strength than our experiments and so the parameters were estimated and improved through trial and error to optimise the fitting of the template profile with the observed plasminogen activation rate data. It was not possible to achieve any reasonable matching of model and raw data in this way. The results of the simulations are shown in figure 5.6 along with the actual kinetic data obtained in section 3.3.2.2. The simulated curves are not as broad as the experimental results for itPA in low NaCl (buffer D), and for itPA in high NaCl (buffer B), figure 5.6. This is

likely to be to the complex nature of unfractionated heparin, which is made up of a mixture of sizes of oligosaccharides that also have variable structures. Hence, each concentration of heparin will be made up of various heparin molecules that may have different affinities for itPA and plasminogen. In fact, the notion of a molar concentration is spurious and approximate which also complicates the simulations. The very heterogeneous nature of unfractionated heparin also explains why it was not possible to find a reasonable model to fit to the Biacore data discussed in section 4.3.2.4. However the simulated curves generated do suggest that the interaction between itPA and plasminogen with heparin is higher affinity at lower concentrations of NaCl (buffer D), itPA, K_D = 0.01 μM and plasminogen K_D = 0.05 μM compared to higher concentrations of NaCl (buffer B); itPA, K_D = 1 μM and glu-plasminogen K_D = 3 μM, as expected. In both buffers itPA has a higher affinity for heparin than plasminogen. It may be possible to identify more complicated schemes that the one shown in figure 5.1, involving multiple heparin ligands to improve the model data, but this has not been successful so far. Further work on this system may be more successful if purified fractions of heparin were used or synthetic heparin analogues with consistent structure.

Reaction No	Reaction	Kinetic Parameters	
		itPA in low NaCl (buffer D)	itPA in high NaCl (buffer B)
1	S + E = ES	k1 = 1.0e+06 k2 = 3.0e+02	k1 = 1.0e+06 k2 = 3.0e+02
2	ES -> E + P	k = 2.0e+01	k = 2.0e+01
3	F + A = AF	k1 = 1.0e+06 k2 = 1.0e-02	k1 = 1.0e+06 k2 = 1.0e+00
4	AF + G = AFG	k1 = 1.0e+06 k2 = 5.0e-02	k1 = 1.0e+06 k2 = 3.0e+00
5	F + G = FG	k1 = 1.0e+06 k2 = 5.0e-2	k1 = 1.0e+06 k2 = 3.0e+00
6	FG + A = AFG	k1 = 1.0e+06 k2 = 1.0e-02	k1 = 1.0e+06 k2 = 1.0e+00
7	AFG -> AF + E	k = 6.0e-02	k = 6.0e+02
8	E + F = EF	k1 = 1.0e-09 k2 = 1.0e+02	k1 = 1.0e-09 k2 = 1.0e+02
9	A + G = AG	k1 = 1.0e+06 k2 = 6.0e+01	k1 = 1.0e+06 k2 = 6.0e+01
10	AG -> A + E	k = 5.0e-02	k = 5.0e-02

Table 5.5: The kinetic rate constants for each of the reactions used to model plasminogen activation by itPA in buffer B and buffer D, with heparin as a template. Kinetic parameters are in units of $M^{-1}s^{-1}$ for forward reactions, k1 and k, and in units of s^{-1} for reverse reactions, k2.

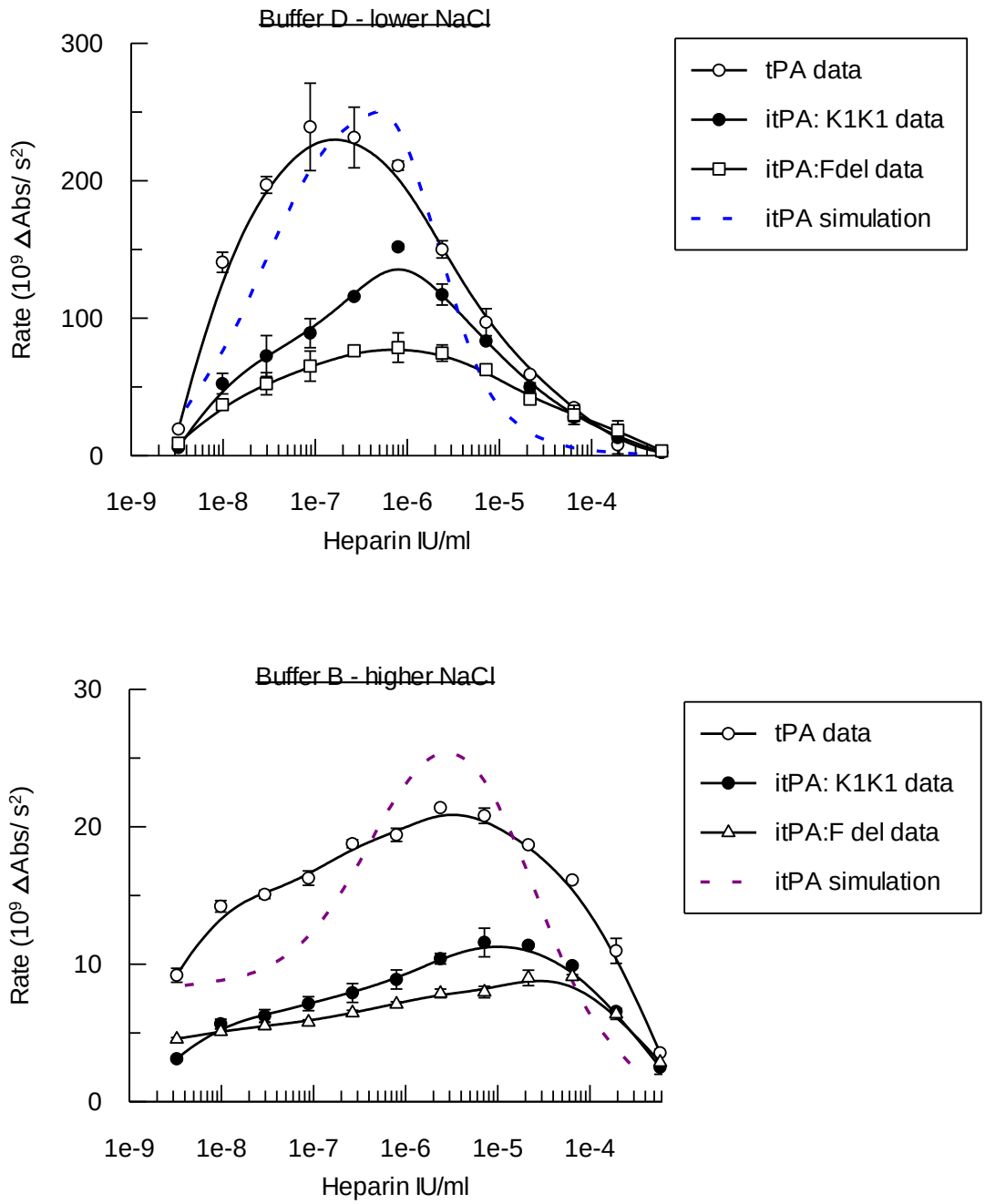


Figure 5.6: Simulation of itPA and kinetic data of itPA, itPA: F del and itPA: K1K1stimulated by heparin to activate plasminogen in buffer D and buffer B. Simulation of itPA (dashed line) and kinetic data (points and lines) of plasminogen activation by 0.826 nM of itPA, itPA: F del and itPA: K1K1 in buffer B and buffer D. The KD values for itPA in buffer D (lower NaCl) = 0.01 µM and buffer B (higher NaCl) = 1 µM and the k_{cat} values were buffer D = 0.06 s^{-1} and buffer B = 0.06 s^{-1}. itPA: F del and itPA: K1K1 were not simulated but it can be seen that they show a similar pattern to itPA with a broad activation peak but the rates are lower.

CHAPTER 6: DISSCUSION

Since the development of tPA as a therapeutic in 1980's and 90's (Collen, 1985; Collen et al, 1989) a number of thrombolytic agents for the treatment of MI and ischemic stroke have been developed in the hope of improving mortality and morbidity. These new thrombolytics were designed to try to reduce bleeding events, loss of circulating fibrinogen and plasminogen, decrease clearance from the body and allow for easier administration. The large majority of these new thrombolytics were domain variants of tPA and some of these new thrombolytics are shown in table 6.1. (Weitz et al, 2003) However none of these new therapeutics showed much improvement clinically compared to tPA, although there have been some improvements in administration (Verstraete, 2000), which can be as a bolus rather than infusion. One of the major goals cited for improvement was to increase fibrin binding and hence fibrinolysis. A large number of studies have been performed to identify the domains and understand their mechanisms of action in enhancing tPA binding to fibrin resulting in plasminogen activation and fibrin lysis (Bakker et al, 1995; Bosma et al, 1988; Bringmann et al, 1995; Burck et al, 1990; Collen et al, 1988; Collen et al, 1990; De Serrano and Castellino, 1994a; De Serrano and Castellino, 1994b; De Serrano and Castellino, 1992; de Vries et al, 1989; de Vries et al, 1990; Fischer and Kohnert, 1997; Gething et al, 1988; Horrevoets et al, 1994; Hoylaerts et al, 1982; Kagitani et al, 1985; Kawasaki et al, 1993; Keyt et al, 1994; Kohnert et al, 1992; Langer-Safer et al, 1991; Larsen et al, 1988; Lijnen et al, 1990; Longstaff et al, 2011; Martin et al, 1992; Obukowicz et al, 1990; Rydzewski and Castellino, 1993; Toschi et al, 1998; van Zonneveld et al, 1986b; van Zonneveld et al, 1986a; Verheijen et al, 1986; Wilhelm et al, 2004). However these studies have not led to a vastly improved thrombolytic enzyme, as judged by clinical trial results. To date, attempted improvements in thrombolytics have been based on the simple assumption that increased fibrin specificity and fibrin binding will automatically lead to improved thrombolytics, but these simple

considerations have never been justified or borne out in clinical trials. A detailed understanding of the enzymology of PA in a fibrin clot may open the way for improved thrombolysis.

Therapeutic	Structure	Improvements	shortfalls
Reteplase	K2P domains of tPA	Increased half-life enabling bolus injection and more rapid reperfusion	no significant difference in efficacy or safety compared to Alteplase
Tenectaplase	tPA analogue modified at three sites: T103N, N117Q, KHHR(296-299)AAAA	Decreased clearance, more fibrin specificity (less fibrinogen depletion) and more PAI-1 resistance	no significant decrease in mortality compared to Alteplase
Lanoteplase	K1K2P domains of tPA, with a mutation Asn117Gln (a glycosylation site) in the K1 domain	Decreased clearance and increased fibrinolytic potency.	Significantly increased intracranial hemorrhage in patients
Monteplase	tPA analogue with a mutation Cys84Ser in epidermal growth factor domain	Decreased clearance	Similar rates of bleeding complications as Alteplase
Pamiteplase	tPA analogue with K1 domain deleted and a mutation Arg275Glu.	Decreased clearance	No significant improvement in safety

Table 6.1. Some of the newly developed thrombolytics with their improvements and shortfalls.

To investigate plasminogen activation and fibrinolysis further, tPA variants were expressed in an insect cell expression system along with insect versions of commercial therapeutic proteins Alteplase and Reteplase. The insect versions of the commercial therapeutic proteins were expressed to account for differences in glycosylation patterns of the different expression systems so that protein structures could be compared in a like versus like way. Glycosylation has been implicated in a number of properties of tPA as stated in section 1.6. of the introduction. The differences in the glycosylation of the proteins from different expression systems was observed when viewing these proteins by SDS-PAGE which showed differences in molecular weight between the commercially available tPA and the tPA expressed in the insect system.

Therapeutic product Actilyse, migrated to ~ 62 kDa region, which corresponds with published molecular weights of between 61kDa and 67 kDa (European Pharmacopoeia, 1998) and the predicted molecular weight of 61 kDa, which is calculated from the amino acid sequence only and does not take into account any glycosylation. The itPA appears to have a lower molecular weight than the Actilyse, migrating to about the 60 kDa region of the gel, amino acid analysis was performed on this variant and it was found to be full length. This difference in molecular weight is likely to be due to the differences in glycosylation between the insect cell expressed protein (itPA) and the mammalian expressed protein (Actilyse). Mammalian cells express proteins with carbohydrates that are more complex than proteins expressed in insect systems and therefore the mammalian expressed proteins are likely to be heavier. The itPA: K1K1 variant has a higher molecular weight than the itPA, of about 62 kDa about the same as Actilyse, even though it has a predicted molecular weight, from the amino acid sequence, that is the same as the itPA. The difference in molecular weight is again probably due to glycosylation. tPA has four potential Asn glycosylation sites, only

three of which are glycosylated, the forth site at position 218 in the K2 domain does not. One at position 448 in the serine protease domain and another at position 117 in the K1 domain are both glycosylated 100% of the time (Pohl et al, 1984). The third site at position 184 in the K2 domain is only glycosylated in 50% of proteins (Pohl et al, 1987). The itPA: K1K1 variant has two K1 domains, therefore containing two Asn 117 glycosylation sites that are glycosylated 100% of the time on all molecules, whereas itPA will only have 50% of molecules with two sites glycosylated, therefore the itPA: K1K1 is likely to be heavier. The irPA has a molecular weight of ~42 kDa which is heavier than the rPA, which runs to its expected molecular weight of 40 kDa. This may again be due to glycosylation as rPA is produced in *E.coli* and hence has no glycosylation, whereas in irPA there are two glycosylation sites one in the K2 domain and one in the protease domain. The differences in glycosylation may affect fibrin binding and activity, and may account for some of the differences between results obtained in this study using rPA and irPA. A vast array of different expression systems and sources of tPA and variants have been used in studies into the interaction with and stimulation by fibrin, see table 6.2, other factors that could possibly introduce variability could be the method used to measure fibrin binding, the condition of the fibrin e.g. if the fibrin is partially degraded exposing more C-terminal lysines (Grailhe et al, 1994; van Zonneveld et al, 1986b) or when using deletion mutants the choice of amino acids where the domains start and finish (Gething et al, 1988).

Plasminogen activator	Source	Reference
tPA (F-G-K1-K2-P)	Human melanoma cells	Bosma et al. 1988
	CHO	Bakker et al. 1995
	CHO	Lijnen et al. 1990
	Simian cells	Gething et al. 1988
	African green monkey kidney	Larsen et al. 1988
	Mouse Lkt-	de Vires et al. 1989
	Human uterus	Hoylaerts et al. 1982
	Sf9 insect cells	Jarvis et al. 1989
	E.coli	Martin et al 1992
F-G-K2-K1-P	CHO	Bakker et al. 1995
F-G-K2-K2-P	CHO	Lijnen et al. 1990
G-K1-K2-P	Simian cells	Gething et al. 1988
	CHO	Bakker et al. 1995
	Mouse Lkt- cells	de Vires et al. 1989
	E.coli	Kagitani et al. 1985
	African green monkey kidney	Larsen et al. 1988
F-G-K2-P	Simian cells	Gething et al. 1988
	Mouse Lkt- cells	de Vires et al. 1989
G-K2-K1-P	CHO	Bakker et al. 1995
F-K1-K2-P	African green monkey kidney	Larsen et al. 1988
F-K2-K2-P	CHO	Lijnen et al. 1990
G-K2-K2-P	CHO	Lijnen et al. 1990
K1-K2-P	Simian cells	Gething et al. 1988
	African green monkey kidney	Larsen et al. 1988
	CHO	Lijnen et al. 1990
F-G-P	Mouse Lkt- cells	de Vires et al. 1989
	Simian cells	Gething et al. 1988
F-P	Mouse Lkt- cells	de Vires et al. 1989
K1-P	Mouse Lkt- cells	de Vires et al. 1989
K2-P	Mouse Lkt- cells	de Vires et al. 1989
	E.coli	Kohnert et al. 1992
	Syrian hamster cells	Burck et al. 1990
K2	E.coli	De Serrano and Castellino. 1994a
P	Simian cells	Gething et al. 1988
	Mouse Lkt- cells	de Vires et al. 1989

Table 6.2. Some of the tPA and variants expressed for studies into the properties of tPA and their source or expression system.

It is generally believed that fibrin binding by tPA is via the F and K2 domains (Bakker et al, 1995; de Vries et al, 1989; Horrevoets et al, 1994; Larsen et al, 1988; Lijnen et al, 1990; van Zonneveld et al, 1986a; Verheijen et al, 1986) although this may be a simplification as others have found that the K1 domain and the G domain also bind to or are stimulated by fibrin (Gething et al, 1988; Larsen et al, 1988; Rydzewski and Castellino, 1993) and Bennet et al. (1991) found through alanine scanning that there are residues throughout the molecule that are involved in the interaction of tPA with fibrin, including many in the P domain (Bennett et al, 1991). Many templates in addition to fibrin have been found to bind and stimulate tPA, such as fibrinogen (and fragments) (Bringmann et al, 1995; Lucas et al, 1983; Thelwell and Longstaff, 2007), heparin (Pâques et al, 1986; Stein et al, 1989), denatured proteins and amyloids (Gebbink et al, 2009; Maas et al, 2007). Templates stimulate tPA activity by a so-called co-localisation mechanism such that tPA and plasminogen associate with the template and are brought into close proximity, giving higher local concentrations, thus increasing the rate of plasminogen activation (Sinniger et al, 1999). This is a slightly different interpretation than the simple mechanism of ternary complex formation that requires strict binding of tPA and plasminogen to adjacent sites on the template (Longstaff et al, 2008; Longstaff and Thelwell, 2005). In this project binding of tPA to fibrin, fibrinogen, heparin and lysine templates have been investigated using tPA and tPA variants. To generate precise results from these experiments the concentration of each variant needed to be known. There is no easy active site titration for tPA (Urano et al, 1988) and so it was not possible to determine the exact quantity of active enzyme in each preparation of tPA and variants. Consequently, protein assays were performed and amidolytic activities were measured and used to establish an active enzyme concentration. All variants were proteolytically active against S2288 and any differences between variants were explored using 95 % confidence intervals, no differences between the domain variants were found to be statistically significant. These

results suggest that amidolytic activity is only a function of the serine protease domain and this activity if it agrees with protein concentration is a reasonable measure of the enzyme concentration. The results presented in Chapter 3.3.1 do not suggest major differences in enzyme activities between domain variants. Thus where variants were studied in the presence of templates and where stimulation of activity was found it was ascribed to enhancement by the templates and co-localisation with plasminogen. However, some caution is needed in following this line of reasoning as some changes in tPA structure away from the protease domain can affect the intrinsic activity of tPA. This can be seen in this work when going from scitPA to tcitPA (e.g. figure 3.3 for activity on S2288) and previously with several substrates. (Longstaff et al, 2007).

Fibrinogen as a template for tPA activity is controversial and some workers point out that fibrinogen should not promote tPA activity in the circulation (Nieuwenhuizen, 2001). This makes sense as activation of tPA throughout the system would lead to loss of circulating plasminogen and fibrinogen. One way to avoid this problem takes the view that when fibrin is formed, cryptic sites are exposed which bind tPA and plasminogen and promote plasmin generation. A lot of work has gone into finding these sites (Medved and Nieuwenhuizen, 2003), but with limited success (Doolittle, 2008). An alternative view is that gross structural changes in fibrin lead to the formation of cross β structures and this results in binding sites for tPA, via finger (discussed in (Longstaff et al, 2011)). However, some groups maintain that fibrinogen binding is physiologically relevant for tPA and this has been investigated and highlighted by the groups developing Desmoteplase, for example, who claim it is more fibrin specific, precisely because it binds to fibrinogen with lower affinity than does tPA (Bringmann et al, 1995; Kruithof et al, 1984; Stewart et al, 1998). Other groups maintain that fibrinogen is a respectable stimulator of tPA (Eastman et al, 1992; Kruithof et al, 1984). In the present study it was found that fibrinogen stimulates tPA-mediated plasminogen

activation following a template model, i.e. with no saturation but bell shaped curves with fibrinogen concentration.

The results from the kinetic experiments with fibrinogen as a template showed that both F and K2 domains are involved and plasminogen activation is greatest where both domains are available (itPA). The presence of the K2 domain was more important than the F domain for plasminogen activation to occur, in agreement with the work on Desmoteplase mentioned above (Desmoteplase has no equivalent to the K2 domain). Interestingly, there appeared to be a synergistic effect when both F and K2 were present in itPA since the activation rate was greater than the sum of the activities of tPA:K1K1 and tPA: F del under the same conditions (see figure 3.4). However a more complicated model of binding involving sites other than F and K2 appear to be supported by results from two variants containing the K2 domain but not the F domain which were shown to be stimulated to different extents. The irPA variant (K2P only) was always found to have lower activity than itPA: F del, again suggesting the involvement of multiple domains or binding sites. Work by Bennet et al (Bennett et al, 1991) showed that residues in the K1 but mainly the P domain were involved in interactions with fibrinogen, but these results did not correlate with our results obtained using the P and K1P variants which showed little or no fibrinogen stimulated activity. Furthermore itPA: K1K1 showed less activity than itPA: F del. The involvement of the G domain (implicated by some in binding to fibrin (Collen et al, 1990; Gething et al, 1988; Larsen et al, 1988)) is also contained in the itPA: K1K1 variant. However, these observations may also suggest that caution is needed when changing the structure of tPA. Some groups have identified subtle interactions between domains, hence deleting domains may have wider repercussions on the behaviour of tPA (Novokhatny et al, 1991) and could change the orientation of binding sites normally exposed in full length tPA (Smith, 1986).

Interestingly, because it is K2 and not the F domain that appears to be most significant for stimulation by fibrinogen the notion that binding to fibrinogen is not specific and is due to the same mechanism as tPA binding to denatured proteins (Gebbink et al, 2009) is not supported. According to these proposals tPA binds to a wide range of proteins, including fibrin, through cross β structures, primarily via the F domain. Processes such as freeze drying or the addition of chemicals such as EDTA that are generally performed on fibrinogen used in the laboratory could change and denature the protein (Haddeland et al, 1994). However, our results indicate a different mechanism in the case as tPA and fibrinogen acting mainly through the K2 domain.

The scitPA (R275E) – non cleavable variant and tcitPA provided a simple system for investigating kinetics, binding (Biacore) and modelling in fibrinogen. The weaker affinity of tctPA seen in Biacore studies (section 4.3.2.3) and elsewhere (Eastman et al, 1992; Stewart et al, 1998) seemed to be adequate to explain the reduced activity in the presence of fibrinogen, according to the modelling presented in Chapter 5, figure 5.3. However, it might be expected that the tctPA has an increased $k_{cat,}$ which is seen in figure 3.3 and elsewhere (Thelwell and Longstaff, 2007) when looking at amidolytic activity with no template. Although every care was taken to treat the samples the same, after plasmin-Sepharose treatment it was not possible to measure protein concentration as the plasmin cleavage buffer interferes with the protein assay, hence there could be some differences in protein concentration in these experiments. Hence some caution is needed in reading the model values used for k_{cat} for tcitPA in Chapter 5.

The other soluble template used to investigate activity of the variants was heparin which like fibrinogen appears to follow a template profile. As with fibrinogen, heparin stimulated activation was best with full length itPA but unlike fibrinogen, the F domain was more important than the K2 domain, agreeing with previously published results (Edelberg et al,

1991; Liang et al, 2000; Pâques et al, 1986; Rijken and Jie, 1996; Stein et al, 1989). Again a difference was observed between the irPA and itPA: F del, where the itPA: F del > irPA, highlighting the importance of the overall structure as well as the individual domains in tPA activity. Previous studies into heparin stimulation of tPA activity have shown ionic strength has an effect on the interaction (Rijken et al, 1993; Rijken and Jie, 1996; Young et al, 1992), this was also noted in this study with itPA and variants, where more stimulation by heparin is seen at lower ionic strength. All variants were stimulated 10-fold in buffer with a lower NaCl concentration (37.5 mM) compared to buffer with 75 mM NaCl indicating that the interaction of both the F and the K2 domain is weakened by the presence of NaCl, whereas previously Reteplase was shown to be more affected than tPA (Rijken and Jie, 1996). The strength of plasminogen binding is also likely to be affected and will likely be responsible for the some reduction in plasminogen activation as it has been shown previously to be more affected than tPA (Rijken et al, 1993). Previously it has been shown that at physiological ionic strength heparin does not stimulate tPA activity (Rijken et al, 1993; Rijken and Jie, 1996; Young et al, 1992) and so is unlikely to cause problems such as systemic plasminogen depletion and fibrinogenolysis that were predicted when the interaction between tPA and heparin was first noted (Andrade-Gordon and Strickland, 1986). Results from the current studies do show it is possible to reduce the likelihood of heparin stimulation of plasminogen activation further by deleting the F domain. Furthermore, the interaction of heparin with tPA and plasminogen is still important in respect to the modelling as it provides an example of a template that is not a substrate for plasmin (unlike fibrinogen) which decreases the complexity of the modelling. .

It was hoped that binding studies that included itPA and variants with fibrinogen and heparin would provide equilibrium or kinetic constants that could be used in modelling studies. However, these binding studies were not entirely successful. The domains of tPA involved in binding to fibrinogen and fibrin were investigated initially using fibrinogen immobilized onto

the surface of microtitre plates. The drawback of this method and when investigating binding to immobilized ligands using the Biacore (discussed in more detail later) has the potential for changing the proteins. The process of adsorption of the immobilization chemistry used, as well as washing steps could denature the proteins and as a result observed binding could be a result of the tPA having an affinity for denatured proteins (Gebbink et al, 2009). Furthermore immobilization on surfaces has been shown to result in modification of the functional properties of the fibrinogen (Riedel et al, 2011). It has been shown that fibrinogen absorbs onto surfaces in two orientations, side on, when immobilised at low concentrations and end on at high concentrations (> 200 μg/ ml). High concentrations result in the molecules being tightly packed together with only one end of the molecule being accessible. In both orientations the central E domain is also inaccessible to antibodies and Fab fragments to this region (Dyr et al, 1998). This means that tPA binding sites in fibrinogen may be hidden in immobilised fibrinogen. Another possibility could be that sites that would not normally be available to bind could be exposed, which was found by Tsurupa et al (2010) when investigating α2-antiplasmin binding to fibrinogen. They found that α2-antiplasmin bound to fibrin and surface adsorbed fibrinogen but not fibrinogen in solution (Tsurupa et al, 2010). Immobilized fibrinogen has also been shown to polymerise and form a 3 dimensional network, more like a fibrin mesh that soluble fibrinogen molecules (Koo et al, 2010) and so binding to immobilized fibrinogen is more like binding to fibrin. However, in this present study itPA and variants were shown to bind to immobilized fibrinogen (on microtitre plates and carboxymethylated dextran on Biacore sensor surface chips), and using a range of activator concentrations binding to fibrinogen immobilized on microtitre plates showed the same pattern of binding as was observed in the kinetic experiments, that F+K2 > K2 > F for binding. The results of the plate binding assays with scitPA (R275E) and tcitPA were quite

variable but like with the kinetic results showed that sctPA (R275E) > tcitPA, when tested over a range of activator concentrations

One problem with investigating binding using the microtitre plate system is that the amount of itPA and variants bound to fibrinogen is measured using activity and differences in plasminogen activation activity by the variants may complicate the interpretation of binding. One attempt to overcome these issues was to use itPA and variants expressed fused to GFP. Another method to fluorescently label tPA is chemical labelling, using a fluorescent label such as FITC but this is method is more difficult to control as it is difficult to ensure that optimal conjugation between variants due to differences amino acid sequence and structure (Holmes and Lantz, 2001). Expression of the tPA-GFP as a fusion protein ensures that there is one GFP molecule fused to each tPA/ variant molecule and we decided at the outset to add the GFP protein to the C-terminal of tPA (the protease domain) to limit any effects of the new domain on the N-terminal binding domains. The GFP fusion proteins expressed for this project were not very successful in the binding assays used in this work. However, they have been employed effectively in confocal microscopy studies (Longstaff et al, 2011; Varju et al, 2011). There is possibly some potential in the future for binding studies, but sensitivity might be an issue, monitoring the fluorescence of the GFP is less sensitive than enzyme activity measurements, including using the activity of bound tPA and enzyme linked immunoabsorbance measurements.

Results from plate binding studies were generally successful in showing relative affinities of the different tPA variants to immobilised fibrinogen, but Biacore studies were more promising in terms of potentially providing the constants required. In theory, SPR using Biacore technology is a good way to look at binding irrespective of enzyme activity and it can also be used to generate detailed measurements of the binding affinities and kinetic constants for the interactions between relevant molecules. However, there were a number of

technical problems with Biacore studies that meant it was difficult to derive binding parameters from simple binding models. Furthermore, when values were derived and input into the simulations, they did not appear to be consistent with the results generated in kinetic experiments. The technical problems found when using Biacore were connected to both ligands and analytes. First of all, it was not possible to find a suitable way of immobilising fibrinogen to form a stable surface via antibodies, which would be gentle and allow for replenishing of fresh ligand between injections of analytes. Direct chemical immobilisation was used but there is a concern that fibrinogen will be damaged during the immobilisation or during subsequent use and regeneration of the sensor chip surface. Immobilisation of heparin was also problematical and there appeared to be non-specific binding to the streptavidin surface. Non-specific binding and the fact that tPA and plasminogen binding to heparin is likely to be complex meant that no binding models were found to fit the response curves. However, generally speaking the binding response level seen with itPA and the variants on immobilised heparin did fit with the results from the kinetic experiments that the F domain binds more than the K2 domain.

Further problems in all Biacore studies were probably caused by tPA insolubility issues. Although measures were taken to improve solubility this meant that the subsequent binding studies were performed under conditions that were quite different from the kinetic studies used to develop the simulations and kinetic models. The importance of the buffer can be seen in Biacore experiments with sc/tcitPA compared with itPA and variants, which generated quite different binding curves. No single set of optimised conditions was found or used to bring the results of the interaction between itPA and fibrinogen in line with the interaction with heparin and the kinetic experiments. High concentrations of HEPES based buffers appeared to be best in terms of keeping tPA soluble but were not employed in kinetic studies. Nevertheless, binding of scitPA (R275E) and tcitPA to fibrinogen was found to produce a

reasonable set of binding curves which could be fitted well to two models, the heterogeneous ligand and the two-step models. Both models showed that the results agreed with the results of the kinetics that sctPA binds with higher affinity than tcitPA. The results of the two models gave K_D values of scitPA (R275E) = 68 nM and tcitPA = 113 nM from the two-step binding model and scitPA (R275E) = 46 nM and tcitPA = 135 nM from the heterogeneous binding model major component. The fittings for itPA and variants binding to fibrinogen for the reasons explained above are not totally convincing and the latest technical recommendations for fitting Biacore curves suggest much lower RU values. Figure 4.2 does however show variation in binding to fibrinogen that fits with the results of the kinetics in terms of response levels and plasminogen activation rates and gives some idea of how much tPA-fibrinogen complex can form that is available for plasminogen activation. However there is an interpretation from the kinetics and modelling looking at the peak optima that suggests itPA: K1K1 binds with higher affinity than itPA: F del, even though the plasminogen activation rate is higher with itPA: F del (see figure 3.2.). One possibility is that there is a different number of binding sites available for F than K2 binding. The lower k_{cat} used for reaction 7 in the model for itPA: K1K1 binding to fibrinogen (see table 5.4) may be reinterpreted as a reaction with the same k_{cat} as tPA but there is less of it. Thus AFG is either changing slowly to AF + E (low k_{cat}) or there is less AFG. There could be less AFG because it doesn't form well because of weak binding but if this was the case then the optimum fibrinogen concentration would be lower. The alternative might be that there are fewer binding sites for itPA: K1K1 thus it does not form as much AFG. The K_D values generated from Biacore fitting were itPA = 158 nM, itPA: K1K1 = 4.6 μM and itPA: F del = 1.8 μM. When these values were used in the modelling they were found to generate different results from the kinetic results and alternative values were sought to make the model fit the data. As discussed above this may be reasonable as there were some difficulties associated with

binding studies. In addition, conditions used for the kinetics work were different from the conditions used for the binding studies in other ways, for example and the concentration of tPA is also different in kinetic experiments. In these kinetic studies the tPA concentration was typically < 1 nM and in Biacore it is between in the 10 and 100+ nM. Of course another possibility is that the binding model that was used to fit the data is wrong. These observations may help explain why the parameters estimated from Biacore studies were not successful when input into the kinetic modelling program. However, it may not be ultimately possible to use Biacore to get estimates for kinetic or equilibrium constants if the modes of binding are in reality very complex and difficult to fit to convenient models. In this case it is reasonable to explore different possible kinetic models and find which fit the data best across the widest range of conditions.

Binding of plasminogen to the fibrinogen surface was in line with the expectations; glu-plasminogen was too weak to generate binding constants and lys-plasminogen was measurable to some extent. Low affinity binding of glu-plasminogen to templates was used in modelling but detailed studies with lys-plasminogen were not performed.

Literature values of K_D for tPA and Pgn binding to intact fibrinogen are not common. Stewart et al (Stewart et al, 1998) identified a high affinity interaction between tPA and fibrinogen of 760 nM and there are a number of published values for binding of tPA and plasminogen binding to fibrin and fibrinogen fragments. Nesheim et al found that lys-plasminogen had a K_D of 0.25 μM and tPA bound with two distinct binding sites for F and K2 domain, with K_D values of 130 nM and 610 nM respectively (Nesheim et al, 1990). Other K_D values for lys-plasminogen with fibrin were found to be 10 μM (Lucas et al, 1983),1μM (Horrevoets et al, 1996) and 0.5 μM (Bok and Mangel, 1985). Values for glu-plasminogen were in the order of 25-40 μM (Bok and Mangel, 1985; Horrevoets et al, 1996; Lucas et al, 1983) and 1 μM (Fleury and Angles-Cano, 1991).

Studying fibrin as a template is technically difficult due to the heterogeneous (solid) nature of the fibrin network compared to using the soluble templates described above. The methods used in this investigation have allowed for precise kinetic data to be generated in fibrin. When investigating the kinetics of fibrin stimulated plasminogen activation by tPA the concentration of fibrin cannot be varied, as it is with soluble templates. However, plasminogen concentration added to the fibrin clot can be varied to generate estimates for apparent K_M and k_{cat} values ("apparent" as values are dependent on the assay system used). Varying plasminogen concentration allows for good comparisons between variants by using k_{cat}/K_M. An alternative approach was to look at the relative potencies by fixing plasminogen concentration but varying activator and using Combistats to compare variant activities with itPA as a standard. Both approaches have their merits. The second approach using a standard is useful in biological assays because of the inherent variability found between assays. The absolute measurements of activity tend to be highly variable but some of the variability can be smoothed out by expressing the results relative to a standard included in every assay; the principle of biological standardisation as practiced by NIBSC/WHO (Longstaff et al, 2009). Even for relatively simple, well defined assay systems such as the clear fibrin clot overlay system used here (Longstaff and Whitton, 2004), there is variability when the same samples are measured in different laboratories, highlighting the problems of making absolute measurements (Longstaff et al, 2007).

As with fibrinogen and heparin, stimulation (and hence binding) by fibrin was shown to be best when both the F and the K2 domain are available to bind. When initial rates of plasminogen activation and rates to 20% fibrin lysis were investigated the F domain was shown to be more important than the K2 domain. As the assay progressed and the rates to 50% fibrin lysis were looked at, the K2 domain was seen to become more important. This is likely to be due an increase in K2 binding sites (C-terminal lysines), generated as plasmin is

produced and breaks down the fibrin. Initial binding is thought to occur using the F domain and as plasminogen activation begins plasmin is generated, which in turn begins to breakdown fibrin producing C-terminal lysines (eg see (Longstaff et al, 2011)). This allows binding of the tPA through the K2 domain and plasminogen possibly via K1 and K4 domains (Trexler and Patthy, 1983; Vali and Patthy, 1984). These observations suggest that modelling the kinetics of plasminogen activation in fibrin will need to be more complex than with soluble templates but the experimental systems in place, including fibrin-based assay systems and domain variants of tPA, will allow for thorough investigation of possible models. The differences in activity between the itPA: F del and irPA that were seen with fibrinogen and heparin templates were also observed in fibrin. Detailed investigation of the role of C-terminal lysines was performed by comparing the initial rates of plasminogen activation of the variants in three different types of fibrin (1) CPB-treated fibrin, which removes C-terminal lysines; (2) plasmin-treated fibrin, which generates C-terminal lysines; (3) normal fibrin that has had no treatment, fibrin will change from native fibrin with no C-terminal lysins to fibrin with C-terminal lysines. Increased activity was seen with irPA (K2 domain binding) in plasmin-treated fibrin compared to normal fibrin but no difference was observed between the variants that contain the F domain (itPA: F del was not tested in this system). In CPB-treated fibrin the the activity of irPA (K2 domain binding) was greatly reduced, see section 3.3.3.3. itPA did not appear to be significantly affected by the removal of C-terminal lysines, a small reduction in activtiy was observed and was atributed to a reduction in plasminogen binding. These results confirm the importance of C-terminal lysines for the K2 domain to bind to fibrin as shown by van Zonneveld et al, 1986 (van Zonneveld et al, 1986b) and Kagitani et al, 1985 (Kagitani et al, 1985) who both found that the K2 domain of tPA bound fibrin via C-terminal lysines. Interestingly, when there were no C-terminal lysines available after CPB treatment, the activity of the itPA: K1K1 variant (F domain binding only)

increased relative to itPA. This was only observed in the assays with fixed plasminogen and varied activator and not in assays with fixed activator and varied plasminogen, this may have been due to variability between assays. Further work with models and simulation of plasminogen activation in fibrin may help better understand all the details of what is going on these complicated systems.

Lysine analogues are useful antifibrinolytic drugs and helpful reagents in helping to understand the significance of lysine binding kringle domains in studies of fibrinolysis. The significance of lysines in fibrino(ogen) binding was further confimed when using a range of concentrations of lysine analogue 6-aminohanoic acid in the plate binding assay, where it was seen that 6-aminohexanoic acid only inhibited binding of variants that had the K2 domain and had no affect on the variants that had the K2 domain deleted. CPB is a more stable analogue of TAFI a physiological carpoxypeptidase fibrinolysis inhibitor. There have been a number of conflicting epidemiological studies on whether increased levels of TAFI can increase the risk of cardiovascular disease and reduce the effectiveness of treatment with tPA (Juhan-Vague et al, 2002; Ladenvall et al, 2007; Leebeek et al, 2005; Morange et al, 2002; Morange et al, 2003). These results indicate that treatment with activators that contain the F domain may still be effective in patients with high concentrations of TAFI in their circulation, whereas treatment with rPA may not be as effective. Some of the questions surrounding the physiological importance of TAFI may be addressed in the future using models of plasminogen activation in the presence of fibrin, with added CPB or TAFI. The systems applied in this study using CPB-treated and plasmin-treated fibrin, in conjunction with tPA domain variants, will help in the development of realistic models to help understand the control of tPA activity and the significance of initial binding events and the exact role of C-terminal lysine development. Initial studies have been published (Longstaff et al, 2011).

Investigating binding to immobilized fibrin is even more difficult than using immobilised fibrinogen. It is also not clear what the effect of thrombin treatment on immobilised fibrinogen is, it is unlikely to make real fibrin but this type of surface has been used before (Angles-Cano, 1986; Fleury et al, 1993). It has been shown that with immobilized fibrinogen the pattern of release of fibrinopeptides "A" and "B" was different to that seen with fibrinogen in solution (Riedel et al, 2011). Thrombin binds to the central region and catalyses cleavage of fibrinopeptides, revealing knobs "A" and "B" which interact with holes "a" and "b" in nearby fibrinogen molecules, beginning the process of fibrin polymerisation (Blomback, 1996). Immobilised fibrin formed by thrombin treatment of low concentrations of immobilised fibrinogen was found to be more like real fibrin (Riedel et al, 2011). Fibrinogen was immobilised onto microtitre plates and on Biacore sensor surface chips at high concentrations in this study and so is even less likely to be like real fibrin. Results of plate binding assays in section 4.3.1.1, table 4.3. showed that itPA and scitPA (R275E) required more 6-aminohexanoic acid to block binding to immobilized fibrinogen than to immobilized fibrin, indicating that binding to fibrinogen was tighter, which is not what we would expect from real fibrin, however in general results from this method were variable and more repeats would be needed to confirm this. Similarly when binding to a "fibrin" surface was investigated using the Biacore the K_D values generated from fitting to the two step binding model showed that binding of scitPA and tcitPA was higher affinity to fibrinogen; K_D = 68 nM and 113 nM respectively, than to fibrin; K_D = 92 nM and 128 nM respectively. However, fitting the same data to the heterogeneous binding model suggested that binding to fibrin was higher affinity K_D = 30 nM and 79 nM for scitPA (R275E) and tcitPA, than binding to fibrinogen, K_D = 46 nM and 135 nM for scitPA (R275E) and tcitPA.

Immobilised lysine is an interesting support and represents a clearly defined chemical surface that resembles C-terminal lysine. However, it does not have the other amino acids of

fibrinogen surrounding it that could make a more extended binding site, so the results may be unrepresentative of C-terminal lysines in fibrin(ogen). Lysine analogues have been used a lot to investigate lysine binding of kringle domains in tPA and plasminogen by a number of techniques such as NMR (Battistel et al, 2009; Byeon et al, 1995; Hu et al, 1994). Results of binding of the variants to immobilized lysine were not as expected itPA: K1K1 was seen to bind to lysine, while poor binding of the irPA and itPA: F del was observed. The reason for this is unknown and previous work had shown has shown good binding of tPA and rPA commercial products (Dr Colin Longstaff, personal communication), further work is needed to address this question. No difference was observed between itPA, scitPA and tcitPA binding to lysine but this may be expected.

The results of the simple template model with soluble templates are reasonable and suggest the same approach might be used for fibrin. Fibrin will be more complicated but the assay used in this study (Longstaff and Whitton, 2004) was designed with this in mind and is amenable to simulations. Work has been started on this. The principle is similar to the situation where fibrinogen is used as template, but there are a few more considerations such as a term for diffusion of the chromogenic substrate (S-2251) through the clot after it is added to the surface of the clot with the activator. However, these additional terms are simple to add using this type of modelling software with numerical simulation. The ultimate aim of the work is to develop a model that looks at the whole time course of clots and takes into account the stimulation due to C-terminal lysine generation, which creates extra binding sites for plasminogen and tPA and includes terms for the breakdown and complete degradation of fibrin. The practical work presented in chapter 3.3.3 using fibrin treated with plasmin (to generate C-terminal lysines from the start of the reaction) or including CPB (to eliminate C-terminal lysine formation) is designed to generate data to help with the development and validation of such a model.

6.1. Future work

Improvements could be made on the models with fibrin as described above and to build up the complexity of these models in fibrin and with soluble templates. More physiologically relevant systems could be developed to include inhibitors such as TAFI, α2-antiplasmin and PAI-1. Other methods need to be developed to get more reliable K_D (or kinetic) values for binding of tPA and plasminogen to templates. This could involve improving methods using GFP fusion proteins and testing more conditions on the Biacore. New tPA variants could be made such as a variant with both the GF and the F domain deleted with the aim of trying to keep the structure of variants similar to full length tPA, ensuring that all of the intermolecular interactions between the domains are intact. Variants of plasminogen could be designed. Small amounts of a cyan fluorescent protein derivative of plasminogen has been produced which can be used in Fluorescence Resonance Energy Transfer (FRET) studies with GFP-tPA to understand the mechanism and affinities of template binding. These experiments could be repeated in plasma which would be more similar to physiological conditions as the system that has been investigated in this study is a simplification of what is really happening in a fibrin clot.

Ultimately all these studies might help develop better plasminogen activators and thrombolytic drugs, especially for stroke where very limited options are available for treatment right now. These kinds of studies can provide systems to measure activities of thrombolytics, new and old, in vitro that really reflect in vivo activity. This is especially helpful for novel drugs before lots of money is wasted on clinical trials. The currently available thrombolytics have not really improved on tPA because there are still significant side effects such as bleeding events, and the only significant improvements have been in

administration due to increased half-life and reduced plasma clearance leading to the ability to administer through bolus injection rather than infusion over a period of hours. The development of tPA itself as a second generation thrombolytic did not show much improvement on 1st generation thrombolytics such as streptokinase and urokinase which are not fibrin specific, despite tremendous optimism and expectation. The disappointments following the clinical trials of tPA and 3rd generation thrombolytics may have been avoided if better models of fibrinolysis were available allowing for proper rational drug design.

7.0 Reference List

Agnelli, G., Pascucci, C., Cosmi, B., and Nenci, G. G. (1990) Effects of therapeutic doses of heparin on thrombolysis with tissue-type plasminogen activator in rabbits. *Blood.*, 76, 10: 2030 - 2036.

Altmann, F., Staudacher, E., Wilson, I. B., and Marz, L. (1999) Insect cells as hosts for the expression of recombinant glycoproteins. *Glycoconj.J.*, 16, 2: 109 - 123.

Andrade-Gordon, P. and Strickland, S. (1990) Fractionation of heparin by chromatography on a tissue plasminogen activator-Sepharose column. *Proc.Natl.Acad.Sci U.S.A.*, 87, 5: 1865 - 1869.

Andrade-Gordon, P. and Strickland, Sidney. (1986) Interaction of heparin with plasminogen activators and plasminogen: effects on the activation of plasminogen. *Biochemistry*, 25, 14: 4033 - 4040.

Angles-Cano, E. (1986) A spectrophotometric solid-phase fibrin-tissue plasminogen activator activity assay (SOFIA-tPA) for high-fibrin-affinity tissue plasminogen activators. *Anal.Biochem.*, 153, 2: 201 - 210.

Bakker, A. H. F., Rehberg, E. F., Marotti, K. R., and Verheijen, J. H. (1995) The Position of the Structurally Autonomous Kringle-2 Domain Influences the Functional Features of Tissue-Type Plasminogen-Activator. *Protein Engineering*, 8, 3: 293 - 300.

Baneyx, François. (1999) Recombinant protein expression in Escherichia coli. *Current Opinion in Biotechnology*, 10, 5: 411 - 421.

Banyai, L., Varadi, A., and Patthy, L. (1983) Common evolutionary origin of the fibrin-binding structures of fibronectin and tissue-type plasminogen activator. *FEBS Lett.*, 163, 1: 37 - 41.

Battistel, M. D., Grishaev, A., An, S. S., Castellino, F. J., and Llinas, M. (2009) Solution structure and functional characterization of human plasminogen kringle 5. *Biochemistry.*, 48, 43: 10208 - 10219.

Bennett, W. F., Paoni, N. F., Keyt, B. A., Botstein, D., Jones, A. J., Presta, L., Wurm, F. M., and Zoller, M. J. (1991) High resolution analysis of functional determinants on human tissue- type plasminogen activator. *Journal of Biological Chemistry*, 266, 8: 5191 - 5201.

Biacore AB (1998),BIAtechnology handbook Biacore AB,

Biacore AB. (2003) Biacore Sensor Surface Handbook. October 2003, AA:

Bisswanger, H (2008),Enzyme Kinetics Principles and Methods 2 edn, Wiley-VCH, Weinheim,

Bizzarri, Ranieri, Serresi, Michela, Luin, Stefano, and Beltram, Fabio. (2009) Green fluorescent protein based pH indicators for in vivo use: a review. *Analytical and Bioanalytical Chemistry*, 393, 4: 1107 - 1122.

Bjork, I. and Nordenman, B. (1976) Acceleration of the reaction between thrombin and antithrombin III by non-stoichiometric amounts of heparin. *Eur.J.Biochem.*, 68, 2: 507 - 511.

Blomback, B. (1996) Fibrinogen and fibrin--proteins with complex roles in hemostasis and thrombosis. *Thromb Res.*, 83, 1: 1 - 75.

Bok, R. A. and Mangel, W. F. (1985) Quantitative characterization of the binding of plasminogen to intact fibrin clots, lysine-sepharose, and fibrin cleaved by plasmin. *Biochemistry*, 24, 13: 3279 - 3286.

Boland, A., Dundar, Y., Bagust, A., Haycox, A., Hill, R., Mujica, Mota R., Walley, T., and Dickson, R. (2003) Early thrombolysis for the treatment of acute myocardial infarction: a systematic review and economic evaluation. *Health Technol.Assess.*, 7, 15: 1 - 136.

Boose, J. A., Kuismanen, E., Gerard, R., Sambrook, J., and Gething, M. J. (1989) The single-chain form of tissue-type plasminogen activator has catalytic activity: studies with a mutant enzyme that lacks the cleavage site. *Biochemistry*, 28, 2: 635 - 643.

Bosma, P, Rijken, D, and Nieuwenhuizen, W. (1988) Binding of tissue-type plasminogen activator to fibrinogen fragments. *European Journal of Biochemistry*, 172, 2: 399 - 404.

Bringmann, P., Gruber, D., Liese, A., Toschi, L., Kratzchmar, J., Schleuning, W. D., and Donner, P. (1995) Structural features mediating fibrin selectivity of vampire bat plasminogen activators. *Journal of Biological Chemistry*, 270, 43: 25596 - 25603.

Brown, Angus M. (2001) A step-by-step guide to non-linear regression analysis of experimental data using a Microsoft Excel spreadsheet. *Computer Methods and Programs in Biomedicine*, 65, 3: 191 - 200.

Brown, J. H., Volkmann, N., Jun, G., Henschen-Edman, A. H., and Cohen, C. (2000) The crystal structure of modified bovine fibrinogen. *Proc.Natl.Acad.Sci U.S.A*, 97, 1: 85 - 90.

Burck, P. J., Berg, D. H., Warrick, M. W., Berg, D. T., Walls, J. D., Jaskunas, S. R., Crisel, R. M., Weigel, B., Vlahos, C. J., McClure, D. B., and . (1990) Characterization of a modified human tissue plasminogen activator comprising a kringle-2 and a protease domain. *Journal of Biological Chemistry*, 265, 9: 5170 - 5177.

Byeon, I. J., Kelley, R. F., Mulkerrin, M. G., An, S. S., and Llinas, M. (1995) Ligand binding to the tissue-type plasminogen activator kringle 2 domain: structural characterization by 1H-NMR. *Biochemistry.*, 34, 9: 2739 - 2750.

Cercek, B., Lew, A. S., Hod, H., Yano, J., Reddy, N. K., and Ganz, W. (1986) Enhancement of thrombolysis with tissue-type plasminogen activator by pretreatment with heparin. *Circulation*, 74, 3: 583 - 587.

Chesebro, J. H., Knatterud, G., Roberts, R., Borer, J., Cohen, L. S., Dalen, J., Dodge, H. T., Francis, C. K., Hillis, D., and Ludbrook, P. (1987) Thrombolysis in Myocardial Infarction (TIMI) Trial, Phase I: A comparison between intravenous tissue plasminogen activator and intravenous streptokinase. Clinical findings through hospital discharge. *Circulation*, 76, 1: 142 - 154.

Christensen, Ulla. (1985) C-terminal lysine residues of fibrinogen fragments essential for binding to plasminogen. *FEBS Letters*, 182, 1: 43 - 46.

Collen, D. (1985) Human tissue-type plasminogen activator: from the laboratory to the bedside. *Circulation.*, 72, 1: 18 - 20.

Collen, D. (1999) The plasminogen (fibrinolytic) system. *Thromb.Haemost.*, 82, 2: 259 - 270.

Collen, D. and Lijnen, H. R. (1991) Basic and clinical aspects of fibrinolysis and thrombolysis. *Blood*, 78, 12: 3114 - 3124.

Collen, D., Lijnen, H. R., Bulens, F., Vandamme, A. M., Tulinsky, A., and Nelles, L. (1990) Biochemical and functional characterization of human tissue-type plasminogen activator variants with mutagenized kringle domains. *J Biol Chem.*, 265, 21: 12184 - 12191.

Collen, D., Lijnen, H. R., Todd, P. A., and Goa, K. L. (1989) Tissue-type plasminogen activator. A review of its pharmacology and therapeutic use as a thrombolytic agent. *Drugs.*, 38, 3: 346 - 388.

Collen, D., Stassen, J. M., and Larsen, G. (1988) Pharmacokinetics and thrombolytic properties of deletion mutants of human tissue-type plasminogen activator in rabbits. *Blood*, 71, 1: 216 - 219.

Collen, Desire and Lijnen, H. Roger. (1995) New thrombolytic agents and strategies. *Bailliere's Clinical Haematology*, 8, 2: 425 - 435.

Cornish Bowden, A (2004),Fundamentals of Enzyme Kinetics by Cornish Bowden 3 rd Edition edn, Portland Press, London and Miami, 1-68

Davies, M. J. and Thomas, A. C. (1985) Plaque fissuring--the cause of acute myocardial infarction, sudden ischaemic death, and crescendo angina. *Br.Heart J.*, 53, 4: 363 - 373.

de Paz, Jose L., Noti, Christian, B÷hm, Friederike, Werner, Sabine, and Seeberger, Peter H. (2007) Potentiation of Fibroblast Growth Factor Activity by Synthetic Heparin Oligosaccharide Glycodendrimers. *Chemistry & Biology*, 14, 8: 879 - 887.

De Serrano, V and Castellino, F. J. (1994a) Involvement of tyrosine-76 of the kringle 2 domain of tissue-type plasminogen activator in its thermal stability and its omega-amino acid ligand binding site. *Biochemistry.*, 33, 12: 3509 - 3514.

De Serrano, V and Castellino, F. J. (1994b) Role of the strictly conserved tryptophan-25 residue in the stabilization of the structure and in the ligand binding properties of the kringle 2 domain of tissue-type plasminogen activator. *Biochemistry.*, 33, 6: 1340 - 1344.

De Serrano, Vesna S. and Castellino, Francis J. (1992) The cationic locus on the recombinant kringle 2 domain of tissue-type plasminogen activator that stabilizes its interaction with .omega.-amino acids. *Biochemistry*, 31, 47: 11698 - 11706.

de Vries, C., Veerman, H., Koornneef, E., and Pannekoek, H. (1990) Tissue-type plasminogen activator and its substrate Glu-plasminogen share common binding sites in limited plasmin-digested fibrin. *Journal of Biological Chemistry*, 265, 23: 13547 - 13552.

de Vries, C., Veerman, H., and Pannekoek, H. (1989) Identification of the domains of tissue-type plasminogen activator involved in the augmented binding to fibrin after limited digestion with plasmin. *Journal of Biological Chemistry*, 264, 21: 12604 - 12610.

Dolovich, L. R., Ginsberg, J. S., Douketis, J. D., Holbrook, A. M., and Cheah, G. (2000) A meta-analysis comparing low-molecular-weight heparins with unfractionated heparin in the treatment of venous thromboembolism: examining some unanswered questions

regarding location of treatment, product type, and dosing frequency. *Arch Intern Med.*, 160, 2: 181 - 188.

Doolittle, R. F. (2008) Searching for differences between fibrinogen and fibrin that affect the initiation of fibrinolysis. *Cardiovasc.Hematol.Agents Med Chem.*, 6, 3: 181 - 189.

Dorner, A. J., Bole, D. G., and Kaufman, R. J. (1987) The relationship of N-linked glycosylation and heavy chain-binding protein association with the secretion of glycoproteins. *The Journal of Cell Biology*, 105, 6: 2665 - 2674.

Dunn, E., Philippou, H., Ariëns, R., and Grant, P. (2006) Molecular mechanisms involved in the resistance of fibrin to clot lysis by plasmin in subjects with type 2 diabetes mellitus. *Diabetologia*, 49, 5: 1071 - 1080.

Dyr, J. E., Tich², I., Jirouskovβ, M., Tobiska, P., Slav∅k, R., Homola, J., Brynda, E., Houska, M., and Suttnar, J. (1998) Molecular arrangement of adsorbed fibrinogen molecules characterized by specific monoclonal antibodies and a surface plasmon resonance sensor. *Sensors and Actuators B: Chemical*, 51, 1-3: 268 - 272.

Eastman, D., Wurm, F. M., van, Reis R., and Higgins, D. L. (1992) A region of tissue plasminogen activator that affects plasminogen activation differentially with various fibrin(ogen)-related stimulators. *Biochemistry.*, 31, 2: 419 - 422.

Edelberg, J. M., Conrad, H. E., and Pizzo, S. V. (1991) Heparin Oligosaccharides Enhance Tissue-Type Plasminogen-Activator - A Correlation Between Oligosaccharide Length and Stimulation of Plasminogen Activation. *Biochemistry*, 30, 45: 10999 - 11003.

Edelberg, J. M. and Pizzo, S. V. (1990) Kinetic-Analysis of the Effects of Heparin and Lipoproteins on Tissue Plasminogen-Activator Mediated Plasminogen Activation. *Biochemistry*, 29, 25: 5906 - 5911.

European Pharmacopoeia. (1998) European Pharmacopoeia. 3rd, 1170 -

Falk, E. (1991) Coronary thrombosis: pathogenesis and clinical manifestations. *Am.J.Cardiol.*, 68, 7: 28B - 35B.

Farrell, P. J., Behie, L. A., and Iatrou, K. (1999) Transformed Lepidopteran insect cells: new sources of recombinant human tissue plasminogen activator. *Biotechnol.Bioeng.*, %20;64, 4: 426 - 433.

Fischer, S. and Kohnert, U. (1997) Major mechanistic differences explain the higher clot lysis potency of reteplase over alteplase: lack of fibrin binding is an advantage for bolus

application of fibrin-specific thrombolytics. *Fibrinolysis and Proteolysis*, 11, 3: 129 - 135.

Fleury, V. and Angles-Cano, E. (1991) Characterization of the binding of plasminogen to fibrin surfaces: the role of carboxy-terminal lysines. *Biochemistry*, 30, 30: 7630 - 7638.

Fleury, V., Loyau, S., Lijnen, H. R., Nieuwenhuizen, W., and ngles-Cano, E. (1993) Molecular assembly of plasminogen and tissue-type plasminogen activator on an evolving fibrin surface. *Eur.J Biochem.*, 216, 2: 549 - 556.

Folk, J., Gladnre, J. A., and Laki, K. (1959) The thrombin-induced formation of co-fibrin. II. Preliminary amino acid sequence studies on peptides A and B. *Journal of Biological Chemistry*, 234, 1: 67 - 70.

Francis, C. W., Marder, V. J., and Barlow, G. H. (1980) Plasmic degradation of crosslinked fibrin. Characterization of new macromolecular soluble complexes and a model of their structure. *J.Clin.Invest*, 66, 5: 1033 - 1043.

Furlong, A. M., Thomsen, D. R., Marotti, K. R., Post, L. E., and Sharma, S. K. (1988) Active human tissue plasminogen activator secreted from insect cells using a baculovirus vector. *Biotechnol.Appl.Biochem.*, 10, 5: 454 - 464.

Fuss, C., Palmaz, J. C., and Sprague, E. A. (2001) Fibrinogen: structure, function, and surface interactions. *J.Vasc.Interv.Radiol.*, 12, 6: 677 - 682.

Gandhi, Neha S. and Mancera, Ricardo L. (2008) The Structure of Glycosaminoglycans and their Interactions with Proteins. *Chemical Biology & Drug Design*, 72, 6: 455 - 482.

Gardlund, B, Hessel, B, Blomback, B, Maruerie, G, and Murano, G. (1977) Primary Structure of Human Fibrinogen. Characterization of Disulfide-Containing Cyanogen-Bromide Fragments. *European Journal of Biochemistry*, 77, 3: 595 - 610.

Gebbink, Martijn F. B. G., Bouma, Barend, Maas, Coen, and Bouma, Bonno N. (2009) Physiological responses to protein aggregates: Fibrinolysis, coagulation and inflammation (new roles for old factors). *FEBS Letters*, 583, 16: 2691 - 2699.

Genentech Inc. (2005) Package insert for Activase (Alteplase).

Gething, M. J., Adler, B., Boose, J. A., Gerard, R. D., Madison, E. L., McGookey, D., Meidell, R. S., Roman, L. M., and Sambrook, J. (1988) Variants of human tissue-type

plasminogen activator that lack specific structural domains of the heavy chain. *EMBO J.*, 7, 9: 2731 - 2740.

Gorkun, O. V., Veklich, Y. I., Medved, L. V., Henschen, A. H., and Weisel, J. W. (1994) Role of the alpha C domains of fibrin in clot formation. *Biochemistry*, 33, 22: 6986 - 6997.

Grailhe, P., Nieuwenhuizen, W., and Angles-Cano, E. (1994) Study of tissue-type plasminogen activator binding sites on fibrin using distinct fragments of fibrinogen. *Eur.J.Biochem.*, 219, 3: 961 - 967.

Green, Michael. (1990), "[5] Avidin and streptavidin," in Methods in Enzymology Avidin-Biotin Technology, Volume 184 edn,Ed Meir Wilchek and Edward(ed.), Academic Press, 51-67.

Griffith, M. J. (1982) The heparin-enhanced antithrombin III/thrombin reaction is saturable with respect to both thrombin and antithrombin III. *J Biol.Chem.*, 257, 23: 13899 - 302.

Gurfinkel, E. P., Manos, E. J., Mejail, R. I., Cerda, M. A., Duronto, E. A., Garcia, C. N., Daroca, A. M., and Mautner, B. (1995) Low molecular weight heparin versus regular heparin or aspirin in the treatment of unstable angina and silent ischemia. *J Am Coll Cardiol.*, 26, 2: 313 - 318.

Haddeland, U., Sletten, K., Bennick, A., and Brosstad, F. (1994) Freeze-dried fibrinogen or fibrinogen in EDTA stimulate the tissue-type plasminogen activator-catalysed conversion of plasminogen to plasmin. *Blood Coagul.Fibrinolysis*, 5, 4: 575 - 581.

Hansen, L., Blue, Y., Barone, K., Collen, D., and Larsen, G. R. (1988) Functional effects of asparagine-linked oligosaccharide on natural and variant human tissue-type plasminogen activator. *Journal of Biological Chemistry*, 263, 30: 15713 - 15719.

Harrison, R. L. and Jarvis, D. L. (2007) Transforming lepidopteran insect cells for continuous recombinant protein expression. *Methods Mol.Biol.*, 388:299-316., 299 - 316.

Heussen, C., Joubert, F., and Dowdle, E. B. (1984) Purification of human tissue plasminogen activator with Erythrina trypsin inhibitor. *Journal of Biological Chemistry*, 259, 19: 11635 - 11638.

Hirsh, J., Warkentin, T. E., Shaughnessy, S. G., Anand, S. S., Halperin, J. L., Raschke, R., Granger, C., Ohman, E. M., and Dalen, J. E. (2001) Heparin and low-molecular-weight heparin: mechanisms of action, pharmacokinetics, dosing, monitoring, efficacy, and safety. *Chest.*, 119, 1 Suppl: 64S - 94S.

Hochschwender, S. M. and Laursen, R. A. (1981) The lysine binding sites of human plasminogen. Evidence for a critical tryptophan in the binding site of kringle 4. *Journal of Biological Chemistry*, 256, 21: 11172 - 11176.

Holmberg, A., Blomstergren, A., Nord, O., Lukacs, M., Lundeberg, J., and Uhlen, M. (2005) The biotin-streptavidin interaction can be reversibly broken using water at elevated temperatures. *Electrophoresis.*, 26, 3: 501 - 510.

Holmes, Kevin L. and Lantz, Larry M. (2001), "Protein labeling with fluorescent probes," in Methods in Cell Biology and Cytometry, Volume 63, Part 1 edn,Ed Zbigniew Darzynkiewicz, Harry A. C.(ed.), Academic Press, 185-204.

Horrevoets, A. J., Smilde, A., de Vries, C., and Pannekoek, H. (1994) The specific roles of finger and kringle 2 domains of tissue-type plasminogen activator during in vitro fibrinolysis. *Journal of Biological Chemistry*, 269, 17: 12639 - 12644.

Horrevoets, Anton J. G., Pannekoek, Hans, and Nesheim, Michael E. (1996) A Steady-state Template Model That Describes the Kinetics of Fibrin-stimulated [Glu1]- and [Lys78]Plasminogen Activation by Native tissue-type Plasminogen Activator and Variants That Lack Either the Finger or Kringle-2 Domain. *Journal of Biological Chemistry*, 272, 4: 2183 - 2191.

Hotchkiss, A., Refino, C. J., Leonard, C. K., O'Connor, J. V., Crowley, C., McCabe, J., Tate, K., Nakamura, G., Powers, D., Levinson, A., and . (1988) The influence of carbohydrate structure on the clearance of recombinant tissue-type plasminogen activator. *Thromb.Haemost.*, 60, 2: 255 - 261.

Hoylaerts, M., Rijken, D. C., Lijnen, H. R., and Collen, D. (1982) Kinetics of the activation of plasminogen by human tissue plasminogen activator. Role of fibrin. *Journal of Biological Chemistry*, 257, 6: 2912 - 2919.

Hu, C. K., Kohnert, U., Wilhelm, O., Fischer, S., and Llinas, M. (1994) Tissue-type plasminogen activator domain-deletion mutant BM 06.022: modular stability, inhibitor binding, and activation cleavage. *Biochemistry.*, 33, 39: 11760 - 11766.

Invitrogen Life Sciences (2004), "An efficient site-specific transposition system to generate baculovirus for high-level expression of recombinant proteins," in Bac-to-Bac® Baculovirus Epression System, Version D edn.

Jacobsson, I., Hook, M., Pettersson, I., Lindahl, U., Larm, O., Wiren, E., and von, Figura K. (1979) Identification of N-sulphated disaccharide units in heparin-like polysaccharides. *Biochemical Journal*, 179, 1: 77 - 87.

Jarvis, D. L., Fleming, J. A., Kovacs, G. R., Summers, M. D., and Guarino, L. A. (1990) Use of early baculovirus promoters for continuous expression and efficient processing of foreign gene products in stably transformed lepidopteran cells. *Biotechnology (N.Y.).*, 8, 10: 950 - 955.

Jarvis, D. L. and Summers, M. D. (1989) Glycosylation and secretion of human tissue plasminogen activator in recombinant baculovirus-infected insect cells. *Molecular and Cellular Biology*, 9, 1: 214 - 223.

Jarvis, D. L., Summers, M. D., Garcia, A., Jr., and Bohlmeyer, D. A. (1993) Influence of different signal peptides and prosequences on expression and secretion of human tissue plasminogen activator in the baculovirus system. *J Biol Chem.*, 268, 22: 16754 - 16762.

Jarvis, Donald L. and Finn, Eric E. (1995) Biochemical Analysis of the N-Glycosylation Pathway in Baculovirus-Infected Lepidopteran Insect Cells. *Virology*, 212, 2: 500 - 511.

Johnsson, B., Lofas, S., and Lindquist, G. (1991) Immobilization of proteins to a carboxymethyldextran-modified gold surface for biospecific interaction analysis in surface plasmon resonance sensors. *Anal.Biochem.*, 198, 2: 268 - 277.

Jönsson, U., Fagerstam, L., Ivarsson, B., Johnsson, B., Karlsson, R., Lundh, K., Lofas, S., Persson, B., Roos, H., Ronnberg, I., and . (1991) Real-time biospecific interaction analysis using surface plasmon resonance and a sensor chip technology. *Biotechniques.*, 11, 5: 620 - 627.

Jonsson, U., Fagerstam, L., Lofas, S., Stenberg, E., Karlsson, R., Frostell, A., Markey, F., and Schindler, F. (1993) Introducing a biosensor based technology for real-time biospecific interaction analysis. *Ann.Biol.Clin.(Paris).*, 51, 1: 19 - 26.

Juhan-Vague, I., Morange, P. E., Aubert, H., Henry, M., Aillaud, M. F., Alessi, M. C., Samnegard, A., Hawe, E., Yudkin, J., Margaglione, M., Di, Minno G., Hamsten, A., and Humphries, S. E. (2002) Plasma thrombin-activatable fibrinolysis inhibitor antigen concentration and genotype in relation to myocardial infarction in the north and south of Europe. *Arterioscler.Thromb.Vasc.Biol.*, 22, 5: 867 - 873.

Kagitani, H., Tagawa, M., Hatanaka, K., Ikari, T., Saito, A., Bando, H., Okada, K., and Matsuo, O. (1985) Expression in E. coli of finger-domain lacking tissue-type plasminogen activator with high fibrin affinity. *FEBS Lett.*, 189, 1: 145 - 149.

Kawasaki, T., Katoh, M., Kaku, S., Gushima, H., Takenaka, T., Yui, Y., and Kawai, C. (1993) Thrombolysis with intracoronary administration of YM866, a novel modified

tissue-type plasminogen activator, in a canine model of coronary artery thrombosis. *Jpn.J.Pharmacol.*, 63, 3: 319 - 325.

Keyt, B. A., Paoni, N. F., Refino, C. J., Berleau, L., Nguyen, H., Chow, A., Lai, J., Pe+¦a, L., Pater, C., and Ogez, J. (1994) A faster-acting and more potent form of tissue plasminogen activator. *Proceedings of the National Academy of Sciences of the United States of America*, 91, 9: 3670 - 3674.

Kohnert, Ulrich, Rudolph, Rainer, Verheijen, Jan H., Jacoline, E., Weening-Verhoeff, D., Stern, Anne, Opitz, Ulrich, Martin, Ulrich, Lill, Helmut, Prinz, Heinrich, Lechner, Max, Kresse, Georg B., Bucket, Peter, and Fischer, Stephan. (1992) Biochemical properties of the kringle 2 and protease domains are maintained in the refolded t-PA deletion variant BM 06.022. *Protein Engineering*, 5, 1: 93 - 100.

Koo, J., Rafailovich, M. H., Medved, L., Tsurupa, G., Kudryk, B. J., Liu, Y., and Galanakis, D. K. (2010) Evaluation of fibrinogen self-assembly: role of its alphaC region. *J Thromb Haemost.*, 8, 12: 2727 - 2735.

Kruithof, E. K., Tran-Thang, C., Ransijn, A., and Bachmann, F. (1984) Demonstration of a fast-acting inhibitor of plasminogen activators in human plasma. *Blood*, 64, 4: 907 - 913.

Ladenvall, C., Gils, A., Jood, K., Blomstrand, C., Declerck, P. J., and Jern, C. (2007) Thrombin activatable fibrinolysis inhibitor activation peptide shows association with all major subtypes of ischemic stroke and with TAFI gene variation. *Arterioscler.Thromb.Vasc.Biol.*, 27, 4: 955 - 962.

Langer-Safer, P. R., Ahern, T. J., Angus, L. B., Barone, K. M., Brenner, M. J., Horgan, P. G., Morris, G. E., Stoudemire, J. B., Timony, G. A., and Larsen, G. R. (1991) Replacement of finger and growth factor domains of tissue plasminogen activator with plasminogen kringle 1. Biochemical and pharmacological characterization of a novel chimera containing a high affinity fibrin-binding domain linked to a heterologous protein. *J Biol Chem.*, 266, 6: 3715 - 3723.

Larsen, G. R., Henson, K., and Blue, Y. (1988) Variants of human tissue-type plasminogen activator. Fibrin binding, fibrinolytic, and fibrinogenolytic characterization of genetic variants lacking the fibronectin finger-like and/or the epidermal growth factor domains. *Journal of Biological Chemistry*, 263, 2: 1023 - 1029.

Leatherbarrow, RJ. (2003) *Grafit*, Version 5.0.6. *Stains, UK: Erithacus Software, Ltd*,

Leebeek, F., Goor, M., Guimaraes, A., Brouwers, G., Maat, M., Dippel, D., and Rijken, D. (2005) High functional levels of thrombin-activatable fibrinolysis inhibitor are

associated with an increased risk of first ischemic stroke. *Journal of Thrombosis and Haemostasis*, 3, 10: 2211 - 2218.

Liang, Jun F., Li, Yongtao, and Yang, Victor C. (2000) The Potential Mechanism for the Effect of Heparin on Tissue Plasminogen Activator-Mediated Plasminogen Activation. *Thrombosis Research*, 97, 5: 349 - 358.

Lijnen, H. R., Nelles, L., Van Hoef, B., De Cock, F., and Collen, D. (1990) Biochemical and functional characterization of human tissue-type plasminogen activator variants obtained by deletion and/or duplication of structural/functional domains. *Journal of Biological Chemistry*, 265, 10: 5677 - 5683.

Lijnen, H. Roger and Collen, Desire. (1995) 1 Mechanisms of physiological fibrinolysis. *Bailliere's Clinical Haematology*, 8, 2: 277 - 290.

Lippincott-Schwartz, Jennifer and Patterson, George H. (2003) Development and Use of Fluorescent Protein Markers in Living Cells. *Science*, 300, 5616: 87 - 91.

Litvinov, R. I., Gorkun, O. V., Galanakis, D. K., Yakovlev, S., Medved, L., Shuman, H., and Weisel, J. W. (2007) Polymerization of fibrin: Direct observation and quantification of individual B:b knob-hole interactions. *Blood*, 109, 1: 130 - 138.

Lo, H. R. and Chao, Y. C. (2004) Rapid Titer Determination of Baculovirus by Quantitative Real-Time Polymerase Chain Reaction. *Biotechnology Progress*, 20, 1: 354 - 360.

Longstaff, C., Merton, E., and Sinniger, V. (1995) A comparison of cultured cells with other promoters of tissue plasminogen activator kinetics. *Fibrinolysis*, 9, 178 - 187.

Longstaff, C. and Thelwell, C. (2005) Understanding the enzymology of fibrinolysis and improving thrombolytic therapy. *FEBS Lett.*, 579, 15: 3303 - 3309.

Longstaff, C., Whitton, C., Thelwell, C., and Belgrave, D. (2007) An international collaborative study to investigate a proposed reference method for the determination of potency measurements of fibrinolytics in absolute units. *J.Thromb.Haemost.*, 5, 2: 412 - 414.

Longstaff, C. and Whitton, C. M. (2004) A proposed reference method for plasminogen activators that enables calculation of enzyme activities in SI units. *J.Thromb.Haemost.*, 2, 8: 1416 - 1421.

Longstaff, C., Whitton, C. M., Stebbings, R., and Gray, E. (2009) How do we assure the quality of biological medicines? *Drug Discov.Today.*, 14, 1-2: 50 - 55.

Longstaff, C., Williams, S, and Thelwell, C. (2008) Fibrin binding and the regulation of plasminogen activators during thrombolytic therapy. *Cardiovascular and Hematological Agents in Medicinal Chemistry*,

Longstaff, Colin, Thelwell, Craig, Williams, Stella C., Silva, Marta M. C. G., Szabo, L., and Kolev, Krasimir. (2011) The interplay between tissue plasminogen activator domains and fibrin structures in the regulation of fibrinolysis: kinetic and microscopic studies. *Blood*, 117, 2: 661 - 668.

Lorand, L. (1952) Fibrino-peptide. *Biochemical Journal*, 52, 2: 200 - 203.

Lucas, M. A., Fretto, L. J., and McKee, P. A. (1983) The binding of human plasminogen to fibrin and fibrinogen. *Journal of Biological Chemistry*, 258, 7: 4249 - 4256.

Ma, Q., Zhou, L., Ma, L., and Huo, K. (2006) Directional and direct cloning strategy for high-throughput generation of recombinant baculoviruses. *Biotechniques.*, 41, 4: 453 - 458.

Maas, Coen, Hermeling, Suzanne, Bouma, Barend, Jiskoot, Wim, and Gebbink, Martijn F. B. G. (2007) A Role for Protein Misfolding in Immunogenicity of Biopharmaceuticals. *Journal of Biological Chemistry*, 282, 4: 2229 - 2236.

Marks, Rory M., Lu, Hong, Sundaresan, Renuka, Toida, Toshihiko, Suzuki, Atsushi, Imanari, Toshio, Herníiz, María J., and Linhardt, Robert J. (2001) Probing the Interaction of Dengue Virus Envelope Protein with Heparin: Assessment of Glycosaminoglycan-Derived Inhibitors. *Journal of Medicinal Chemistry*, 44, 13: 2178 - 2187.

Martin, U., Fischer, S., Kohnert, U., Opitz, U., Rudolph, R., Sponer, G., Stern, A., and Strein, K. (1992) Pharmacokinetic and thrombolytic properties of unglycosylated recombinant tissue-type plasminogen activator (BM 06.021) produced in *Escherichia coli*. *Naunyn-Schmiedeberg's Archives of Pharmacology*, 346, 1: 108 - 113.

Martin, U., Fischer, S., Kohnert, U., Rudolph, R., Sponer, G., Stern, A., and Strein, K. (1991) Pharmacokinetic properties of an Escherichia-coli-produced recombinant plasminogen activator (BM 06.022) in rabbits. *Thromb.Res.*, 62, 3: 137 - 146.

McCluskey, E. R., Refino, C. J., Zioncheck, T. F, and Chin, R. Y (2003), "Tenectaplase: Biochemistry, Pharmacology, and Clinical Experience," in New Therapeutic Agents in Thrombosis and Thrombolysis, Second edn,Ed Sasahara, A. A and Loscalzo, J, Marcel Decker, Ink, New York, Basel, 501-511.

McKee, Patrick A., Rogers, Larry A., Marler, Eric, and Hill, Robert L. (1966) The subunit polypeptides of human fibrinogen. *Archives of Biochemistry and Biophysics*, 116, 271 - 279.

Medved', L. V., Gorkun, O. V., Manyakov, V. F., and Belitser, V. A. (1985) The role of fibrinogen alpha C-domains in the fibrin assembly process. *FEBS Lett.*, 181, 1: 109 - 112.

Medved, L., Litvinovich, S., Ugarova, T., Matsuka, Y., and Ingham, K. (1997) Domain structure and functional activity of the recombinant human fibrinogen gamma-module (gamma148-411). *Biochemistry*, 36, 15: 4685 - 4693.

Medved, L. and Nieuwenhuizen, W. (2003) Molecular mechanisms of initiation of fibrinolysis by fibrin. *Thromb.Haemost.*, 89, 3: 409 - 419.

Medved, L., Tsurupa, G., and Yakovlev, S. (2001) Conformational changes upon conversion of fibrinogen into fibrin. The mechanisms of exposure of cryptic sites. *Ann.N.Y.Acad.Sci*, 936, 185 - 204.

Mendes, P., Hoops, S., Sahle, S., Gauges, R., Dada, J., and Kummer, U. (2009) Computational modeling of biochemical networks using COPASI. *Methods Mol.Biol.*, 500:17-59., 17 - 59.

Mendes, Pedro. (1997) Biochemistry by numbers: simulation of biochemical pathways with Gepasi 3. *Trends in Biochemical Sciences*, 22, 9: 361 - 363.

Mickelson, J. K., Simpson, P. J., Jackson, C. V., and Lucchesi, B. R. (1988) Protection of myocardial function and coronary vasculature by streptokinase. *J Cardiovasc.Pharmacol.*, 12, 2: 186 - 195.

Morange, P. E., Henry, M., Frere, C., and Juhan-Vague, I. (2002) Thr325IIe polymorphism of the TAFI gene does not influence the risk of myocardial infarction. *Blood*, 99, 5: 1878 - 1879.

Morange, P. E., Juhan-Vague, I., Scarabin, P. Y., Alessi, M. C., Luc, G., Arveiler, D., Ferrieres, J., Amouyel, P., Evans, A., and Ducimetiere, P. (2003) Association between TAFI antigen and Ala147Thr polymorphism of the TAFI gene and the angina pectoris incidence. The PRIME Study (Prospective Epidemiological Study of MI). *Thromb.Haemost.*, 89, 3: 554 - 560.

Mousa, Shaker A. (2010), "Heparin and Low-Molecular Weight Heparins in Thrombosis and Beyond," in Anticoagulants, Antiplatelets, and Thrombolytics, 663 edn,Ed Mousa, Shaker A.(ed.), Humana Press, 109-132.

Mulloy, Barbara and Forster, Mark J. (2000) Conformation and dynamics of heparin and heparan sulfate. *Glycobiology*, 10, 11: 1147 - 1156.

Mulloy, Barbara and Linhardt, Robert J. (2001) Order out of complexity - protein structures that interact with heparin. *Current Opinion in Structural Biology*, 11, 5: 623 - 628.

Mutch, Nicola J., Engel, Ruchira, Uitte de Willige, Shirley, Philippou, Helen, and Ariëns, Robert A. S. (2010) Polyphosphate modifies the fibrin network and down-regulates fibrinolysis by attenuating binding of tPA and plasminogen to fibrin. *Blood*, 115, 19: 3980 - 3988.

Nader, H. B., Chavante, S. F., dos-Santos, E. A., Oliveira, F. W., de-Paiva, J. F., Jer+¦nimo, S. M. B., Medeiros, G. F., de-Abreu, L. R. D., Leite, E. L., de-Sousa-Filho, J. F., Castro, R. A. B., Toma, L., Tersariol, I. L. S., Porcionatto, M. A., and Dietrich, C. P. (1999) Heparan sulfates and heparins: similar compounds performing the same functions in vertebrates and invertebrates? *Brazilian Journal of Medical and Biological Research*, 32, 529 - 538.

Nesheim, M., Fredenburgh, J. C., and Larsen, G. R. (1990) The dissociation constants and stoichiometries of the interactions of Lys-plasminogen and chloromethyl ketone derivatives of tissue plasminogen activator and the variant delta FEIX with intact fibrin. *Journal of Biological Chemistry*, 265, 35: 21541 - 21548.

Nesheim, M. E., Tracy, R. P., and Mann, K. G. (1984) "Clotspeed," a mathematical simulation of the functional properties of prothrombinase. *J Biol.Chem.*, 259, 3: 1447 - 1453.

NICE. (2010) Drugs for early thrombolysis in the treatment of acute myocardial infarction - Final Appraisal Determination from the National Institute for Clinical Excellence. *http://www.nice.org.uk/article.asp?a=36672,*

Nieuwenhuizen, W, Vermond, A, Voskuilen, M, Traas, D W, and Verheijen, J. (1983a) Identification of a site in fibrin(OGEN) which is involved in the acceleration of plasminogen activation by tissue-type plasminogen activator. *Biochimica et Biophysica Acta (BBA) - Protein Structure and Molecular Enzymology*, 748, 1: 86 - 92.

Nieuwenhuizen, W. (2001) Fibrin-mediated plasminogen activation. *Ann.N.Y.Acad.Sci*, 936, 237 - 246.

Nieuwenhuizen, Willem, Verheijen, Jan H., Vermond, Anton, and Chang, Glenn T. G. (1983b) Plasminogen activation by tissue activator is accelerated in the presence of

fibrin(ogen) cyanogen bromide fragment FCB-2. *Biochimica et Biophysica Acta (BBA) - General Subjects*, 755, 3: 531 - 533.

Novokhatny, V. V., Ingham, K. C., and Medved, L. V. (1991) Domain structure and domain-domain interactions of recombinant tissue plasminogen activator. *Journal of Biological Chemistry*, 266, 20: 12994 - 13002.

Obukowicz, Mark G., Gustafson, Mark E., Junger, Kurt D., Leimgruber, Richard M., Wittwer, Arthur J., Wun, Tze Chein, Warren, Thomas G., Bishop, Bruce F., and Mathis, Karl J. (1990) Secretion of active kringle-2-serine protease in Escherichia coli. *Biochemistry*, 29, 41: 9737 - 9745.

Olden, Kenneth, Bernard, Bruno A., Humphries, Martin J., Yeo, Tet Kin, Yeo, Kiang Teck, White, Sandra L., Newton, Sheila A., Bauer, Hans C., and Parent, J. Brian. (1985) Function of glycoprotein glycans. *Trends in Biochemical Sciences*, 10, 2: 78 - 82.

Pâques, E. P., Stöhr, H. A., and Heimburger, N. (1986) Study on the mechanism of action of heparin and related substances on the fibrinolytic system: Relationsship between plasminogen activators and heparin. *Thrombosis Research*, 42, 6: 797 - 807.

Parekh, Raj B., Dwek, Raymond A., Rudd, Pauline M., Thomas, Jerry R., Rademacher, Thomas W., Warren, T., Wun, T. C., Hebert, B., and Reitz, B. (1989) N-Glycosylation and in vitro enzymic activity of human recombinant tissue plasminogen activator expressed in Chinese hamster ovary cells and a murine cell line. *Biochemistry*, 28, 19: 7670 - 7679.

Pennica, D., Holmes, W. E., Kohr, W. J., Harkins, R. N., Vehar, G. A., Ward, C. A., Bennett, W. F., Yelverton, E., Seeburg, P. H., Heyneker, H. L., Goeddel, D. V., and Collen, D. (1983) Cloning and expression of human tissue-type plasminogen activator cDNA in E. coli. *Nature*, 301, 5897: 214 - 221.

Petri, T., Langer, G., Bringmann, P., Cashion, L., Shallow, S., Schleuning, W.-D., and Donner, P. (1995) Production of vampire bat plasminogen activator DSPA [alpha]1 in CHO and insect cells. *Journal of Biotechnology*, 39, 1: 75 - 83.

Pizzo, Salvatore V., Schwartz, Martin L., Hill, Robert L., and McKee, Patrick A. (1972) The Effect of Plasmin on the Subunit Structure of Human Fibrinogen. *Journal of Biological Chemistry*, 247, 3: 636 - 645.

Pohl, G, Kenne, L, Nilsson, B, and Einarsson, M. (1987) Isolation and characterization of three different carbohydrate chains from melanoma tissue plasminogen activator. *European Journal of Biochemistry*, 170, 1-2: 69 - 75.

Pohl, Gunnar, Kaellstroem, Margareta, Bergsdorf, Nils, Wallen, Per, and Joernvall, Hans. (1984) Tissue plasminogen activator: peptide analyses confirm an indirectly derived amino acid sequence, identify the active site serine residue, establish glycosylation sites, and localize variant differences. *Biochemistry*, 23, 16: 3701 - 3707.

Prendergast, Franklyn G. and Mann, Kenneth G. (1978) Chemical and physical properties of aequorin and the green fluorescent protein isolated from Aequorea forskalea. *Biochemistry*, 17, 17: 3448 - 3453.

Privalov, P. L. and Medved', L. V. (1982) Domains in the fibrinogen molecule. *Journal of Molecular Biology*, 159, 4: 665 - 683.

Quinlan, D. J., McQuillan, A., and Eikelboom, J. W. (2004) Low-molecular-weight heparin compared with intravenous unfractionated heparin for treatment of pulmonary embolism: a meta-analysis of randomized, controlled trials. *Ann.Intern Med.*, 140, 3: 175 - 183.

Rao, A. K., Pratt, C., Berke, A., Jaffe, A., Ockene, I., Schreiber, T. L., Bell, W. R., Knatterud, G., Robertson, T. L., and Terrin, M. L. (1988) Thrombolysis in Myocardial Infarction (TIMI) Trial--phase I: hemorrhagic manifestations and changes in plasma fibrinogen and the fibrinolytic system in patients treated with recombinant tissue plasminogen activator and streptokinase. *Journal of the American College of Cardiology*, 11, 1: 1 - 11.

Riedel, Tomas, Suttnar, Jiri, Brynda, Eduard, Houska, Milan, Medved, Leonid, and Dyr, Jan E. (2011) Fibrinopeptides A and B release in the process of surface fibrin formation. *Blood*, 117, 5: 1700 - 1706.

Rijken, D. C., de Munk, G. A., and Jie, A. F. (1993) Interaction of plasminogen activators and plasminogen with heparin: effect of ionic strength. *Thromb.Haemost.*, 70, 5: 867 - 872.

Rijken, D. C. and Jie, A. F. H. (1996) Interaction of reteplase with heparin. A comparison between reteplase and alteplase. *Blood Coagulation & Fibrinolysis*, 7, 5:

Rijken, D. C., Otter, M., Kuiper, J., and van Berkel, T. J. (1990) Receptor-mediated endocytosis of tissue-type plasminogen activator (t-PA) by liver cells. *Thromb.Res.Suppl.*, 10:63-71., 63 - 71.

Robbins, Kenneth C., Summaria, Louis, Hsieh, Betty, and Shah, Rajnikant J. (1967) The Peptide Chains of Human Plasmin. Mechanism of Activation of Human Plasminogen to Plasmin. *Journal of Biological Chemistry*, 242, 10: 2333 - 2342.

Rosenberg, R. D. and Lam, L. (1979) Correlation between structure and function of heparin. *Proc.Natl.Acad.Sci U.S.A.*, 76, 3: 1218 - 1222.

Rydzewski, A. and Castellino, F. J. (1993) The Effector Roles of Kringle 1 and Kringle 2 in the Enzymatic Properties of Recombinant Tissue-Type Plasminogen Activator as Revealed by Generation of Recombinant Molecules Containing Each Kringle Linked to the Protease Domain. *Archives of Biochemistry and Biophysics*, 300, 1: 472 - 482.

Saito, A. and Munakata, H. (2007) Analysis of plasma proteins that bind to glycosaminoglycans. *Biochimica et Biophysica Acta - General Subjects*, 1770, 2: 241 - 246.

Schielen, W. J., Adams, H. P., van Leuven, K., Voskuilen, M., Tesser, G. I., and Nieuwenhuizen, W. (1991) The sequence gamma-(312-324) is a fibrin-specific epitope. *Blood*, 77, 10: 2169 - 2173.

Schielen, Wim J. G., Voskuilen, Marijke, Tesser, Godefridus I., and Nieuwenhuizen, Willem. (1989) The Sequence Aalpha -(148-160) in Fibrin, but not in Fibrinogen, is Accessible to Monoclonal Antibodies. *Proceedings of the National Academy of Sciences*, 86, 22: 8951 - 8954.

Schmidt, F. R. (2004) Recombinant expression systems in the pharmaceutical industry. *Applied Microbiology and Biotechnology*, 65, 4: 363 - 372.

Schuck, Peter. (1997) Use of Surface Plasmon Resonance to Probe the Equilibrium and Dynamic Aspects of Interactions Between Biological Macromolecules. *Annual Review of Biophysics and Biomolecular Structure*, 26, 1: 541 - 566.

Shimomura, Osamu, Johnson, Frank H., and Saiga, Yo. (1962) Extraction, Purification and Properties of Aequorin, a Bioluminescent Protein from the Luminous Hydromedusan, Aequorea. *Journal of Cellular and Comparative Physiology*, 59, 3: 223 - 239.

Sinniger, V., Merton, R. E., Fabregas, P., Felez, J., and Longstaff, C. (1999) Regulation of tissue plasminogen activator activity by cells. Domains responsible for binding and mechanism of stimulation. *Journal of Biological Chemistry*, 274, 18: 12414 - 12422.

Smalling, R. W. (1997) Pharmacological and clinical impact of the unique molecular structure of a new plasminogen activator. *European Heart Journal*, 18, suppl F: 11 - 16.

Smith, R. A. (1986) An active-site titrant for human tissue-type plasminogen activator. *Biochemical Journal*, 239, 2: 477 - 479.

Soeda, Shinji, Kakiki, Motoharu, Shimeno, Hiroshi, and Nagamatsu, Atsuo. (1987) Localization of the binding sites of porcine tissue-type plasminogen activator and plasminogen to heparin. *Biochimica et Biophysica Acta (BBA) - Protein Structure and Molecular Enzymology*, 916, 3: 279 - 287.

Soeda, Shinji, Ohki, Hirohiko, Shimeno, Hiroshi, and Nagamatsu, Atsuo. (1989) Further characterization of the binding of plasminogen to heparin: evidence for the involvement of lysine residues. *Biochimica et Biophysica Acta (BBA) - Protein Structure and Molecular Enzymology*, 999, 1: 29 - 35.

Stein, P. L., van Zonneveld, A. J., Pannekoek, H., and Strickland, S. (1989) Structural domains of human tissue-type plasminogen activator that confer stimulation by heparin. *Journal of Biological Chemistry*, 264, 26: 15441 - 15444.

Steiner, H., Pohl, G., Gunne, H., Hellers, M., Elhammer, A., and Hansson, L. (1988) Human tissue-type plasminogen activator synthesized by using a baculovirus vector in insect cells compared with human plasminogen activator produced in mouse cells. *Gene.*, 20;73, 2: 449 - 457.

Stewart, Ronald J., Fredenburgh, James C., and Weitz, Jeffrey I. (1998) Characterization of the Interactions of Plasminogen and Tissue and Vampire Bat Plasminogen Activators with Fibrinogen, Fibrin, and the Complex of d-Dimer Noncovalently Linked to Fragment E. *Journal of Biological Chemistry*, 273, 29: 18292 - 18299.

Stryer, L. (1978) Fluorescence Energy Transfer as a Spectroscopic Ruler. *Annual Review of Biochemistry*, 47, 1: 819 - 846.

Suenson, E, Lützen, O, and Thorsen, S. (1984) Initial plasmin-degradation of fibrin as the basis of a positive feed-back mechanism in fibrinolysis. *European Journal of Biochemistry*, 140, 3: 513 - 522.

Takada, Yumiko, Urano, Tetsumei, and Takada, Akikazu. (1994) Effects of heparan sulfate analogue or other sulfated polysaccharides on the activation of plasminogen by t-PA or u-PA. *Thrombosis Research*, 73, 5: 301 - 311.

Thelwell, C. and Longstaff, C. (2007) The regulation by fibrinogen and fibrin of tissue plasminogen activator kinetics and inhibition by plasminogen activator inhibitor 1. *J.Thromb.Haemost.*, 5, 4: 804 - 811.

Theroux, P., Ouimet, H., McCans, J., Latour, J. G., Joly, P., Levy, G., Pelletier, E., Juneau, M., Stasiak, J., deGuise, P., and . (1988) Aspirin, heparin, or both to treat acute unstable angina. *N.Engl.J Med.*, 319, 17: 1105 - 1111.

Tong, X. and Smith, L. M. (1992) Solid-phase method for the purification of DNA sequencing reactions. *Anal.Chem.*, 64, 22: 2672 - 2677.

Topol, E. J., George, B. S., Kereiakes, D. J., Stump, D. C., Candela, R. J., Abbottsmith, C. W., Aronson, L., Pickel, A., Boswick, J. M., and Lee, K. L. (1989) A randomized controlled trial of intravenous tissue plasminogen activator and early intravenous heparin in acute myocardial infarction. *Circulation*, 79, 2: 281 - 286.

Toschi, L., Bringmann, P., Petri, T., Donner, P., and Schleuning, W. D. (1998) Fibrin selectivity of the isolated protease domains of tissue-type and vampire bat salivary gland plasminogen activators. *European Journal of Biochemistry*, 252, 1: 108 - 112.

Trexler, M., Vali, Z., and Patthy, L. (1982) Structure of the omega-aminocarboxylic acid-binding sites of human plasminogen. Arginine 70 and aspartic acid 56 are essential for binding of ligand by kringle 4. *Journal of Biological Chemistry*, 257, 13: 7401 - 7406.

Trexler, Maria and Patthy, Laszlo. (1983) Folding Autonomy of the Kringle 4 Fragment of Human Plasminogen. *Proceedings of the National Academy of Sciences*, 80, 9: 2457 - 2461.

Tsai, Yu-Chen Hu, en-Hsin Lo, Ding-Gang Yang, and Jen-Te Lu. (2007) Factors influencing the production and storage of baculovirus for gene delivery: An alternative perspective from the transducing titer assay. *Enzyme and Microbial Technology*, 40, 5: 1345 - 1351.

Tsien, R. Y. (1998) The green fluorescent protein. *Annu.Rev.Biochem.*, 67:509-44., 509 - 544.

Tsurupa, G. and Medved, L. (2001a) Fibrinogen alpha C domains contain cryptic plasminogen and tPA binding sites. *Ann.N.Y.Acad.Sci*, 936, 328 - 330.

Tsurupa, G. and Medved, L. (2001b) Identification and Characterization of Novel tPA- and Plasminogen-Binding Sites within Fibrin(ogen) alphaC-Domains. *Biochemistry*, 40, 3: 801 - 808.

Tsurupa, G., Yakovlev, S., McKee, P., and Medved, L. (2010) Noncovalent interaction of alpha(2)-antiplasmin with fibrin(ogen): localization of alpha(2)-antiplasmin-binding sites. *Biochemistry.*, 49, 35: 7643 - 7651.

Urano, T., Urano, S., and Castellino, F. J. (1988) Reaction of tissue-type plasminogen activator with 4-methylumbelliferyl-p-guanidinobenzoate hydrochloride. *Biochem.Biophys.Res.Commun.*, 150, 1: 45 - 51.

Vali, Z. and Patthy, L. (1984) The fibrin-binding site of human plasminogen. Arginines 32 and 34 are essential for fibrin affinity of the kringle 1 domain. *Journal of Biological Chemistry*, 259, 22: 13690 - 13694.

van Zonneveld, A. J., Veerman, H., MacDonald, M. E., van Mourik, J. A., and Pannekoek, H. (1986a) Structure and function of human tissue-type plasminogen activator (t-PA). *J.Cell Biochem.*, 32, 3: 169 - 178.

van Zonneveld, A. J., Veerman, Harry, and Pannekoek, Hans. (1986b) Autonomous Functions of Structural Domains on Human Tissue-Type Plasminogen Activator. *Proceedings of the National Academy of Sciences*, 83, 13: 4670 - 4674.

Varadi, Andras and Patthy, Laszlo. (1983) Location of plasminogen-binding sites in human fibrin(ogen). *Biochemistry*, 22, 10: 2440 - 2446.

Varju, I., Sotonyi, P., Machovich, R., Szabo, L., Tenekedjiev, K., Silva, M. M., Longstaff, C., and Kolev, K. (2011) Hindered dissolution of fibrin formed under mechanical stress. *J Thromb Haemost.*, %20. doi: 10.1111/j.1538-7836.2011.04203.x., 10 - 7836.

Verheijen, J. H., Caspers, M. P., Chang, G. T., de Munk, G. A., Pouwels, P. H., and Enger-Valk, B. E. (1986) Involvement of finger domain and kringle 2 domain of tissue-type plasminogen activator in fibrin binding and stimulation of activity by fibrin. *EMBO J.*, 5, 13: 3525 - 3530.

Verheijen, J. H., Nieuwenhuizen, W., and Wijngaards, G. (1982) Activation of plasminogen by tissue activator is increased specifically in the presence of certain soluble fibrin(ogen) fragments. *Thrombosis Research*, 27, 4: 377 - 385.

Verstraete, M. (2000) Third-generation thrombolytic drugs. *Am.J.Med.*, 109, 1: 52 - 58.

Voskuilen, M., Vermond, A., Veeneman, G. H., van Boom, J. H., Klasen, E. A., Zegers, N. D., and Nieuwenhuizen, W. (1987) Fibrinogen lysine residue A alpha 157 plays a crucial role in the fibrin-induced acceleration of plasminogen activation, catalyzed by tissue-type plasminogen activator. *Journal of Biological Chemistry*, 262, 13: 5944 - 5946.

Wagner, R., Geyer, H., Geyer, R., and Klenk, H. D. (1996) N-acetyl-beta-glucosaminidase accounts for differences in glycosylation of influenza virus hemagglutinin expressed in insect cells from a baculovirus vector. *J.Virol.*, 70, 6: 4103 - 4109.

Wallen, P., Bergsdorf, N., and Ranby, M. (1982) Purification and identification of two structural variants of porcine tissue plasminogen activator by affinity adsorption on fibrin. *Biochim.Biophys.Acta*, 719, 2: 318 - 328.

Waller, M, Mack, S, Martin, U, and Minella, P. A (2003), "Clinical and Preclinical Profile of the Novel Recombinant Plasminogen Activator Reteplase," in New Therapeutic Agents in Thrombosis and Thrombolysis, Second edn,Ed Sasahara, A. A and Loscalzo, J, Marcel Decker, Ink, New York, Basel, 479-500.

Weinstein, M. J. and Doolittle, R. F. (1972) Differential specificities of the thrombin, plasmin and trypsin with regard to synthetic and natural substrates and inhibitors. *Biochim.Biophys.Acta*, 258, 2: 577 - 590.

Weisel, J. W. and Medved, L. (2001) The structure and function of the alpha C domains of fibrinogen. *Ann.N.Y.Acad.Sci*, 936, 312 - 327.

Weisel, J. W., Stauffacher, C. V., Bullitt, E., and Cohen, C. (1985) A model for fibrinogen: domains and sequence. *Science*, 230, 4732: 1388 - 1391.

Weitz, J. I., Hirsh, J., Giugliano, R. P, Mousa, Shaker A., Willerson, J. T, Goldhaber, S. J, and Verstraete, M. (2003), "New Therapeutic Agents in Thrombosis and Thrombolysis," 2nd Edition edn,Ed Sasahara, A. A and Loscalzo, J, Marcel Dekker, New York, 1-707.

Weitz, J. I., Kuint, J., Leslie, B., and Hirsh, J. (1991) Standard and low molecular weight heparin have no effect on tissue plasminogen activator induced plasma clot lysis or fibrinogenolysis. *Thromb.Haemost.*, 65, 5: 541 - 544.

Wells, T. N. and Fersht, A. R. (1986) Use of binding energy in catalysis analyzed by mutagenesis of the tyrosyl-tRNA synthetase. *Biochemistry.*, 25, 8: 1881 - 1886.

WHO. (2007) The Atlas of Heart Disease and Stroke.

Wilhelm, S. E., Lounes, K. C., and Lord, S. T. (2004) Investigation of residues in the fibrin(ogen) gamma chain involved in tissue plasminogen activator binding and plasminogen activation. *Blood Coagulation & Fibrinolysis*, 15, 6: 451 - 461.

Williams, D. O., Borer, J., Braunwald, E., Chesebro, J. H., Cohen, L. S., Dalen, J., Dodge, H. T., Francis, C. K., Knatterud, G., and Ludbrook, P. (1986) Intravenous recombinant tissue-type plasminogen activator in patients with acute myocardial infarction: a report from the NHLBI thrombolysis in myocardial infarction trial. *Circulation*, 73, 2: 338 - 346.

Wittwer, Arthur J., Howard, Susan C., Carr, Linda S., Harakas, Nikos K., Feder, Joseph, Parekh, Raj B., Rudd, Pauline M., Dwek, Raymond A., and Rademacher, Thomas W. (1989) Effects of N-glycosylation on in vitro activity of Bowes melanoma and human

colon fibroblast-derived tissue plasminogen activator. *Biochemistry*, 28, 19: 7662 - 7669.

Yakovlev, S., Makogonenko, E., Kurochkina, N., Nieuwenhuizen, W., Ingham, K., and Medved, L. (2000) Conversion of Fibrinogen to Fibrin: Mechanism of Exposure of tPA- and Plasminogen-Binding Sites. *Biochemistry*, 39, 51: 15730 - 15741.

Yakovlev, Sergiy, Gorlatov, Sergey, Ingham, Kenneth, and Medved, Leonid. (2003) Interaction of Fibrin(ogen) with Heparin: Further Characterization and Localization of the Heparin-Binding Site. *Biochemistry*, 42, 25: 7709 - 7716.

Yang, Z., Kollman, J. M., Pandi, L., and Doolittle, R. F. (2001) Crystal structure of native chicken fibrinogen at 2.7 A resolution. *Biochemistry*, 40, 42: 12515 - 12523.

Yang, Z., Mochalkin, I., and Doolittle, R. F. (2000) A model of fibrin formation based on crystal structures of fibrinogen and fibrin fragments complexed with synthetic peptides. *Proc.Natl.Acad.Sci U.S.A*, 97, 26: 14156 - 14161.

Yonekawa, O., Voskuilen, M., and Nieuwenhuizen, W. (1992) Localization in the fibrinogen gamma-chain of a new site that is involved in the acceleration of the tissue-type plasminogen activator-catalysed activation of plasminogen. *Biochemical Journal*, 283, 1: 187 - 191.

Young, Timothy N., Edelberg, Jay M., Stack, Sharon, and Pizzo, Salvatore V. (1992) Ionic modulation of the effects of heparin on plasminogen activation by tissue plasminogen activator: The effects of ionic strength, divalent cations, and chloride. *Archives of Biochemistry and Biophysics*, 296, 2: 530 - 538.

Zhang, Fuming, Fath, Melissa, Marks, Rory, and Linhardt, Robert J. (2002) A Highly Stable Covalent Conjugated Heparin Biochip for Heparin-Protein Interaction Studies. *Analytical Biochemistry*, 304, 2: 271 - 273.

Zhang, Lijuan (2010), "Glycosaminoglycan (GAG) Biosynthesis and GAG-Binding Proteins," in Progress in Molecular Biology and Translational Science Glycosaminoglycans in Development, Health and Disease, Volume 93 edn,Ed Lijuan, Zhang(ed.), Academic Press, 1-17.